Aspects of Respiratory Heat Transfer in Asthma.

Robert Farley
BSc (Hons), MSc (Bioengineering).

Submitted for the degree of
Doctor of Philosophy

at The University of Glasgow,

University Department of Clinical Physics & Bioengineering
and The Department of Respiratory Medicine
Western Infirmary, Glasgow.

October 1988

Il mio tesi e in memoria della mia nonna. Guardando indietro, della di tutta la mia famiglia, era forse la scoltore principale della mia caraterre.

Aspects of Respiratory Heat Transfer in Asthma.

Summary

During the winter some asthma suffers are incapable of exertion without provoking bronchoconstriction. The rate of respiratory heat exchange (RHER) is proposed as a stimulus of exercise induced asthma. A respiratory test was required to determine heat loss sensitivity. A pumped cold air supply was developed (-22°C, 150 l/min air flowrate) to effect airway cooling during either a hyperventilation or exercise challenge. A microcomputer based data acquisition unit was programmed to record the real-time RHER and permit a trend analysis of expirate temperatures. In two independent hyperventilation challenges, both involving asthmatic and normal subjects, RHER in the asthmatics correlated with the post challenge fall in FEV_1 ($r=0.96$ $n=7$; $r=0.85$ $n=9$). Evidence of an air conditioning deficiency in asthma was found. Attenuation of RHER was by a purpose built humidifier (38°C 100%RH, 150 l/min air flowrate). The device was combined with a numerical model of simultaneous heat and water vapour transfer in order to describe the thermodynamic factors influencing airway heat exchange. Minimising RHER inhibited airway dysfunction in 11 asthmatics after exercise. Invasive measurement in 11 anaesthetised patients of airway temperature was undertaken to determine the site of maximal heat loss. An oral-pharyngeal temperature gradient of 15°C during tidal inspiration of ambient air was found. A catheter-like humidity probe was developed. In 6 subjects tidally inspired ambient air was found to be subsaturated (minima: 80% RH, 34°C) at the mid trachea. Trans mucosal water flow proximal to the trachea was measured as 0.21 ml/min. The larynx may host the airway site from which the bronchial response to heat loss is triggered.

Acknowledgments

Thanks are extended to Dr KR Patel for financial and advisory support throughout the course of the work, in particular the opportunity to attend international meetings with the wider scientific community was greatly appreciated. Thanks also to Dr AT Elliot for reading and critising the work and general 'guidance through the system'.

The technical help of the respiratory staff: Rita Jack, Ian Wade, Aileen Vetters and Jacqueline Scally and the consistant secretarial support of Mrs J Peter, Knightswood Hospital, was appreciated.

Thanks to Mr R Donnet, Mr W Squire and staff of the Mechanical Workshop, Department of Clinical Physics and Bioengineering for advice on and the production of various pieces of hardware. Also to Mrs M Finlayson for photography, Mrs I Hepburn of the general office and staff in the electronics laboratory, DCPB.

The invasive procedures described in this work were executed carefully and reliably by clinical staff at: Knightswood Hospital bronchoscopy theatre, thanks in particular to Sister E Hutcheson and staff, also at the Western Infirmary orthopaedic theatre thanks in particular to Dr J Dougall and staff.

The help of all those who volunteered to participate in the work is greatly appreciated.

Aspects of Respiratory Heat Transfer in Asthma.

Contents. Page.

1. Introduction.

This thesis summarises the findings over a three year period 1985-88 in respect of the development and clinical evaluation of an air conditioning facility for use in the diagnosis of asthma. Studies have also been undertaken to invasively record intra thoracic heat transfer. Chapter 1 furnishes the reader with the principles and terminology of heat transfer, airway physiology and the pathology of asthma. The hypothesis which has directed the research is then described. Supporting literature to each aspect of the project is given at the point of presentation. Some of the work has been published.

1.1. The need.

Subzero temperature air when inhaled can induce bronchoconstriction (airway narrowing) in asthma sufferers. In western Scotland winter temperatures of less than -10°C are not uncommon and pose a seasonal period of discomfort and inconvenience to native asthmatics.

Airway sensitivity to cold air arises with exercise or spontaneous deep breathing, termed hyperventilation. Not all asthmatics are susceptible to exercise induced asthma (EIA) or hyperventilation induced asthma (HIA). Of those that are, cold air inhalation serves to exacerbate the bronchoconstriction which follows either challenge. Respiratory challenges leading to both HIA and EIA can be expected to confer a relatively high rate of heat loss from the airway tissue compared to that encountered during resting ventilation. Exercise induced asthma is a well documented phenomena. Less attention has been given to hyperventilation as it has been regarded as a subset of exercise. For example the airway heat loss that occurs during a hyperventilation challenge has been proposed as a

model of heat loss in exercise (section 3.1).

A combined hyperventilation and cold air challenge could offer the clinician the means to test patients responsiveness to airway heat loss without the physiological stress of exercise. Subjects with heart disorders are candidates for such a test wherein the risk to health in diagnosing asthma would be less than with a test involving exercise.

It has generally been the case that a newly referred asthmatic must wait until the winter months before a diagnosis with respect to cold air can be made. A cold air facility in the lung function laboratory and available throughout the year to challenge a hyperventilating or exercising patient is needed.

Exercise in the lung function laboratory is normally performed on a cycle ergometer or a treadmill. In both cases the work of exercise is calculated from the patient's tractive effort and can be correlated with the level of post exertional bronchoconstriction (figure 3.01).

A similar index of 'air conditioning effort' is required to quantify the severity of a cold air challenge.

1.2. Quantifying respiratory heat loss.

The respiratory tract can be regarded as a "black box" into which unconditioned air is inspired. Exhaled air emerges at some temperature less than the body core temperature but warmer than the inspirate and in a state of full water vapour saturation. The net thermal load on the airway can be described by the energy input necessary to condition the inspirate.

Enthalpy is the thermodynamic property which describes the energy content of a moving gas. It comprises internal energy and the work done in transferring unit mass of gas into or out of the system under consideration. Thus:

$h = u + P.v$ where h: enthalpy. J/kg K
P: gas pressure. N/m^2
u: internal energy. J
v: specific volume. m^3/kg

In practice the change in enthalpy between two states is required rather than absolute enthalpy:

$$d(h)_{1,2} = d(u)_{1,2} + d(P.v)_{1,2}$$

The thermodynamic relation describing the change in enthalpy for a superheated gas can be found using the gas laws (Rogers and Mayhew[47] 1983) and is written as:

$$d(h)_{1,2} = C_p.d(T)_{1,2} \qquad .....1$$

where C_p: Specific heat at constant pressure. J/kg K
T: Absolute temperature. K

At ambient conditions dry air is highly superheated. C_p is approximately constant and no phase changes occur. However, water can exist in liquid or vapour phases. The enthalpy of water vapour at equilibrium with the liquid phase is:

$h_g = h_f + h_{fg}$ where subscripts g: vapour phase
f: liquid phase
fg: enthalpy of evaporation.

h_{fg} is sometimes known as the latent heat of evaporation.

When the liquid phase is absent the enthalpy can rise above the saturation value (h_g) and the vapour is described

as superheated. Hence $h_g > (h_f + h_{fg})$. This arises when in a mixture of air and water vapour the relative humidity is less than unity. Measured values of enthalpy are recorded in tables and charts (Stoecker and Jones[68] 1981) to enable calculation of energy changes.

In a mixture of dry air and water vapour the enthalpy is:

$$h = m_a.[h_a + w.h_g]$$

where m_a: mass of air in unit mass of mixture. kg
w: specific vapour content. kg/kg
found by $w = m_{wv}/m_a$ m_{wv}: mass of water vapour

The specific water vapour content w is a direct function of its partial pressure in air and can be deduced from the psychrometric relation given in section 2.4.4.

Dry air and water vapour are inhaled at temperature T_i with mass flows m_{ai} dry air and m_{wvi} water vapour. Exhaled air has a temperature T_e with mass flows m_{ae} dry air and m_{wve} water vapour. The energy balance describing this system comprises four elements:

i) the enthalpy content of the inspirate;
ii) the heat lost by the airway;
iii) the enthalpy of the additional water supplied at body temperature to the air and
iv) the enthalpy content of the expirate.

or: iv) = i) + ii) + iii),

$$h_{ae} + w_e.h_{ge} = [h_{ai} + w_{ai}.h_{gi}] + Q + [(w_e - w_i).h_{fb}] \quad \ldots 2$$

Where subscripts denote a: dry air
b: body condition
e: exhalation condition
i: inspiratory condition and
Q denotes heat loss.

Rearranging equation 2 and substituting with equation 1:

$$w_i.(h_{gi} - h_{fb}) + Q = C_p.[T_e - T_i] + w_e.\ (h_{ge} - h_{fb})$$

or writing RHE (respiratory heat exchange) for Q:

$$RHE = C_p.[T_e - T_i] + w_e.(h_{ge} - h_{fb}) - w_i.(h_{gi} - h_{fb})$$

Expressed in terms of the respiratory heat exchange rate (RHER) J/s or W and assuming m_a remains constant:

$$RHER = m_a.(C_p.[T_e - T_i] + w_e.(h_{ge} - h_{fb}) - w_i.(h_{gi} - h_{fb}))$$

The solution requires prior knowledge of three enthalpy values. Thermodynamic data for water vapour at temperatures and humidities typical to those encountered in this work are taken from the tables of reference 68. It is assumed that evaporation in the airway leaves the exhaled air fully saturated at the temperature of exhalation.

T_b=37°C; h_{fb}=155 kJ/kg. C_{pa} = 1.005 kJ/kg K.

T_e=32°C; RH=100% w_e=0.0308 kg/kg; h_{fe}=134 kJ/kg;
h_{fge}=2426 kJ/kg; h_{ge}=2560 kJ/kg

T_i=20°C; RH=45% w_i=0.0065 kg/kg; h_{fi}=84 kJ/kg;
h_{fgi}=2504 kJ/kg; h_{gi}=2538 kJ/kg (at saturation).

The enthalpy of the superheated inspired water vapour can be taken to be that at the saturation condition (Stoecker and Jones[68] 1981). Substituting values into the formula for RHER yields:

$$RHER=70.64(m_a) \text{ kJ/kg.}$$

Now if it is assumed that $h_{fb} \approx h_{fi} \approx h_{fe}$ and given that $h_{fg}=h_g-h_f$:

$$RHER = m_a.[C_{pa}(T_e - T_i) + w_e.h_{fge} - w_i.h_{fgi}]$$

Now $h_{fge} \approx h_{fgi}$ thus:

$$RHER = m_a.[C_{pa}(T_e - T_i) + h_{fge}.(w_e - w_i)] \qquad ....3$$

and substituting values yields RHER = 74.27(m_a) or an error of less than 5%.

From the tables[68] the specific volume of dry air at 32°C is 0.9066 m^3/kg and for water vapour 29.57 m^3/kg. Thus the mass flow m_a of dry air can be estimated by:

$$V_t = m_a.v_a + m_{wv}.v_{wv}$$

V_t: total volume flowrate. m^3/s
v: specific volume. kg/m^3

with $m_{wv}=w_e.m_a$

$$V_t = m_a.v_a + w_e.m_a.v_{wv}$$

Inserting values:

$$m_a \approx V_t/(1.82)$$

The mass flowrate of dry air can be derived from measurements of respired air volume and air flowrate respectively. Thus knowledge of inspiratory and expiratory air conditions together with ventilation rate is required to quantitate the severity of a thermal burden. An example of RHER calculation is given in section 3.4.2 wherein a typical heat exchange rate in ambient air during tidal breathing is about 13 W.

Exercise challenge severity is normally preset and the patient must develop and maintain a specified tractive effort. This can take the form of simply keeping up with the treadmill or matching the brake power set on the cycle ergometer. Breath by breath measurement of RHE and RHER provides a means of maintaining a constant severity of burden in the thermal challenge. Chapter 2 describes the method by which these measurements were made and displayed.

1.3. Structure and function of the human airway.

A synopsis is given of the structure and function of the human airway which has been derived from the medical texts of Best & Taylor (1983)[1], Crofton & Douglas (1981)[2] and Tortora & Anagnostakos (1984)[3].

1.3.1. Airway structure.

The respiratory system is the means by which air is conducted to the alveolar blood - gas barrier, where diffusive gas exchange occurs. The airway has been arbitrarily divided at the level of the main carina (base of the trachea and site of the first airway division) into upper and lower portions.

The upper respiratory tract comprises the mouth , nose, pharynx, larynx and trachea. Figure 1.01 illustrates these structures; the dimensional data have been taken from the airway casting work of Hanna and Scherer (1986)[4].

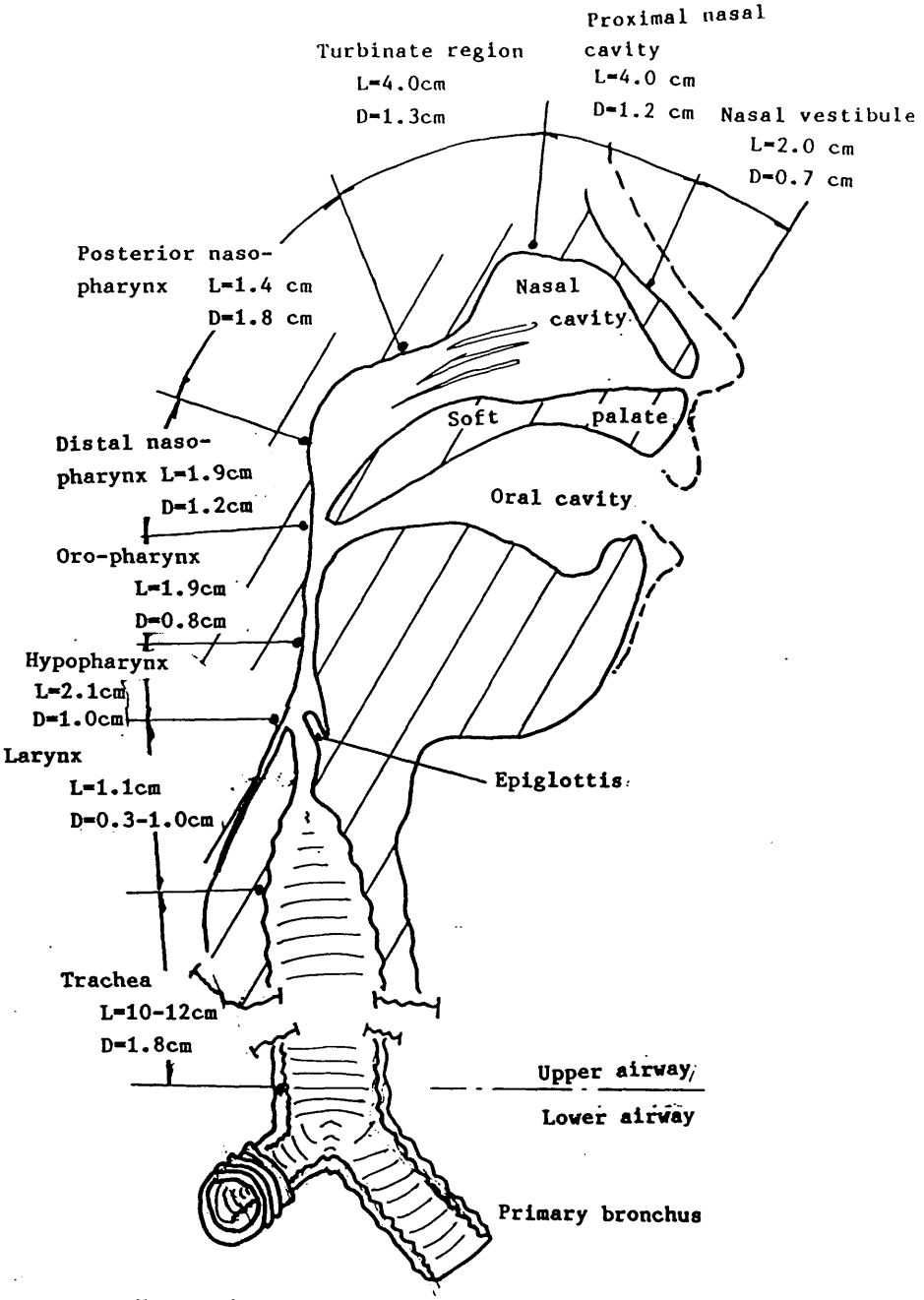

Upper airway structure.
Dimensions after Hanna & Scherer (1986 a)

Figure 1.01:

The nose provides particulate filtering and an olfactory facility. There is an absence of the fine ciliary hairs in the nasal vestibule, generally present in the upper airway, and it is believed that the nose is the terminal site in the muco - ciliary clearance process, described in section 1.3.2. The wall of the nasal cavity is highly vascularised and exudes watery secretions both of which serve to rapidly humidify and warm the tidal inspirate. The turbinate region comprises a series of longitudinally orientated folds which enhance air turbulance in the nose. Its importance as an air conditioner is illustrated by the laryngeal soreness encountered in exercise with oral breathing, especially in cold air conditions.

The pharynx comprises two structures divided by the soft palate. The naso - pharynx meets the region of the turbinates at the rear of the nasal cavity and becomes congruent with the oro - pharynx distal to ('below') the oral cavity. The pharynx acts as a passage way for food and air. Constructed of skeletal muscle it is funnel-like in configuration and extends 11 cm. The pharynx terminates at the mid - neck proximal to ('above') the epiglottis which seals the laryngeal airway during a swallowing manoeuvre. The food bolus is directed into the oesophagus the entrance to which lies posterior to ('behind') the larynx.

The larynx includes the vocal cords or glottis and geometrically is a venturi. It is formed by highly mobile cartilagenous elements and has recently been described by Engel (1987)[5] as an organ of respiration. This proposal followed observations of diametrical constriction and dilation during exertional expiration and inspiration respectively. A dilated glottis was proposed to reduce the resistance to inspiration whereas expiratory narrowing would promote some back pressure, or hyperinflation, in the lower airway and thus prevent total airway collapse.

The trachea, or windpipe, extends 12 cm from the larynx to the main carina,the first division in the airway. It

lies anterior to ('in front of') the oesophagus. In cross - section the trachea is elliptical with the coronal diameter some 25% greater than the sagittal. It is formed of semi - lunar cartilagenous rings and has a 2 cm range in longitudinal mobility according to body position and movement.

At the carina the airway branches into right and left primary bronchi and therafter subdivides progressively until the alveolar level. The first division is characterised by a right offset due to the proximity of the heart and great vessels. The right primary bronchus is about 1.5 cm in length and subdivides into three major lobes, independent regions of ventilation. The lobes are described by their relative position, these being upper, middle and lower lobes. The left primary bronchus is about 5 cm in length and the lung comprises two major lobes, upper and lower. The bronchi are formed by cartilagenous rings which extend some 15 - 25 generations into the airway from the carina. Structural changes in the bronchi arise as the generations increase with the emergence of cartilage plates. As the cartilage abandons its circumferential distribution so the bronchial muscle becomes disposed longitudinally in a spiral manner. Thus muscular contraction results in a reduction in airway length and diameter. The smallest bronchus is estimated to have an inner diameter or 'lumen' of 1 mm. Beyond this point the bronchioli subdivide for a further 3 or 4 generations prior to the terminal bronchiole. Approximately 20 terminal bronchioli are derived from each small bronchus. Weibel (1967)[6] correlated the bronchial tree structure with an exponential decrease in diameter and length for each successive airway generation. The model was termed 'dicotomous bifurcation': progressive binary division.

The terminal bronchioli meet sacs of elastic tissue termed lobules. These contain the highly vascularised alveoli and are the blood - gas interface by which

metabolic respiration occurs. The blood - gas barrier is about 2.5 um thick. There are an estimated 300 million alveoli in each lung, each of a diameter of less than 0.25 mm, yielding a total surface area for gas exchange of 40 - 80 m^2.

1.3.2. The airway wall.

Evaporative water vapour uptake and convective heat transfer to the inspired air is derived from the airway wall. Between the upper airway and bronchi a three layer airway wall structure is evident. This comprises the mucosa, the submucosa and a fibrocartilagenous layer which includes the smooth muscle. Figure 1.02 illustrates the airway cross section at the trachea.

The mucosa or mucus membrane consists of epithelium onto which are located an abundance of ciliary cells. There are about 200 ciliary fibrils attached to the cell, each 5um long, with some 1500-2000 million cilia per cm^2 of upper airway. The cilia serve to transport particulate debris out of the respiratory tract by means of a consecutive wave action of about 21 beats/min. Depending on the size of the debris muco ciliary clearance rates of between 2.5-35 mm/min arise. The ciliary escalator is unaffected by body orientation or sleep. Excessive mucus production can impede the muco ciliary clearance action as can airway drying, observed by Horstmann et al (1977)[7]. With the exception of the anterior nasal cavity and the posterior larynx the upper airway is coated with this ciliated and mucus secreting epithelium. Ciliary density declines with progression through the upper airway and into the bronchi. A corresponding decline in mucus secreting elements is also evident; thus the airway wall becomes inherently drier with increasing generations of bronchi. The mucosa is limited by strands of interweaving fibrils which form the basement membrane.

Figure 1.02:

Airway cross section at the trachea

After Crofton & Douglas (1981)

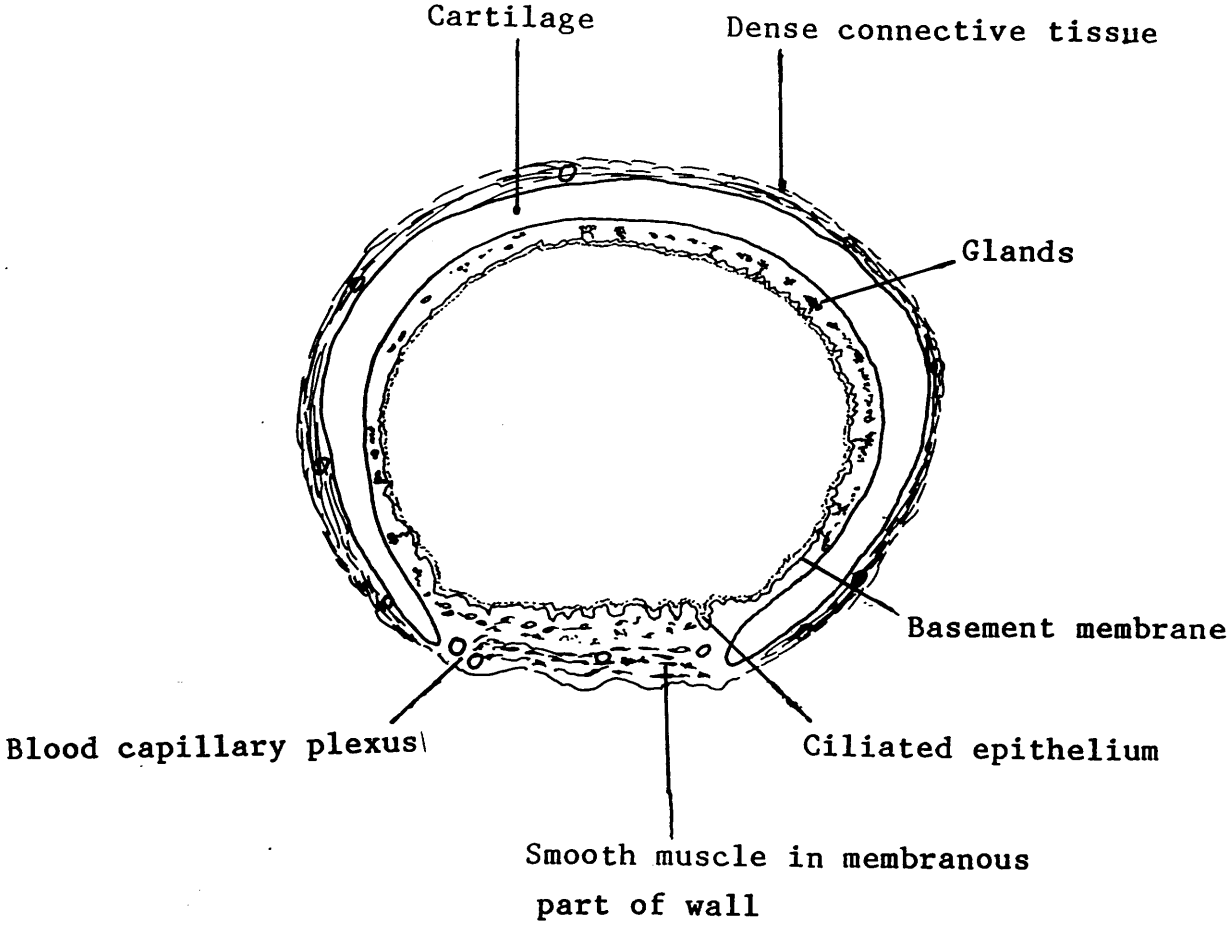

Located in the elastic fibres of the sub mucosa is a blood capillary plexus which oxygenates and supplies heat to the epithelium. Pre and post capillary vessels are located in the deeper elastic tissues. The submucosa also hosts the the mucus secreting glands and goblet cells. Mucus is a viscous fluid which serves to waterproof the airway, lubricate the mucociliary escalator and has some anti infective properties. Sensory receptors are also sited in the sub mucosa. Chemical, mechanical and thermal irritants directed at the larynx can stimulate a cough reflex: an explosive discharge of air followed by rapid glottic closure. The presence of chemo, thermo and mechano receptors is accompanied by autonomic nerves which regulate muscle tone and vaso diameter in the sub mucosal capillary plexus. Both vagal (constrictor) and sympathetic (dilator) nervous pathways are present. More recently Barnes (1986)[8] has identified a third, the non-cholinergic, non-adrenegic nervous pathway. Under normal circumstances this provides for a certain degree of muscle tone by the release from the nerve terminals of acetylcholine. Variations in the level of acetylcholine alters the smooth muscle tone. The tracheo bronchial nerve supply could be derived from the laryngeal supply. Balliere et al (1975)[9] have catergorised thermal stimuli as a cutaneous sensation allied to touch although the precise nature of thermoreceptors is unknown. Toratora and Anaknostakos (1984)[3] believe thermoreceptors could be free nerve endings projecting into the submucosa. Receptor stimulation forms one end of a 'reflex arc'. At the other a motor neuron fires a muscle element which results in a contractile or extensor manoeuvre. These manoeuvres can influence vaso-diameter or size of the airway lumen. Receptor stimulation is characterised by the 'all or none' principle wherein a sub threshold stimulus will not activate the motor neuron. Stimuli greater than the threshold level fires the neuron resulting in a muscle reflex. Rapidly recurrent stimulation can promote the

development of a receptor tolerance to the stimuli, termed 'accommodation', and the magnitude of the reflex declines. A common example is the sensation felt when first entering a hot bath and that felt shortly after. Increasing the area of stimulation and thus the number of receptors results in the 'recruitment' of more motor neurons and a graded extensor or contractile response arises.

The fibrocartilagenous layer comprises connective tissues, smooth muscle and the larger vessels of the pulmonary blood supply. Narrowing of the airway lumen follows from contraction of the smooth muscles herein.

1.4. Airway dysfunction in the asthmatic.

1.4.1. A short history.

Sakula (1988)[10] in "A history of Asthma" cites features commonly associated with the disorder being identified by Arab physicians from 980 AD. Sir John Floyer (1698) correlated the climate and seasons with asthmatic episodes. Long sea voyages and strong coffee were recommended to inhibit the symptoms. Presumably the moisture content of the bracing sea air conferred some protective effect upon the airway (section 3.1) as almost certainly would have the caffeine in coffee which possesses bronchodilator properties. Franz Reissen (1808) identified bronchial muscle and proposed that its tone was related to the size of the lumen during asthmatic episodes. In 1835 Francis Ramadge established the London Infirmary for Asthma, Consumption and other diseases of the Chest. Work there correlated asthma with allergies to house dust mites, fleas and ticks. Technical advancement followed from the need to quantitate airway function and in 1846 John Hutchinson patented the first spirometer. His spirometry principle remains central to the diagnosis of pulmonary disorders.

Since that time there has been a plethora of clinical and technical advancement in respiratory medicine. Indeed this thesis is one aspect of that trend. However, asthma remains a disorder for which there is no universal definition.

1.4.2. The pathology of asthma.

Clark and Godfrey (1983)[11] describe asthma as episodes of wheezy breathlessness with intervals of complete freedom from symptoms. It represents diffuse airways obstruction which causes a resistance to respiratory airflow. Hyperinflation of the lung due to obstructive trapping of expiratory air and mucus plugging of the lumen may be present. In most asthma sufferers some airways obstruction follows exercise. This phenomena is not universal and, as will be illustrated, there are those asthmatics who can tolerate exercise. Diagnosis also involves testing for enhanced reactivity to specific (known) and non - specific (unknown) stimuli.

Hypersecretion from the airway wall and oedema (watery swelling) of the submucosa are common symptoms as is hypertrophy (excessive growth) of the bronchial smooth muscle. Vasodilation of the blood capillary plexus in the submucosa and sensitisation of the airway by the ingression of inflammatory cells are also associated with the asthmatic airway. With the appropriate stimuli these cells are believed to release mediator substances which provoke bronchoconstriction (section 3.7.1). Figure 1.03 illustrates the tracheal lumen in this diseased state.

Inner city dwellers are ten times more likely to suffer from asthma than pertains nationally (Andrews, 1986)[12] and the Asthma Research Council recorded 1764 deaths from the disease in 1984 (Hedges, 1986)[13]. Asthma presently affects some 2.5 million Britons (Hodgkinson, 1986).[14]

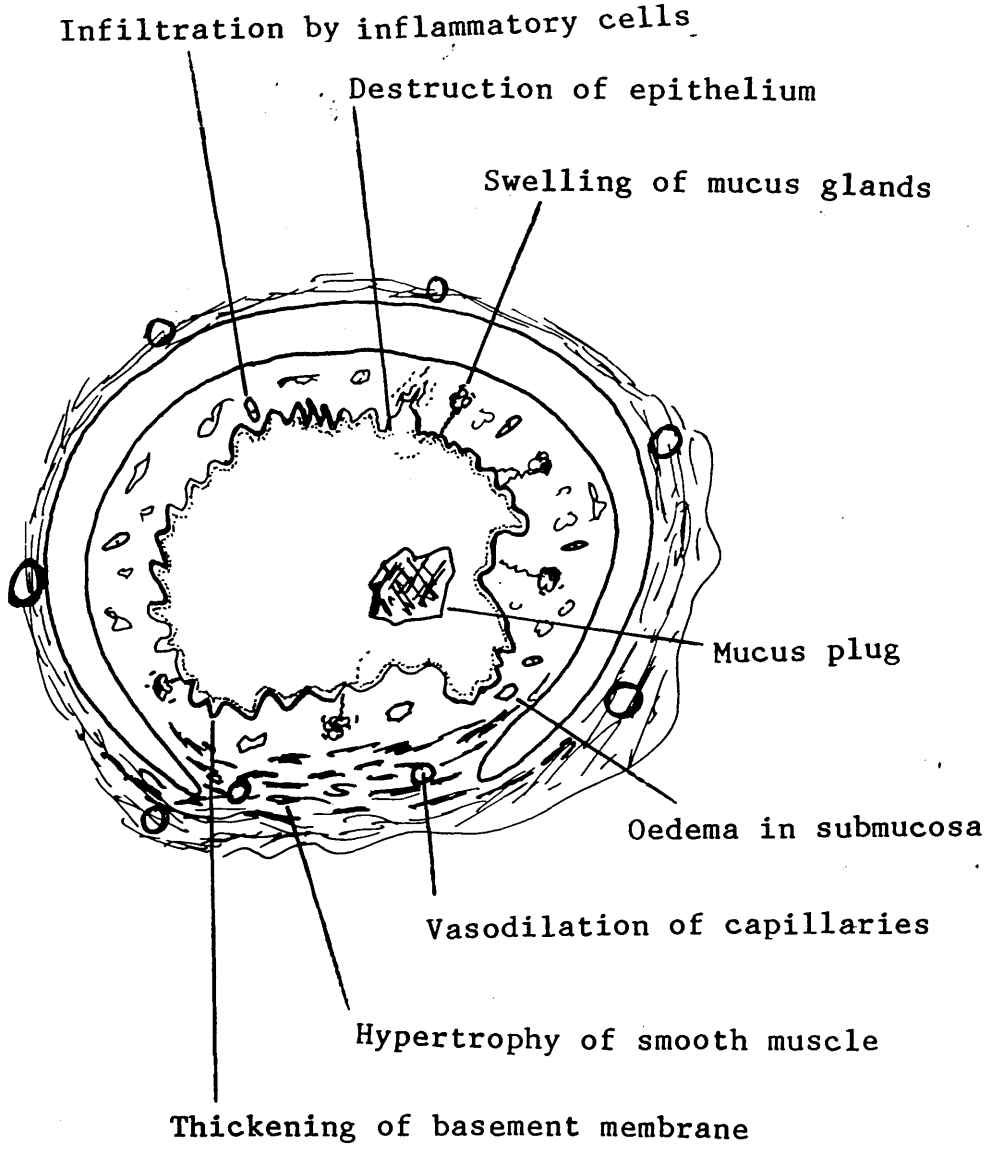

Tracheal lumen in asthma.
The bronchi would exhibit
identical features, but without
structural cartilage.

Figure 1.03:

1.5. Quantifying lung function.

1.5.1. Airway volumes.

Pulmonary ventilation involves the rhythmic mass movement of air up and down the respiratory passages. Inspiration involves an upward and outward movement of the ribs accompanied by a flattening of the diaphragm causing an increase in the thoracic volume. The reduction in thoracic air pressure sucks ambient air into the airway. Quiet expiration is a passive manoeuvre relying on the recoil of the elastic tissues. During exercise expiration is assisted by voluntary contraction of the rib cage. Rhythmicity, rate and depth of breathing are controlled by the autonomic respiratory centre to ensure adequate alveolar ventilation.

Tidal volume is that amount of air respired and has a resting value in adults of about 500 ml. Of this 150 ml occupies the anatomical dead space and has no direct role in alveolar gas exchange. The active 350 ml is termed the alveolar volume. By contraction of the abdominal muscles a further 500 ml can be expired, termed the Expiratory Reserve Volume (ERV). A residual air volume of 1200 ml remains in the airway. This is normally less than 30% of Total Lung Capacity (TLC) obtained by full inspiration. Exertional expiration of a full inspiration yields the Forced Vital Capacity (FVC). Normally FVC is 80% of TLC.

1.5.2. The spirometer.

Forced vital capacity can be recorded on a dry wedge spirometer. The dry wedge comprises a breathing tube through which the patient expires into a wedge shaped bellows. The rate at which the bellows are filled and the final volume achieved represent important lung function parameters. The dry wedge spirometer used in this work was

an independently calibrated 'Vitalograph' (Vitalograph Ltd, Buckingham UK). It comprises a platter which traverses a slideway fixed onto the device casing and a laterally mobile stylus, mechanically linked to the bellows. The platter motion is breath activated. As expiration begins so the platter traverses the slideway and the stylus moves down. The platter takes six seconds to cross the slideway during which maximal expiration is maintained. The tracing produced represents the time course cumulative volume of the expiration.

Figure 1.04 illustrates the tracings obtained from a normal male (age 25 yrs) and an asthmatic female (age 21 yrs). The main index of lung function is the Forced Vital Capacity in 1 second, FEV_1, illustrated by the initial gradient of the curves. FEV_1 is influenced by the level of effort in assisting expiration and the degree of airway obstruction present. The absolute quantities between the two subjects are not of primary importance as thoracic volumes and airway mobility vary among individuals. In normal lung function FEV_1 is expected to exceed 80% of FVC and this ratio is sufficient to identify airway dysfunction. Comparison of the actual FEV_1 and FVC with the predicted normal FEV_1 and FVC can also be done in order to relate the absolute quantities to a normal population of equal gender, height, weight and age. The asthmatic subject exhibited an FEV_1 of 41% of FVC whereas in the normal this was 91%.

The effect on an individual of an airway challenge such as bronchoconstrictor agents, exercise or cold air is quantified by comparison of the pre and post challenge FEV_1. The percentage change is expressed as:

$$\text{Change} = \frac{[FEV_1\ (\text{Pre}) - FEV_1\ (\text{Post})]}{FEV_1\ (\text{Pre})} \times 100\%$$

Figure 1.04: Forced expiratory tracings obtained from the dry wedge spirometer

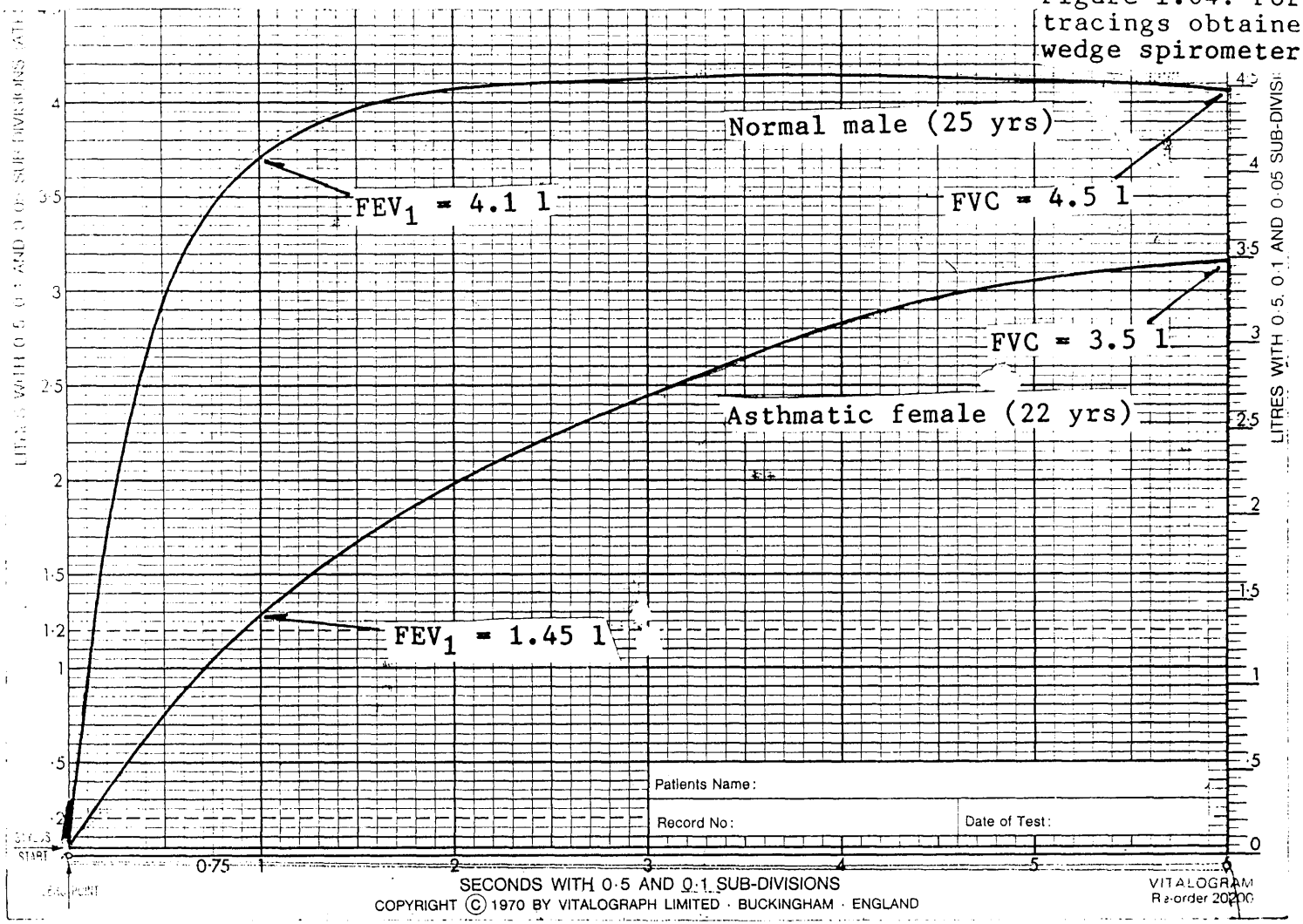

This expression was used throughout the present work. Typically a mild asthmatic may experience a fall in FEV_1 of between 10-20% after a brisk treadmill walk whereas a normal subject would be expected to exhibit a 5% rise in FEV_1.

1.6. The hypothesis.

The hypothesis was based upon the intuitive notion that the behaviour of many physical systems is rate dependent. With regard to the airway the rate of respiratory heat exchange is assumed to directly influence the receptors of the sub mucosa and may lead to the reflex events described in section 1.2.2. A threshold airway heat exhange rate and thereafter a cumulative airway response with increasing RHER is expected. The hypothesis was:

The rate of respiratory heat exchange arising in a thermal burden can be correlated with the resultant changes in FEV_1.

The sphere of research was widened to investigate the site of a maximal heat transfer in the airway. This location could be presumed to host the initiator of the events leading to bronchoconstriction.

To fulfil the hypothesis the construction of air handling facilities and protocols was required capable of conditioning the inspirate to yield a range of thermal burdens. Flexibility and applicability to the exercise and hyperventilation regimes were necessary. The programme of work was divided into three broad areas:

1. Mechanical development of a cold air facility for use in the respiratory laboratory. This also required a microcomputer based recording system to generate real time values of RHER. Chapter 2 describes the cold air unit. A clinical evalutaion of the effects of varying RHER using the device is presented in chapter 3.

2. The effect of minimising RHER by inhalation of tropical grade air was examined. A novel air humidifier capable of producing body core condition air for use in exercise was built and is described in chapter 4. An evaluation of RHER in exercise using both the humidifier and the cold air unit is given in chapter 5.

3. The site of maximal in vivo heat transfer was investigated. Direct measurements of intra thoracic air temperature during ambient and cold air breathing were made, detailed in chapter 6. This work prompted measurements of airway air humidity. The purpose built probe and invasive study for this are described in chapter 7.

2. Cold air generation and data acquisition.

2.1. Past Techniques.

Early thermal challenge studies by Millar et al (1965)[15] involved patients breathing -20°C air for 7 minutes in a refrigeration room owned by the Dundee Cold Storage Company.

Simonsen et al (1967)[16] in observing the broncoconstrictive effect of various irritants used air actively pumped at 20 l/min through a coiled pipe immersed in dry ice and acetone. Patients breathed the chilled air off one arm of a 't' piece. Exercise ventilation levels are typically 50-60 l/min. The device was not applied to an exercise test.

Strauss et al (1977)[17] describe an isopropyl alcohol heat exchanger through which subjects sucked the cooled air during an exercise challenge. However the mechanical suction effort required to overcome the heat exchanger coil resistance can itself lead to bronchoconstriction. No comment with regard to back pressure effects was made. Deal et al (1979)[18] have also adopted this system in studies relating to lung function in dry air and Magussen and Reuss (1983)[19] have built a similar device whereby patients breathe from a reservoir of cold air.

The advantages of the passive system are its simplicity and low cost. Its effectiveness as a means of inducing bronchoconstriction is evident although there exists some doubt as to whether heat exchanger resistance to air flow was considered a contributory factor. The rate at which the subject inhales and length of heat exchanger coil immersed in coolant under these circumstances will also influence the temperature of inspired air.

To the authors knowledge there is one commercial cold

air generator for use in the respiratory laboratory manufactured by Jaeger GmbH (RHES, Wurzburg, West Germany). It is shown in figure 2.01 and is of the passive variety. Subjects inhale cold air (-25°C) through an alcohol coolant heat exchanger mounted on an adjustable boom. Refrigeration of the coolant occurs in a remote unit housed under the boom. A 30 litre balloon, continuously filled by bottled dry air and connected to the heat exchanger, serves as a reservoir from which the patient inhales and also as a target for tidal volume control. In addition to the problems associated with a passive system the machine cost in excess of £10,000 (1987 price) and did not appear compatible with a treadmill exercise test due to the limited reach of the boom and bulk of the heat exchanger - mouthpiece assembly.

The following describes the pumped cold air system designed in the present work which has been published (Farley and Patel[70], 1989). It is capable of generating air temperatures as low as -28°C at an air flow of up to 150 l/min.

2.2. Cold air Production.

The means by which the cold air was produced is detailed in four parts relating to: air compression; predrying; air cooling and air delivery. Figure 2.02 shows this sequence.

2.2.1. Compressor.

Laboratory air was drawn into a single phase four vane oiless rotary compressor, (ECB8 Edwards Vacuum Co. Coventry, UK), operating at 0.5 bar, 150 l/min air flowrate. This was housed in a purpose built box, designed by the author, of 25mm thick chipboard lined with 25mm gauge acoustic foam (NCC25, Bestobell Ltd, Leicester, UK) which adequately attenuated the machine noise.

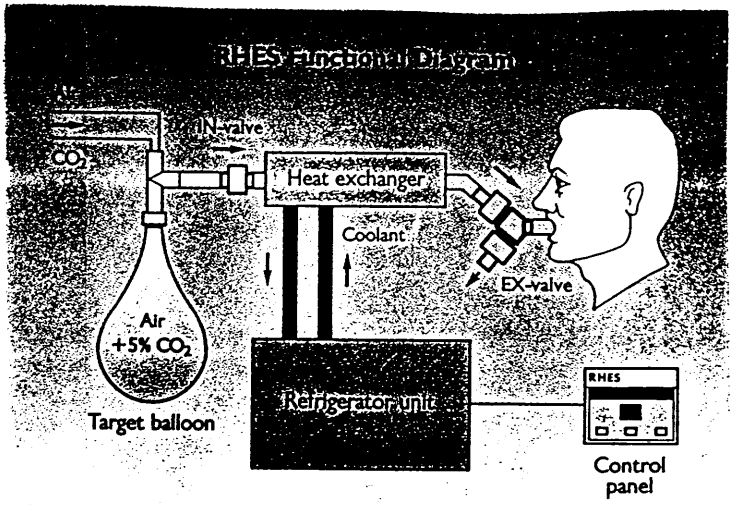

Figure 2.01: Jaeger cold air unit. The targeting balloon is sighted by the patient in order to maintain constant ventilation.

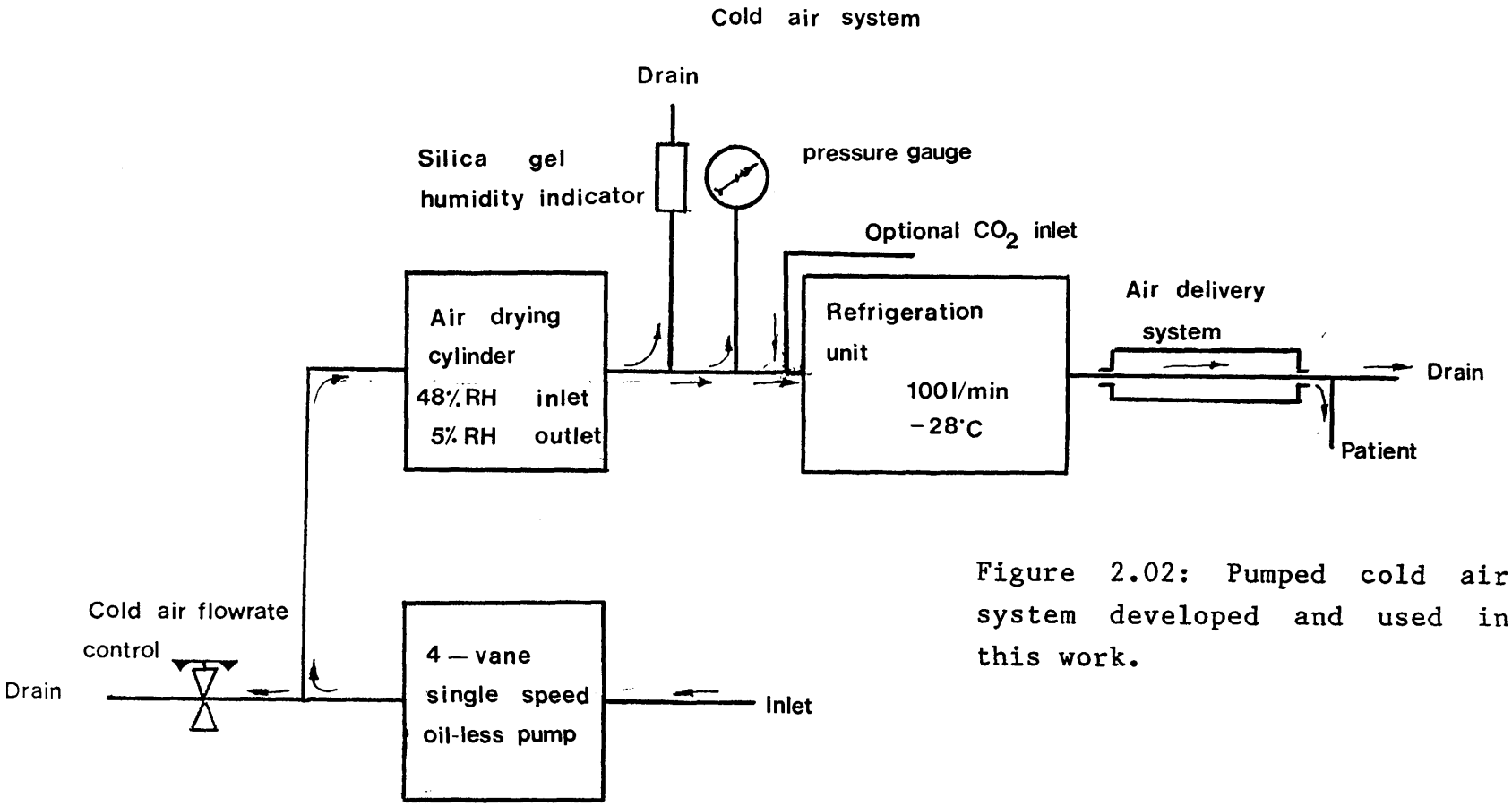

Figure 2.02: Pumped cold air system developed and used in this work.

2.2.2. Air Drying.

Air was then piped via a 12.5mm ID rubber tubing into a vessel containing anhydrous zeolite pellets (sodium aluminosilicate: type 5A Molecular Sieve, Kochlite Ltd, Edinburgh, UK). The unit was specially built in order to avoid using expensive bottled dry air to supply the cold air refrigerator, which was initially found prone to internal blockage by the freezing out of water carried in ambient air.

Figure 2.03 illustrates the air drier which comprised a vertically orientated cylindrical chamber of ABS plastic divided at its mid section by a non sealing baffle. A cotton wool filter on top of the baffle followed by 1kg of zeolite pellets filled the upper half of the chamber. Along its mid line, through the baffle, projected a copper inlet pipe. Two air outlet pipes projected into the lower portion of the chamber and the entire unit was made airtight by a steel compression ring over each endcap coupled by four lengths of 4mm studding.

The effectiveness of the air drier was determined by pumping air through the cold air system as shown in figure 2.04 and periodically sampling the air condition at the drier outlet using a wetted wick swing hygrometer (Gallenkemp Ltd, East Kilbride, UK). Ambient air temperature and humidity were 18°C and 56%RH respectively. The test was conducted for 100 minutes and air flow set to 120 l/min. Initially the exit air temperature from the drier increased associated with the heat of compression and chemical absorption of water vapour, figure 2.05. After 30 minutes the exit air temperature began to fall caused by a decline in chemical heating by water retention in the zeolite. Figure 2.06 illustrates the exit air water vapour content, which after 30 minutes rose markedly. Ambient and bottled dry air conditions are shown for comparison. The

Figure 2.03: Air drying cylinder. This was built in order to avoid using expensive bottled air.

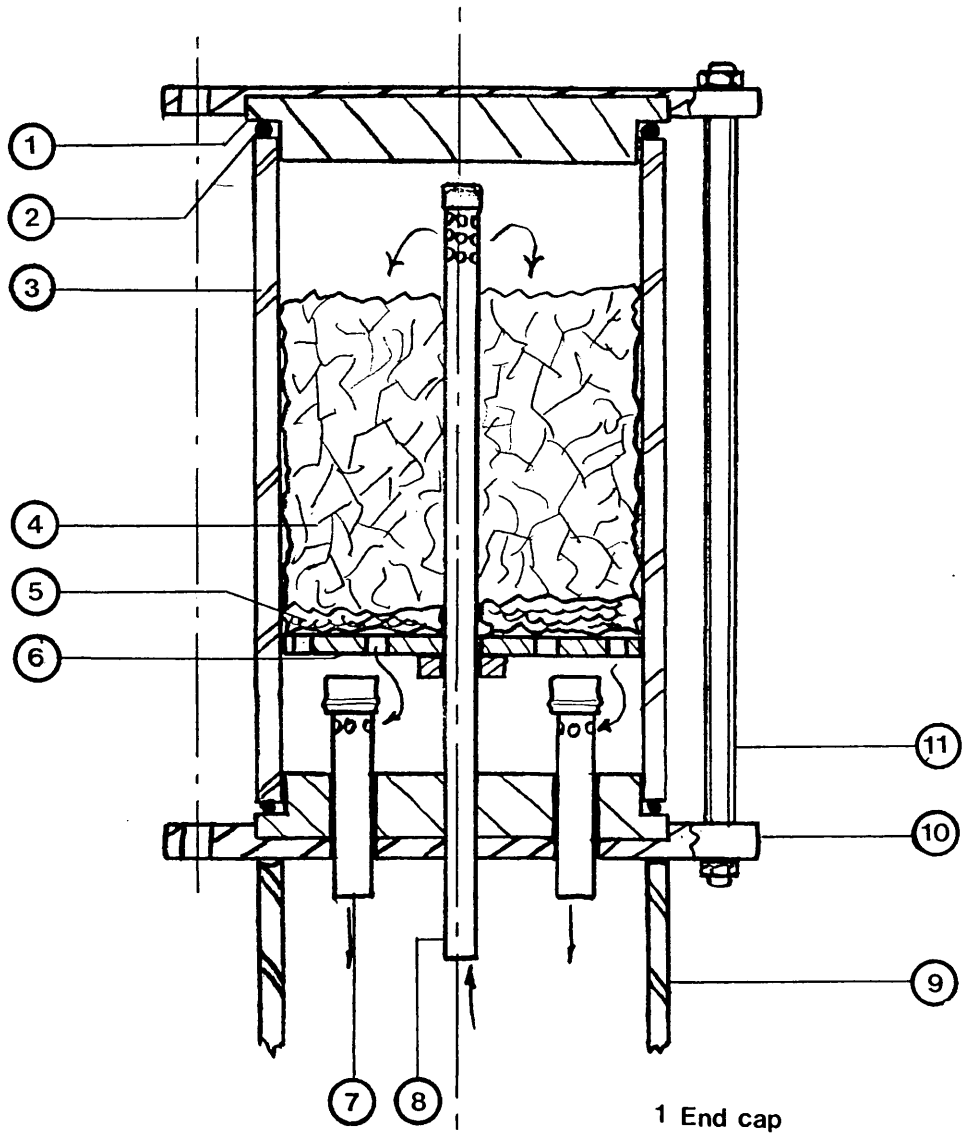

1 End cap
2 'O' ring
3 Casing
4 Zeolite drying agent
5 Cotton wool filter
6 Support baffle
7 Outlet to refrigerator
8 Inlet from pump
9 Stand
10 Compression ring
11 Compression studding

Performance:

Agent life 30 mins
Inlet - 48%RH
Outlet - 5%RH
Flow - 100l/min

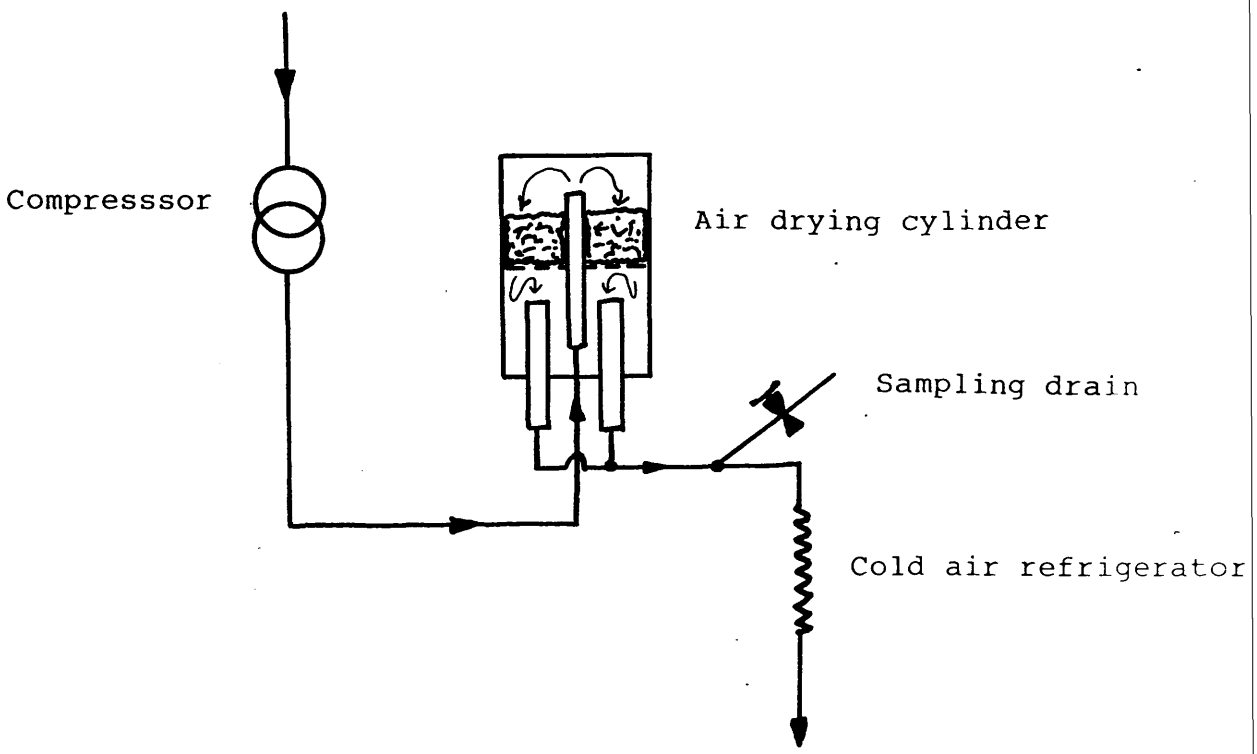

Figure 2.04: Evaluation of air drying cylinder effectiveness. Air samples were intermittently drawn from the drain.

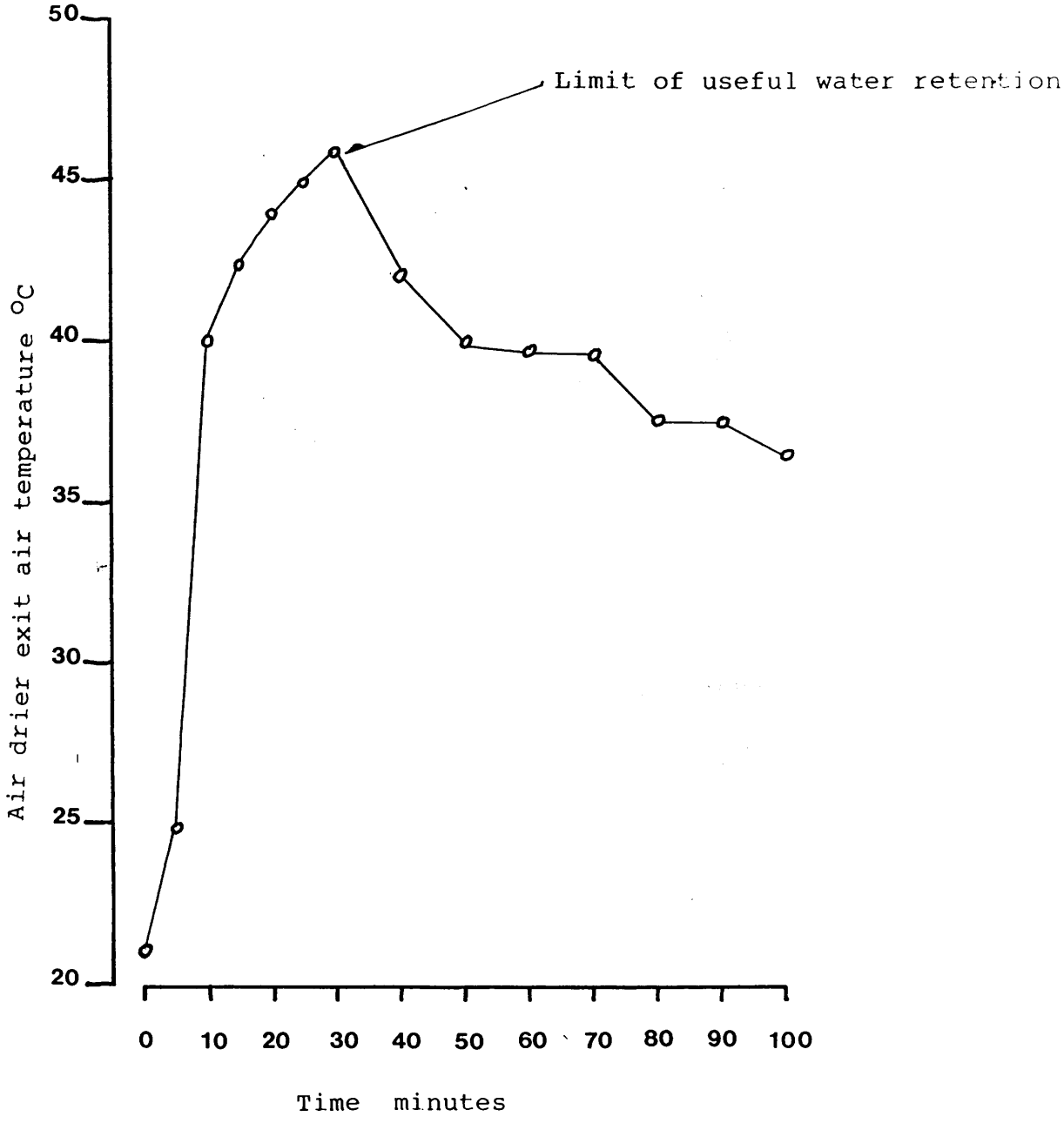

Figure 2.05: Exit air temperature from the drying cylinder. The peak temperature corresponds to the limit of water vapour retention.

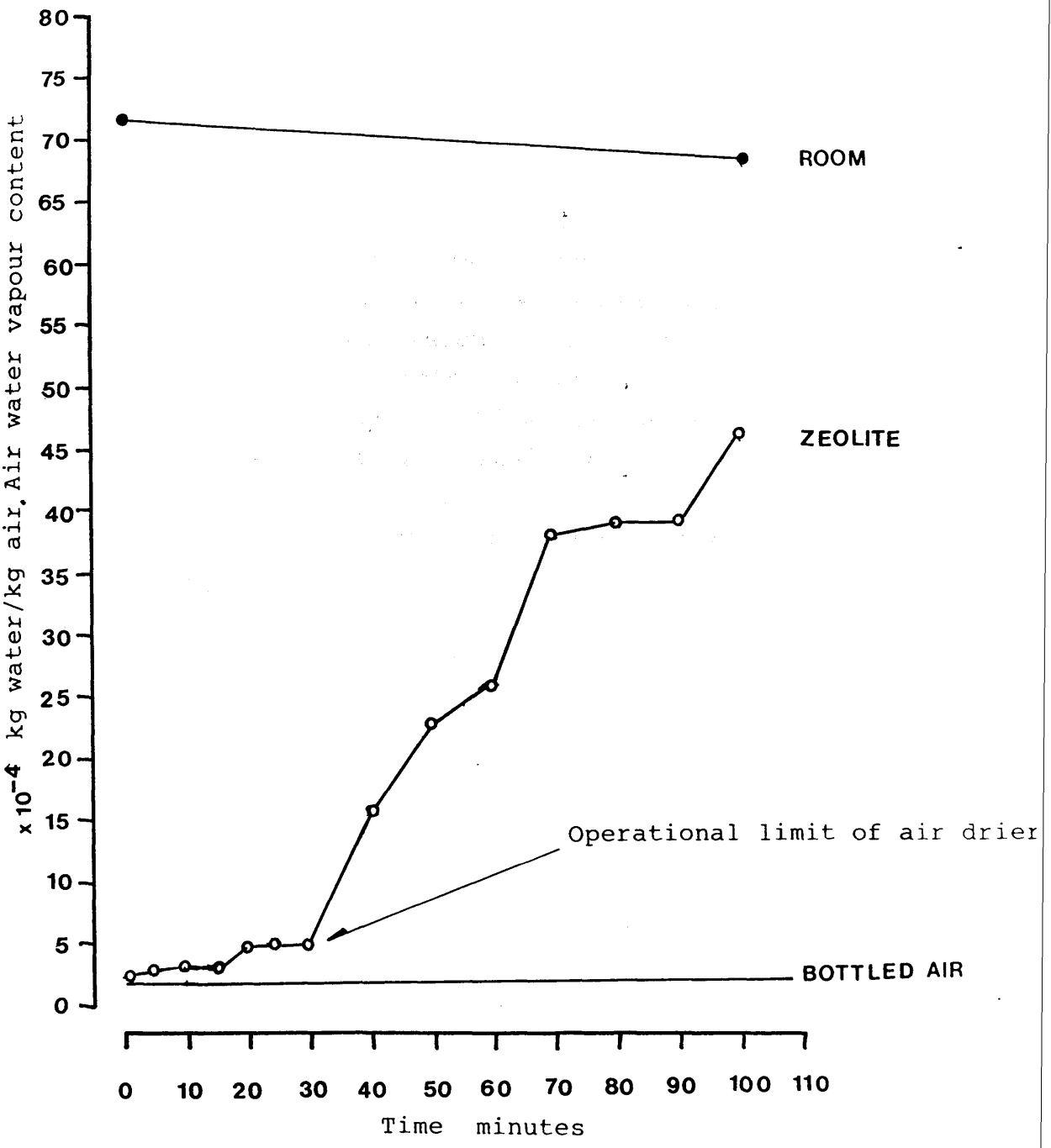

Figure 2.06: Exit air water vapour content from the air drier. An operational limit of about 30 minutes was apparent for 1 kg of zeolite crystals.

operating limit of the air drier was therefore set to 30 minutes which would allow six 5 minute challenges before regeneration of the zeolite became necessary. Regeneration of the zeolite was done by baking at 250°C for about 3 hours.

2.2.3. Cooling

Air cooling was achieved by passing the dry air stream through a heat exchanger designed and built by the Kooltech Company, (ACU1, Glasgow, UK). The machine was based on the standard single stage vapour compression cycle using refrigerant R502 and its internal working is illustrated in figure 2.07. The important elements of this cycle are compression, condensation, expansion and evaporation of the refrigerant.

At the compression stage refrigerant vapour is raised to a pressure of about 18 bar in a hermetically sealed reciprocating compressor after which it passes to the condenser. Ambient air forced across the condenser cooling coils reduces the refrigerant temperature causing it to condense. The refrigerant emerges as a saturated liquid (a fog) and enters the expander. This is a device comprising a length of capillary tubing which reduces the operating pressure to about 1 bar by friction encountered in the narrow bore. A partial return to the vapour state occurs accompanied by a decline in temperature. The refrigerant then enters the evaporator: the component by which heat exchange occurs. In order to rewarm, the refrigerant extracts heat from the dry air stream and evaporates back into a vapour prior to compression again.

The machine was found to be capable of cooling dry air flowing at up to 150 l/min to -28°C from an inlet temperature of 20°C.

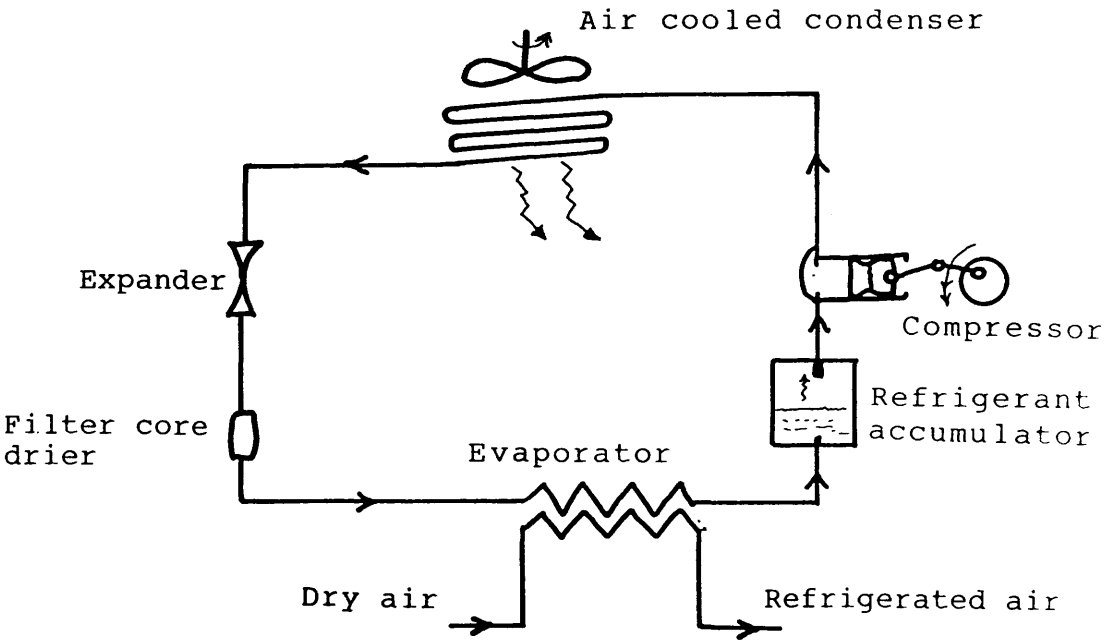

Figure 2.07: Single stage vapour compression cycle. The device was air cooled and used R502 refrigerant, similar to a domestic freezer.

2.2.4. Air delivery.

The air delivery system comprised a vacuum insulated boom to pipe the cold air to the patient and a non-rebreathing valve assembly allowing respiration off the conditioned air stream.

2.2.4i. Vacuum boom.

In order to preserve the low temperature of the exit air from the refrigerator a vacuum insulated boom was designed by the author. Figure 2.08 shows its construction which was based on an established vacuum jacket syphon tube used to transport liquid helium from storage to application, described by Rose-Innes (1973)[20]. The copper boom comprised a 1 meter length of 15mm OD thin wall tube encased in a 35mm OD pipe. Five equi-spaced square polythene spacers 2mm thick supported the inner tube and restricted conductive heat transfer by the minimal contact of each corner with the outer tube. Linkage to the cold air unit was via a turned polythene adapter. An 8mm diameter brass syphon valve located at the boom mid-section allowed connection to a vacuum source. At the delivery end of the boom the inner tube projected 80mm from the jacket.

The boom was evacuated by a 2 stage vacuum pump (Edwards 2SC20A, Notts, UK) to produce an estimated vacuum of less than 1mm Hg. Without airflow the refrigerator was allowed to cool until its thermostat switched the machine off. With the air flowrate adjusted to 120 l/min, the boom inlet and exit temperatures were then simultaneously recorded for 12 minutes by a 't' type thermocouple and the 'Microlink' data acquisition system described in section 2.3. Ambient air temperature was 23°C.

After 12 minutes the evacuated boom exit temperature was -21.5°C. Airflow was stoppped and the refrigerator allowed to run until the thermostat again switched the

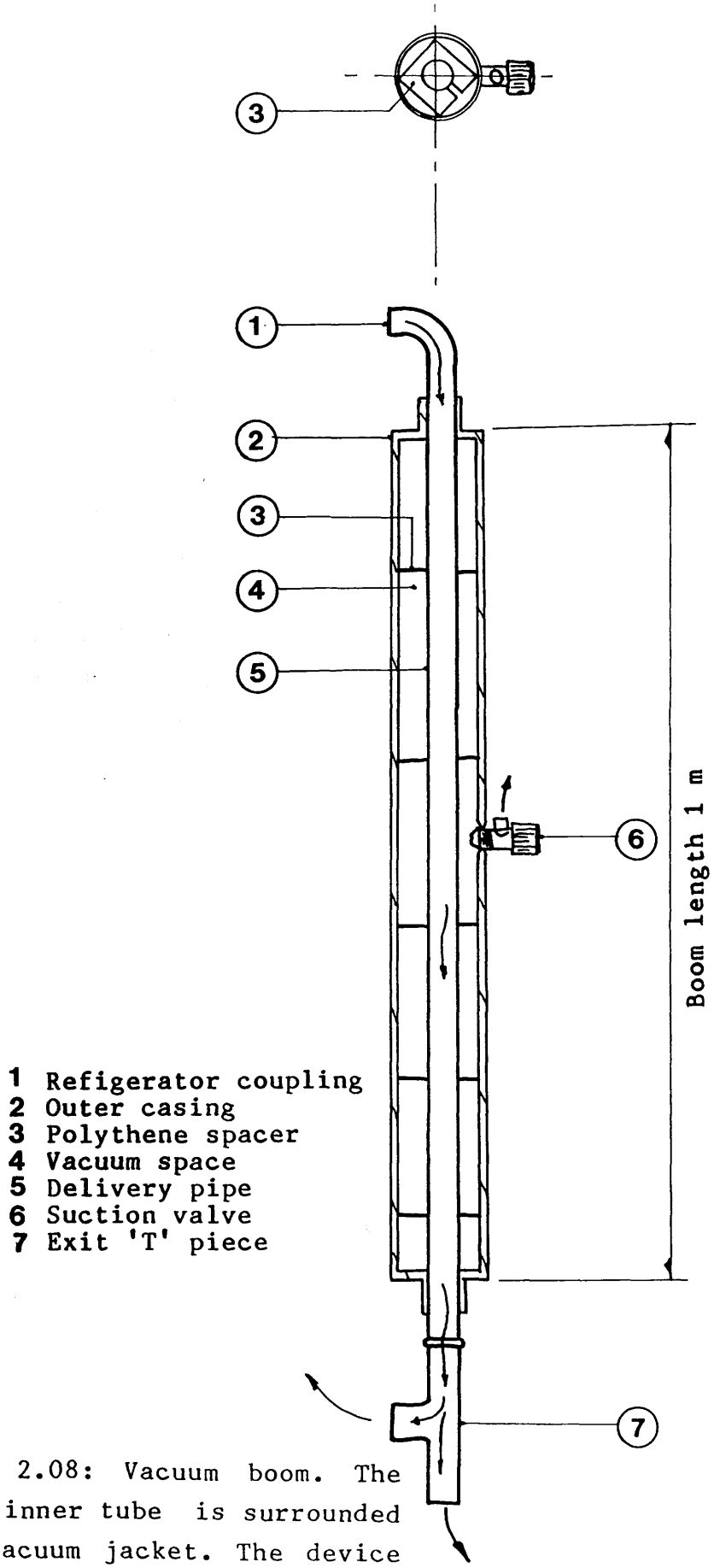

Figure 2.08: Vacuum boom. The copper inner tube is surrounded by a vacuum jacket. The device was fabricated from standard DIY plumbing fittings.

machine off. The vaccum was filled with ambient air and the test repeated. Without evacuation the boom exit temperature was -17.4°C, illustrated in figure 2.09. Both temperatures are within the range quoted by other workers and are acceptable for clinical use. The time course of the exit air temperature indicated that a five minute pre-challenge cooling period was required.

Later experience with the refigerator yielded an evacuated boom exit temperature as low as -28°C, achieved by overiding the thermostat. This practice was not adopted as it tended to result in earlier icing of the evaporator coil and appeared effective during the winter months when cold air was least required.

2.2.4ii. Non-rebreathing valve assembly.

To allow the patient to breathe off the conditioned air stream a standard non-rebreathing valve, (Gas Messung, Dortmund, West Germany, type 72), was connected via its inspiratory port to a plastic 't' piece located at the delivery end of the boom. As the patient inspired so the inspiratory port opened to the cold air stream. Expired air was vented through a second port to air temperature and air flowrate measuring instruments. The original valve is sketched in figure 2.10 and was determined, by filling with water, to have a dead space volume of 46 ml common to inspired and expired air.

Accurate measurement of expired air temperature is crucial in determining respiratory heat exchange rate (section 1.3) and it became apparent that this dead space volume should be minimal. Modifications to this component are described in succession to the clinical tests performed with the cold air system.

Figure 2.09: Vacuum boom evaluation. A 5 minute pretest cooling period was apparent

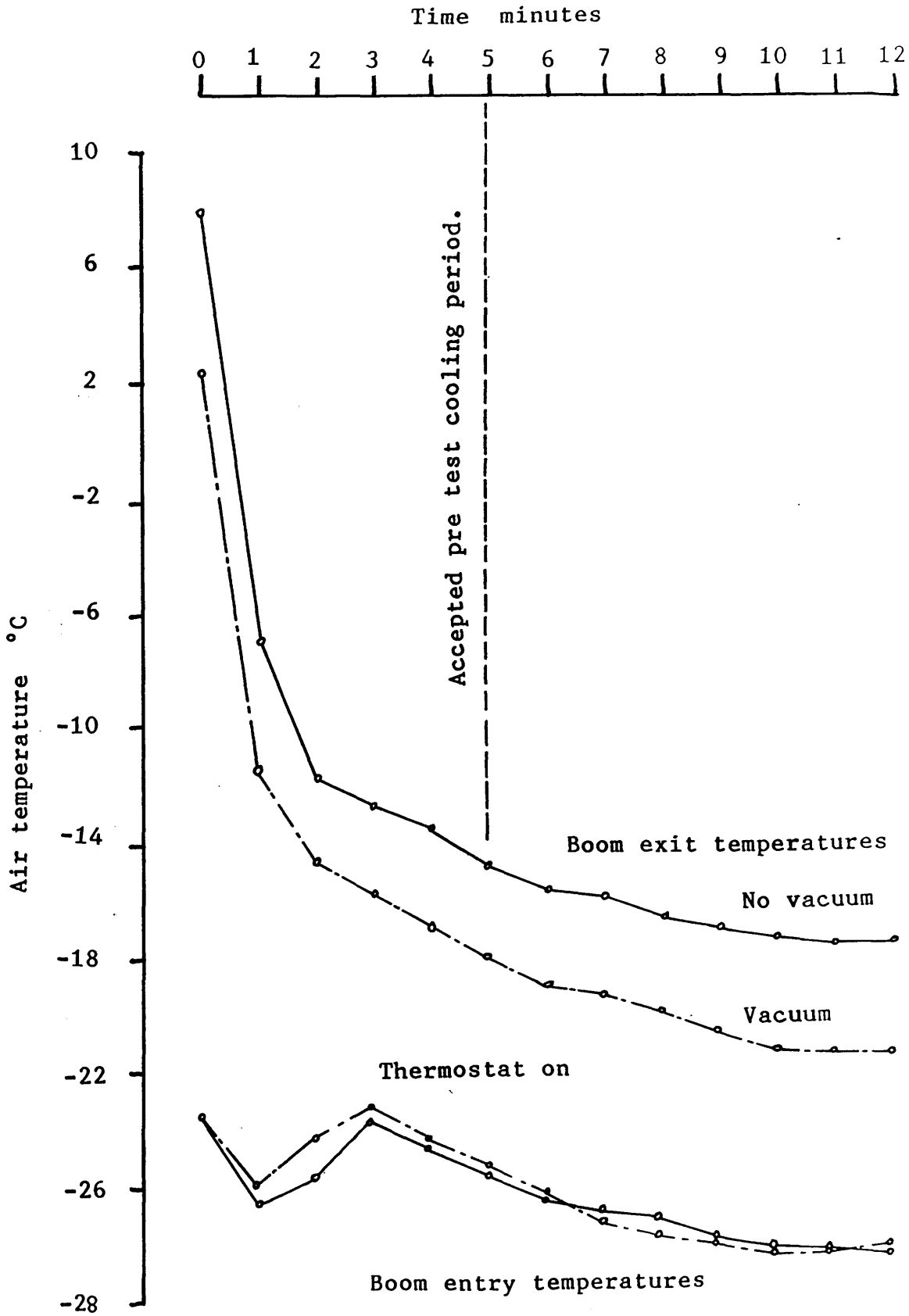

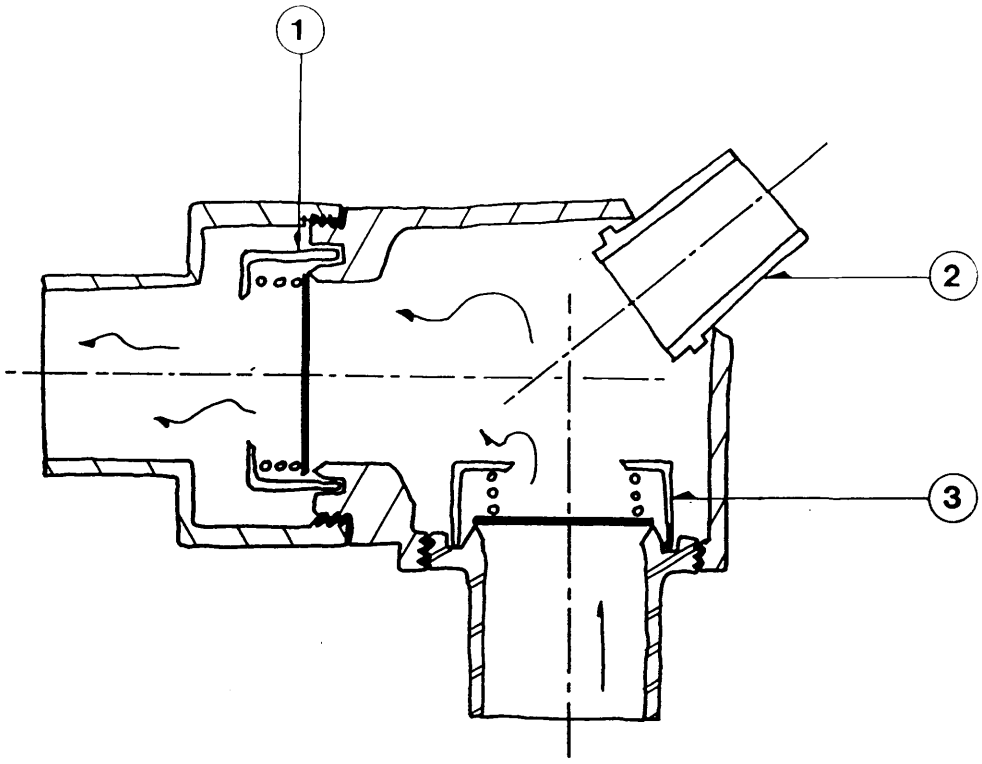

Gas Messung Type 72 Non Rebreathing valve (Full Scale)
Dead space volume enclosed between valves: 46 ml

1 Expiratory leaflet valve
2 Mouthpiece adaptor
3 Inspiratory leaflet valve

Figure 2.10: Non rebreathing valve, cast perspex. The disc leaflets are cut from a mica wafer.

2.3. Data acquisition hardware.

Software described in section 2.3.2. was written to capture, process, display and retain the real time per breath values of respiratory heat exchange rate during a thermal burden. Necessary for this was knowledge of the inspiration and expiration air condition and the mass flow of air respired described in section 1.2. The data acquisition hardware and transducers used to obtain this information are described.

2.3.1. Microcomputer interfacing.

A 'Microlink' data acquisition unit purchased from Biodata Ltd (Birmingham, UK 1986) was used to select and sample voltage outputs from the devices measuring air temperature and air flowrate. The 'Microlink' consisted of eight rack mounted modules. These were: a $\pm$15V +5V power supply unit; a controller multiplexer; a 12 bit analogue to digital converter (A-12D); four selectable gain analogue inputs (AN-1) and a thermocouple amplifier (TC-16) which provided for 10 independent thermocouple inputs. The 'Microlink' was interfaced with an Apricot 1200ap xi microcomputer (768k) via an IEEE488 communications card slotted into one of the microcomputer's internal expansion ports. An assembly language command routine, (supplied by Biodata Ltd), enabled access to the various 'Microlink' facilities from data aquisition and processing software written by the author in MSBASIC.

This data acquisition system was used throughout the present work.

2.3.2. Temperature measurement.

A 't' type thermocouple (RS Ltd, copper - copper/nickel BS4937) having a measuring range of of -200°C to +200°C and an output of 42 uV/°C was chosen for the present application. It was used with the thermocouple amplifier TC-16, described in section 2.3.1. which was also supplied with a platinum resistance wire cold junction reference (Biodata, RTD) housed in a foam insulated box. Output voltage from the thermocouple amplifier was sampled by the microcomputer via the 'Microlink' and converted into its celsius temperature value using an algebraic formula quoted by the manufacturer (Lines 750-830 of appendix 2).

Step response time of the thermocouple was determined by exposure to a water plunge test using the apparatus illustrated in figure 2.11. The thermocouple was taped to a connecting rod which projected 15 mm below a piston and the apparatus was clamped such that the thermocouple junction lay 1mm above the surface of a water bath. At bottom dead centre the thermocouple would just penetrate this surface. A 31g bolt, (weighed with a Mettler P-1200 balance), was dropped from a height of 140mm onto the piston crown (weight 5.5g) which, on impact, plunged the thermocouple into the water. From calculations based on the principle of conservation of momentum the step period was estimated to be 0.5mSec, detailed in appendix 1. Tepid and cold tap water was used to generate a 10°C step rise and a 7°C step fall in temperature respectively both of which were repeated three times. The 'Microlink' data acquisition system described in section 2.3.1 measured the temperature of the thermocouple every 25mSec (40Hz). Software written in MSBASIC continuously recorded these samples over a 10 second period during which the step occurred and a listing is given in appendix 2.

Figure 2.12 illustrates the typical step rise and step fall characteristics found. Target temperature was

Figure 2.11: Step test evaluation of the 'T' type thermocouple. The cylinder and piston were formed from a syringe.

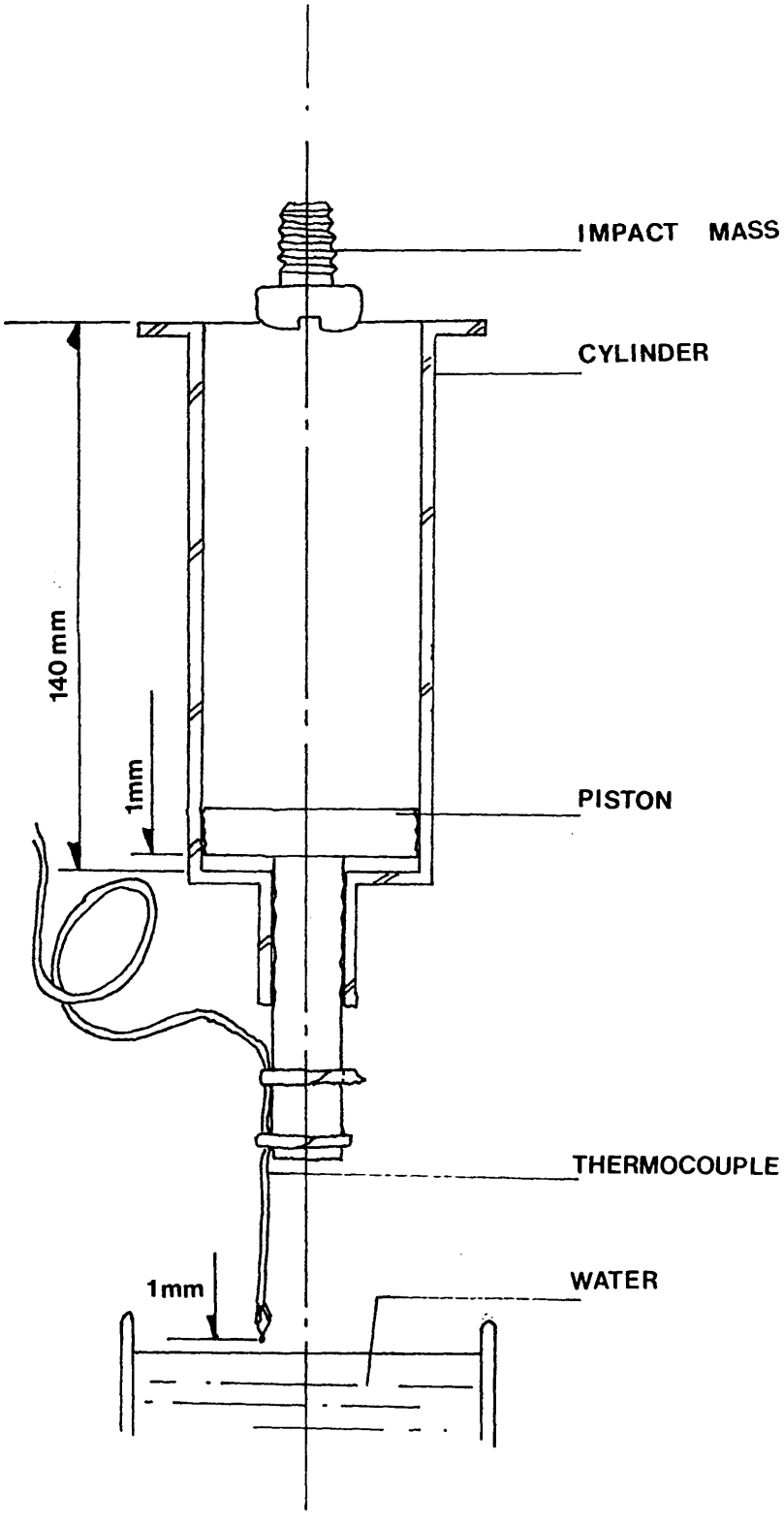

Figure 2.12: Response time characteristic of the thermocouple. A 100% response was obtained within 50 msec.

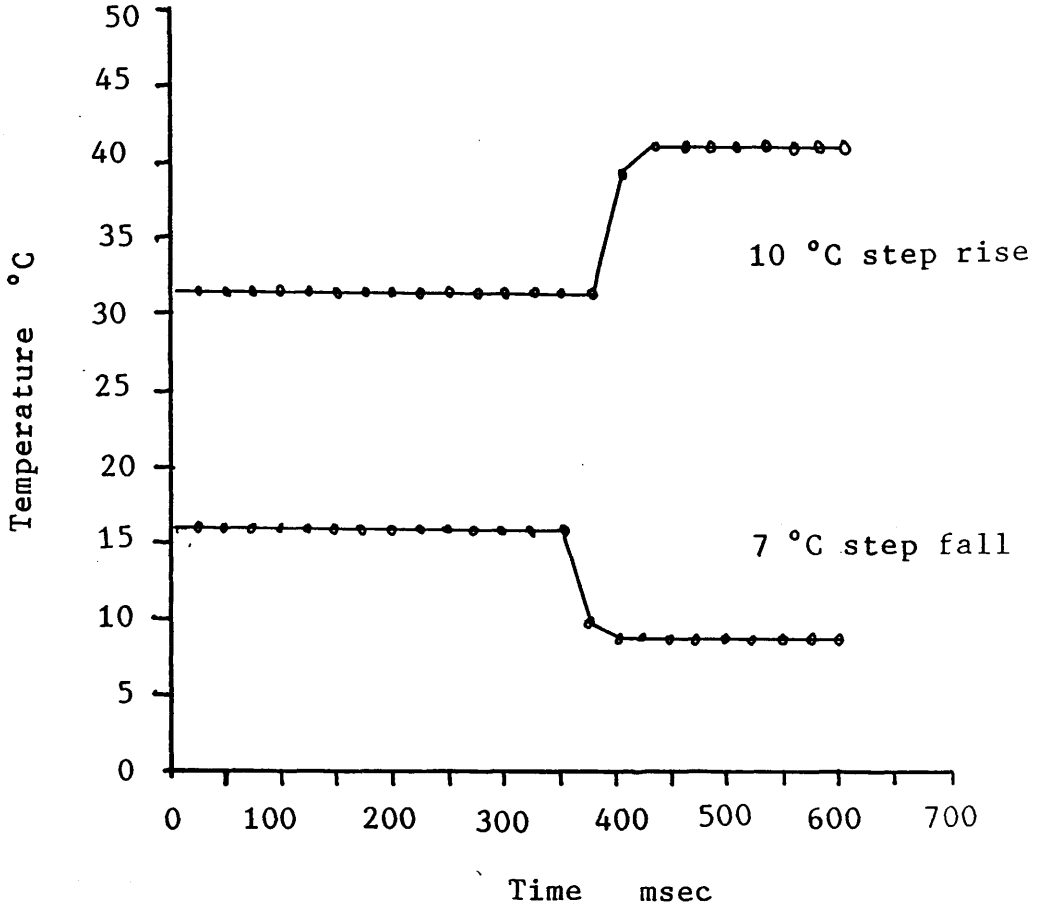

evaluated by measuring that prevalent during the last five seconds of the test. The step period was determined by noting the sampling cycle when temperature rise began and the cycle when the target was achieved. Full response was obtained in both tests within two sample cycles (50mSec), that achieved after 25mSec being 90% of target for the 7°C step fall and 82% of target for the 10°C step rise.

A typical expiration period of 2.5-3 s during tidal breathing can be expected compared to approximately 1 s during exercise. Moreover the air in the expiratory port of the non-rebreathing valve does not experience the large inspiration-expiration swing in temperature expected in the dead space volume. On this basis the response time of the thermocouple was considered suitable for use down stream of the expiratory port.

2.3.3. Airflow measurement.

A pneumotachograph flowhead (F300L) and electrospirometer (CS5) supplied by Mercury Instruments (East Kilbride, UK) were used to determine airflow rate in the range 0-300 l/min and tidal volume in the range 0-3 l. The electrospirometer gave a 0-1V output suitable for remote sensing using the 'Microlink'.

The device operates as follows. A gauze diaphragm located at the mid-section of the flowhead impedes respired airflow causing a slight pressure differential between inlet and outlet. A pressure tapping at each side of the gauze feeds into the electrospirometer. The pressure difference between the tappings is detected by an optical transducer wherein a hermetically sealed reflective foil disc, (each surface of which is exposed to one of the tappings), becomes deformed. Variations in the intensity of light scattered from the foil are directly proportional to the airflow rate through the pneumotachograph.

Early experience with the flowhead highlighted a tendency

of the gauze to block with expired water causing instability and overestimates of airflow rate, especially during cold air hyperventilation when condensation readily occurred. To prevent this a 6 Watt heating element (Fleisch 2395, GDR), cannibalised from a broken pneumotachograph, was attached upstream of the present flowhead and thermal contact between the two enhanced using a heat sink compound. This led to a flowhead casing temperature of 60°C and the modification is illustrated in figure 2.13.

Figure 2.14 illustrates the experimental means by which the performance of the heated flowhead was assessed. Ambient air was conditioned to 85%RH 40°C by bubbling it through a 5 litre bath of hot water at 15 l/min. Periodic measurement of airflow rate using the data acquisition system (section 2.3.1) was made over a 15 minute exposure. The heated flowhead yielded a consistently stable output whereas the unheated version became unstable after about 5 minutes, illustrated in figure 2.15.

Calibration of the electrospirometer was done using the apparatus schematically shown in figure 2.16. Connected to the flowhead was an independently calibrated 0-200 l/min rotameter (Rotameter Manufg. Co. Croyden, UK, Series 1000) which was used as the standard for airflow rate measurement. Compressed air in the ranges 0-100 l/min and 0-200 l/min was directed through the system, these rates corresponding to the selectable sensitivity of the electrospirometer. Output from the amplifier was digitised and stored using the data acquisition system described previously and is plotted in figure 2.17 against the calibration air flowrate. For both range settings the electrospirometer gave a linear electrical output with analogue to digital conversion number (AtoD) and the transfer coefficients were found from a regression test to be:

Figure 2.13: Mercury flowhead and Fliesch pneumotach heater. The heat sink compound ensured good thermal contact.

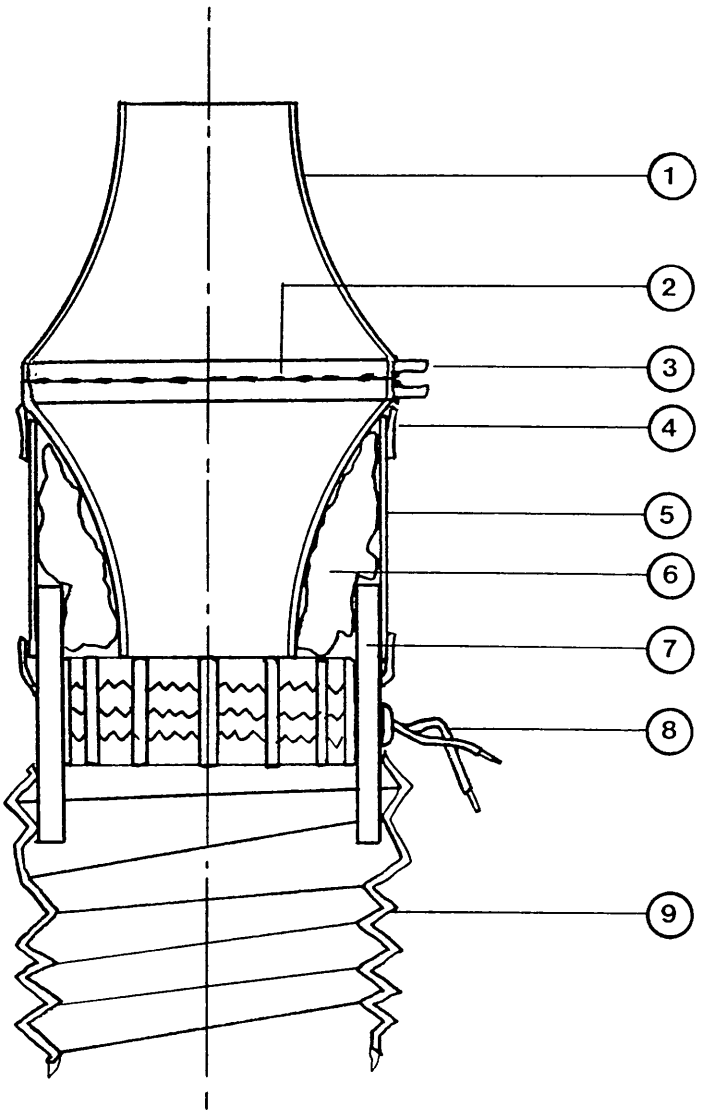

1 F300L Flowhead casing
2 Diaphram
3 Pressure tapping
4 Tape binding
5 Flowhead - heater coupling
6 Heat sink compound
7 Heater
8 Power cable
9 Inlet hose

0.24096 l/min per AtoD ..... 0-100 l/min range, r=0.99; 0.7% error at full scale deflection
0.80000 l/min per AtoD ..... 0-300 l/min range, r=0.99; 2.8% error at full scale deflection

2.4. Software.

Access to the 'Microlink' unit was set up via the assembly language programme 'ULINKB' (Biodata Ltd) entered at the operating system level.

Control of the 'Microlink' unit, data processing, display and storage was done using software written by the author in interpreted MSBASIC. Although slower than compiled programming langauges, (FORTRAN-77, TURBO PASCAL and 'C'), MSBASIC was immediately available for use with the 'Microlink'. It executed with sufficient speed (25 Hz) to enable representative sample collection for real time display of the per breath RHE. Figure 2.18 illustrates the four sequential features of the programme developed for use with the cold air system. These were: user interaction; trigger; main data collection and algebraic processing. A full software listing is given in appendix 3 which is referred to (line numbers) in the following.

2.4.1. User interaction.

The cold air system MSBASIC programme 'RHE5' opened with a request for initial conditions of the experiment including a choice regarding cold or ambient air inhalation (lines 130-330). Figure 2.19 illustrates this initialisation. If cold air was selected then the inspiratory air temperature was recorded by means of the thermocouple located at the inspiratory port of the non-rebreathing valve (section 2.2.4ii) and the associated water content later evaluated based on full saturation.

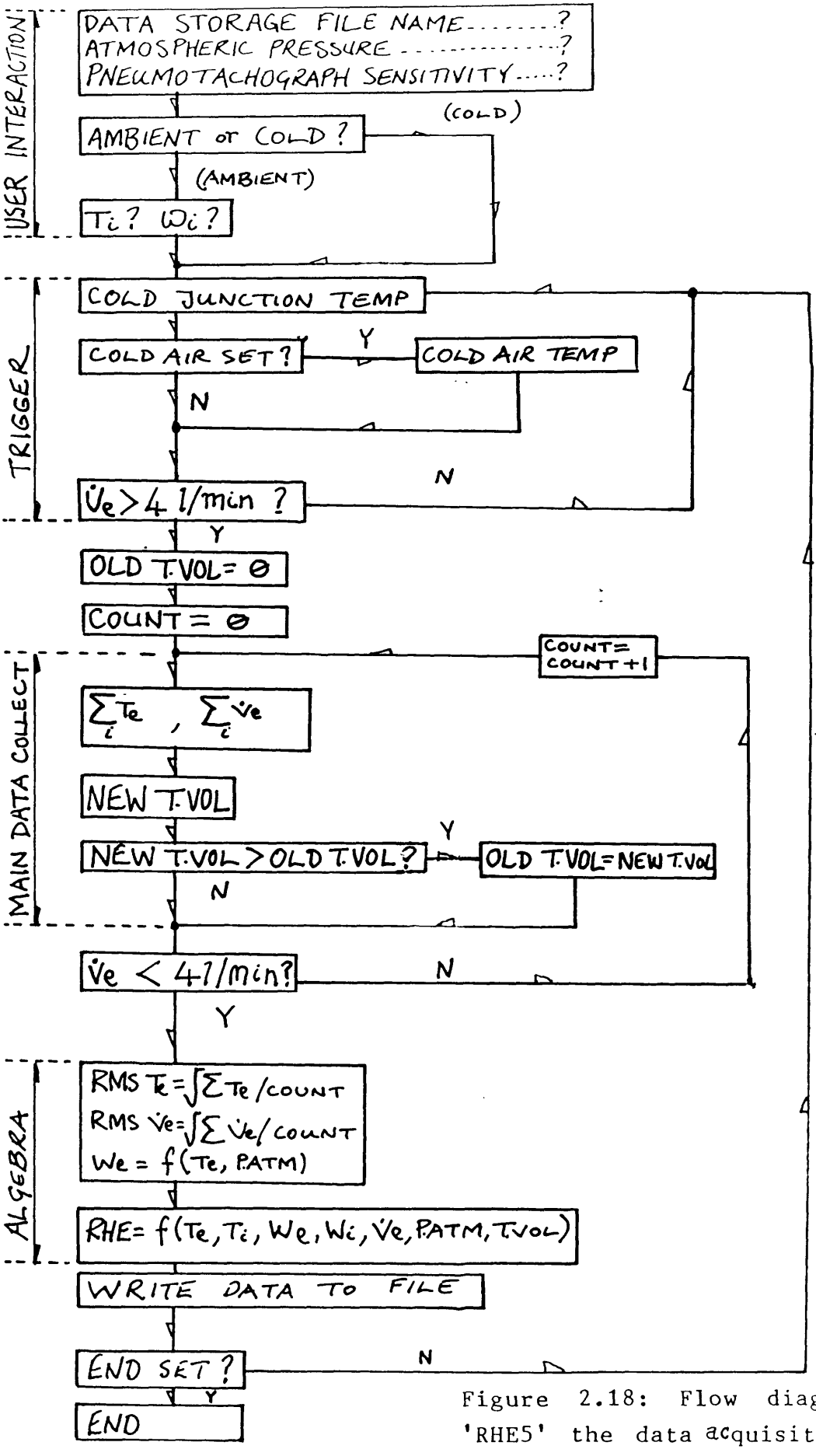

Figure 2.18: Flow diagram of 'RHE5' the data acquisition and processing software developed for the cold air facility.

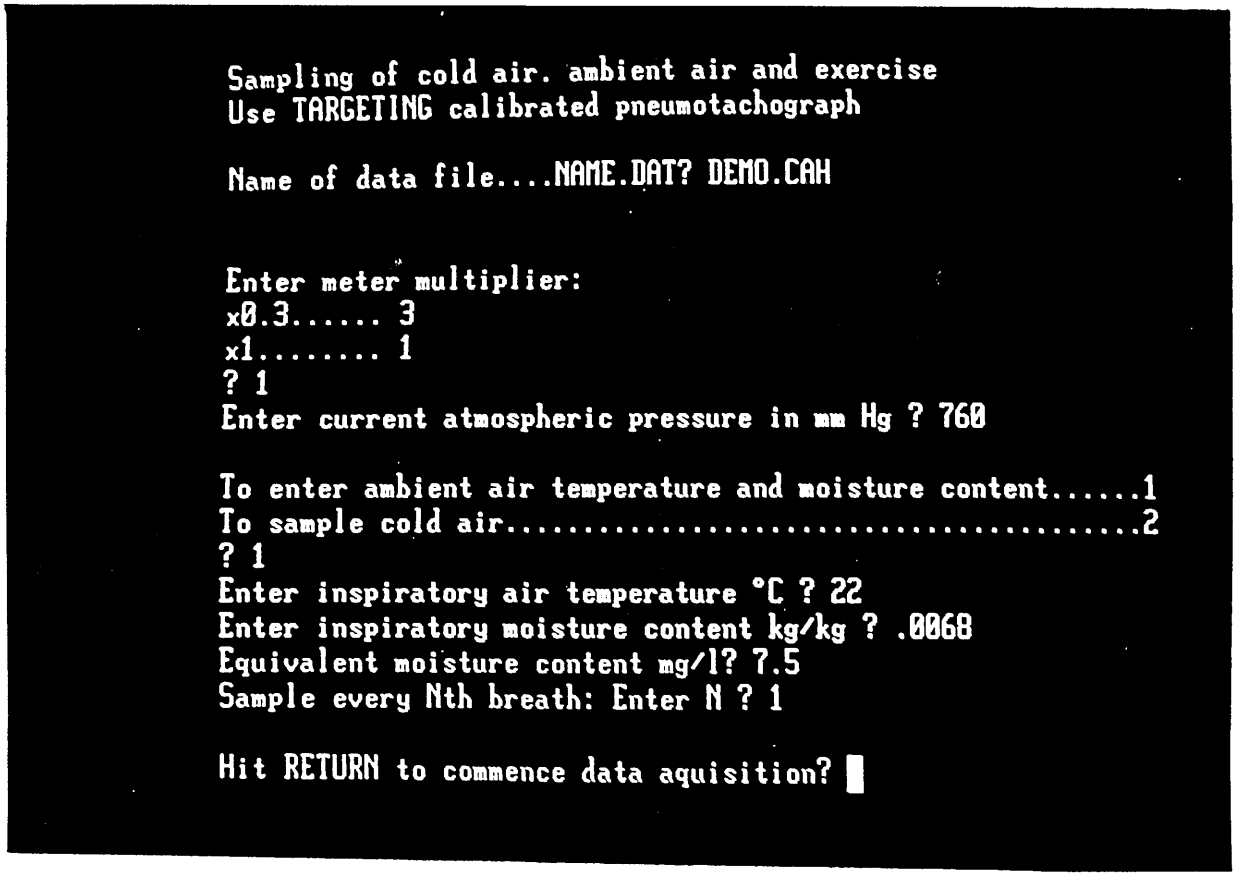

Figure 2.19 Initial prompts for data collection. The user enters a filename for data storage and the inspiration air conditions.

2.4.2. Trigger.

Data acquisition commenced during the expiratory phase. The instantaneous air flowrate threshold for this was set at 4 l/min which in the range of normal tidal airflow corresponded to an ommission of about 5% of the expiration period (section 2.4.3). During the sub threshold 'wait' stage continuous monitoring of the thermocouple cold junction reference temperature, expiratory air flowrate and, if necessary, inspiratory cold air temperature were made (lines 600-800).

2.4.3. Main data collection.

Expiratory airflow in excess of 4 l/min started the data acquisition phase from which the subsequent real time calculations were made. Temperature, tidal volume and ventilation rate of expired air were sampled at 20 Hz (lines 910-1060).

Air temperature rises throughout part of the expiratory phase and air flowrate also varies throughout expiration. The Root Mean Square (RMS) values of both temperature and air flowrate were derived after each expiration as these represented the constant value equivalent to the sample spectra encountered. The RMS was obtained by integration of all expired air sample values and is formally defined as:

$$X_{RMS} = \sqrt{\sum (x_i)^2 / n}$$

Each digital value read from the analogue to digital (AtoD) converter was squared and added to the last (lines 1030-1040). A count was kept of the number of data acquisition cycles made during an expiration (line 1020). Immediately after end expiration the sum of squares was divided by the count value, the square root being the RMS of the sampled signal.

The variation in expiratory air flowrate and air temperature during tidal breathing of ambient air (20 °C) is illustrated in figure 2.20. This was obtained by inserting a thermocouple directly into the mouth, inspiring nasally and expiring orally through the pneumotachograph. Data collection was by the 'Microlink' unit, described in section 2.3.1. at a rate of 25Hz. The RMS expiratory air flowrate and air temperature were derived using the equation in the foregoing, using a Minitab statistics programme. RMS airflow was found to be approximately 2/3 that of peak airflow. Values of air flow greater than the RMS pertained for approximately 50% of the expiratory phase and airflow rates within 90% of the peak pertained for about 20% of the expiratory phase. The period over which RMS air temperature was derived was defined by the ventilation trigger. A slight temperature lag with ventilation was observed; discussed in section 6.4. The RMS air temperature corresponded to approximately 3/4 of peak temperature and values greater than the RMS were prevalent over 60% of the expiration phase. During exercise involving vigorous treadmill running peak expiratory air flowrates of 200 l/min were found with a corresponding RMS airflow of 120 l/min.

Tidal volume was found by detecting the maximum tidal volume signal from the electrospirometer (line 1050) during the data collection phase.

2.4.4 Data processing.

Transformation of the RMS AtoD value of expired air temperature into its celsius equivalent was performed using an algorithm supplied by Biodata Ltd (line 1130-1190). RMS air flowrate was obtained by multiplication of the AtoD value with the relevant scaler described in section 2.3.3. Expired water content was derived on the assumption of full saturation (lines 1900-1920). This was performed using a

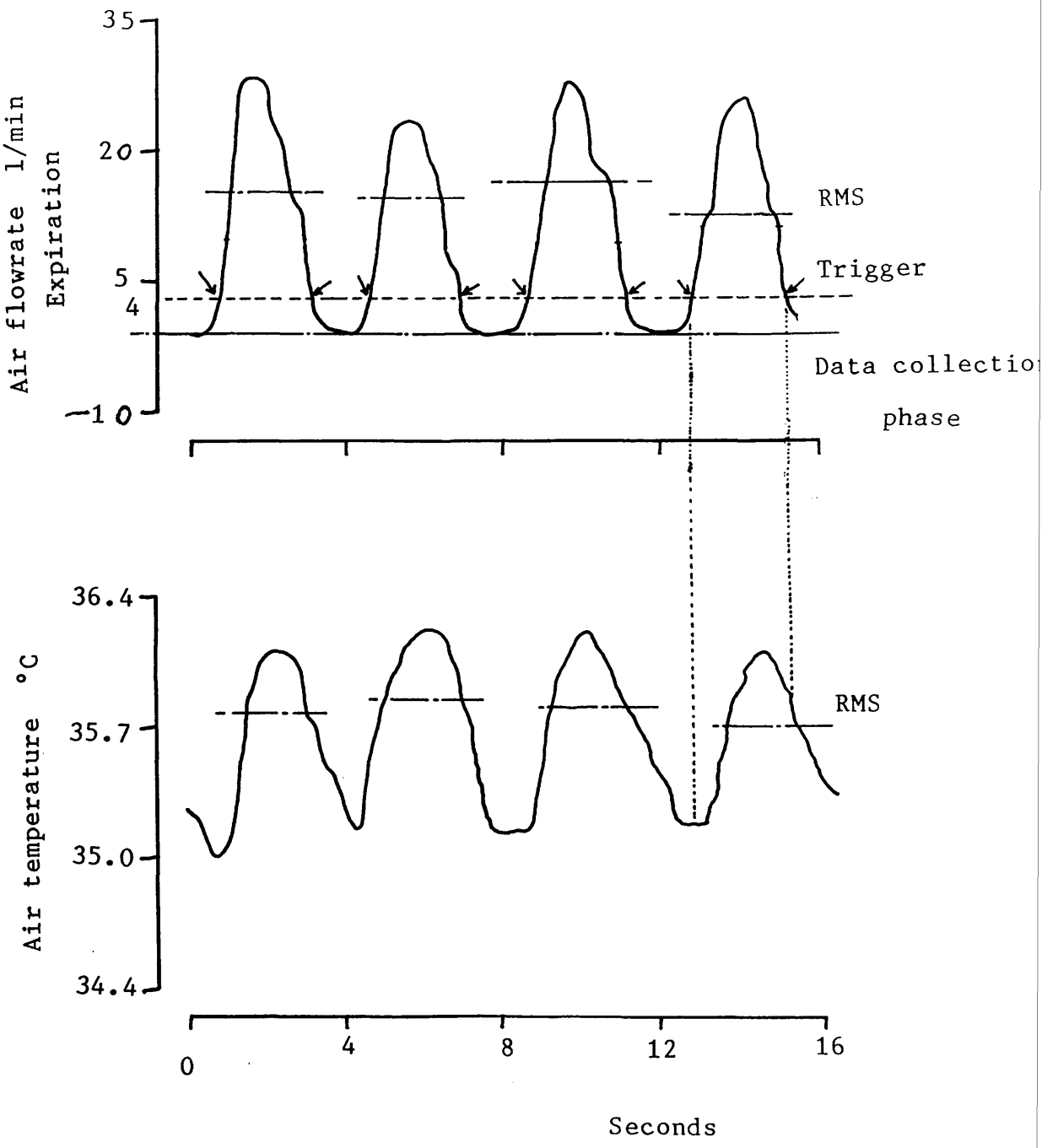

Figure 2.20: Typical tracings of expiratory air temperature and flowrate obtained using the 'Microlink' for tidal breathing.

psychrometric relation for the partial pressure of water vapour in air (Gardner 1972)[21]:

$$P_w = 6.108 \cdot \exp(A \cdot T_w/(T_w-B)$$

where: P_w vapour pressure mb
T_w Air temperature °C
A = 17.269388 and B = 237.3

The actual full saturation water vapour content is given by:

$$W_{act} = 0.622 \cdot P_w/(P_{atm}-P_w)$$

where: W_{act} Water vapour content kg_{water}/kg_{air}
P_{atm} Atmospheric pressure mb

Appendix 4 gives a graph of the actual full saturation water content over -20 to 40 °C air temperature range and the predicted water content using the Gardner formula. An error of less than 0.5% between predicted and actual values was found.

The per breath respiratory heat exchange rate (RHER) was computed on the basis of equation 3, given in section 1.1.2 (lines 1500-1915) and requires knowledge of ventilation rate; air temperature; water vapour content; the latent heat of water (h_{fg}) and the specific heat of air (C_{pa}). The software contained algorithms for the interpolation of h_{fg} and C_{pa} which were derived from thermodynamic tables and are given in appendix 5. An error of less than 1% of actual values pertained for these algorithms.

During inspiration all the measured and derived values were written to a disc file and displayed in real time, shown in figure 2.21. After the challenge data were

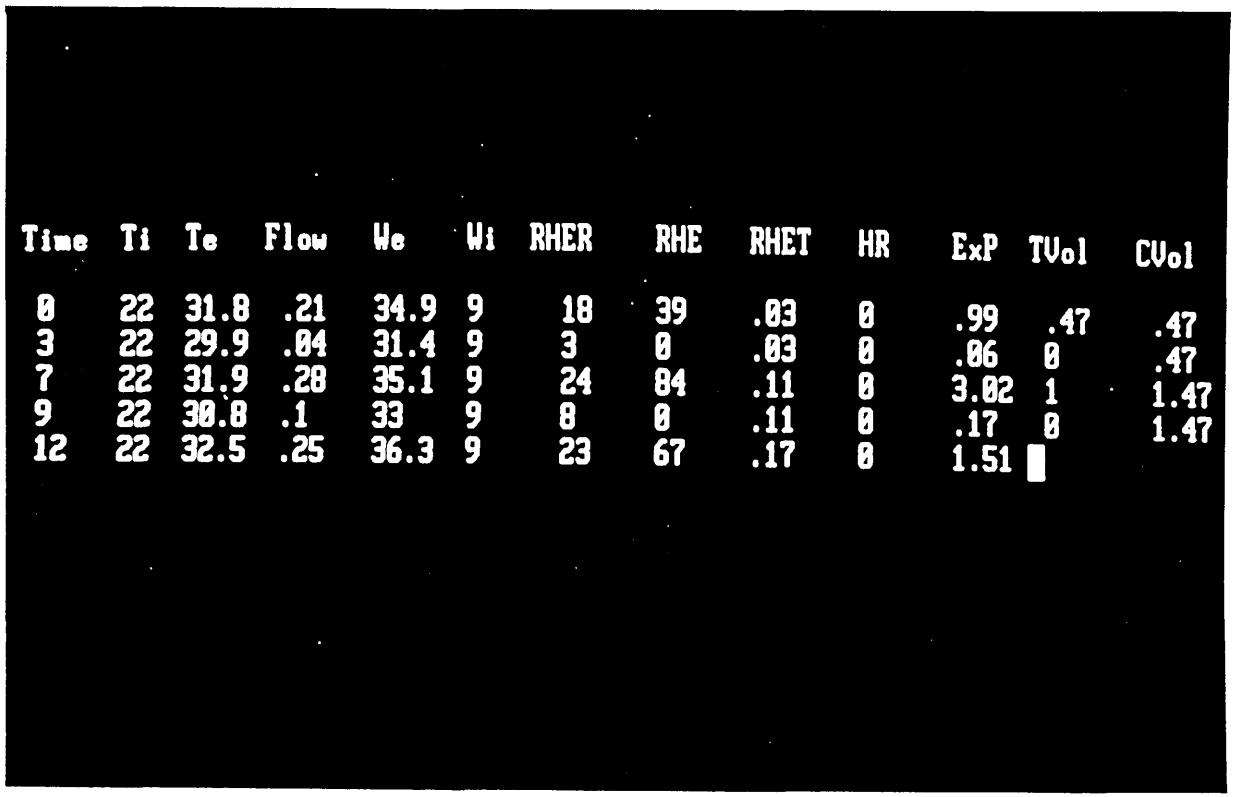

Time	Ti	Te	Flow	We	Wi	RHER	RHE	RHET	HR	ExP	TVol	CVol
0	22	31.8	.21	34.9	9	18	39	.03	0	.99	.47	.47
3	22	29.9	.04	31.4	9	3	0	.03	0	.06	0	.47
7	22	31.9	.28	35.1	9	24	84	.11	0	3.02	1	1.47
9	22	30.8	.1	33	9	8	0	.11	0	.17	0	1.47
12	22	32.5	.25	36.3	9	23	67	.17	0	1.51		

Figure 2.21: Real time output from the RHE5 software. The rate of respiratory heat loss and associated parameters are displayed during inspiration.

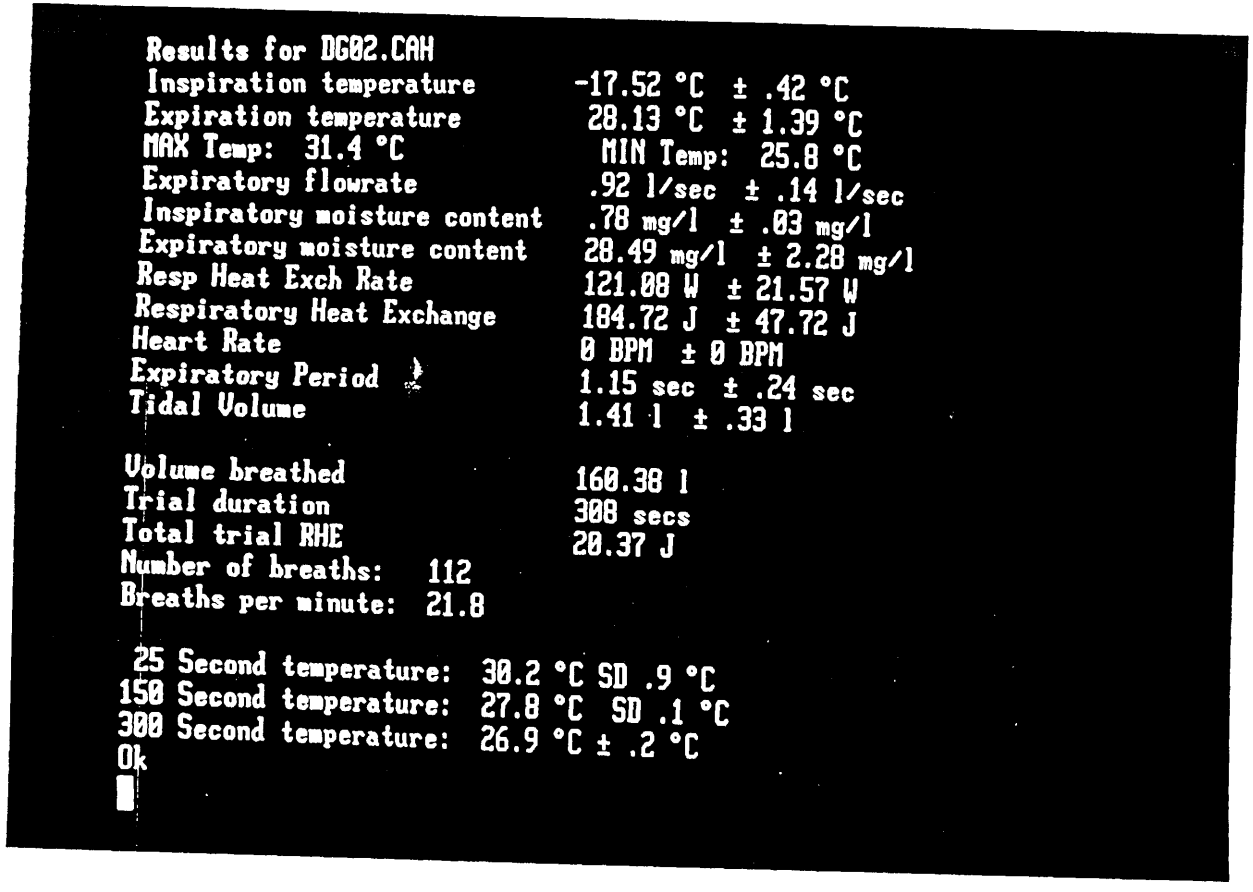

Figure 2.22: Data summary. This provided a means of tabulating heat loss parameters for a group.

summarised and displayed or printed, for later analysis, shown in figure 2.22.

2.5. Overview.

The system described generates a cold air thermal burden and simultaneously evaluates the airway respiratory heat exchange rate in the clinical environment. It is illustrated in figure 2.23 for use in conjuction with a treadmill test. The modular nature of the device allows the data aquisition system to be used in unrelated experiments. A source of dried ambient air is also available either by reheating at the refigerator outlet or by using directly the charge from the air drying unit. Experiments relating to this are included in a pilot study of respiratory heat exchange rate in asthmatics, presented in the next chapter.

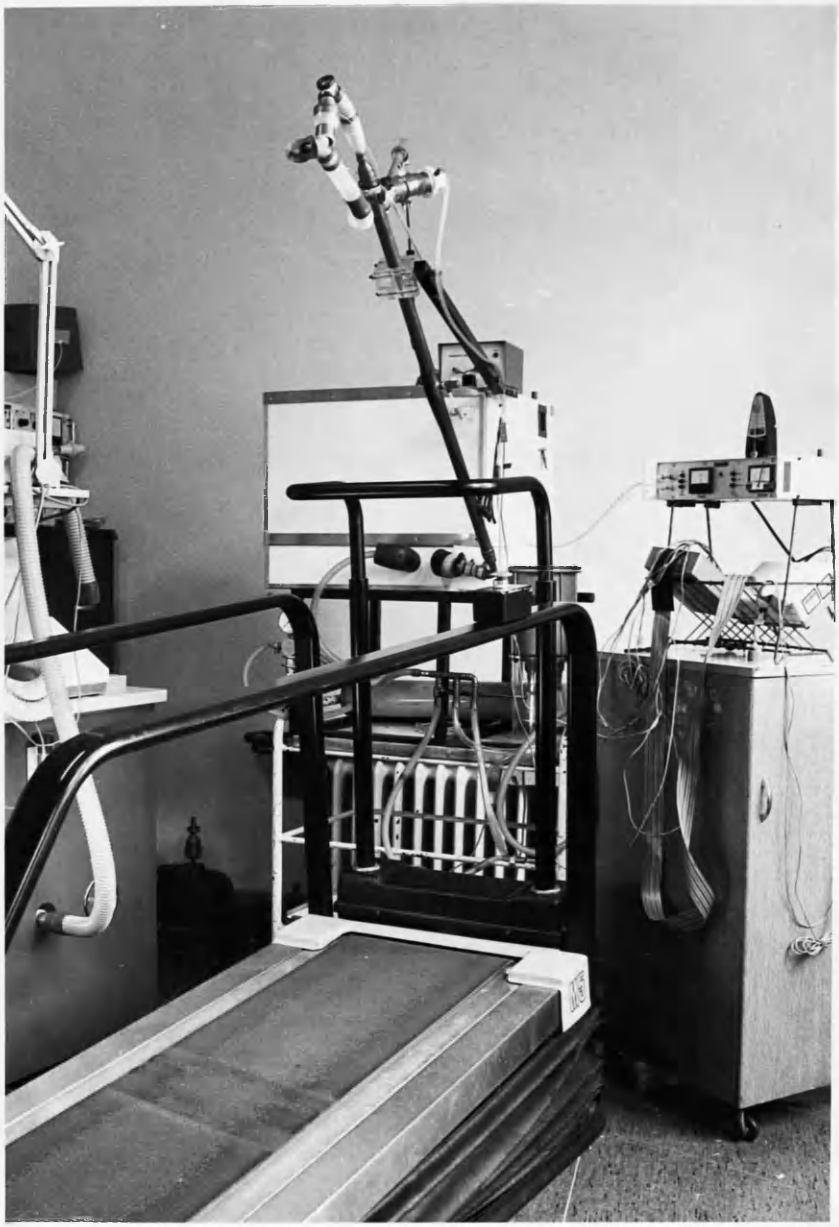

Figure 2.23: The pumped cold air unit set up for use with a treadmill exercise challenge.

Figure 2.14: Flowhead evaluation. Air from the water bath emerges fully saturated.

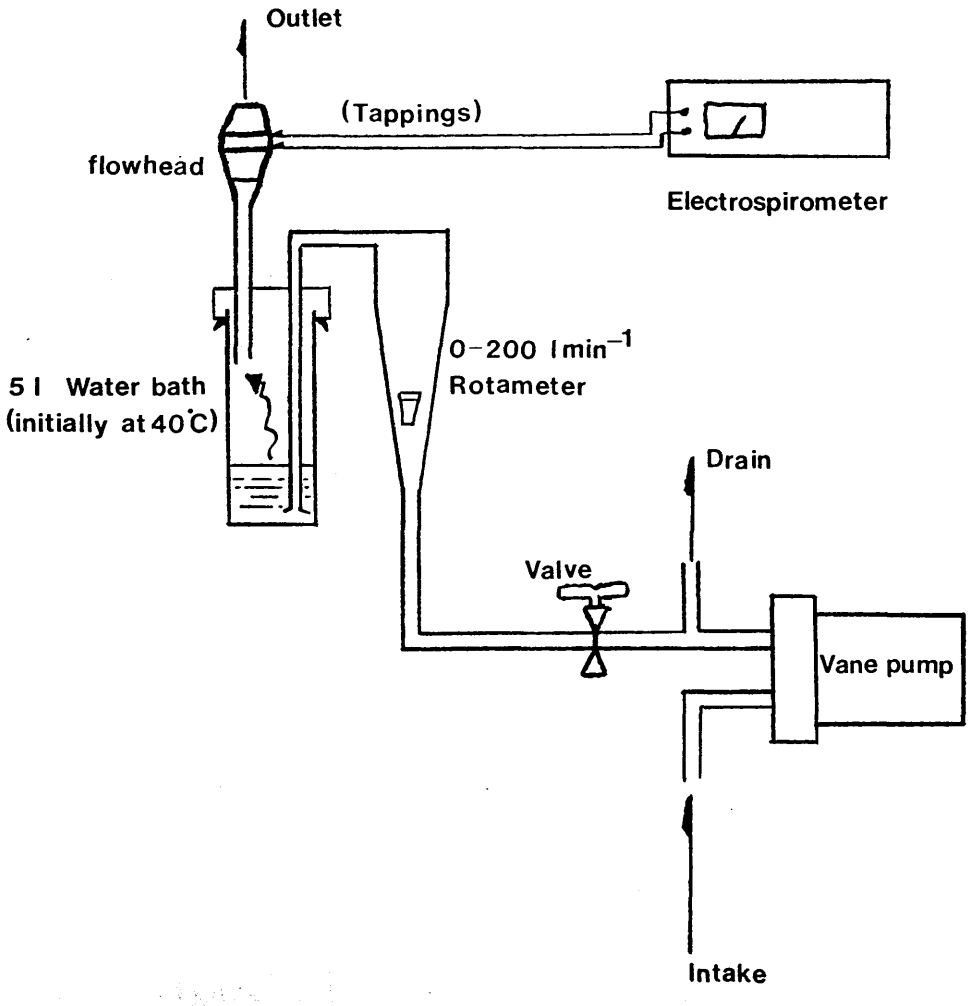

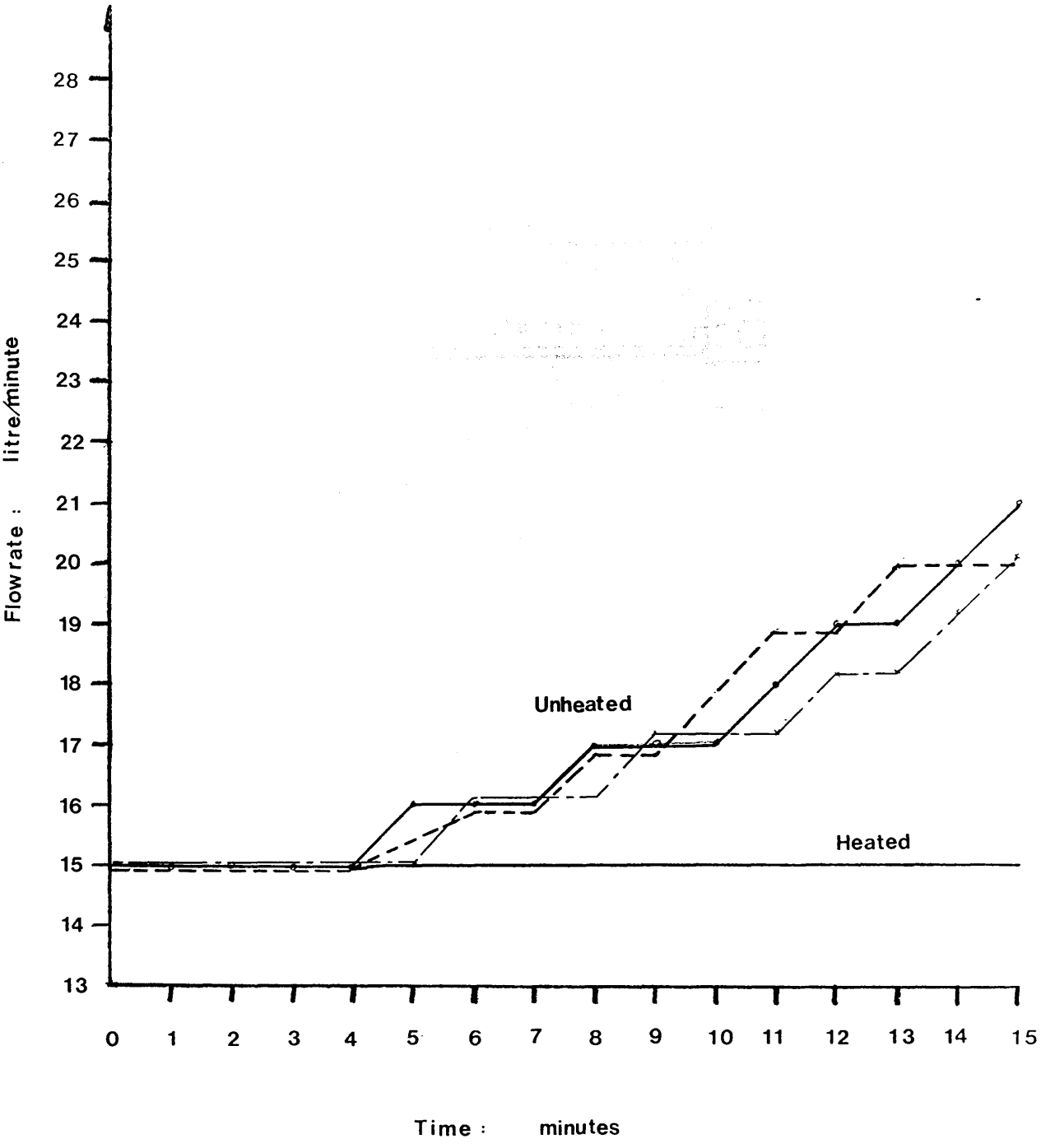

Figure 2.15: Effect on a heated and an unheated pneunmotach. Condensate formation on the unheated diaphragm causes blockage of the pressure tappings and an unstable output.

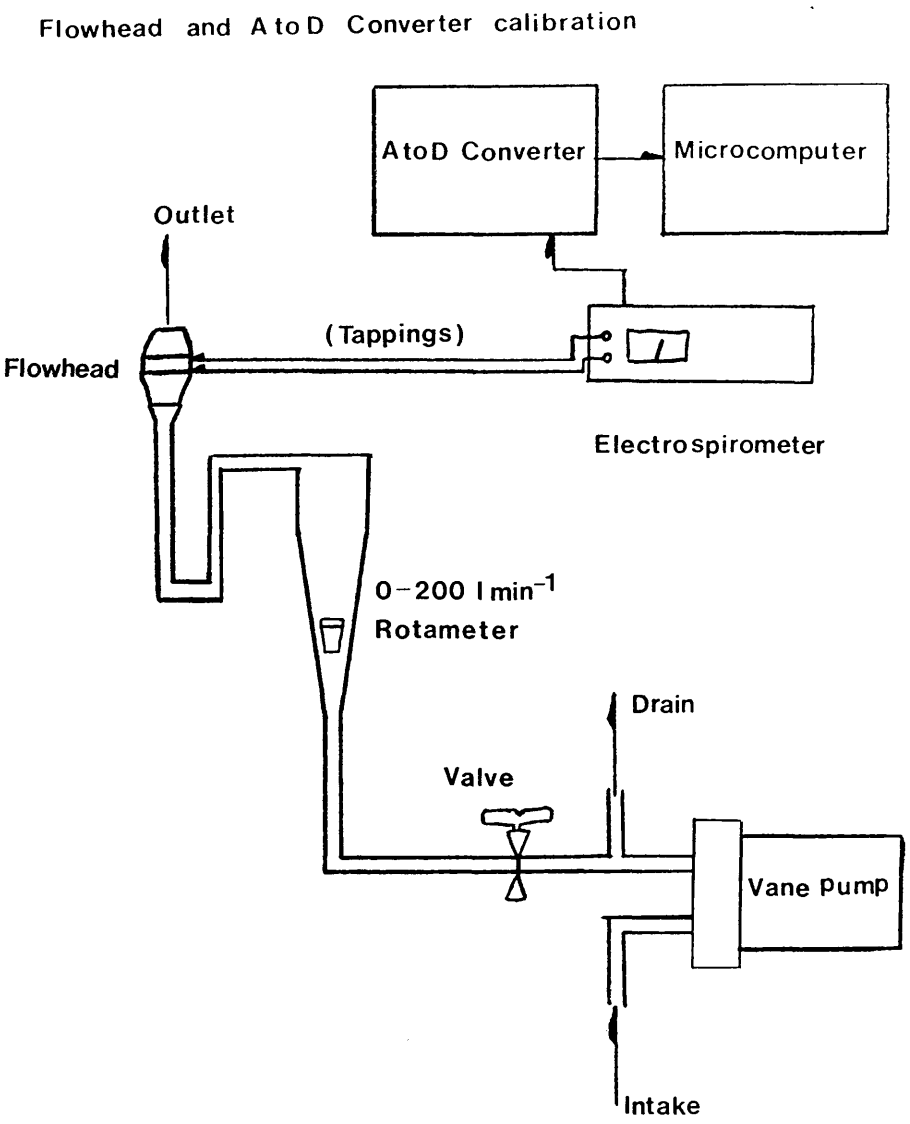

Figure 2.16: Calibration method of pneumotachograph using an independently calibrated rotameter.

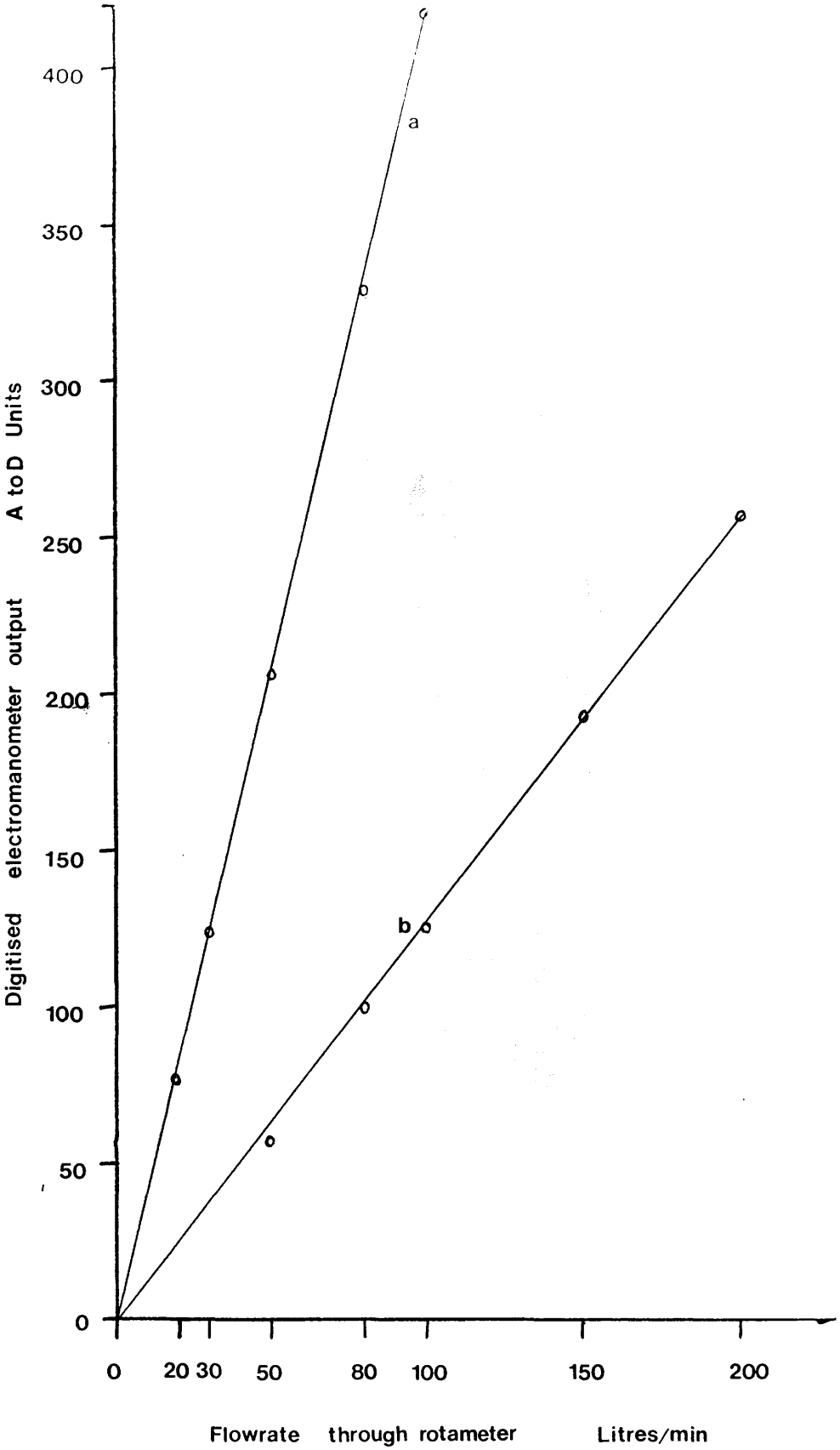

Figure 2.17: Calibration line for pneumotachograph at high and low sensitivity.

3. Hyperventilation induced asthma and respiratory heat loss

3.1. Introduction.

Studies into exercise induced asthma (EIA) have led to interest in the roles of airway drying and cooling as mechanisms of bronchoconstriction. The hypothesis for a heat loss role in EIA is supported by the findings of Weinstein et al (1976)[22] who reported different asthmogenicity between swimming and running exercise challenges. Swimming was found to cause minimal or a complete absence of bronchoconstriction. Chen and Horton (1977)[23] also observed a protective effect of humid air from EIA. Bar-Or et al (1977)[24], found little or no airway dysfunction after exercise with warm humid air but typical EIA with dry air. In each of the experiments the protective effect of the moist inspirate was associated with its attenuation of respiratory heat exchange.

Millar et al (1965)[15] demonstrated a fall in FEV_1 of 20% from the rest state in asthmatic subjects exposed to a -20°C environment for 7 minutes. Strauss et al (1977)[17] enhanced EIA by cold air inhalation and Deal et al (1979)[18] proposed cooling of the airway mucosa as the predominant stimulus to EIA. McFadden et al (1982)[25] have measured air temperatures at the third generation airways of 25°C and suggested that airway cooling herein may stimmulate thermoceptors as part of the initial sequence of events leading to EIA. The autonomic pathway by which sensitisation arose was not alluded to. Airway cooling via the hyperventilation encountered with exercise was proposed as the most important stimulus to EIA and differences in asthmogenicity to various levels of exercise were attributed to the imposed heat loss. The protective effect of humid air inhalation was associated with a reduction in

the latent heat of vapourisation from the airway mucosa.

The graded airway response to severity of exercise has been identified by Silverman & Anderson (1972)[26], illustrated in figure 3.01. Anderson (1984)[27] has proposed that airway drying is the predominant stimulus in EIA by causing a transient increase in the osmolarity of the airway epithelium. It was calculated that ambient air hyperventilation required a greater mass of water to humidify the inspirate than was available from a stationary boundary of water 1-20um thick such as that lining the airway to the 7th generation bronchi. Hahn et al (1984)[28] exercised subjects breathing air at different temperatures and matched water vapour content. No significant variation in the airway response which followed was reported despite differences in the imposed airway cooling stress.

Hyperventilation has therefore been suggested as a model of airway heat loss during exercise. Inhalation of various grades of air between cold-dry and warm-humid air during exercise appears to elicit airway responses ranging from severe to mild. If heat loss is important then a graded response should pertain after a range of hyperventilation challenges.

The graded EIA response has been previously interpreted in terms of the source of the thermal burden rather than the actual respiratory heat exhange rate (RHER). Use of the RHER parameter, which can be evaluated for all grades of air, could help in defining the relative roles of airway cooling and drying in the production of hyperventilation induced asthma.

The following discourse seeks to characterise hyperventilation induced asthma first in terms of the exposure time to a fixed rate of heat loss and second to the relative roles of cooling and drying in asthmogenicity. As a consequence of these findings a third study was undertaken to explore the possibility of an air

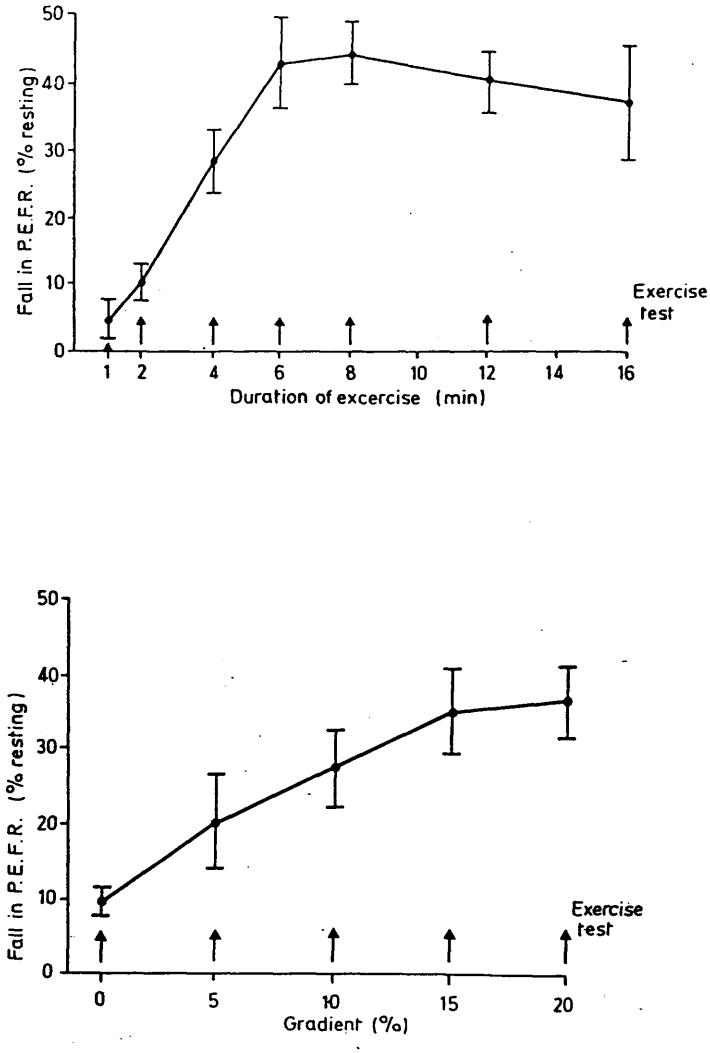

Figure 3.01: Exercise induced asthma can be correlated with severity either by cumulative effort or by increasing work rate. After Anderson (1984)

conditioning defect in asthmatics during hyperventilation. Each work is terminated by a summary which defines the aim of the subsequent study.

3.2. Method: The effect of challenge exposure time in cold air hyperventilation induced asthma.

Eight volunteer patients (4 female) in regular attendance at the hospital chest clinic and taking inhaled anti asthma drugs participated in the study. The mean age of the group was 24.1 (±7.4) yrs with an FEV_1 of 2.77 (±0.66) l or 80.3 (±18.1) % of the mean predicted normal FEV_1. Hospital ethical committee approval and informed consent were obtained.

Pre test lung function was recorded on a dry wedge spirometer (Vitalograph, Buckingham, UK) which was used throughout to measure the post challenge changes in FEV_1. These changes were expressed as the percentage rise or fall in FEV_1 from the baseline value as cited in section 1.4.2.

Subjects were seated at the cold air facility described in section 2.2 and breathed tidally through a rubber mouthpiece. Samples were obtained of resting ventilation and heat exchange rate for 1 minute using the 'Microlink' and the software, described in section 2.4, after which the subject removed the mouth piece. Air flowrate through the refrigerator was set to 120 l/min and the unit allowed to thermally stabilise for 5 minutes (figure 2.09). Hyperventilation induced nausea (hypocapnia) was prevented by adding the accepted standard5% CO_2 to the air supply prior to cooling. The data acquisition programme was reinitialised and subjects commenced breathing at their maximum voluntary ventilation (MVV) for 1 minute. Throughout encouragement was given to inhale deeply. Following exposure to cold air the subject was transferred to the spirometer and the post challenge FEV_1 recorded at

0.5, 1.5, 3, 5-6, 10 minutes and, if required, at greater than 10 minutes. Subjects were allowed a post challenge rest of 30 minutes after which the protocol was repeated twice with exposure times of 3 minutes and later 6 minutes. A six minute exposure had been found by experience to be tolerable to most subjects challenged prior to the study.

3.3. Results

Anthropometric and resting lung function of the subjects is given in table 3.01. Ambient air temperature during the measurements of tidal breathing was 19.4 (±1.38) °C, 41 (±4.5) %RH and 6.9 (±0.8) mg/l. Resting ventilation rate, expired air temperature and respiratory heat exchange rate were 8.67 (±5.15) l/min, 27.6 (±0.9) °C and 11.9 (±4.6) W respectively. The mean inspiratory cold air temperature was -22 (±0.79) °C with MVV's of 28.2 (±14.1) l/min [1 min], 24.1 (±9.9) l/min [3 min] and 24.8 (±8.9) l/min [6 min] throughout the tests. Respiratory heat exchange rate was computed on the basis of RMS expiratory air flowrates which were 24.1 (±7.0) l/min [rest], 57.9 (±18.0) l/min [1 min], 52.4 (±13.0) l/min [3 min] and 50.7 (±11.5) l/min [6 min].

Similar maximum falls in FEV_1 occurred after all the cold air exposures: 13.9 (±9.3) % [1 min], 11.5 (±6.3) % [3 min], 23.3 (±13.4) % [6 min]. Two subjects indicated discomfort due to laryngeal dryness and did not complete the 6 minute challenge although their fall in FEV_1 was after 3 minutes less than 15%. A further two subjects experienced a post challenge fall in FEV_1 of greater than 30% after the 6 minute challenge. Omission of these four patients from the data yielded a 6 minute exposure response of 13.5 (±1.5) (n=4). Figure 3.02 illustrates the time course of the post challenge FEV_1. All the exposures were followed by a recovery to within 10% of the pre test FEV_1

Figure 3.02: Post challenge FEV_1
for each exposure time.

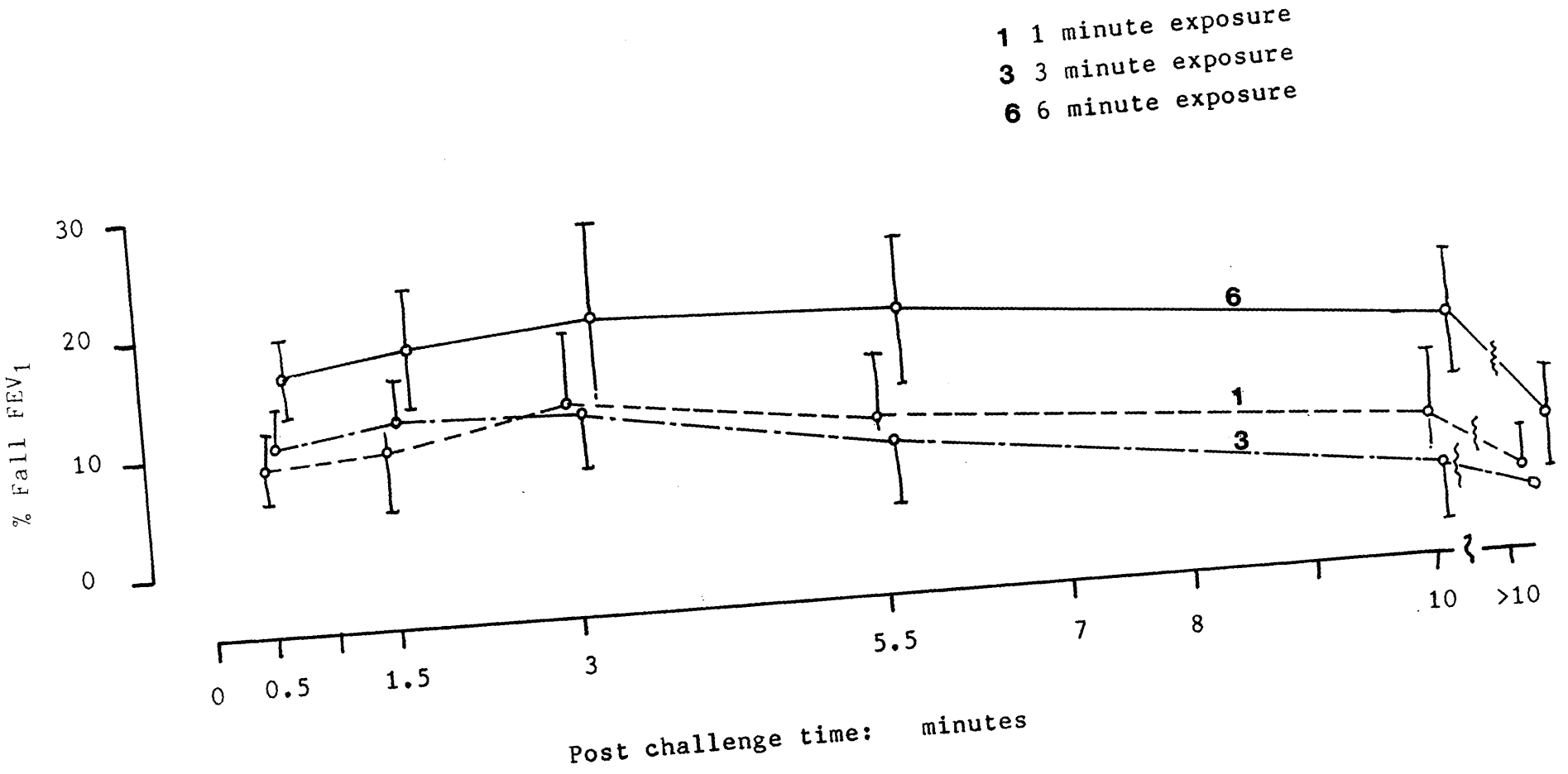

within 10-12 minutes. In each case the peak response occurred 2-3 minutes after the challenge.

Figure 3.03 illustrates the respiratory heat exchange rate imposed on the airway during each exposure and the subsequent % fall in FEV_1. No statistically significant variation in RHER was found between the challenges, the range of which was 44-48 W. The cumulative effect of exposure time to a fixed rate of heat loss is illustrated in figure 3.04. A trend of increasing response to exposure time could intuitively be interpreted although this was not statistically significant.

Table 3.02 summarises the imposed heat loss, airways response and ventilation level of the group.

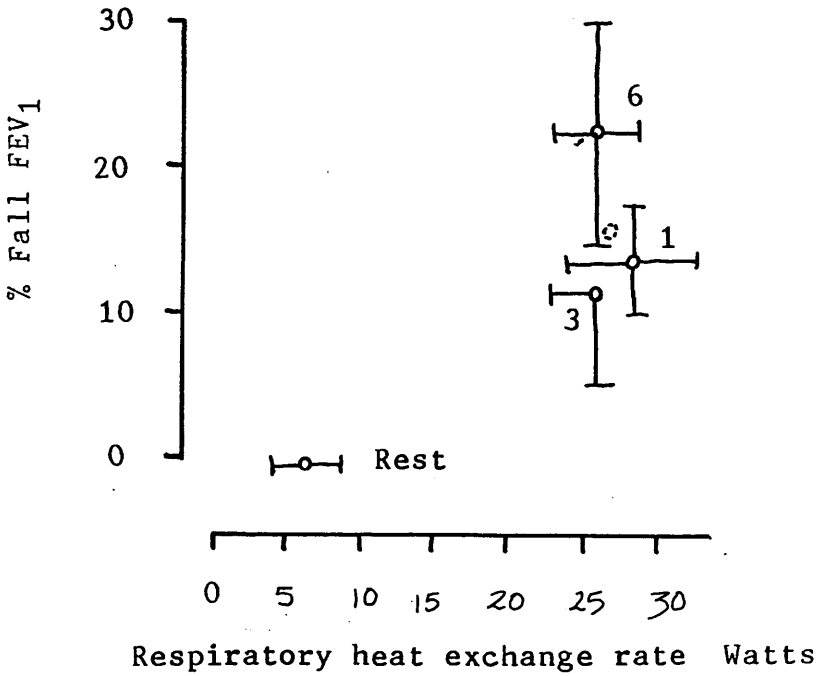

Figure 3.03: Respiratory heat exhange rates imposed during each of the challenges were similar.

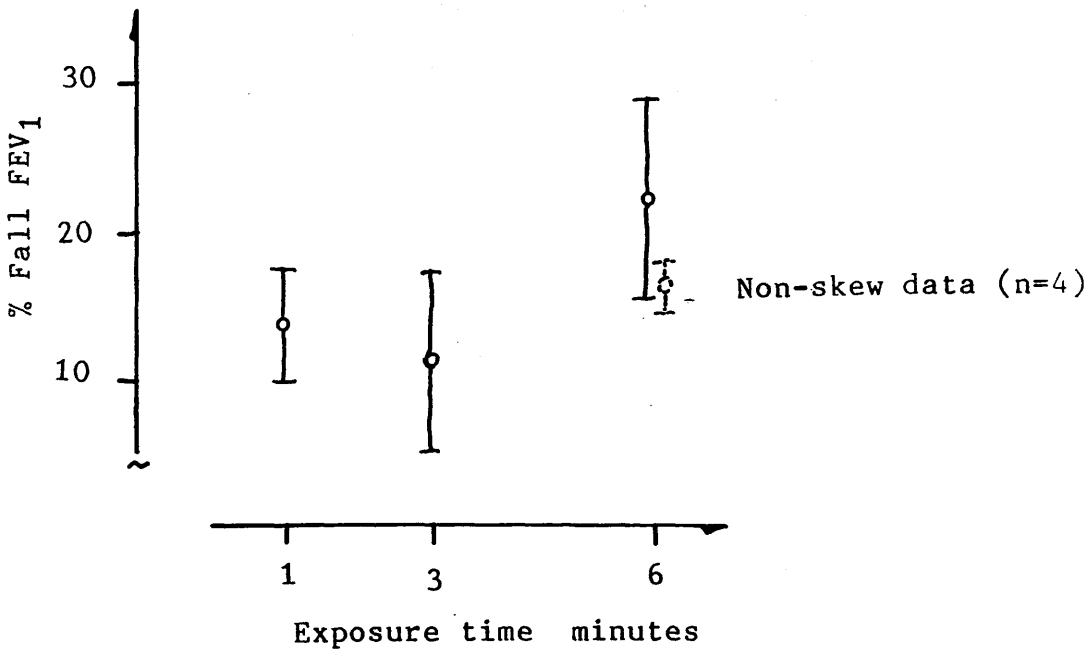

Figure 3.04: Exposure time and $\%FEV_1$

Table 3.01: Patient anthropometric data.

Subject	Sex	Age yrs	Height cm	Rest FEV_1 l	% pred.
1	F	17	160	3.0	91
2	F	19	158	1.92	60
3	F	28	167	3.27	112
4	M	17	178	3.16	77
5	M	36	174	2.95	84
6	F	35	162	2.35	76
7	M	22	174	1.74	50
8	M	19	172	3.78	92
Mean (SD)		24.1 (±7.4)	168.2 (±6.7)	2.77 (±0.66)	80.3 (±18.1)

Table 3.02: Summary of challenge and $\%FEV_1$

Exposure (mins.)	Rest	1	3	6
Vent. (SD) l/min.	8.67 (±5.15)	23.2 (±6.85)	24.2 (±9.9)	24.8 (±8.9)
RHER (SD) W	11.9 (±4.6)	51.2 (±17.0)	46 (±11.9)	45.3 (±10.0)
$\%FEV_1$ (SD)	- -	13.4 (±8.8)	13.1 (±5.8)	23.6 (±13.4)
Time of FEV_1 minima: mins (SD)	- -	3.1 (±0.8)	2.0 (±0.9)	2.8 (±3.3)

3.4. Comments.

3.4.1. Lung function.

The similar responses between the cold air exposures in the adjusted group (n=4) suggests that either the challenges were not identifiably different or that the previous test influenced that following. Without this adjustment a cumulative trend could have been interpreted from the data and would have reasonably been expected, following from the work illustrated earlier in figure 3.01. Section 3.11.1 seeks to address this possibility. Refractoriness, (ie the protective effect of consecutive and similar challenges), has been reported by Ben Dov et al (1982)[29] wherein subjects exercised twice breathing cold air before attaining full recovery from the previous challenge. A warm humid air challenge was found not to provoke bronchoconstriction although the same level of refractoriness was evident in a subsequent cold air challenge. It was concluded that refractoriness was not a function of heat loss but rather of exercise. Assoufi et al (1986)[30] describes an experiment in which asthmatics hyperventilated cold air twice with a 15 minute rest period separating the challenges. No refractoriness arose. Extensions of the rest period to 30 and 60 minutes were also found not to incur a refractory advantage. Neither could a cumulative response be obtained following rest intervals of 5 and 10 minutes. It was concluded that refractory and cumulative response events were confined to exercise induced asthma. The refractory phenomena is allied to the ability of some sports orientated asthma sufferers to 'run through' their asthma. A full natural recovery after the 1 and 3 minute exposures was obtained from the subjects prior to the next test and refractory effects were considered not to have influenced the experiment.

Clark and Godfrey (1983)[11] state that a vigorous 6 minute exercise is typically followed by a peak fall 5-7 minutes after the challenge. Lee et al (1984)[31] and Deal et al (1980)[32] identified a peak response to exercise up to 10 minutes after the challenge. Indeed a slight improvement in lung function after 2-4 minutes is not uncommon (Clark & Godfrey 1983[11]). A post challenge improvement was not observed in the present group. Comparison between cold air hyperventilation and the ambient exercise challenge, cited by Godfrey, is of limited value due to the greater RHE experienced in cold air breathing and the increase in heart rate associated with exercise. Physiologically the challenges are different. This will be alluded to in section 3.7.1.

Respiratory heat exchange comprises sensible (cooling based) and latent (drying based) heat transfers. Studies on exercise induced asthma have led to interest in the role of airway drying and airway cooling as mechanisms of bronchoconstriction, which was described in section 3.1. The nature of the response to various thermal stresses is also in doubt; the cooling argument suggests recruitment of thermoceptors with increasing heat exchange rate and presumably a graded response. The drying argument suggests mediator activity prompted by osmotic changes in the mucosal lining and presumably an 'all or nothing' trigger response.

The present work involved a maximum exposure time of 6 minutes which was chosen on the basis of what appeared to be tolerable to the participating asthmatics. Silverman an Anderson (1972)[26] (figure 3.01) exercised subjects for up to 20 minutes and elicited a cumulative response. If recruitment of thermoceptors with increasing RHER is important in the onset of hyperventilation induced asthma then, for the 6 minute exposure period used, the airway may accomodate a fixed heat loss rate regardless of exposure

time. The linearity or otherwise of the airway response following various magnitudes of RHER remains unanswered.

3.4.2. Errors and modifications.

The expired air temperatures recorded for ambient tidal breathing were lower than expected. This was due to the thermal inertia of the non-rebreathing valve inherent with its relatively large dead space volume. Measurements made by plunging a thermocouple directly into the expired air stream yielded a temperature of between 30°C-32°C during tidal respiration. Thus an underestimate of basal RHE would have been incurred. Using the RHER expression given in section 1.2 and substituting (SI units):

With:

T_i=19.4°C; w_i=6.9 mg/l (0.0059 kg/kg);
T_e=30°C; w_e=30 mg/l (0.0252 kg/kg); h_{fg}=2500 kJ/kg;
C_{pa}=1.005 kJ/Kg K and V_{RMS}=24.1 l/min, m_a=0.000228 kg/s

yields an RHER of 13.2 W

and

T_e=32°C; w_e=33 mg/l (0.0278 kg/kg)

yields an RHER of 15.0 W

against the present RHE of 12.1 W, an error range of 9-21%.

It is likely that this magnitude of error would not have been transposed into the hyperventilation data. The higher respiratory air flowrates and larger volumes of air involved would have retained more heat than the slowly moving bolus of tidal air. Moreover the action of frigid air inhalation can be expected to promote a cooler

expirate. At the time of experiment invitations had been issued to a second independent group of subjects for the following study. Thus no immediate replacement to the non rebreathing valve was made although the following modification in its use was implemented. Measurements of tidal air temperature commenced after two minutes breathing through the mouthpiece, which by experiment was found to yield a stable expired air temperature in the range 28-30°C.

The recorded MVV's of the subjects were comparatively low. McFadden et al (1982)[25] has reported ventilation levels of between 60- 120 l/min in asthmatics breathing cold air during measurements of intra thoracic air temperature. The present group MVV range was 24-28 l/min. A means of objectively varying the ventilation rate of a subject was sought as this would reduce data scatter and allow between subject matching of a thermal burden. In McFadden's experiment subjects exhaled into a rubber bladder which then emptied through a rotameter. The bladder acted as a surge tank smoothing the intermittent expiratory airflow. By sighting the rotameter bob a subject was able to voluntarily maintain a 'constant' ventilation rate. Alternatively the device could have been located on the inspiratory port of the non rebreathing valve . Air flowing into the rotameter would discharge through the bladder and the subject would be required to maintain a constant rate of air 'consumption'. It is likely that the height of the rotameter bob would have oscillated throughout respiration and that peak flows may have been observed and recorded. Without this phenomena a large bladder with an exit restriction necessary to completely smooth the between breath air surges would have presented a resistance to expiration and so interfere with the nature of the challenge. The actual RMS expiratory airflow rate recorded in the present group was about 55 l/min and applying a 2/3 rule of thumb 'RMS/peak constant' yields airflows

compatible with McFadden's data. However the RMS expiratory air flowrate, necessary for the computaion of breath by breath RHER, represents only a portion of the respiratory cycle. It takes no account of the expiratory period or frequency of breathing. Actual ventilation in this study was determined as the product of tidal volume and the number of breaths per minute. The rotameter technique was not considered for the present application due to the extra equipment required and the need for accurate on line measurement of patient ventilation. Ventilation control was subsequently achieved using a method devised by the author called 'target ventilation'.

The electrospirometer included an analogue meter of tidal volume. A target needle taped to the display allowed a subject to exhale a desired volume of air. Synchronisation of the exhalations with a metronome controlled the frequency of breathing. By this method a ventilation target could be established and measured breath by breath, on line, using existing equipment.

3.4.3. Summary.

No significant difference in bronchoconstrictive effect was observed in a small group of asthmatics following exposure to 44-48 W rate of heat loss for 1, 3 and 6 minutes. However the airway response to a range of heat loss rates is unknown as are the relative roles of cooling and drying. The following study alludes to these points and has been published: Farley, Albazzaz & Patel (1988)[33].

3.5. Method: Role of cooling and drying in hyperventilation induced asthma.

Seven patients (4 female) with mild allergic asthma and a baseline FEV_1 of greater than 70% of predicted normal values were enrolled. Seven non smoking volunteer subjects

(3 female) were also studied. The protocol was approved by the hospital ethical committee and informed consent was obtained from each subject.

Cold dry air -23.4 (±0.43) °C and 0.3 mg/l was produced using the facility described in section 2.2. Dried ambient air was generated by redirecting the refrigerator outlet through a 2.5 m bank of thin walled copper tube, designed by the author, and mounted on a heated radiator. It yielded air at 18.5 (±0.52) °C and 0.3 mg/l. Carbon dioxide was added to the inspirate from a bottled supply to 5% of mixture in order to prevent hypocapnia. The two grades of air were administered randomly among the groups on separate visits to the laboratory. Respiratory heat exhange rate was calculated on line using the microcomputer equipment described in chapter 2.

Patients inhaled the conditioned air by target ventilating, (section 3.4.2), at 15, 30 and 60 l/min for 3 minutes each. Normals omitted the 15 l/min challenge. After each hyperventilation challenge FEV_1 was recorded at 0.5, 1.5, 3, 5, 7, 10, 12 and 15 minutes on a dry wedge spirometer at ambient temperature and humidity. The best result in three attempts was recorded and the results again expressed as the maximum percentage fall in FEV_1. Data were subjected to an analysis of variance with a Minitab statistics package.

3.6. Results.

Anthropometric and lung function data on the trial participants are given in table 3.03. Figure 3.05 illustrates the maximum percent fall in FEV_1 for different ventilation rates with cold air and dry ambient air hyperventilation in normal and asthmatic subjects. There was a significantly larger ($p<0.05$) fall in FEV_1 in both groups after cold air than dry ambient air hyperventilation. In the asthmatic group the cold versus

Figure 3.05: Fall in FEV_1 with the ventilation rate. The achieved ventilation undershoots the target at the 60 l/min level.

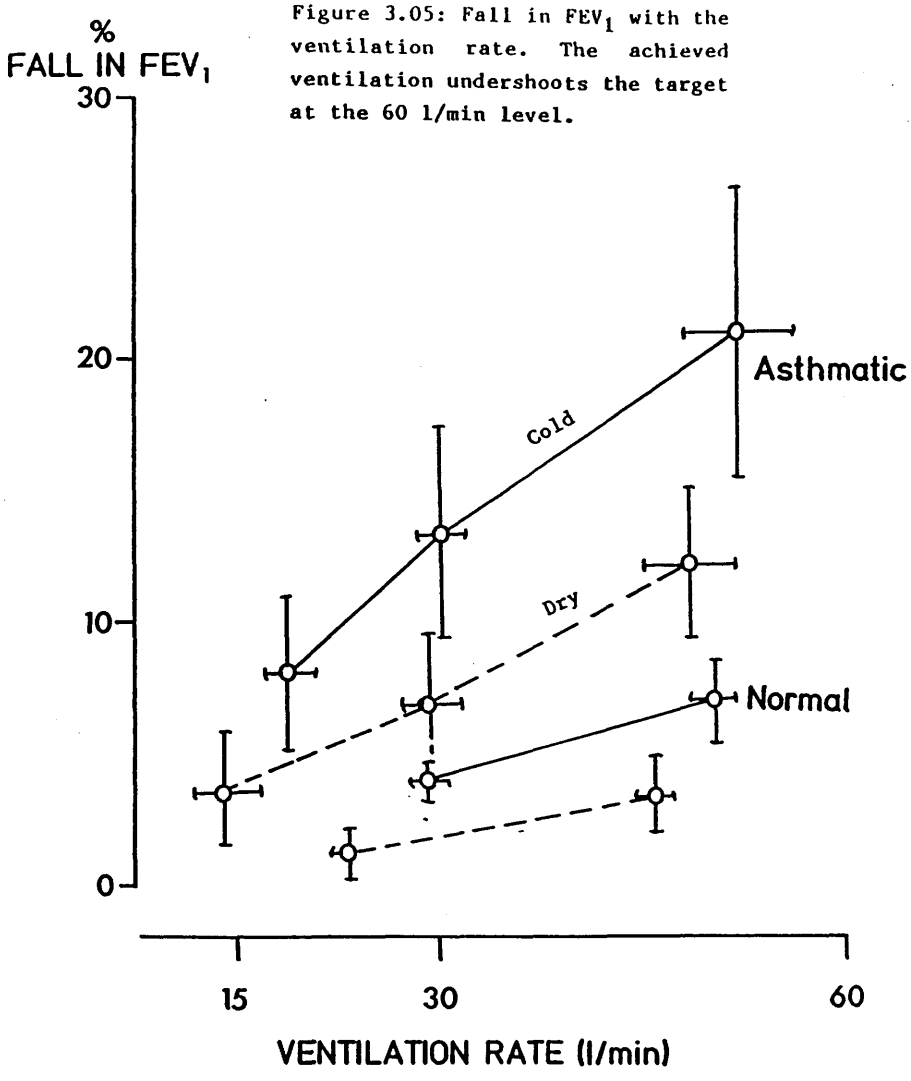

dry $\%FEV_1$ falls were 8 (±4)% vs 3.8 (±4)% [15 l/min] F=8.2; 11.6 (±8)% vs 7 (±4.4)% [30 l/min] F=3.6 NS and 20.7 (±11)% vs 12.3 (±6.3) F=11.4 [60 l/min]. In the normal group smaller $\%FEV_1$ falls were recorded: 4.7 (±1.4)% vs 1.2 (±1.2)% F=24 [30 l/min] and 7.1 (±3.1)% vs 3.3 (±3)% F=11.4 [60 l/min].

In the asthmatic patients increasing ventilation in the cold air challenge was followed by larger falls in FEV_1 ($p<0.05$) whereas in dry ambient air the trend was smaller. Figures 3.06-3.07 illustrate the time course of the airway response after the challenges. The maximum fall in FEV_1 was observed after about 2-5 minutes and recovery to within 5% of baseline FEV_1 was obtained by 20 minutes.

During cold air hyperventilation the expired air temperature was lower than during dry ambient air breathing in both groups (table 3.04). The respiratory heat exchange was computed on the basis of these temperatures and is plotted in figure 3.08 against $\%FEV_1$. In the asthmatic group a linear relation between heat loss rate and the mean falls in FEV_1 for the group was found ($r=0.96$, $\%FEV_1=0.13(RHE)-1.73$); regardless of the type of thermal burden and appeared to conform to some kind of superposition rule. At the 60 l/min ventilation level both groups had an achieved ventilation of about 75% of the target (table 3.05). The contribution of sensible (convective cooling based) and latent (evaporative drying based) heats was examined by separating the net RHER into component form, using the expression given in section 3.4.2 and these are shown for the asthmatic group in table 3.06. The lower expired air temperatures in cold air hyperventilation imply greater airway water retention and less latent heat loss than in ambient air hyperventilation. For the same rate of latent heat loss the associated airway response is greater with cold air than dry ambient air. Higher rates of sensible heat loss (caused by the larger inspiratory expiratory temperature gradient) were followed

Figure 3.06: Post challenge FEV_1 for each exposure time with dry air breathing.

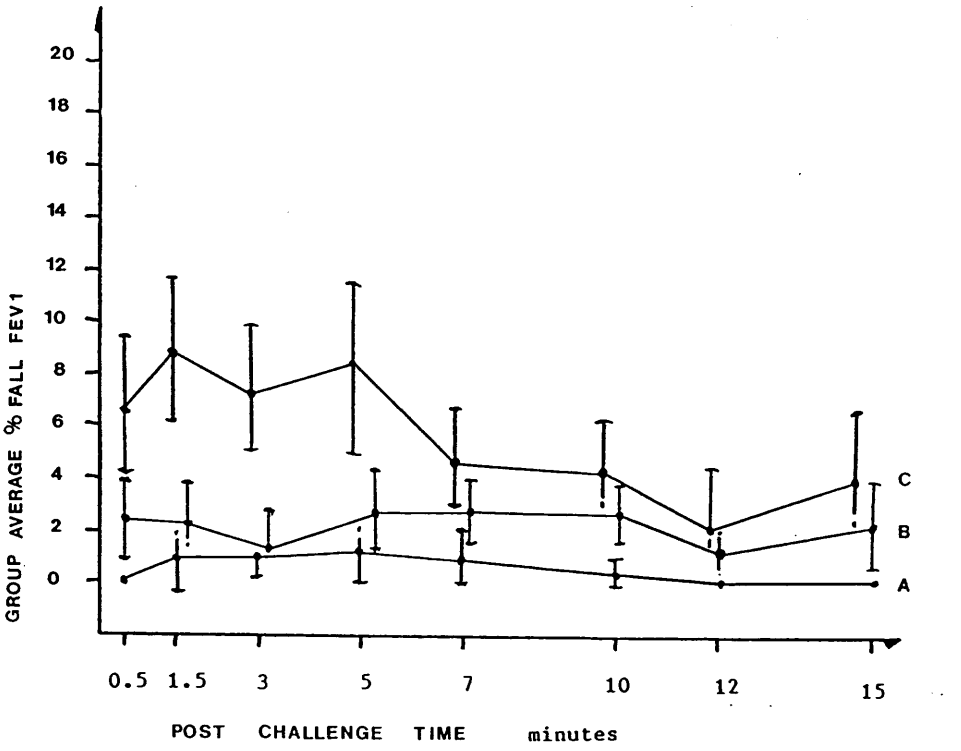

A 15 l/min Target ventilation rate
B 30 l/min Target ventilation rate
C 60 l/min Target ventilation rate

Figure 3.07: Post challenge FEV_1 for each exposure time with cold air breathing.

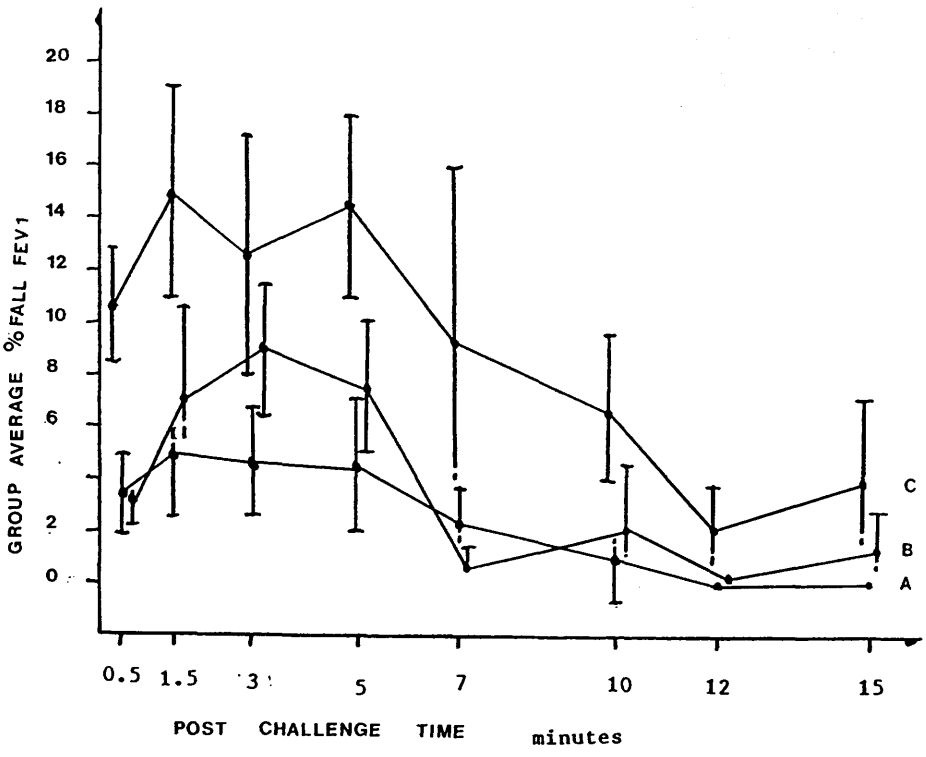

A 15 l/min Target ventilation rate
B 30 l/min Target ventilation rate
C 60 l/min Target ventilation rate

Figure 3.08: % Fall in FEV_1 with the rate of respiratory heat exchange. Regardless of the nature of the thermal burden the RHER - FEV_1 relation falls on a line.

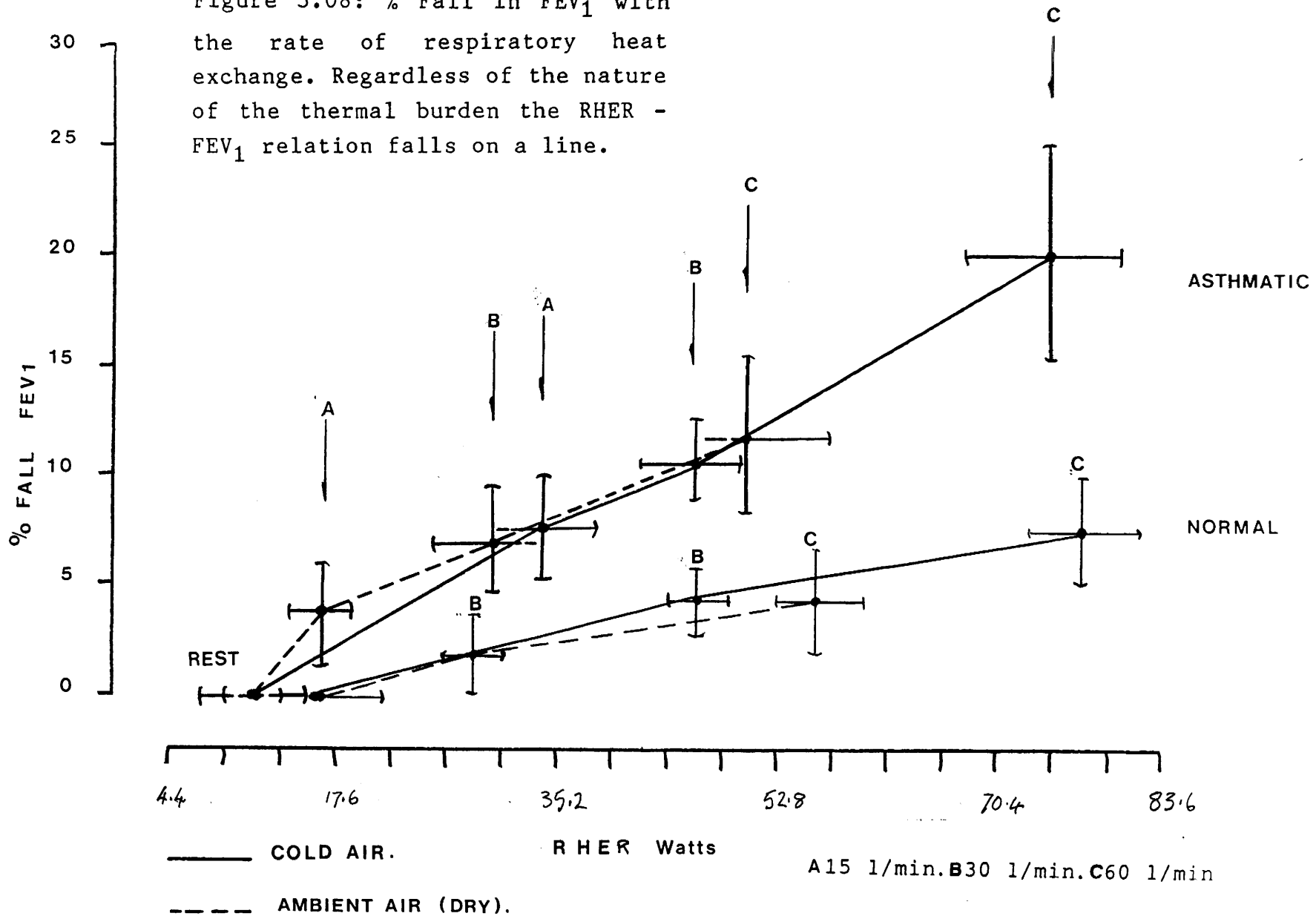

by a greater fall in FEV_1. However, for a given rate of sensible heat loss the subsequent airway responses in cold air and dry ambient air were similar. Enhanced airway cooling appears to provoke a response additional to that elicited from drying.

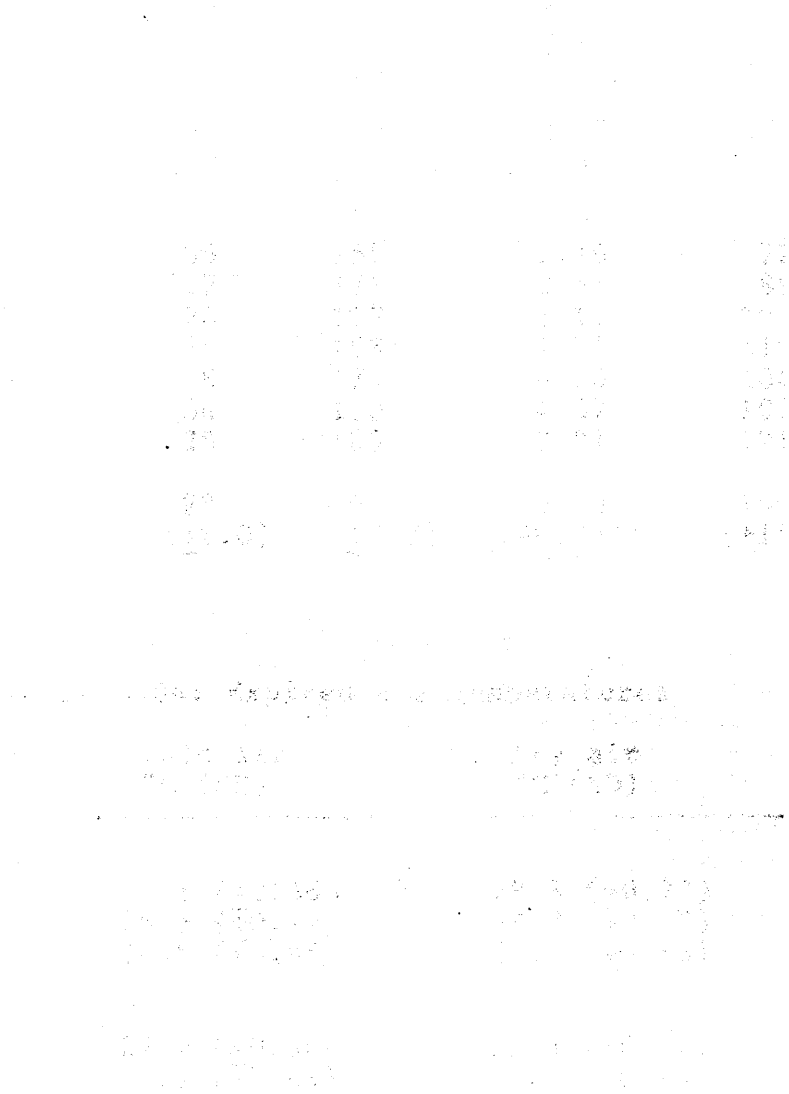

Table 3.03: Anthropometric and lung function data.

Subject	Sex	Age yrs	Height cm	Rest FEV_1 l	% pred.
Asthmatic:					
1	F	35	162	2.62	91
2	F	50	159	2.57	112
3	M	30	188	4.77	106
4	F	28	160	3.13	106
5	F	19	158	2.12	71
6	M	22	163	3.04	98
7	F	36	174	4.31	117
Mean (SD)		31.5 (±9.5)	166.3 (±10.2)	3.22 (±0.9)	100.1 (±15.4)
Normal:					
1	F	39	155	2.16	72
2	M	27	173	3.43	89
3	F	24	163	3.11	100
4	M	24	168	4.25	110
5	M	28	175	4.20	104
6	M	34	180	4.37	107
7	F	20	165	3.87	121
Mean (SD)		28 (±6.0)	168 (±7.7)	3.63 (±0.74)	100.4 (±15.9)

Table 3.04: Expired air temperatures

Vent. target l/min	Cold air °C (SD)	Dry air °C (SD)
Asthmatic (n=7)		
15	27.1 (±0.46)	28.8 (±0.73)
30	26.5 (±0.71)	29.7 (±0.49)
60	26.8 (±0.85)	30.3 (±0.53)
Normal (n=7)		
30	27.2 (±0.66)	29.4 (±0.35)
60	27.1 (±0.66)	30.0 (±0.9)

Table 3.05: Actual vs target ventilation.

Vent: l/min (SD)	Rest (ambient)	15	30	60
Asthmatic:				
Cold	9.9 (±3.8)	17.2 (±0.5)	25.5 (±0.6)	43.8 (±1.2)
Dry	8.1 (±0.9)	13.1 (±0.4)	24.7 (±0.2)	41.3 (±1.1)
Normal:				
Cold	12.2 (±3.3)	--------	29.4 (±0.4)	49.6 (±0.5)
Dry	13.9 (±1.3)	--------	22.9 (±0.7)	45.7 (±0.2)

Table 3.06: Components of heat loss in the asthmatics.

Vent. l/min (SD) Target	Actual	RHER (Watts) Sens.	Lat.	Tot.	$\%FEV_1$ (SD)	H_2O loss g/min
Rest	9.9 (3.8)	3.5	12.3	15.8	-	0.25
Cold air:						
15	17.2 (0.5)	18.0	20.2	38.2	8.0 (5)	0.44
30	25.5 (0.6)	27.7	23.8	51.5	11.6 (8)	0.61
60	43.8 (1.2)	50.2	28.2	78.4	20.7 (11)	1.05
Dry air:						
15	13.1 (0.4)	2.6	18.0	20.6	3.8 (4)	0.40
30	24.7 (0.2)	5.7	28.6	34.3	7.0 (4.4)	0.72
60	41.3 (1.1)	10.1	44.0	54.1	12.3 (6.3)	1.24

Sens.- Sensible heat, via convective cooling; Lat.- Latent heat, via evaporative drying; Tot.- Total rate of heat loss; H_2O loss - Water loss/min based on a fully saturated expirate.

3.7. Comments.

3.7.1. Lung function.

Increasing ventilation during cold and dry ambient air hyperventilation was followed by greater falls in FEV_1, the largest fall in the asthmatic group occuring about 2-5 minutes after the challenges. Moderate airway drying was encountered in both forms of hyperventilation. Water loss rates in the asthmatics were calculated on the basis of a fully saturated expirate of known temperature and actual ventilation rate (table 3.06) During maximal ventilation (60 l/min target) water loss rates of 1.05 g/min (cold air hyperventilation) and 1.24 g/min (dry ambient air hyperventilation) were predicted in contrast to the ambient rest value of 0.25 g/min. Net water loss in cold air hyperventilation was reduced despite the same inspiratory drying stress as in dry ambient air, owing to the greater condensation of water back onto the cool upper airway.

Similar ventilation rates were observed in both groups and are listed in table 3.05. At the 60 l/min target both tended to undershoot the preset rate although the achieved level remained constant throughout the challenge. Table 3.04 summarised the expired air temperatures recorded in the asthmatic and normal groups throughout the challenges. In the asthmatic group slightly lower temperatures were found with increasing ventilation than in the normal group during cold air hyperventilation and a cooling characteristic was evident. No statistical analysis of the temperature data was made due to the insensitivity of the non rebreathing valve reported in section 3.4.2. A redesign of this unit is detailed in section 3.7.2. However, because the inspired air condition and ventilation rates between the groups were similar the finding could be

explained by the presence of an air conditioning defect in the airways of the asthmatics.

Hyperventilation induced asthma is used as a model of the effect of respiratory heat and water loss in exercise induced asthma although the mechanisms remain unclear. Physiological differences between the two types of challenge have been identified. Airway receptors anaesthetised by lignocaine were found not to confer protection from exercise induced asthma (Tullet et al 1982[34]) and it was concluded that direct sensory stimulation by drying or cooling was unlikely. There may be differences in the release of mediators between exercise and hyperventilation induced asthma. Barnes and Brown (1981)[35] reported a rise in histamine concentrations in asthmatic subjects after exercise whereas in normals no change occurred. Hyperventilation produced no histamine rise in either group although both exercise and hyperventilation were followed by similar reductions in peak expiratory flowrate (PEFR). Nagakura and Lee et al (1983)[36] observed neutrophil chemotactic factor release during exercise but none during hyperventilation induced asthma. The two types of challenge elicited the same fall in FEV_1. Similar observations have been made by Deal et al (1980)[32] during a study of antigen provocation versus hyperventilation induced asthma.

Hahn and coworkers (1984)[28] exercised subjects in a temperature of 10-35°C with a fixed water vapour content of 9-10 mg/l. Large reductions in PEFR were observed during the 35°C challenge, although a similar challenge with humidified air (29 mg/l) appeared to confer protection against exercise induced asthma. Epithelial water loss was proposed as the predominant stimulus for exercise induced asthma. Expired air temperature was not recorded. On the assumption that this was about 34°C the maximum range of temperature imposed on the airway would have been 25°C. In the present study the range was up to 60°C and airway

cooling was more severe. Heating air depresses its relative dryness. The mass transport coefficient of water in air, which determines the evaporation rate from a particular region of the airway, depends on the water vapour concentration gradient between the epithelium and airstream and on the local air temperature. For example wet epithelial tissue exposed to air at 40°C and 0.3 mg/l will have twice the water loss rate as that produced by air at -25°C and 0.3 mg/l. It is reasonable to expect that the upper respiratory tract, the zone in initial contact with the inspirate, will have the greatest rates of drying during an arid burden. During an in vivo measurement of intra thoracic air temperature, detailed in chapter 6 pharyngeal temperatures of 34°C were observed with tidal inspiration of 22°C ambient air, giving an oral - pharyngeal temperature gradient of 12°C. A cold air (-18°C) intra thoracic air temperature investigation by McFadden et al (1982)[25] implied an oral - pharyngeal gradient of 40°C and recorded temperatures of 25°C at the third generation bronchial airway during hyperventilation. Direct stimulation of the airways receptors beyond the third generation would appear to be unlikely as this would demand prior stimulation, by severe heat loss, of thermoreceptors in the upper airway.

Throughout the dry ambient air hyperventilation challenge all patients and normals reported a sensation of pharyngeal dryness and four patients also described discomfort at the level of the sternal notch. In all cases the sensation of dryness was distinct during dry ambient air hyperventilation. Only four patients reported dryness after the cold air hyperventilation challenge. This may have been due to differences between patients ability to maintain the ventilation target, the inherently higher transport rates of drying experienced in dry ambient air described earlier or the additional water vapour retention associated with cold air breathing. In the present study the burden of

conditioning was placed on the upper airway, particularly at the oropharynx in keeping with the sensations felt by the subjects.

McFadden et al (1986)[37] has shown that the rate of airway rewarming after a thermal burden influences the severity of exercise induced asthma. If the rate of heat loss is crucial the airway may accommodate heat loss due to steady state hyperventilation of cold air but be unable to do so when exposed to the step change in inspiratory temperature during the period after exertion. In the current work subjects resumed inhalation of room air immediately after the challenges. Because the participants were hyperventilating rather than exercising, ventilation would have returned to resting values almost immediately, giving rise to a lower rewarming burden than would have arisen had postexertional increased ventilation been present. However, steady state accommodation by the airway was implied in the previous experiment wherein asthmatic subjects were exposed to identical rates of respiratory heat loss for 1, 3 and 6 minutes and therafter exhibited similar post hyperventilation decline in FEV_1.

Both drying and cooling appear to influence airway responses. In the dry ambient air hyperventilation challenge low rates of sensible heat loss arose (about 20% of the total RHER), the burden being primarily the action of drying, which was followed by a fall in FEV_1 of 12% at 60 l/min. In cold air hyperventilation a fivefold increase in the level of sensible heat loss rate and latent heat loss rate similar to that experienced in dry ambient air produced a fall in FEV_1 of 20% at 60 l/min. Intuitively, larger numbers of thermoceptors will be stimulated by an increased ventilation rate and may play a role in airway cooling induced bronchoconstriction. An air conditioning deficiency in asthmatics could result in the stimulation of thermoceptors deeper in the airway in addition to the thermal stress on those in the upper respiratory tract.

Without an improved measurement of expired air temperature the existence of such a deficiency cannot be addressed.

3.7.2. Errors and modifications.

The low tidal air temperatures recorded, following the two minute warm up period, lead to a 20% error in the estimation of RHER described in section 3.4.2. In the current non rebreathing valve (figure 2.09) a 'T' type thermocouple was located downstream of the expiratory port, chosen because inspiratory airflow cooling would have led to the formation of expiratory condensate on the thermocouple. This would have depressed the measured expiratory temperature. Moreover, a single thermocouple probe located at the mouth was considered unlikely to respond over the 60°C range of temperature during cold air breathing within a respiratory cycle. Condensate was noted on the inside surface of the non rebreathing valve in proximity to the disc leaflet of the expiratory port.

A new non rebreathing valve (Mk2), designed and built by the author, is illustrated in figure 3.09. The device comprised a polythene 'Y' piece flow separator, drilled to an internal diameter of 10 mm and the existing disc leaflets. Assembled it had a 'between valve dead space' of 31 ml compared to the 46 ml for the Mk1 version and did not present a perceptible resistance to breathing. Initial measurements yielded a tidal expiration temperature of 31-32°C compared to 28-30°C found in the Mk1.

3.7.3. Summary.

A bronchoconstrictive effect in the range 10-20% fall in FEV_1 was observed in a small group of asthmatic patients following three minutes hyperventilation of various grades of air. The post challenge fall in FEV_1 was found to be directly proportional to the imposed heat loss rates in the

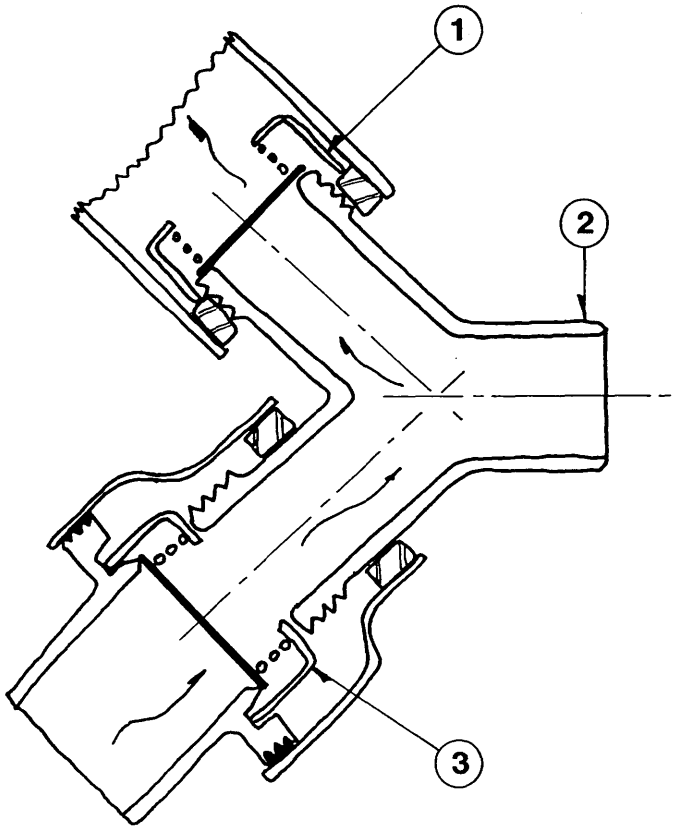

Mk2 Non rebreathing valve (full scale)
Dead space volume between valves: 31 ml

1 Expiratory leaflet valve
2 Mouthpiece adaptor
3 Inspiratory leaflet valve

Figure 3.09:

range 22-88 W. Cold air breathing conferred the greatest heat exchange rates and thereby the largest post challenge responses. A similar challenge in a small group of normal subjects was followed by a fall in FEV_1 of under 5%. The responses in the asthmatic group could be due to thermoceptor stimulation by cooling. The slightly lower expired air temperatures recorded in the asthmatic group may indicate an air conditioning deficiency.

Using the Mk2 non rebreathing valve the following study was done to investigate the existence of an air conditioning deficiency in asthmatics and the work has been published in abstract form: Farley & Patel (1988)[38].

3.8. Method: Rate of airway cooling in hyperventilation induced asthma.

Nine patients (4 female) with mild allergic asthma and a baseline FEV_1 of greater than 80% of predicted normal values were enrolled. Eight non-smoking normal volunteer subjects were also studied. The protocol was approved by the hospital ethical committee and informed consent was obtained.

On three separate visits to the laboratory participants hyperventilated isocapnically, through the Mk2 non-rebreathing valve, ambient air, dry ambient air and cold air. These grades of air were produced using the equipment described in section 3.5. Each was administered randomly among individuals and the challenges were preceded by a two minute period of tidal breathing in order to measure basal heat exchange rate. Data collection and processing was as described in the previous study. Ventilation was maintained for five minutes at targets of 15, 30 and 60 l/min (section 3.4.2). After each challenge recordings of lung function were made using the dry wedge spirometer. A rest period of 30 minutes separated each ventilation level.

A five minute challenge was chosen in order to lengthen

the period of exposure and to allow characterisation of the airway cooling process. This was done by averaging the expired air temperature in three 30 second windows centered at 25, 150 and 280 seconds into the challenge, and is described in detail in section 3.10. The rate of airway cooling (RAC) at a given ventilation level was defined by the author to be the difference between tidal and end challenge expired air temperatures over the five minute period:

$$RAC=(T_{rest} - T_{5\ min})/5\ mins. \quad °C/min$$

Within group data were subjected to an analysis of variance (F test) and between group data to a Student's 'T' test using a Minitab statistics programme.

3.9. Results.

Anthropometric and lung function data are given for the groups in table 3.07.

Respiratory heat exchange rate ranged between 13-88W in the normals whereas this was 13-70 W in asthmatics. The difference was due to the latter having a larger undershoot in ventilation targeting. Similar tidal ventilation, expired air temperature and basal RHER were observed in both groups summarised in table 3.08.

In the asthmatic group higher falls in FEV_1 were again observed in proportion to the imposed rate of heat loss, figure 3.10: $r=0.85$, $\%FEV_1=0.223(RHE)-2.73$. The largest fall in FEV_1 occurred after cold air breathing (60 l/min) of 26.7 ($\pm$11.9)% and was significantly greater ($p<0.05$) than that after ambient air, 12.5 ($\pm$5.4)% $F=8.06$ and dry air, 13.9 ($\pm$9.2)% $F=5.9$. In the normal group cold air hyperventilation at 60 l/min was followed by a decline in FEV_1 of 5.7 ($\pm$2.8)%. Table 3.09 summarises the post challenge responses in each group.

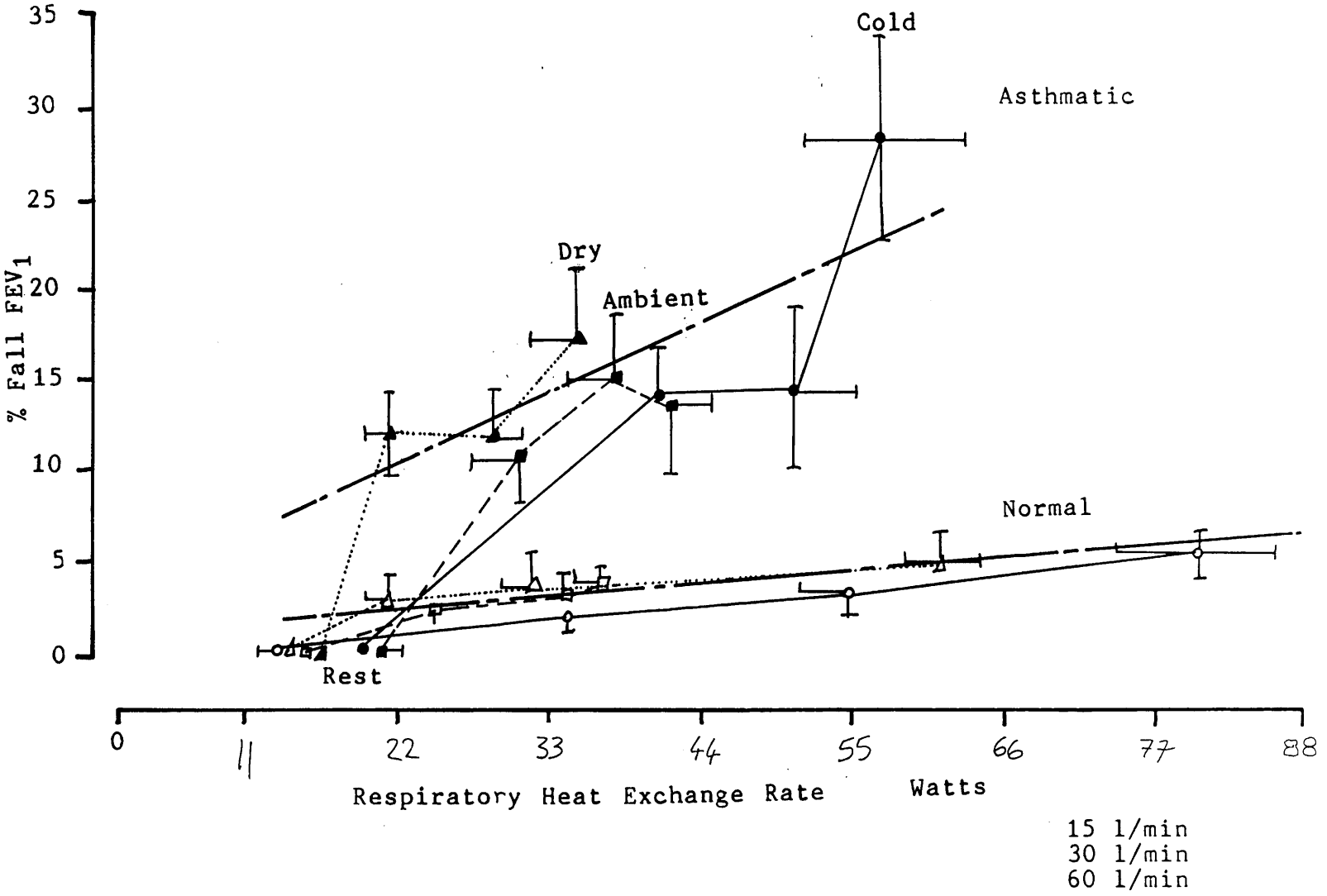

Figure 3.10: % Fall in FEV_1 with the rate of respiratory heat exchange. Again an RHER - FEV_1 linearity is evident.

Figure 3.11 illustrates the typical variation in expired air temperature for a normal subject obtained using the Mk2 non-rebreathing valve during each of the challenges. Cold air breathing conferred the greatest reduction in expired air temperature whereas in ambient air little change was found. The transient peaks and troughs in these loci are attributed to subject swallowing and local mismatching with the ventilation target. Figure 3.12 is an enlargement of the expired air temperature plots during the three 60 l/min challenges. Superimposed onto the curves are three thirty second windows used to determine the local expired air temperature at 25, 150 and 280 seconds into the trial. These values were named T_{25}, T_{150} and T_{300}; 300 seconds being the end trial observation.

Figure 3.13 summarises the local expired air temperatures for all the experiments measured in both asthmatic and normal groups. An airway cooling characteristic was evident, in proportion to the severity of the thermal burden. Measured expired air temperatures throughout the course of the ambient air challenges in the normals were found to be significantly higher ($p<0.05$) than those in the asthmatics by up to 1°C. This could be explained by the inspired ambient air temperature which was generally warmer in the normal group by up to 1.5°C. Expiration temperature in the normal group was higher by about 1°C than in the asthmatic group with dry air breathing, this trend was again found to be statistically significant ($p<0.05$) and inspired dry air temperatures between the groups were similiar. No statistically significant difference in expired air temperature between the two groups was found during the cold air challenges although those in the asthmatic group were slightly lower. Ventilation rates for the groups were matched and are given in table 3.10. Table 3.11 lists the expired air temperature data.

Figures 3.14 and 3.15 illustrate the decline in T_{300} with the ventilation rates attained by the asthmatic and normal

Figure 3.11: Expiratory air temperature in 1 subject throughout the challenges.

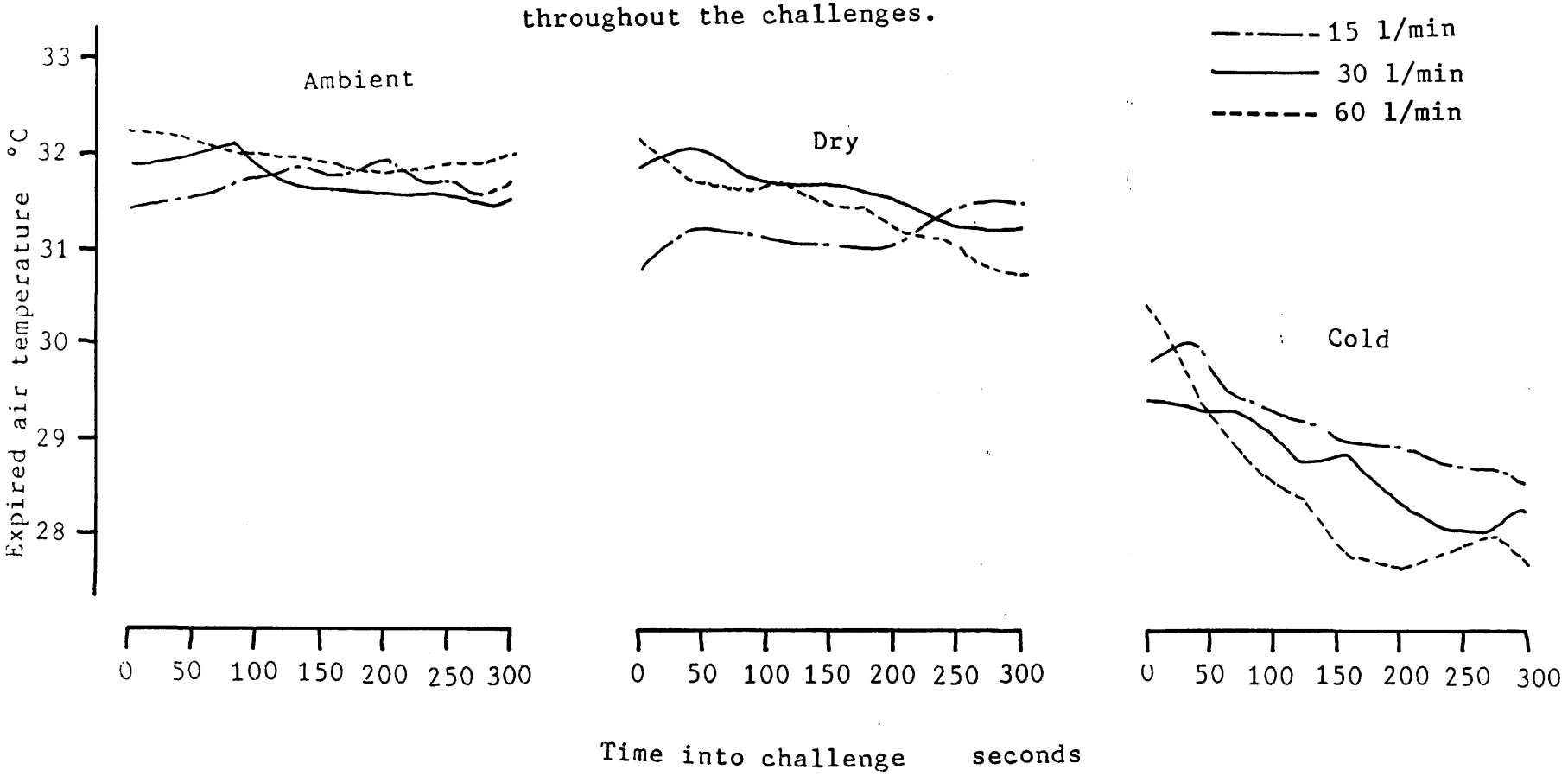

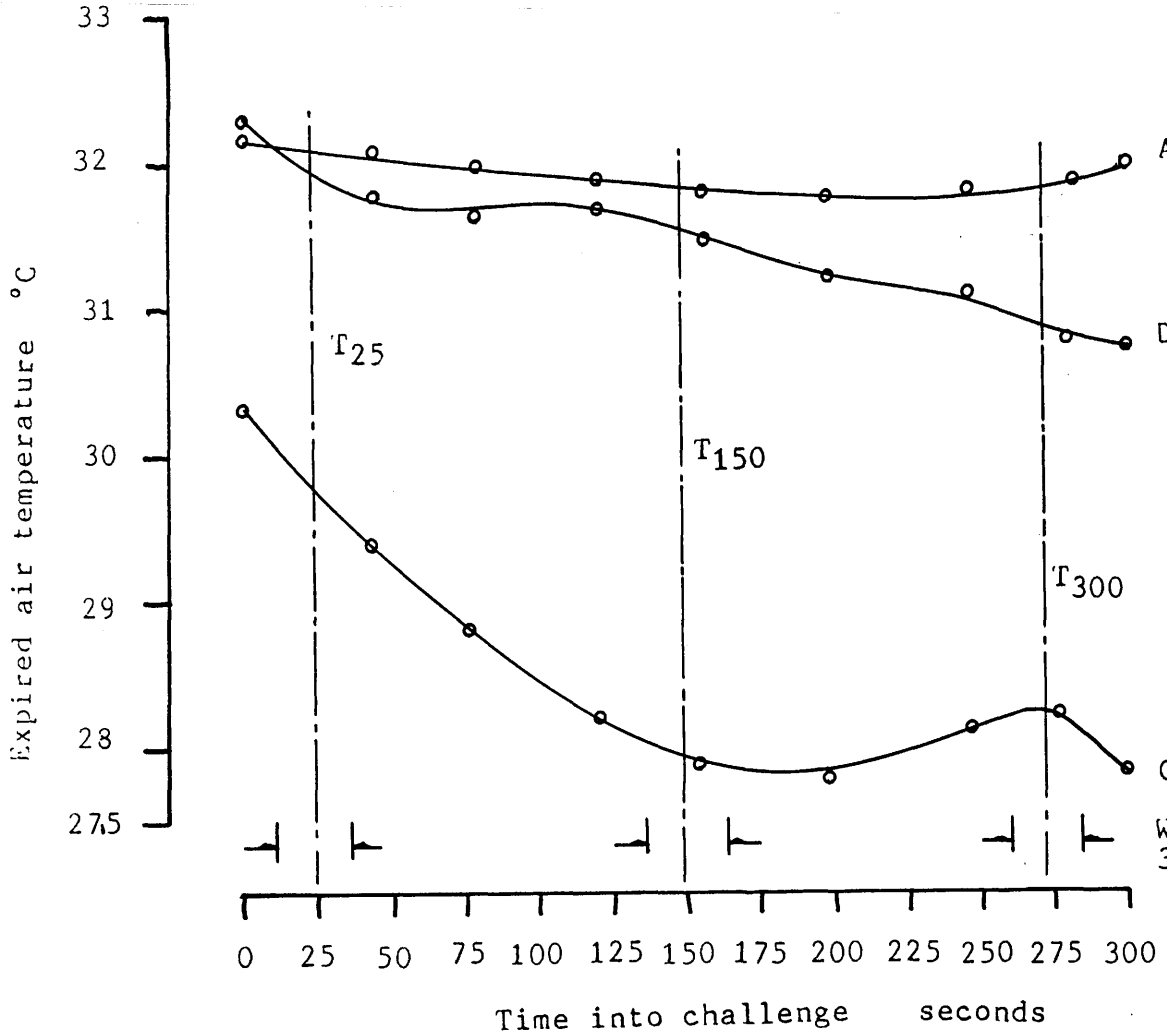

Figure 3.12: Enlargement of 60 l/min data from preceeding diagram. The peak at T_{300} for cold air is an artefact.

Figure 3.13: Expiratory air temperatures in astmatics and normals for all the challenges.

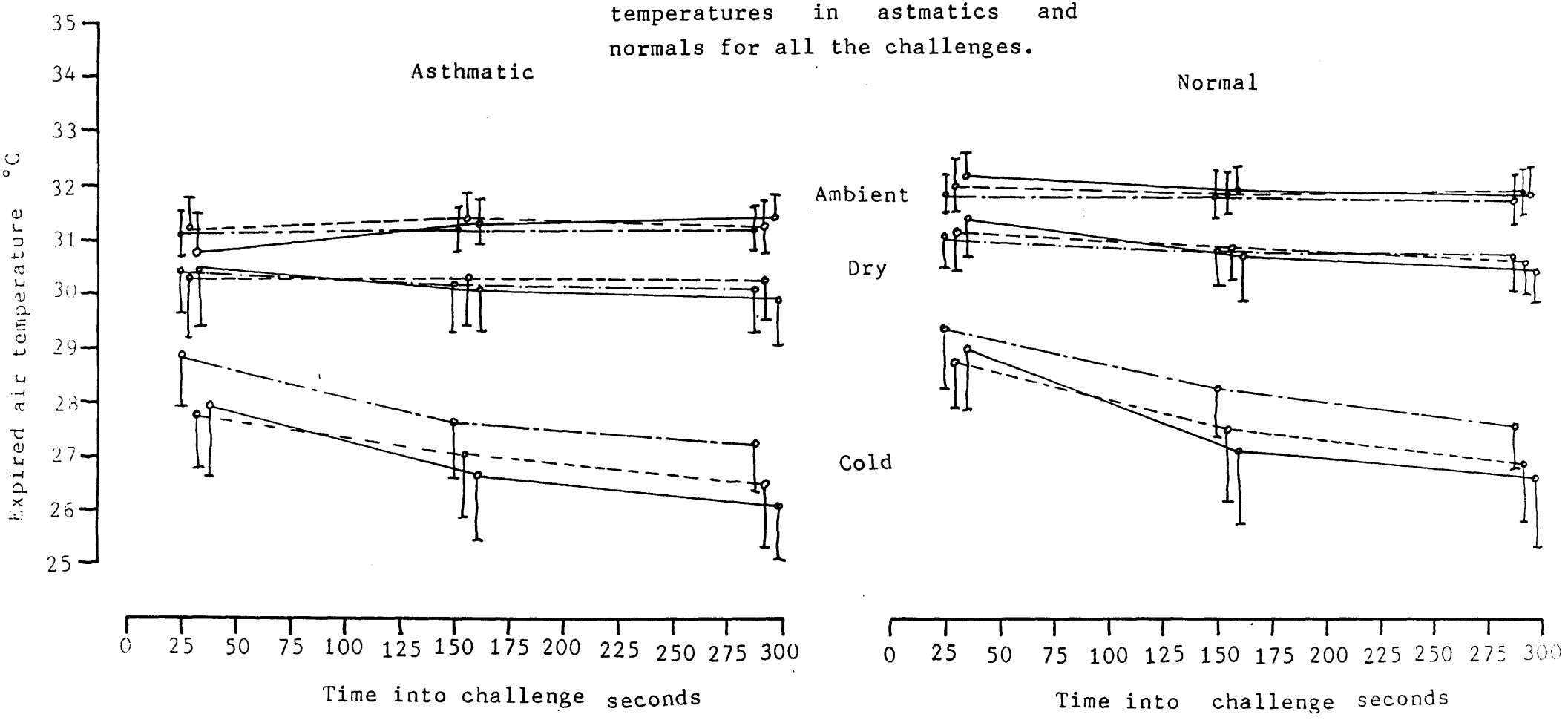

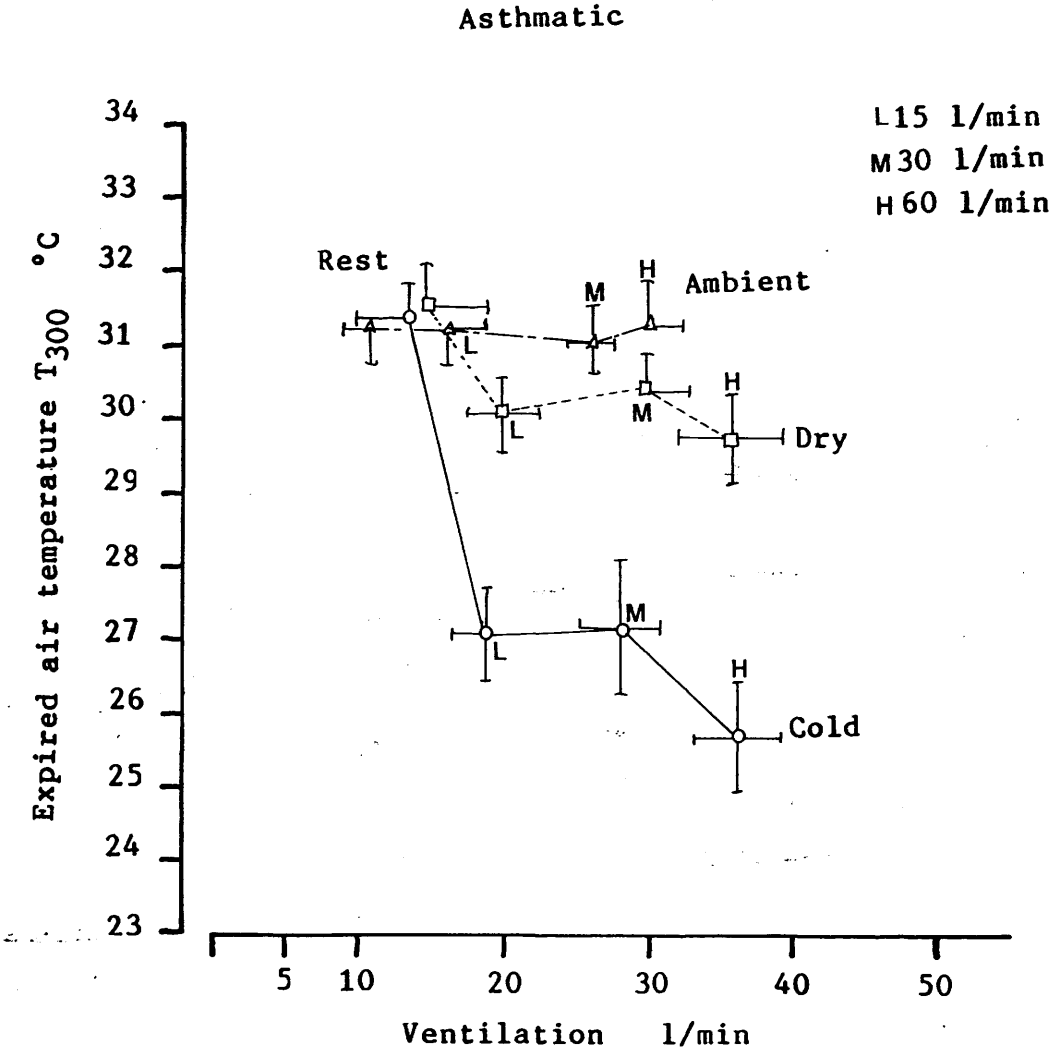

Figure 3.14: T_{300} in the asthmatics and ventilation rate.

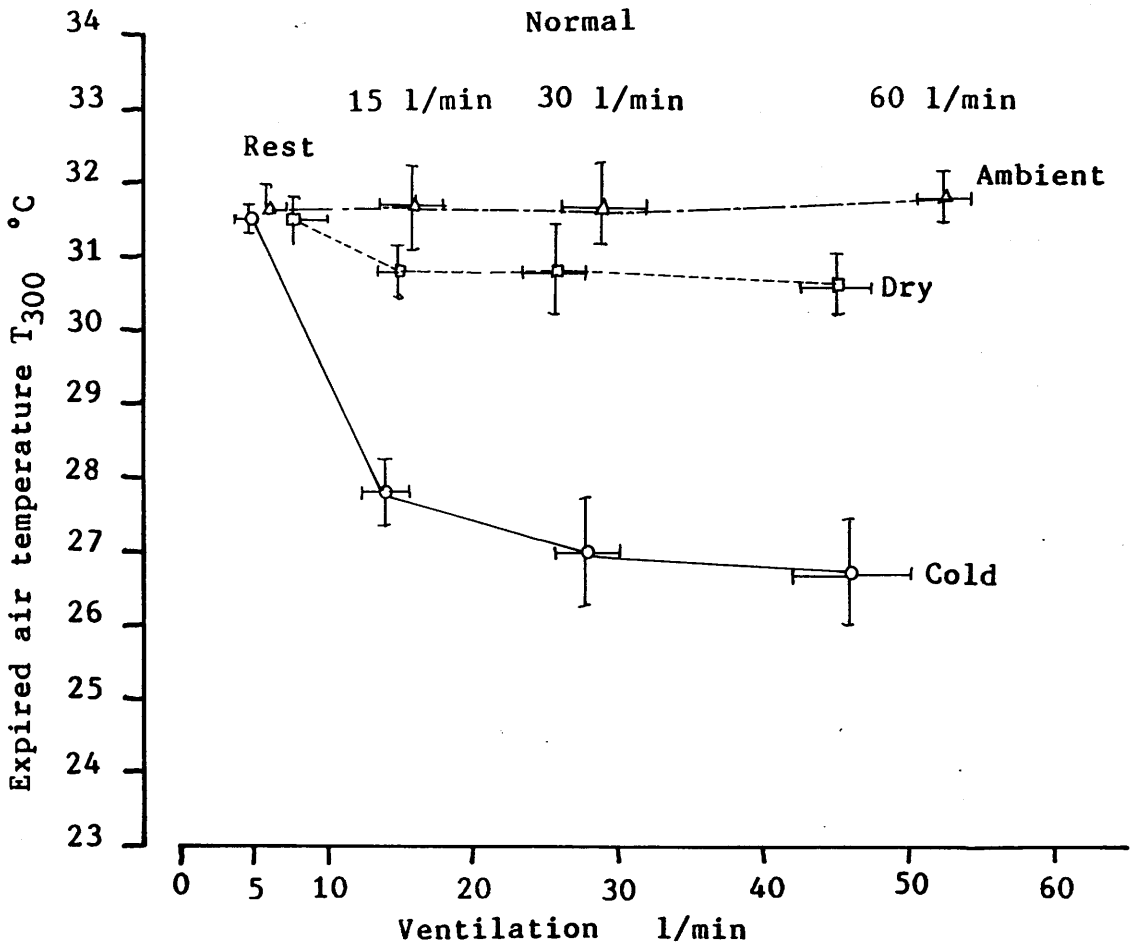

Figure 3.15: T_{300} in the normals and ventilation rate.

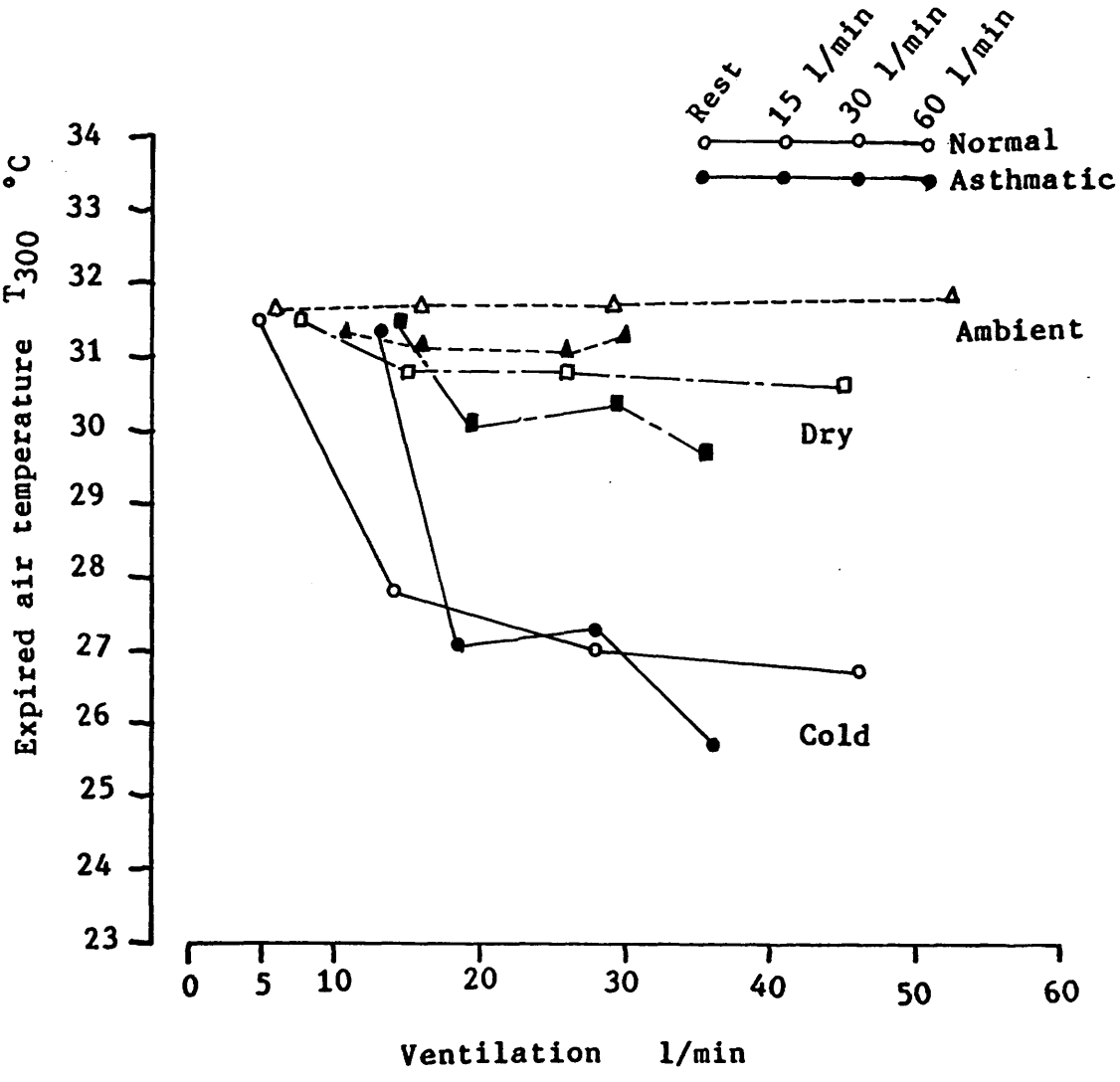

Figure 3.16: Comparison between end challenge expirate temperature in normals and asthmatics. For clarity error bars have been omitted.

groups. For both there was a significant difference ($p<0.05$) in T_{300} between ambient, dry and cold air hyperventilation. The graphs are summarised in figure 3.16 wherein the standard deviation bars have been ommitted for clarity.

The rate of airway cooling was computed using the expression cited in section 3.9. Similar RAC was encountered between the groups of approximately 0-0.1 °C/min (ambient air); 0.2-0.4 °C/min (dry air) and 0.8-1.1 °C/min (cold). Data are summarised in table 3.12. The post challenge responses to these airway cooling rates is plotted in figure 3.17.

Any given RAC was followed by a greater fall in FEV_1 in the asthmatics than in the normals.

Figure 3.17: Rate of airway cooling computed from T_{300} in normals and asthmatics.

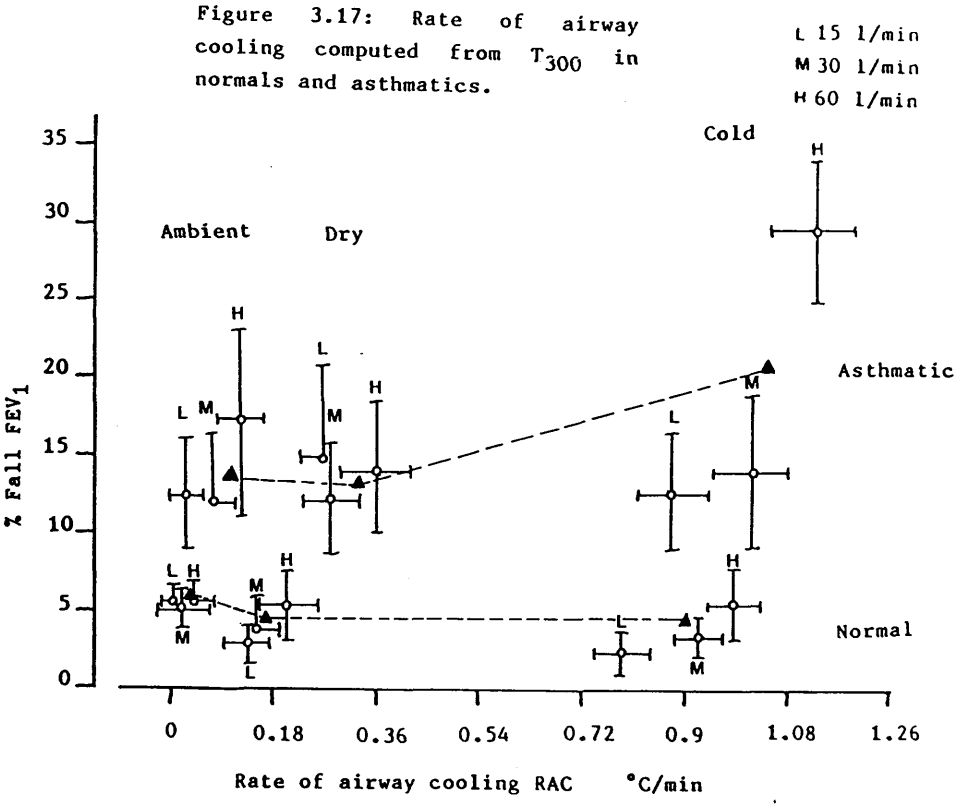

Table 3.07: Anthropometric and lung function data.

Subject	Sex	Age yrs	Height cm	rest FEV_1 l	% pred.
Asthmatic:					
1	F	20	158	2.16	72
2	M	37	167	3.02	86
3	M	36	174	4.43	119
4	F	34	162	2.89	101
5	F	25	166	2.65	82
6	F	39	149	2.00	85
7	M	39	174	2.77	75
8	F	62	156	1.95	88
9	M	49	175	2.06	60
Mean		37.9	164.6	2.66	85
(SD)		(±11.6)	(±8.6)	(±0.74)	(±16)
Normal:					
1	M	29	175	4.39	108
2	F	38	155	2.13	71
3	F	41	160	2.63	99
4	M	23	173	5.46	137
5	M	24	169	4.08	105
6	M	29	171	4.51	117
7	M	24	173	4.05	119
8	M	35	167	4.08	117
Mean		30.4	167.9	3.92	109
(SD)		(±6.4)	(±6.5)	(±0.99)	(±18)

Table 3.08: Basal RHE and ventilation rate.

Mean (SD)	Vent. l/min	T_{exp} °C	RHE. W
Asthmatic	12.63 (±6.2)	31.45 (±0.63)	19.26 (±5.7)
Normal	6.90 (±3.8)	31.55 (±0.62)	33.12 (±3.2)

Table 3.09: Post challenge FEV_1.

Vent. target l/min	15	30	60
Asthmatic: Mean (SD)			
Ambient	12.4 (±5.7)	12.0 (±7.6)	12.5 (±5.4)
Dry	11.8 (±9.2)	15.7 (±15.3)	13.9 (±9.2)
Cold	11.9 (±9.7)	13.9 (±14.1)	26.7 (±11.9)
Normal: Mean (SD)			
Ambient	5.0 (±1.4)	3.3 (±2.8)	3.8 (±2.1)
Dry	3.0 (±1.7)	4.4 (±2.1)	5.1 (±3.8)
Cold	2.8 (±1.6)	3.6 (±0.9)	5.6 (±2.6)

Table 3.10: Actual ventilation rates between groups.

Vent. target l/min Mean (SD)	15	30	60
Asthmatic			
Ambient	16.04 (±2.20)	24.52 (±3.25)	30.15 (±5.7)
Dry	19.02 (±5.86)	29.09 (±4.98)	35.74 (±12.0)
Cold	19.32 (±5.11)	27.30 (±4.99)	36.09 (±14.1)
Normal			
Ambient	15.87 (±3.00	27.50 (±2.24)	52.33 (±6.1)
Dry	14.71 (±2.06)	26.90 (±1.60)	46.70 (±7.2)
Cold	15.01 (±3.30)	28.15 (±3.20)	45.80 (±7.3)

Table 3.11: Expired air temperatures and statistical comparison between groups

Challenge	Expired air temp. (SD) °C Asthmatic	Normal	'T' test Norm>Asth t p<0.05
Ambient 15 l/min			
T_i	19.88 (±1.55)	22.44 (±1.21)	3.7 sig
T_{25}	30.91 (±0.52)	31.91 (±0.39)	4.3 sig
T_{150}	31.16 (±0.40)	31.84 (±0.42)	3.2 sig
T_{300}	31.01 (±0.60)	31.83 (±0.55)	2.8 sig
Ambient 30 l/min			
T_{25}	31.06 (±0.75)	32.01 (±0.41)	3.7 sig
T_{150}	31.09 (±0.41)	31.93 (±0.41)	3.2 sig
T_{300}	31.08 (±0.41)	31.85 (±0.46)	3.6 sig
Ambient 60 l/min			
T_{25}	31.34 (±0.24)	32.34 (±0.30)	7.4 sig
T_{150}	31.23 (±0.41)	31.91 (±0.39)	3.4 sig
T_{300}	31.21 (±0.40)	31.84 (±0.40)	3.0 sig
Dry 15 l/min			
T_i	20.89 (±2.08)	21.25 (±1.82)	-NS-
T_{25}	30.45 (±0.89)	31.26 (±0.74)	NS (sig p<0.1)
T_{150}	30.28 (±0.74)	30.79 (±0.52)	NS (sig p<0.1)
T_{300}	30.10 (±0.70)	30.68 (±0.74)	NS (sig p<0.1)
Dry 30 l/min			
T_i	20.92 (±2.05)	21.16 (±1.78)	-NS-
T_{25}	30.19 (±0.89)	31.26 (±0.74)	2.7 sig
T_{150}	30.20 (±0.67)	30.90 (±0.68)	2.2 sig
T_{300}	30.09 (±0.60)	30.70 (±0.74)	NS (sig p<0.1)
Dry 60 l/min			
T_i	20.81 (±2.13)	21.24 (±1.79)	-NS-
T_{25}	30.27 (±0.86)	31.51 (±0.69)	3.1 sig
T_{150}	30.01 (±0.59)	30.86 (±0.78)	2.4 sig
T_{300}	29.67 (±0.85)	30.65 (±0.57)	2.6 sig
Cold 15 l/min			
T_i	-22.04 (±1.92)	-20.18 (±1.97)	-NS-
T_{25}	28.78 (±1.06)	29.36 (±1.15)	-NS-
T_{150}	27.31 (±1.07)	28.24 (±1.12)	-NS-
T_{300}	27.04 (±0.65)	27.65 (±1.16)	-NS-
Cold 30 l/min			
T_i	-22.63 (±0.95)	-21.24 (±1.60)	-NS-
T_{25}	27.73 (±1.14)	28.83 (±1.07)	-NS-
T_{150}	26.91 (±1.37)	27.49 (±1.40)	-NS-
T_{300}	26.26 (±1.58)	26.88 (±1.30)	-NS-

Table 3.11, continued
Expired air temperatures and statistical comparison between groups

Challenge	Expired air temp. (SD) °C Asthmatic	Normal	'T' test Norm>Asth t $p<0.05$
Cold 60 l/min			
T_i	-22.61 (±1.11)	-20.57 (±1.52)	2.99 sig
T_{25}	27.46 (±1.76)	29.07 (±1.24)	-NS-
T_{150}	26.48 (±1.30)	27.20 (±1.31)	-NS-
T_{300}	25.91 (±1.36)	26.73 (±1.45)	-NS-

T_i inspired air temperature; T_{25}, T_{150} & T_{300} Early, mid and end challenge expiration temperatures; $p<0.1$: 90% confidence level; $p<0.05$: 95% confidence level.

Table 3.12: Rate of airway cooling °C/min

Vent. target l/min (SD)	15	30	60
Asthmatic:			
Ambient	0.16 (±0.02)	0.07 (±0.11)	0.11 (±0.07)
Dry	0.28 (±0.11)	0.27 (±0.08)	0.37 (±0.13)
Cold	0.89 (±0.15)	1.04 (±0.15)	1.13 (±0.19)
Normal:			
Ambient	0.02 (±0.09)	0.01 (±0.06)	0.05 (±0.06)
Dry	0.14 (±0.07)	0.14 (±0.06)	0.21 (±0.10)
Cold	0.78 (±0.17)	0.94 (±0.19)	0.98 (±0.24)

3.10. Comments.

3.10.1. Lung function.

Figure 3.10 illustrates the RHE plotted with the maximum post challenge fall in FEV_1 for both groups. The correlation for the group mean data obtained was $\%FEV_1=0.223(RHE)-2.73$ ($r=0.85$) whereas in the previous study (section 3.6) $\%FEV_1=0.13(RHE)-1.72$ ($r=0.96$), thus supporting the finding that airway response is directly proportional to the rate of heat exchange. The differences between the two correlations can be attributed to the two non-rebreathing valves used. In the present study the mean (SD) airway reponse after the 60 l/min cold air challenge was 26.7 ($\pm$11.9)% and in the previous study 20.7 ($\pm$11.0)%; both being 10-12% greater than the penultimate response. The higher rates of heat loss imposed during this particular challenge may have exceeded a threshold in airway tolerance to RHE and thereby provoked a further reduction in FEV_1. A plateau region of similar responses could be interpreted from figure 3.10 in the range 17.6-48.4 W although no statistical basis for the cut off in RHE could be found. A refractory effect would not have contributed to this observation because refractoriness has been shown by other workers[29,30] not to be present in hyperventilation induced asthma. Indeed had it been so it would have conferred protection against repeated challenges, section 3.4.1. Tiring of the subjects was considered not to have influenced the experiment as care was taken to ensure a full recovery before the final 60 l/min challenge. The rates of airway cooling are plotted in figure 3.17 with the airway response. No statistical basis for an RAC trigger was found although the diagram serves to emphasise the possibility of a 60 l/min cold air

hyperventilation threshold to heat loss. The cold air exposure - time test (section 3.2) raised the possibility of increased response to cumulative heat loss. Intuitively a cooler expirate will be developed with long term cold air hyperventilation. It is conceivable that the airway could accommodate long term exposure to cold but be sensitive to a short term exposure to a large RHER.

The expired air temperatures in the asthmatic group were lower than those in the normal group during ambient air hyperventilation. This phenomenon could have been explained by the slightly higher inspiration temperatures in the normals. However, the trend was repeated during the dry air challenge wherein the inspired air condition was not significantly different. In the cold air challenges a similar observation was made although statistical significance was lost due to the larger variation in expired air temperatures between individuals. This variation corresponds to a higher incidence of subject mismatching with the ventilation target.

At 15 and 30 l/min targets the ventilation rate in each group was matched but at 60 l/min the asthmatics displayed a larger undershoot than the normals. A lower ventilation rate can be expected to have conferred less airway cooling and higher expiration temperatures. Despite this the asthmatic expirate tended to be cooler.

Lower expiration temperatures in the asthmatics implies a cooler airway wall. Spencer (1973)[39] and Lopez-Vidriero and Reid (1983)[40] state that asthma is characterised by mucus plugging of the bronchi, an increase in both the size and number of mucus glands in the bronchial wall and thickening by oedema of the sub epithelial basement membrane (section 1.2). In terms of heat transfer, thickening of the tissues lining the airway would act as an insulating jacket attenuating the passage of heat from the blood capillary plexus to the airstream. Presumably tidal ventilation rates impose a level of heat loss which can be accomodated by the

blood capillary plexus even with the jacket. Alternatively, hypersecretion associated with greater numbers of mucus secreting glands could act as a coolant boundary leading to an increase in the return of heat to the airway wall from the expirate.

At a biochemical level differences have been observed to occur in asthmatics, but not in normals during exercise and hyperventilation challenges such as mediator substance output described in section 3.7.1. Cardiac output will be greater during the exercise challenge thus the possibility of an air conditioning deficiency herein is unknown. Because the tidal expiration temperatures observed in the asthmatic and normal groups were similar it is possible that hyperventilation stimulated airway hypersecretion and/or epithelial thickening by oedema. Both mechanisms could operate simultaneously serving to jacket the airway and reduce expiration temperatures during the challenge.

3.10.2. Errors and modifications.

The Mk2 non rebreathing valve yielded more accurate expiration temperature data which, during tidal breathing, were compatible with that found by direct insertion of thermocouple into the oral airstream. The connecting dead space between the inspiratory port and the cold air supply was approximately 80 ml. Using a direct measurement at the mouth a rewarming gradient between the supply and patient of up to 8°C was found. Cold air had been bled through the valve prior to challenging the patients and this was found to reduce the rewarming gradient to 3-5°C. The largest overestimate in RHER computation are likely to have arisen during the 60 l/min cold air challenge due to greater internal air turbulence especially about the leaflet discs on each non-rebreathing port (figure 3.09). The supply air temperature and ambient air temperature can also be expected to have influenced the size of error. On the basis

of a supply air temperature of -22°C and an expirate of 27°C, using the equation cited in section 3.4.2 and substituting:

T_e=27°C; w_e=27 mg/l (0.0227 kg/kg)
T_i=(-22)°C; w_i=0.3 mg/l (0.0003 kg/kg) and
V_{RMS}=60 l/min m_a=0.000554 kg/s

yields an RHE = 54 W

With T_i=-17°C, RHE=56 W an error of 5%
and T_i=-14°C, RHE=54 W an error of 8%.

A new low dead space and fast response time non rebreathing valve has since been designed by the author and is described in section 8.2.

3.11. Overview of work done.

The magnitude of airway response following a hyperventilation challenge has been found to be in proportion to the imposed rate of respiratory heat exhange (RHER); regardless of the nature of the thermal burden. Cold air breathing caused the highest RHER and was followed by the largest airway responses. Similar airway responses were observed in the range 17-48 W RHER and could be interpreted as the presence of an airway threshold to RHER. These observations could be explained by a thermoceptor role in airway sensitivity to heat loss. However, evidence for a lower temperature expirate in the asthmatic group was found. This could be explained by the presence of airway oedema and/or hypersecretion, provoked during the hyperventilation phase by mediator activity.

Hyperventilation induced asthma has been used as a model of heat loss in exercise induced asthma although physiological and biochemical differences between the two

have been described. The rate of respiratory heat loss per se is an important component in hyperventilation induced asthma. If this pertains for exercise then minimising RHER should attenuate bronchoconstriction.

The site of maximal heat exchange in the airway is of particular interest. If the cumulative effect of respiratory heat loss or the rate of heat loss are crucial in the production of the response then it is reasonable to assume that the location of maximal in vivo cooling and drying is also the area from which the airway response is triggered.

The following chapters allude to these points.

4. Long Axis Air Conditioning.

4.1. Introduction.

Examination of equation 3 (section 1.2) shows that if warm humidified air (32°C-33°C and 100%RH) is inhaled, thus matching the expired air condition, then respiratory heat exchange is suppressed. By negating heat loss in an exercise challenge it is possible to observe the sole effect of physical exertion in provoking an asthmatic response. Long axis air conditioning is the process name chosen to describe the operation of an air heater - humidifier developed by the author for the current study.

The humidifier was also intended as a representation of the air conditioning process in the human airway. Using the device data were generated for a numerical model of long axis air conditioning. This numerical model was pursued in order to describe the thermodynamic factors governing simultaneous heat and water vapour transfer. Following this work an apparatus capable of delivering, in excess of 100 l/min, droplet free humidified air (32°C-38°C, 100%RH) for use in a heat loss free exercise challenge was designed. Chapter 4 deals with the design and development work done in respect of long axis air conditioning and a clinical trial involving heat loss free exercise is presented in chapter 5.

4.2. Types of humidifier available.

Prior to developing the long axis air conditioner several commercially available air humidification systems and their mode of operation were considered. These are classified as either water bath devices or aerosol generators and are generally limited to tidal air flow rates.

Water bath humidifiers are of either the bubble type or proximity type. Bubble type units are widely used in respiratory rehabilitation medicine and operate by passing air through a reservoir of water. Typical performance is 37°C, 100%RH at 30 l/min air flow rate (Inspiron Inc Aerway 300). Proximity devices allow air contact with a wetted wick and yield similar air conditioning performance (Puritan Bennet Inc 7203). Water bath humidifiers suffer from the accumulation of condensed water in the tubes serving the patient (the external airway) thus presenting a drainage problem and are therefore liable to bacterial infection. Without additional immersion heating of the water bath reservoir the conditioned air temperature is below ambient temperature since evaporation requires the absorption of energy as latent heat of evaporation. Bubble devices produce an air stream laden with water droplets. Filtering can attenuate the potentially irritating effect of droplet impaction with the airway but the additional condensate could worsen the drainage problem and causes a reduction in inspired air temperature and water vapour content.

A recent variation on the wetted wick design is a disposable hydrophobic (non-wetting) filter media placed in the external airway. These 'heat and moisture exchangers' are gaining acceptance in anaesthesia and operate by retaining condensed exhaled water which vaporises on the next inspiration. Gravelyn et al (1987)[41] have found these devices effective in preventing hyperventilation induced asthma although because the inspired water content was dependent on the patient's ventilation rate no quantitative comment with regard to heat loss or water loss could be made.

Commercial aerosol generators operate either by jet nebuliser action or the ultrasonic vibration of a piezoelectric crystal. Jet nebulisers comprise a high velocity air stream flowing perpendicular to the end of a

capillary tube. At its opposite end the capillary is immersed in a fluid bath. Fluid drawn up the capillary by the Bernoulli effect is torn into the airstream and fragmented. Aerosol droplets having a diameter in the range 1um-100um (Lichtiger and Moya 1974[42]) are produced. With filtering this can be reduced to 1um-10um. Smaller drops tend to evaporate increasing the vapour concentration in the air stream whereas the larger diameters coalesce, ie "rain out" leading to mechanical impact on the airway. Jet nebulisers are commonly used in the lung function laboratory as an aerosol delivery system and are limited to tidal air flowrates.

Piezoelectric devices such as the Timeter MP500 (Timeter Inc USA) vibrate water drops at a frequency of 1-2MHz producing aerosol diameters in the range 0.5um-5um. A fan drives the mist produced to the patient and an airstream laden with several times the moisture content of air saturated at body temperature is possible. Air flowrate is restricted to 10 l/min.

A variant on this principle is the 'Spinning Top' aerosol generator available from Research Engineers (Shoreditch, London). The device was inspected at the Department of Thoracic Medicine, Royal Free Hospital, (London). It comprises a stainless steel conical platform of 15mm diameter supported by an air bearing. The top spins with a rotational speed of ¼ million RPM. Water droplets directed onto the rotating platform fragment into a water spray having a particle diameter of 22um (Cheah and Davies 1984[43]) with an air flowrate of up to 100 l/min. A droplet laden airstream and the need for particle filtering were anticipated. In addition the device costs £2500 (1986 prices) and requires the development of a housing and water delivery mechanism.

4.3 Design.

The long axis air conditioner was originally intended as a thermodynamic model of the heat and water vapour process occurring in the human airway. Encouraging results from a prototype (Mk 1) led to the development of a version suitable for exercise challenge studies (Mk 2).

In the human airway inspired air is mixed against a wet and warm boundary whose geometry varies both axially and circumferentially. The long axis air conditioner consists of a warm water film drained over the internal surface of a downtube of uniform diameter. Air passed through the tube simultaneously gains heat and water vapour through the process of natural convection and evaporation. Exit air is characterised by an absence of droplets or super saturation inherent in the humidifiers alluded to in section 4.2. Only one similar device was later found to have been built (Gilland and Sherwood, 1934[45]) shown in figure 4.01, which was used to determine the vapour uptake in air from various fluid films.

Figure 4.02 illustrates the salient features of the present Mk 1 device. The mounting and water supply lines have been omitted for clarity. It was built of perspex by the Mechanical Workshop in the Department of Clinical Physics and Bioengineering. At one end of a 23mm ID tube, 1 m long, is press fitted a two piece spray head (2,4). Water enters the head via four inlet ports (located on 4) and is directed through four 2mm holes towards the axial centre of the down-tube. The emergent spray impinges on a hollow diffuser (1) and is deflected onto the inside surface of the downtube. The interfacial gap between the diffuser and downtube is approximately 1.5mm. Airflow forces any drop accumulation on the diffuser lip back into the water film by virtue of entry expansion effects. At the opposite end of the tube a hollow baffle (9) seals the air exit point

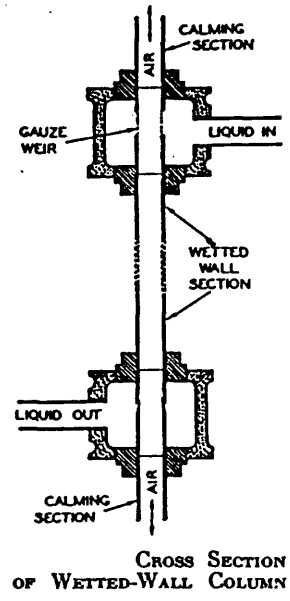

CROSS SECTION OF WETTED-WALL COLUMN

Figure 4.01: Gilland and Sherwood vapour uptake apparatus (1934). The physical principle of operation is identical to the long axis conditioner. Presumably the present spay head would allow a greater water film flowrate.

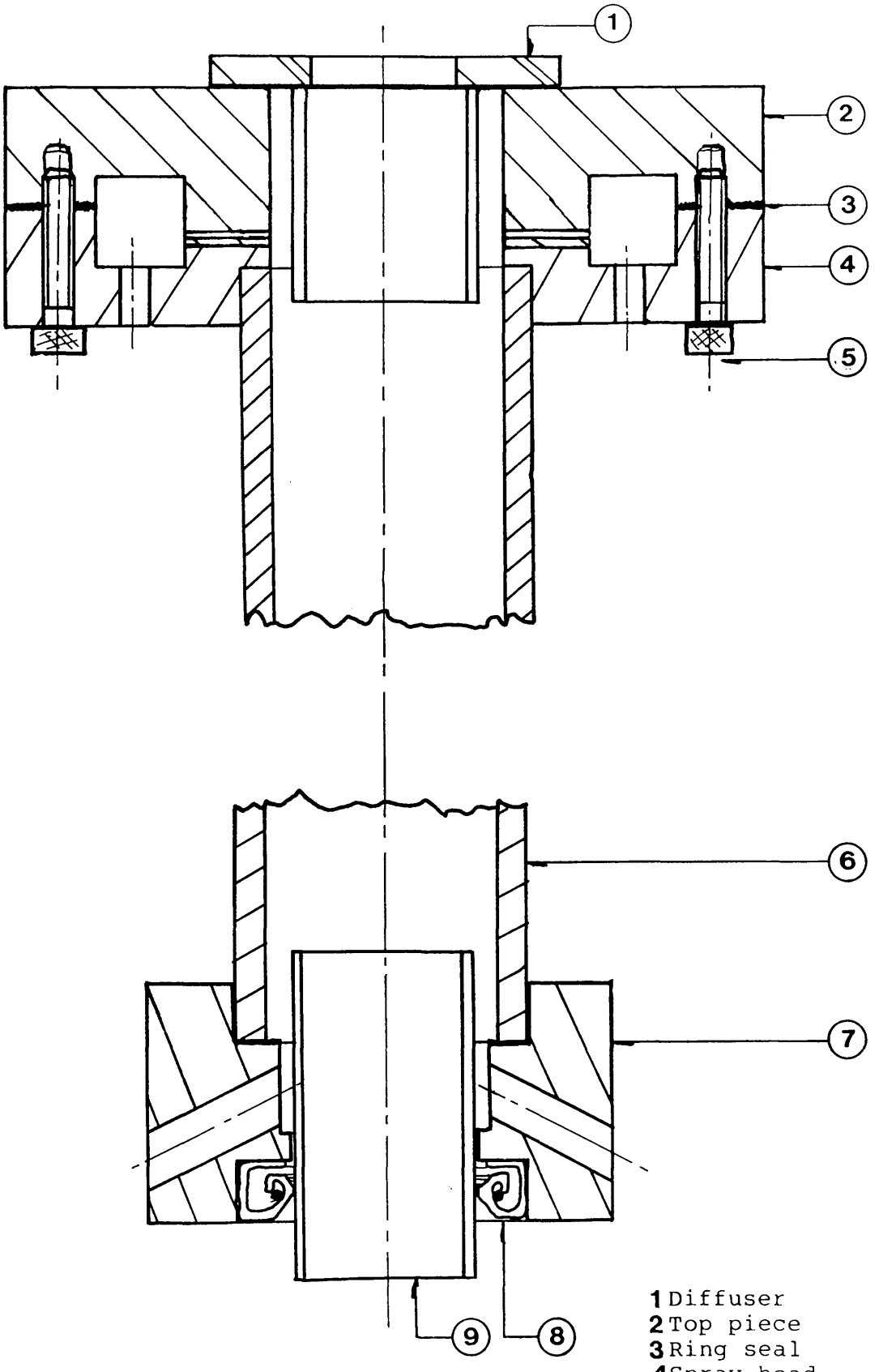

1 Diffuser
2 Top piece
3 Ring seal
4 Spray head
5 Retaining screw
6 Down tube
7 Exhaust cup
8 Lip seal
9 Air exit Baffle

Figure 4.02: The long axis air conditioner. The device was fabricated from perspex bar and tube.

from the film which drains through a manifold (7), again press fitted to the tube.

Water film flowrate was measured by recording the time taken to fill a 1 litre volume located at the film outlet and was typically 40 s yielding a consumption of 1.5 l/min. The passage time of the film through the actual downtube was estimated by timing the washout period of a 10 ml bolus of blue ink injected into the inlet water supply and visually observing the exhaust water. The volume of the inlet and outlet pipes was predetermined by filling with water and the film flowrate was set to 1.5 l/min. Passage time was calculated to be 0.6 s with a corresponding mean film thickness of 0.2 mm. Appendix 7 gives a description of the calculations.

4.4. Evaluation.

4.4.1. Axial rise in air temperature.

In order to fulfill the role as a thermodynamic model of airway heat and water vapour transfer it was necessary to quantify the axial rise in air temperature along the conditioner. These data are later compared with the results of a direct measurement of in vivo air temperature described in chapter 6. This work has been published, Farley & Patel (1988)[48].

Determination of the local air temperature within the conditioner was done using the apparatus shown in figure 4.03. A 'T' type thermocouple was lowered 90cm along the centre line of the conditioner at intervals of 10cm via a 35 SWG copper tension wire restrained mechanically at the entry point. The wire passed through a pinhole central to the base of a plastic tub which was glued to the conditioner exhaust manifold. Air exit was facilitated by means of a 35mm ID plastic conduit, 2m long, glued to one side of the tub. Air was sucked through the conditioner in

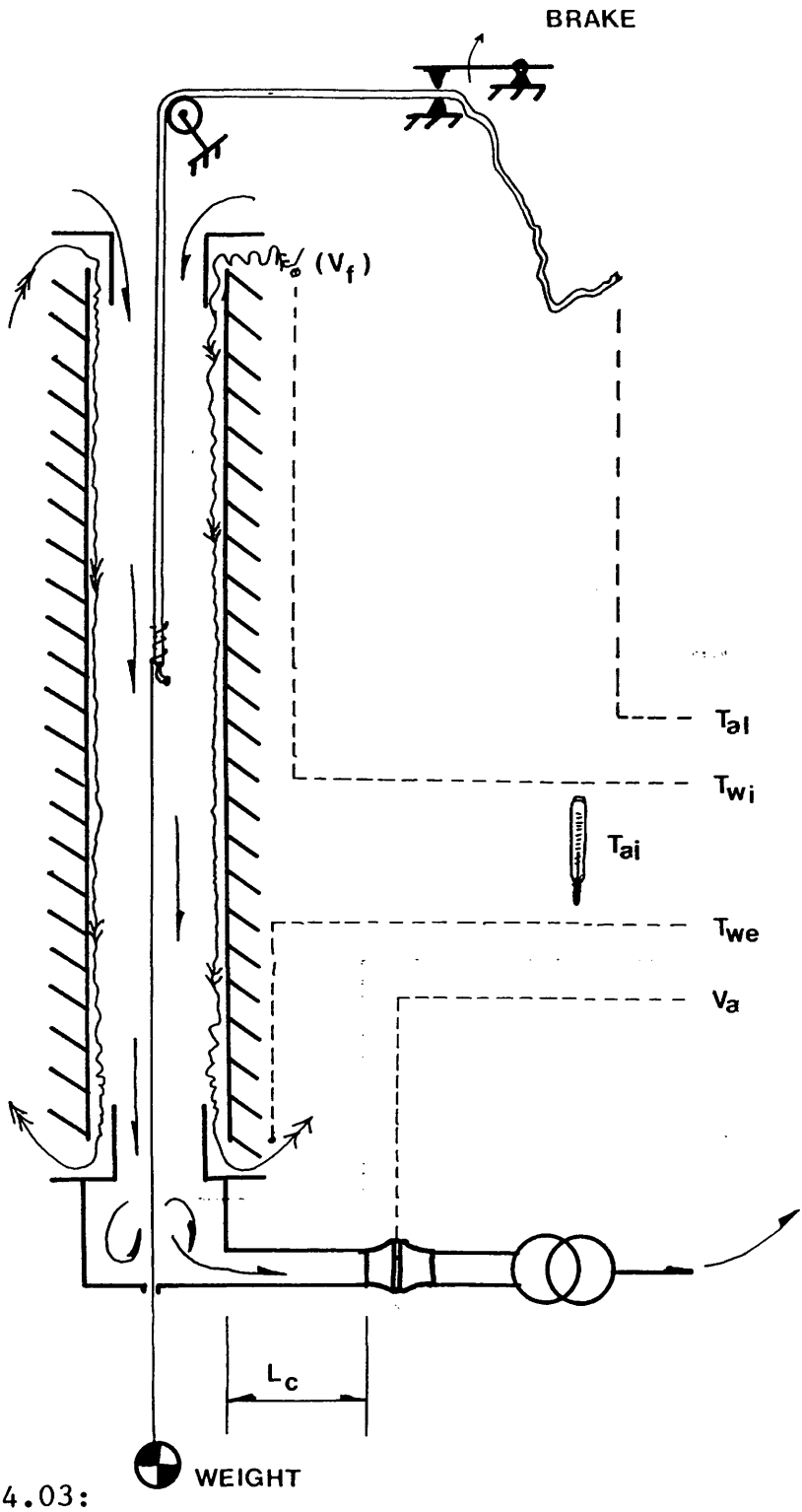

Figure 4.03:
Long axis humidifier: air warming vs exposure length.

T_{ai} : Inlet air temp; T_{al} : Local midstream air temp;
T_{wi} : Inlet water film temp; T_{we}: Exit water film temp;
V_a : Air flowrate; V_f: Film flowrate; L_c : Condensing length 2m.

order to minimise entry effects at flowrates in the range 7.5 l/min to 100 l/min and parallel to the direction of water film flow. Film entry temperature was adjusted to about 38°C by means of mixing the hot and cold tap water supply through a 'Y' piece. This temperature was similar to that expected at the body core and the film was delivered at 1.5 l/min, which by experiment was found to yield a stable and approximately isothermal boundary (section 4.4.2).

The data acquisition system described in section 2.3 was used to collect 100 samples of local air and water film inlet temperatures at 10Hz. The thermocouple was then lowered to the next station and the measurements repeated. Air flowrate was set prior to commencing data acquisition at the first station (0cm).

Figure 4.04 illustrates the long axis rise in air temperature over the range of air flowrate 7.5 l/min to 100 l/min. The mean (SD) film temperature was 38.4°C ($\pm$0.4). For a 90cm exposure length the observed exit air temperature for air having an inlet condition of 23°C 48%RH ranged between 38.5°C (7.5 l/min) and 30.1°C (100 l/min). The family of curves shown are characterised by rapid initial air warming followed by a progressive reduction in the rate of air temperature rise toward an equilibrium temperature with the film boundary.

4.4.2. Exit air temperature.

Ambient air (20°C, 45%RH) was pumped through the long axis air conditioner at air flowrates of 15, 30, 60 and 100 l/min, again parallel to the direction of film flow. Film temperature was varied between 30°C and 50°C at a water flowrate of 1.1-1.2 l/min by mixing the hot and cold water supply described in section 4.4.1. The exit air temperature was monitored using the 'Microlink' to sample voltage from a 'T' type thermocouple taped to the exhaust

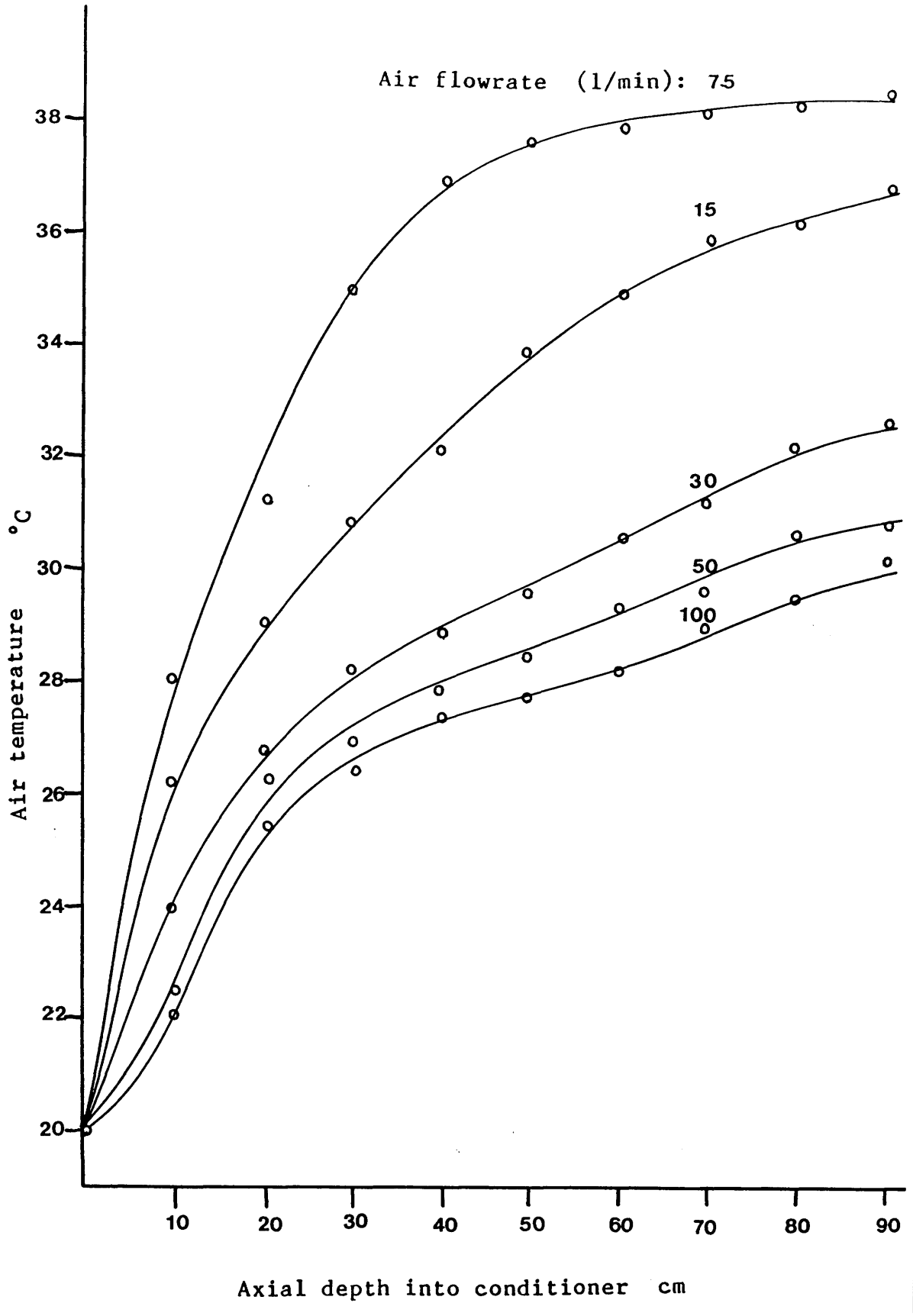

Figure 4.04: Axial rise in air temperature in the conditioner.

manifold.

For any film temperature the exit air temperature was found to be inversely related to the air flowrate through the conditioner, illustrated in figure 4.05. Following exposure to the maximum film temperature of 50°C exit air temperature ranged between 35°C (100 l/min) and 46°C (15 l/min).

In a subsequent parallel versus counter flow evaluation a maximum film temperature of 56°C was obtained, the increase due to the daily fluctuations in the hospital hot water supply. Ambient air of 23°C, 48%RH, was pumped parallel to, and later counter to, the direction of film flow at air flowrates of 15, 30, 50, 75 and 100 l/min. Film flowrate ranged between 1.3-1.4 l/min. Exit air temperature and film inlet and outlet temperatures were monitored with the 'Microlink' system and a 'T' type thermocouple located inside the requisite ports.

In counter flow mode the exit air temperature was found to be consistently higher than that in parallel. At a film temperature of 56°C and air flowrate of 100 l/min these exit air temperatures were 48°C (counter) versus 44.3°C (parallel) and at a film temperature of 30°C, 100 l/min air flowrate, were 27.4°C versus 25°C respectively. Figure 4.06 compares the performance of each mode. Although less efficient the parallel flow configuration was considered mechanically easier to implement for the Mk2 treadmill design described in section 5.1.

When running at full capacity,ie 56°C film temperature, 1.2 l/min film flowrate and 100 l/min air flowrate, the water film temperature was found to decline by 2.5°C over the length of the conditioner. This corresponds to a 4.5% reduction in the inlet temperature of the water whereas a gain of 192% in air temperature arose during full capacity parallel air flow. Figure 4.07 illustrates the marginal cooling of the water film in relation to a line of thermal

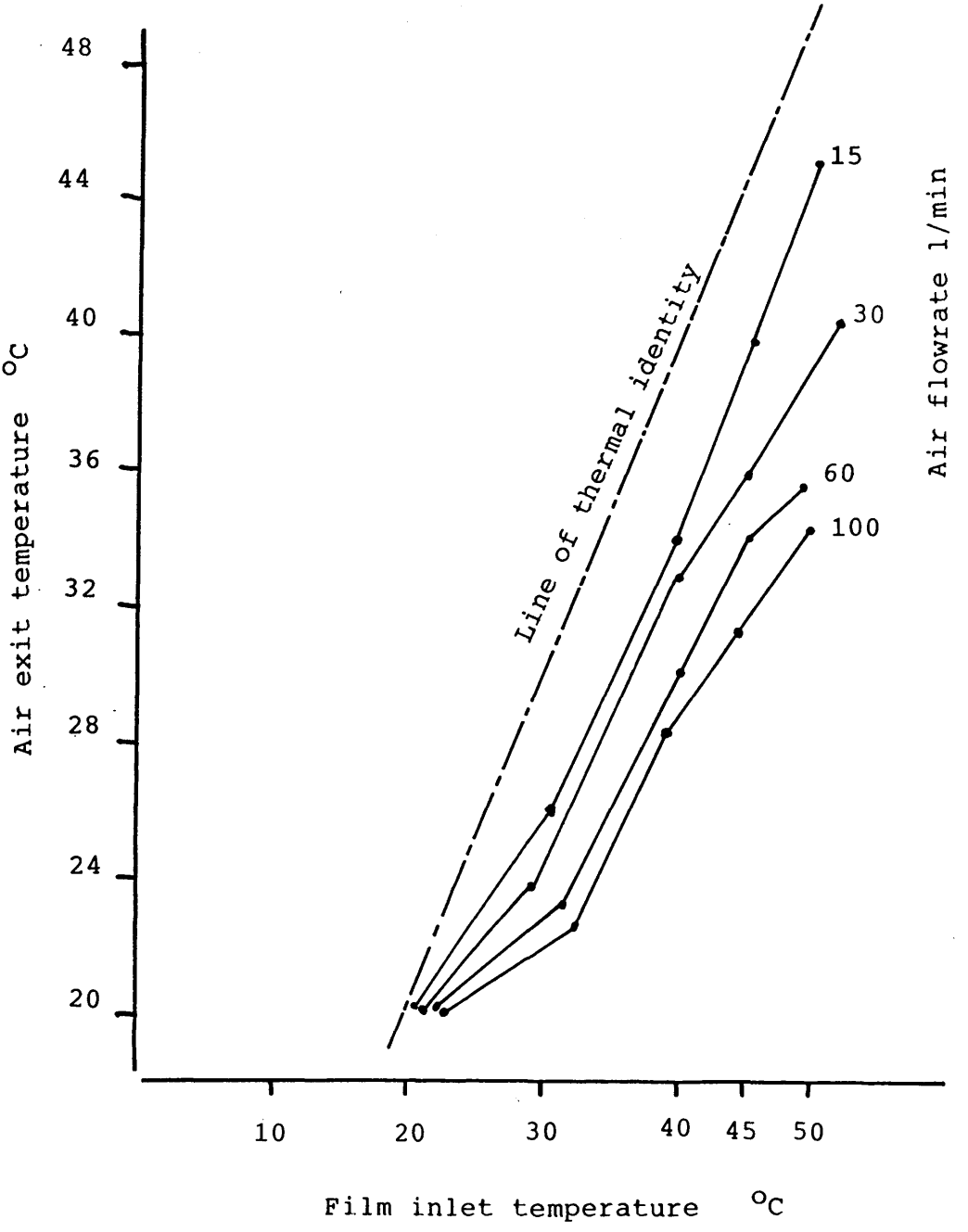

Figure 4.05: Exit air temperature and film inlet temperature.

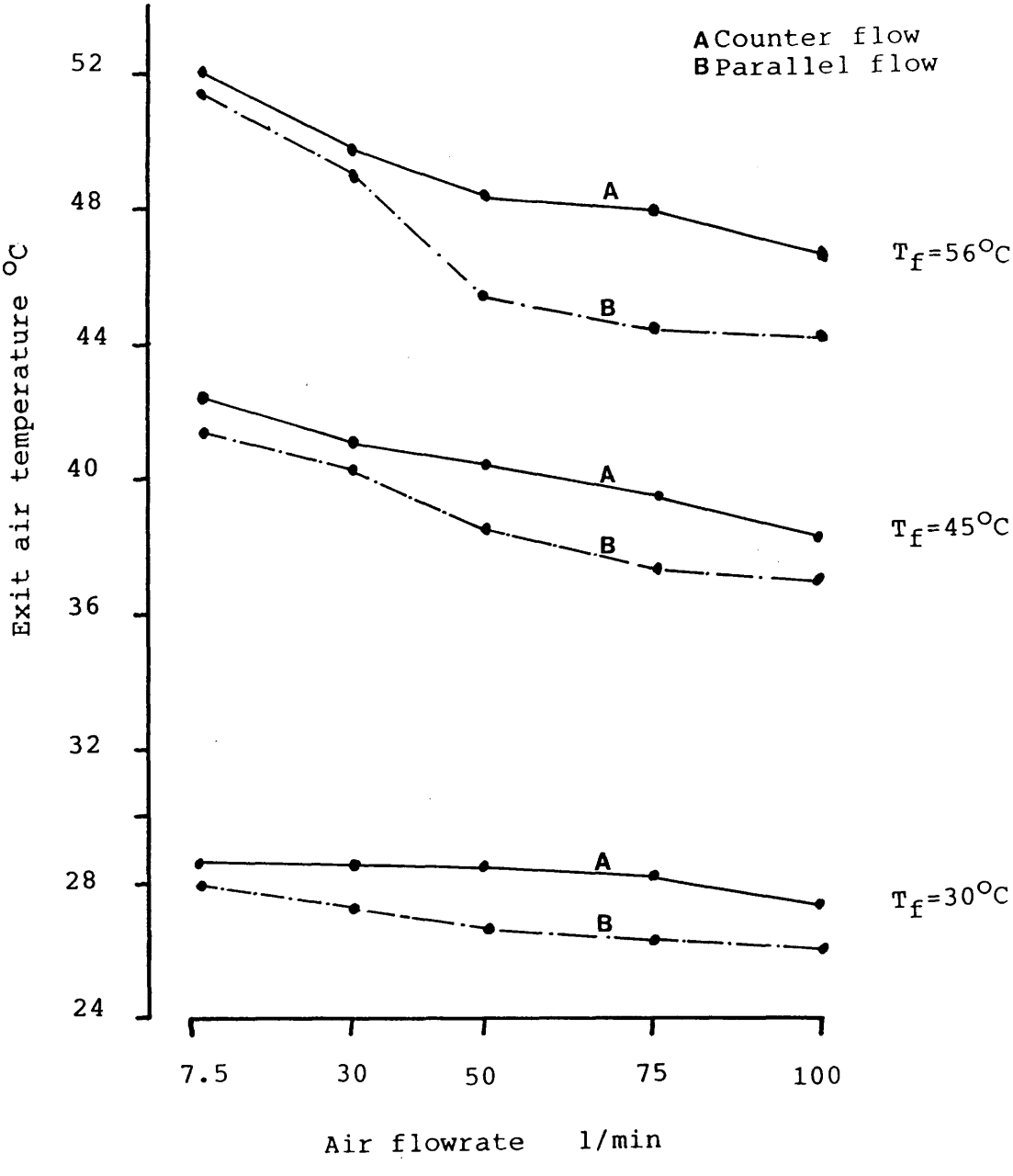

Figure 4.06: Parallel air - film flow compared with counter air - film flow. The counter flow mode was observed to be a more efficient air warmer.

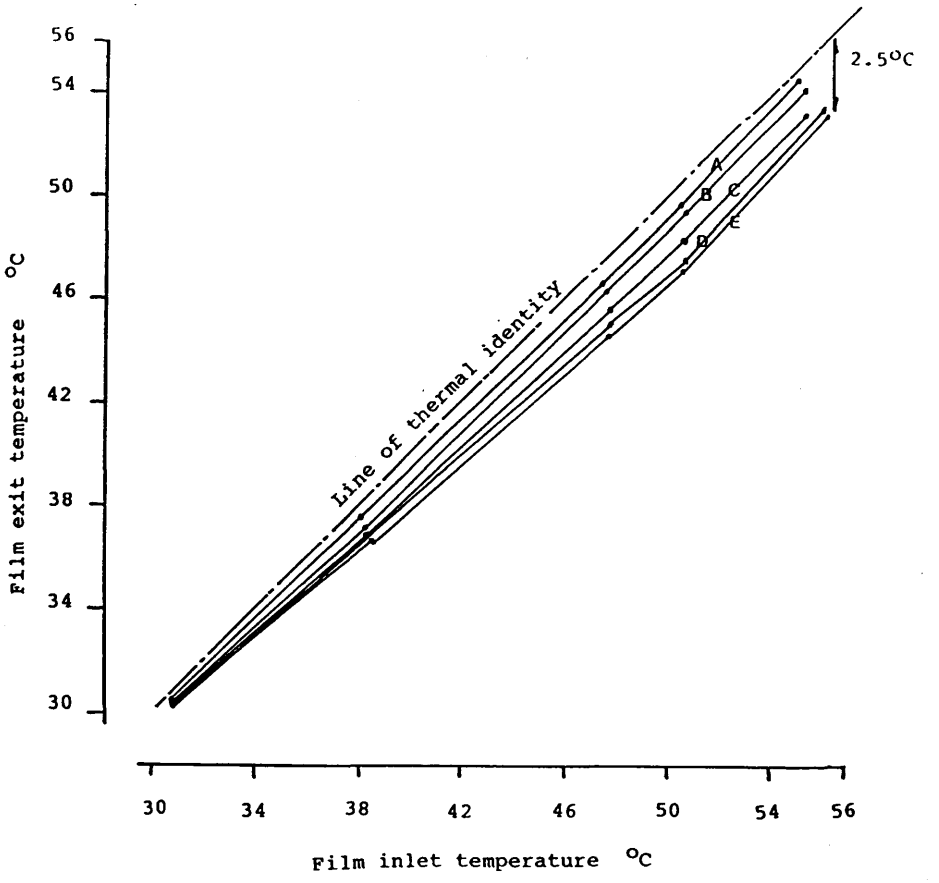

A: 15 l/min; B: 30 l/min; C: 50 l/min; D: 75 l/min; E: 100 l/min

Figure 4.07: Inlet vs Outlet film temperatures with a range of air flowrates. The line of thermal identity is shown: the axial film temperature can be approximately described by its inlet condition.

identity. On this basis the film boundary was considered to be isothermal and described by its inlet temperature.

4.4.3. Humidification.

The design remit was to produce a droplet free conditioned air stream in order to balance airway heat loss arising from conditioning the expirate.

Ambient air (20°C, 45 %RH and 8 mg/l) was pumped in parallel mode through the long axis air conditioner. With the film temperature set to 50°C and air flow to 100 l/min the emergent air temperature was 35°C previously described in section 4.4.2. and illustrated in figure 4.05. Exit water vapour content was determined by first measuring the wet and dry bulb temperatures of the exit air using a swing hygrometer held against the exhaust manifold for approximately 1 minute. Vapour content was then estimated using the psychrometric relation described in section 2.4.4.

For a given air flowrate exit water vapour content was found to be directly related to the film inlet temperature, shown in figure 4.08. Lines of full saturation are also drawn: the percentage ratio between the actual and full saturation curves for a given film temperature and air flowrate yields the relative humidity of the exit air. At a film temperature of 50°C the water vapour content of the exit air was determined to be 31.6 mg/l (100 l/min air flow) or 80%RH at 32°C exit air temperature. Ambient air (22°C, 48%RH and 9.5 mg/l) flowing at 100 l/min when exposed to a 56°C film boundary emerged with a condition of 35°C, 90%RH and 38 mg/l. By comparison a vapour content of 40.4 mg/l (15 l/min air flow) was found or 58%RH at 45.5°C exit air temperature, indicating that the rate of vapour uptake by long axis air conditioning is also dependent on turbulant mixing of air against the film boundary associated with higher air flowrates.

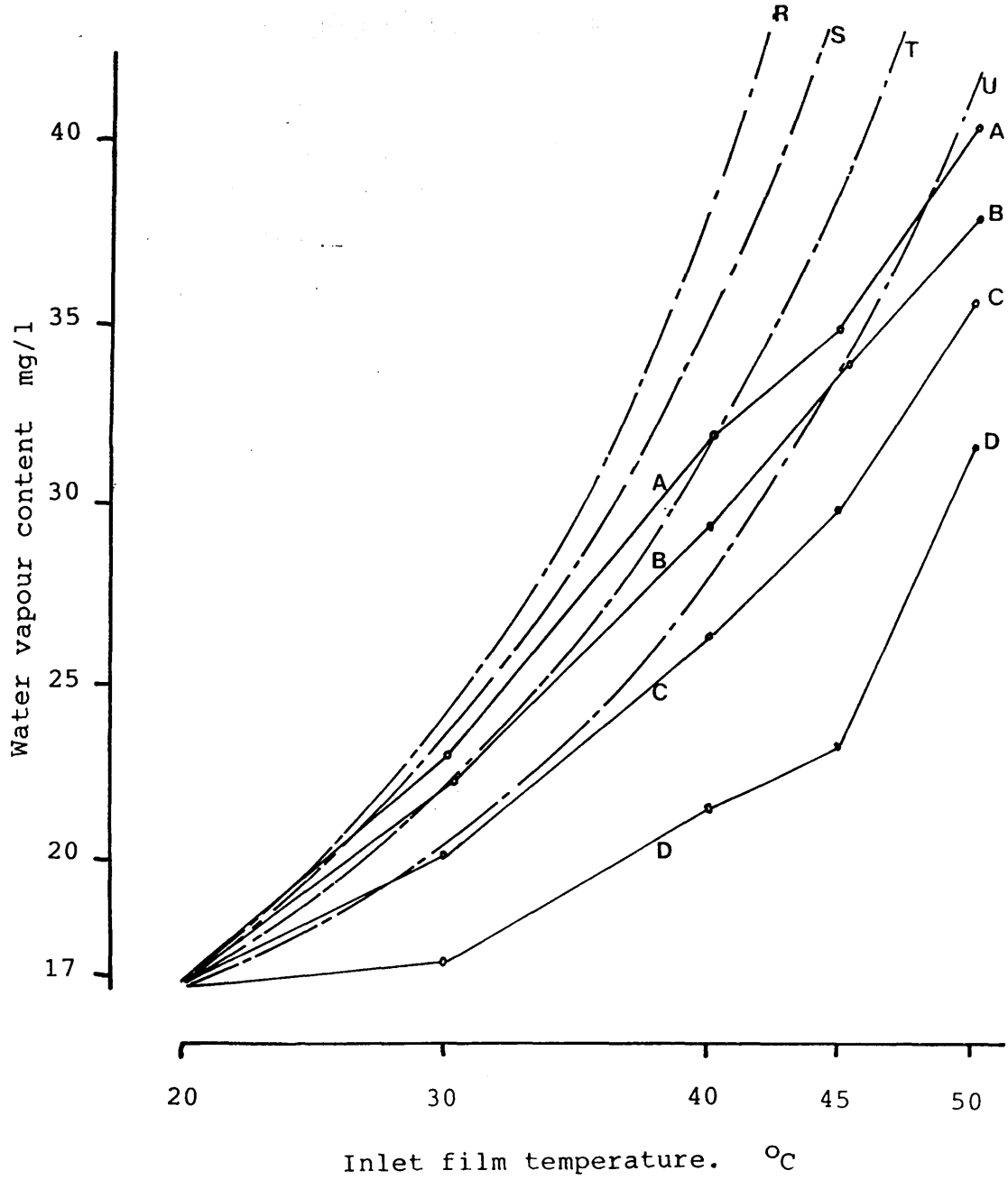

Line of actual water vapour content:
A: 15 l/min; B: 30 l/min; C: 60 l/min; D: 100 l/min

Line of fully saturated water vapour content:
R: 15 l/min; S: 30 l/min; T: 60 l/min; U: 100 l/min

Figure 4.08: Water vapour content of the exit air.

4.5. Finite difference model.

4.5.1. Basic equations.

Water vapour uptake and heat transfer to the free stream occur simultaneously in the long axis air conditioner. An examination of the equations governing this would reveal the principal thermodynamic factors at work. Moreover a better understanding was sought prior to designing the Mk2 long axis device for use clinically. The system of equations used have been described by Hanna and Scherer (1986)[45] as part of a model of distributed heat and water exchange in the human airway. They are derived by the author in appendix 8. The axial rise in air temperature inside the conditioner was numerically modelled using a finite difference predictor-corrector (P-C) algorithm which is given in appendix 9.

Assumptions governing the model were:

i) a steady state airflow;
ii) an isothermal water film boundary;
iii) the existance of a boundary region of fully saturated air at film temperature located at the air-film interface which drives the conditioning process and
iv) negligible axial diffusion of heat and water vapour.

Figure 4.09 illustrates an axial segment of the long axis conditioner with the heat and water vapour gradients arising perpendicular to the direction of air flow. The equations used to predict to axial rise in water vapour content and air temperature were based upon the conservation of mass, momentum and energy. They were:

Figure 4.09: Axial segment in the long axis air conditioner. Notation is given in section 4.5.

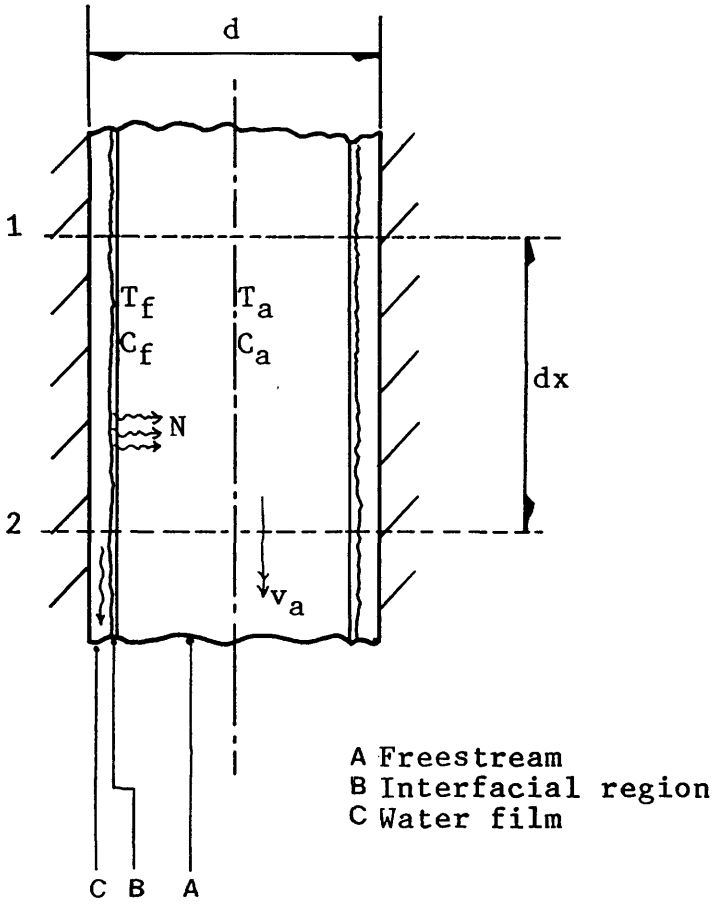

$$N=k_c.(c_f-c_a) \quad \text{.....1}$$

$$v_a.(dC_{12}/dx)=(P/A).k_c.(c_f-c_a) \quad \text{.....2}$$

$$v_a.(dT_{12}/dx)=(P/A.\rho.C_{pa})[h_c+N.C_{pw}.M_w] \quad \text{.....3}$$

Notation for equations.

Symbol	Name	Units
A	Area	m^2
c	Water vapour concentration	mol/cm^3
C_p	Specific heat	J/kg K
d	Down tube diameter	m
dx	Axial segment length	m
D_{ab}	Diffusion coefficient for water vapour in air.	m^2/s
h_c	Heat transfer coefficient	W/m_2 K
k_c	Mass transfer coefficient	m/s
k_t	Thermal conductivity of air	W/m K
L	Representative length	m
m	Mass flowrate of air	kg/s
M_w	Molecular weight of water	kg/kmol
P	Down tube perimeter	m
Pr	Prandtl number	-
ρ	Density	kg/m^3
Q_{conv}	Convective heat transfer rate	W
Q_{sen}	Sensible heat transfer rate	W
Sc	Schmidt number	-
T	Temperature	K
μ	Dynamic viscosity of air	kg/m s
v	Velocity	m/s

Subscripts: a air; w water; f film; 1, 2 axial station.

Equation 1 predicts the flux of water vapour evaporating into the free stream due to the concentration gradient (c_f-c_a) between the interfacial region and the air. Equations 2 and 3 are statements of the conservation of mass and momentum (2) and energy and momentum (3) for the axial segment dx. These were solved using the P-C algorithm described in appendix 9.

Solution to equations 1 to 3 requires values of T_a, c_a, T_f, c_f, k_c and h_c. T_f is considered isothermal and c_f can be derived from the psychrometric relation given in section 2.4.4.

Initially T_a and c_a are known. The heat transfer coefficient h_c was derived from the experimental data presented in section 4.4.2. This was then used to estimate the mass transfer coefficient k_c by means of the energy and mass transport analogy described by Chilton and Colburn, given in Welty (1984)[46].

4.5.2. Derivation of the transport coefficients h_c and k_c.

The parameter h_c describes the flux of heat necessary to raise the air temperature by 1 degree Kelvin. It is a function of the physical properties of the air and the magnitude of the temperature gradient between the film and freestream. Free convection of air has an h_c of 5 - 50 W/m^2 K and boiling water 2500 - 250,000 W/m^2 K (Welty et al 1984). By analogy k_c describes the mass flux of material driven by a concentration gradient and takes the units m/s.

The convective heat transferred from the water film to the air, Q_{conv}, is associated with air warming and is given by the Newton Rate Equation, Rogers and Mayhew (1983)[47]:

$$Q_{conv} = h_c.A.(T_f-T_a)$$

The increase in air temperature over the axial distance dx can also be expressed as a sensible heat gain, Q_{sen}, thus for an air stream of mass flowrate m (kg/s):

$$Q_{sen} = m.C_{pa}.(T_2-T_1)$$

Applying the conservation of energy principle $Q_{sen}=Q_{conv}$, therfore:

$$h_c.A.(T_f-T_a) = m.C_{pa}.(T_2-T_1)$$

or

$$h_c = (m.C_{pa}/A).(T_2-T_1)/(T_f-T_a) \qquad .....4$$

In the calculations T_a was taken to be the midpoint temperature between stations defined as:

$$T_a = T_1+(T_2-T_1)/2 \qquad .....5$$

With an internal diameter of 23 mm and axial segment length of 10 cm the internal surface area A of the downtube was estimated to be 0.00723 m^2. For a given air flowrate v (l/min) the mass flow of air m (kg/s) was estimated by the conversion:

$m = \rho.v/(60).(1000)$ where $\rho=1.255$ kg/m^3.

Multiplying by C_{pa}/A, where C_{pa}=1005 J/kg K yields

$m.C_{pa}/A$= 2.91 (v) which substituted into equation 4 gives

$$h_c=2.91(v).(T_2-T_1)/(T_f-T_a) \quad .....6$$

Using equations 5 and 6, h_c was computed from the experimental data and is presented in appendix 10. Figure 4.10 illustrates the local values of h_c along the conditioner. In general the increased action of entry expansion turbulance associated with the higher air flowrates conferred a greater h_c.

Estimation of k_c was done using the transport analogy described by Chilton and Colburn, in Welty et al (1984)[48] which is summarised as:

$$k_c=h_c/(\rho.C_{pa}).(Pr/Sc)^{0.66}$$

Pr is the Prandtl number describing the ratio between molecular diffusivity of heat and mass. Sc is the Schmidt number describing the ratio between molecular diffusivity of momentum and mass. Both are dimensionless and are described in appendix 11 with the transport analogy. The Chilton - Colburn analogy allows the determination of an unknown transport coefficient from knowledge of another and is valid for Pr in the range 0.6 - 100 and Sc in the range 0.6 - 2500. The present values of Sc and Pr were estimated to be 1.8 and 100.6.

Software for the model was written in MSBASIC and a listing is given in appendix 12. An example of screen output is shown in figure 4.11.

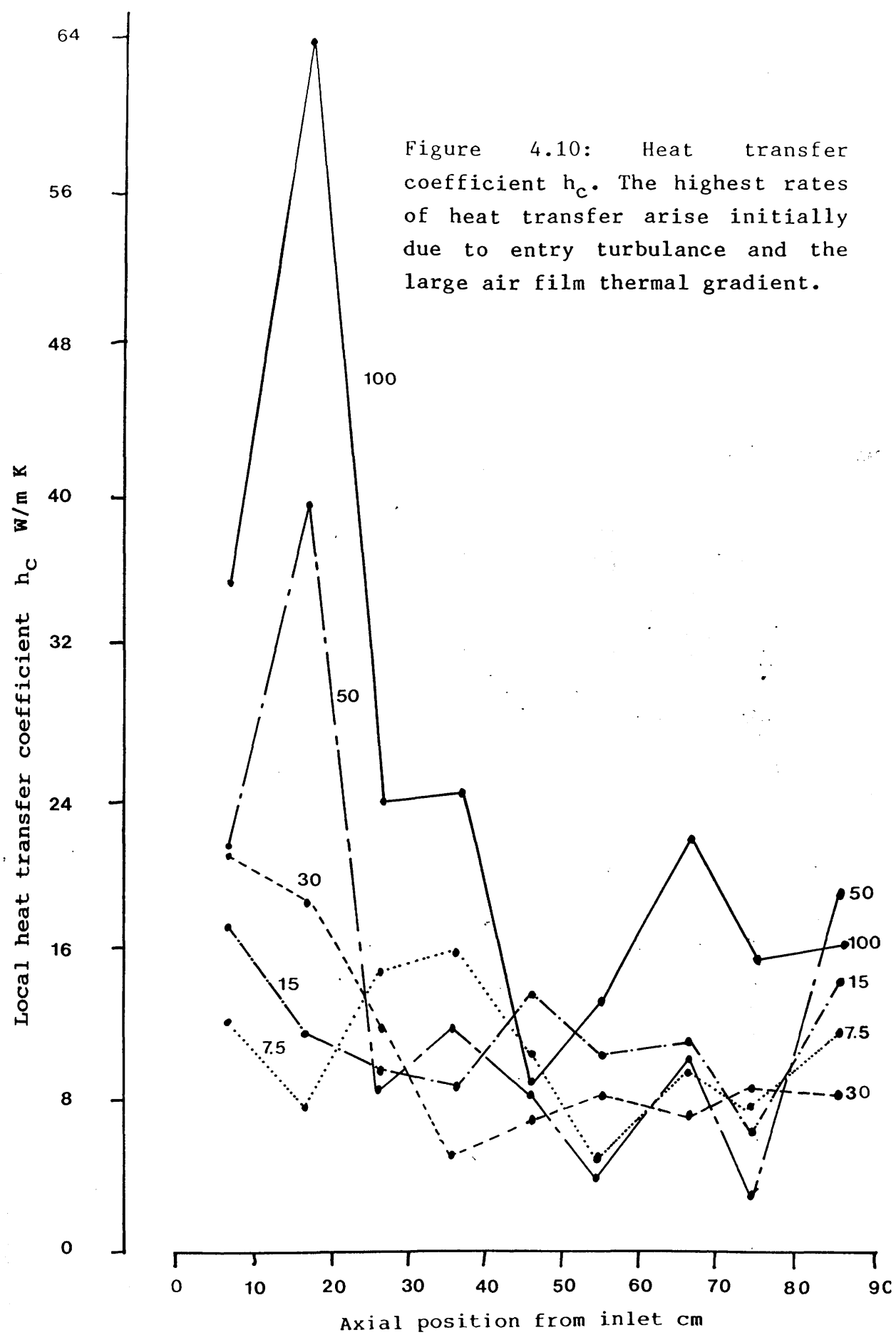

Figure 4.10: Heat transfer coefficient h_c. The highest rates of heat transfer arise initially due to entry turbulance and the large air film thermal gradient.

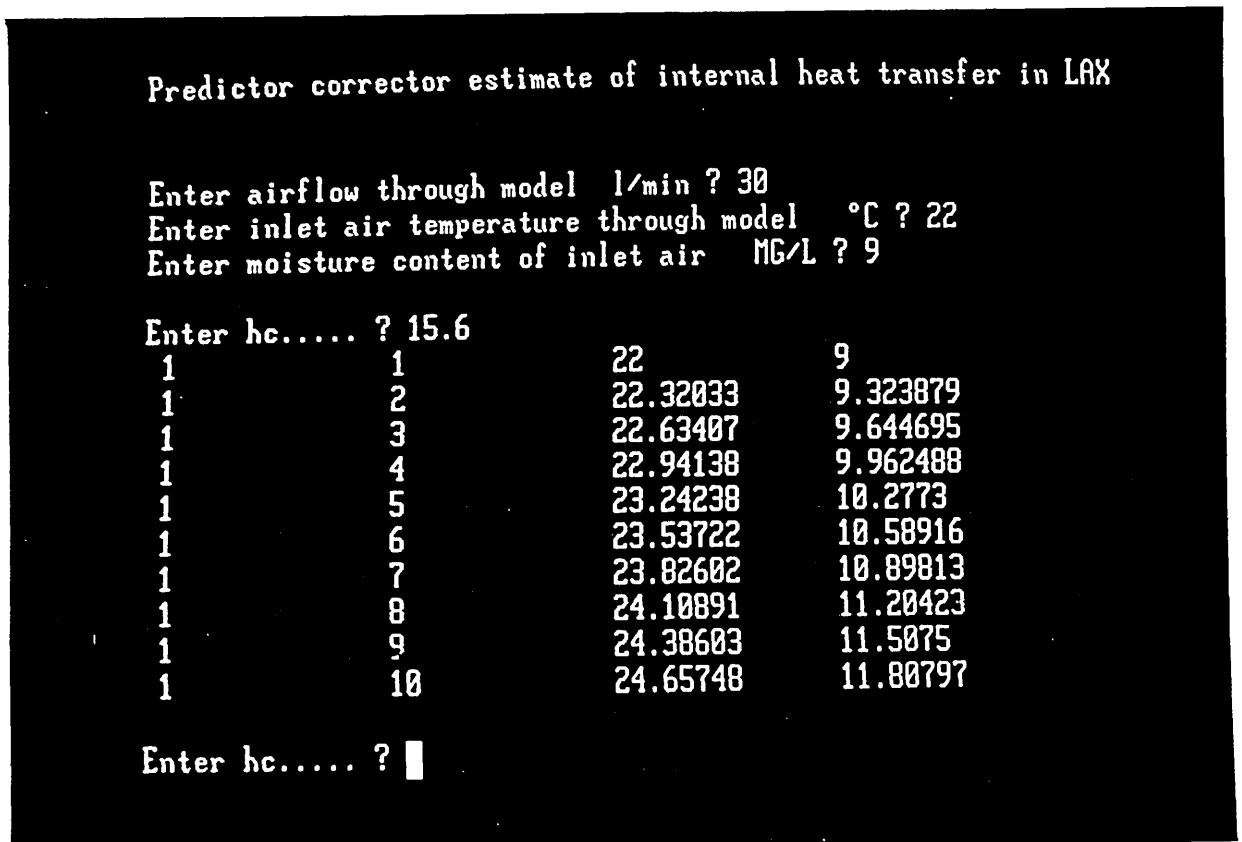

Figure 4.11: Screen output from the numerical model. Values of h_c were entered together with starting values of air temperature and water vapour content. Predicted temperature (°C) left column and water vapour content (mg/l) right column.

4.5.3. Comparison between P-C model and experimental data.

Figure 4.12 shows the predicted axial rise in air temperature which is in agreement with the superimposed experimental values presented in section 5.4.1. The predicted axial rise in water vapour content exhibits the same flowrate dependence observed in the air temperature profile although there is an absence of an initial phase of rapid air humidification. The diagram demonstrates the simultaneity of heat and water vapour transfer.

Actual exit water vapour content was compared with the predicted values in order to inspect the authenticity of the model. For the mid-range of air flowrate (30-75 l/min) the model underestimates water vapour content, figure 4.13. An artificial increase of 25% to the value of k_c marginally improved these estimates and a 100% increase in k_c lead to marginal overestimates of water vapour content. The effect of varying k_c simulates the role of varying geometry along the conditioning surface.

Presumably the entry related turbulance caused by pumping the air through the conditioner during the exit humidity test was not present during the axial rise in temperature test wherein the air was sucked through the device. The transport analogy could not account for this, thus the values of both h_c and k_c are expected to be higher when entry and geometry related turbulance is present. On this basis the human airway will confer more rapid air warming than in the long axis device and this will be described in section 6.5.

Essentially heat and water vapour transfer by long axis air conditioning are simultaneous although air warming achieves the asymptotic value before humidification, due to the low specific heat of air compared with the latent heat of evaporation of water.

Figure 4.12

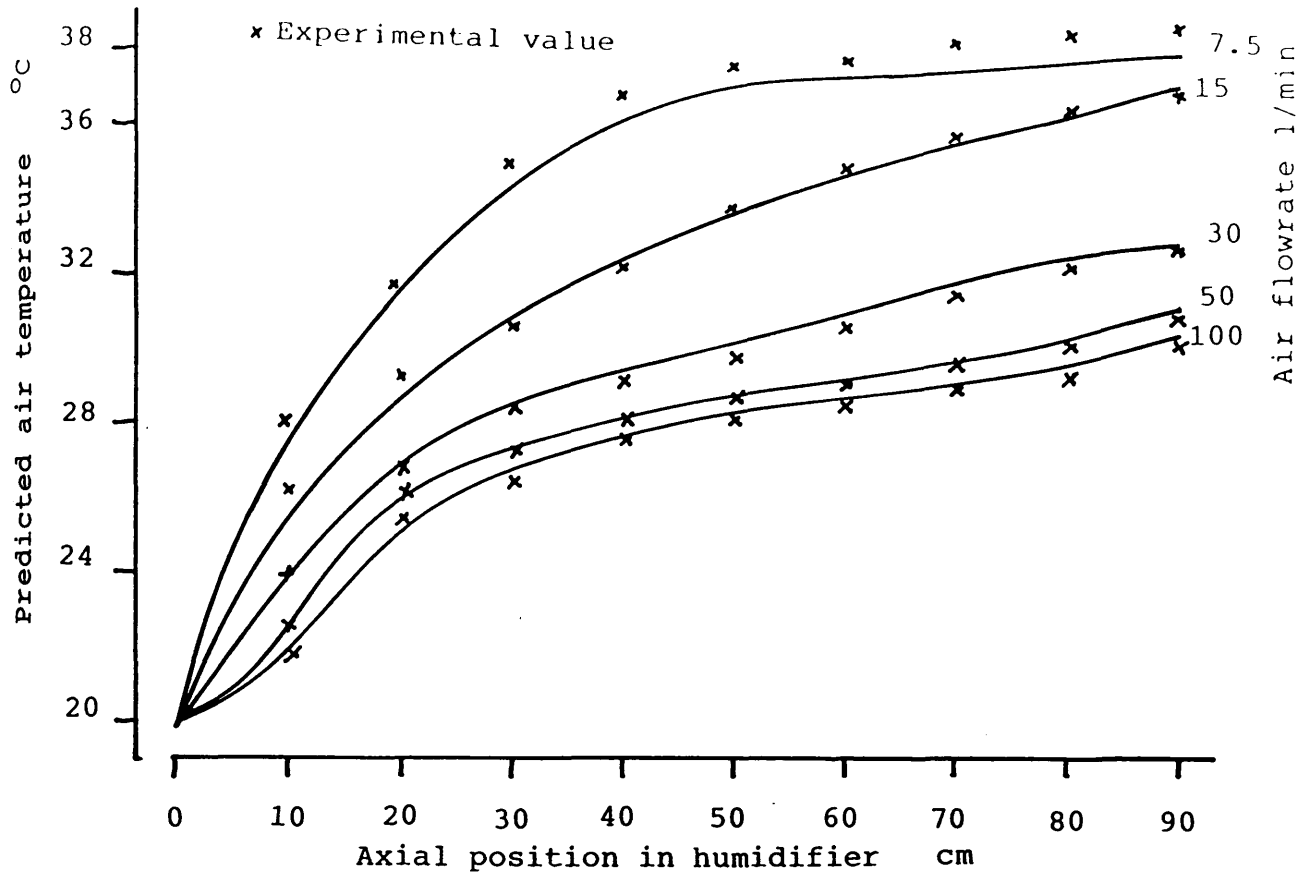
Experimental value
Predicted air temperature °C
38
36
32
28
24
20
7.5
15
30
50
100
Air flowrate l/min
0
10
20
30
40
50
60
70
80
90
Axial position in humidifier cm

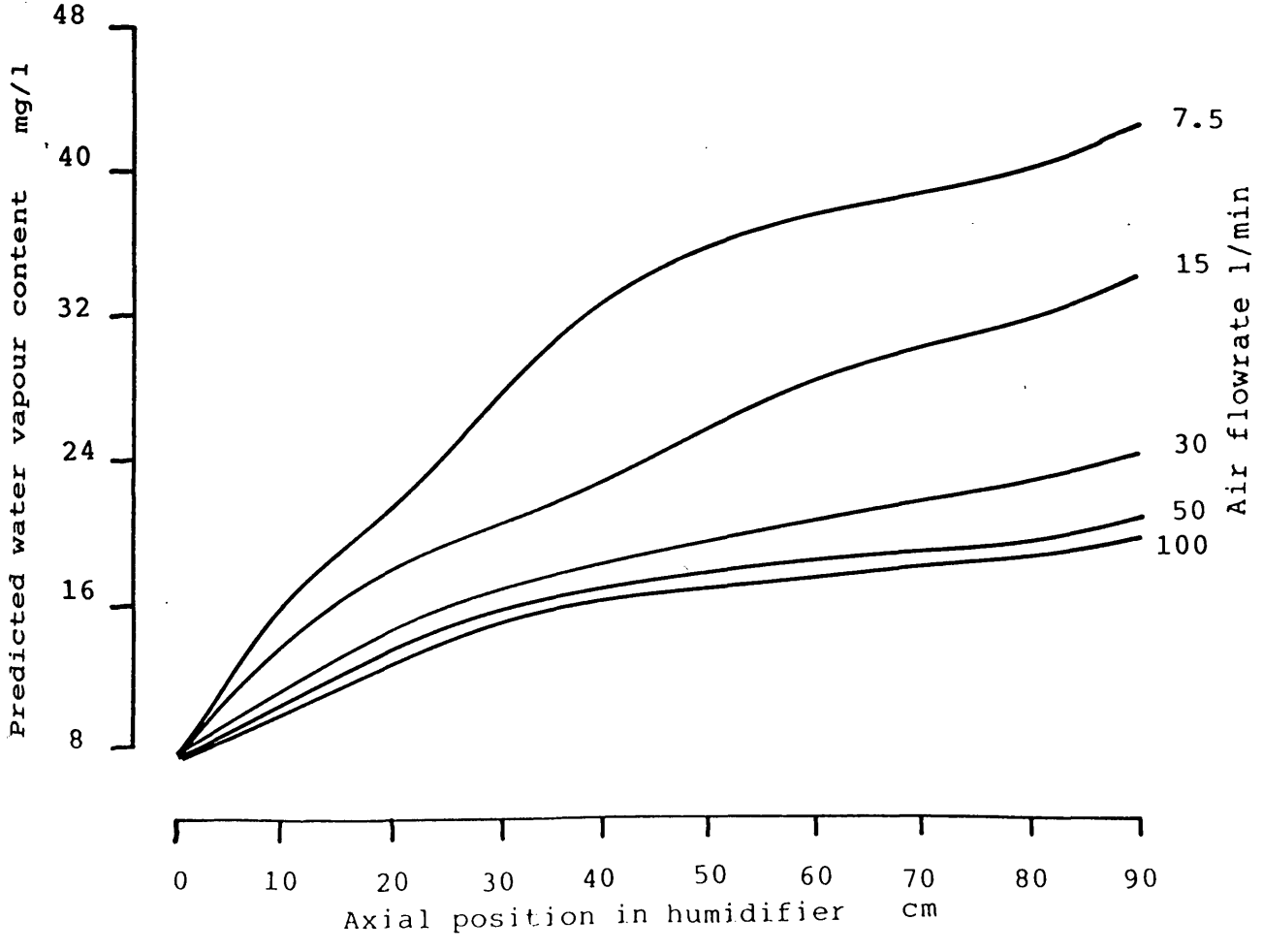
Predicted water vapour content mg/l
48
40
32
24
16
8
7.5
15
30
50
100
Air flowrate l/min
0
10
20
30
40
50
60
70
80
90
Axial position in humidifier cm

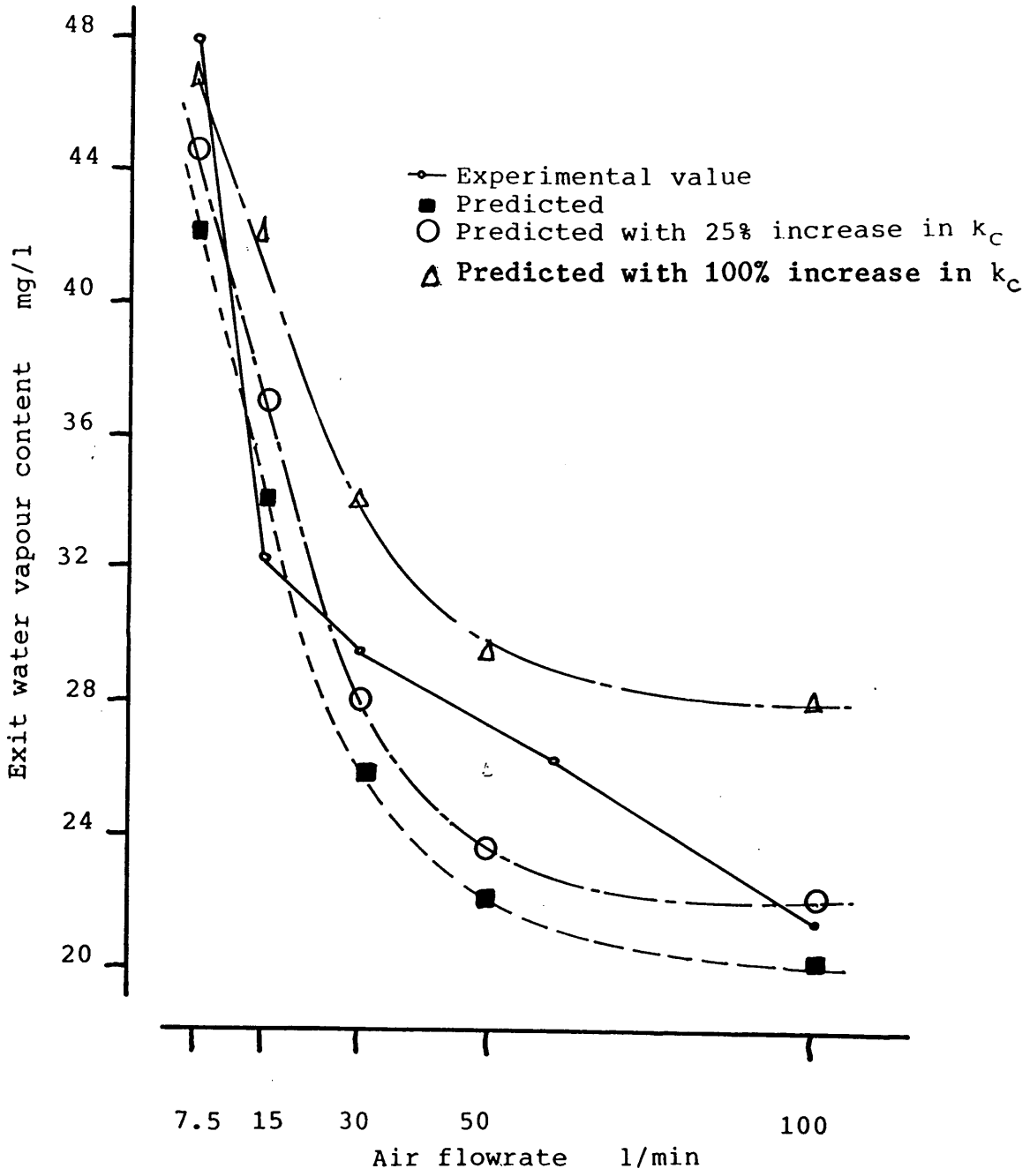

Figure 4.13 Predicted and actual exit water vapour content. The model underestimates reality by 12% (7.5 l/min) and 5% (100 l/min).

4.6. Comments.

The Mk1 prototype long axis air conditioner was found to be capable of conditioning ambient air to a droplet free state of approximately 33°C 80%RH at an air flowrate of 100 l/min. A bend upstream of the conditioner inlet in the air supply conduit will improve the water vapour uptake by enhancing k_c via entry turbulance of the air. This phenomenon was used to modify the performance of the Mk2 long axis air conditioner which yielded an exit air condition of about 33°C, 95-100%RH and is described in section 5.2.

When inhaled, this grade of air will minimise the rate of respiratory heat exchange experienced by the airway.

5. Respiratory heat exchange in exercise induced asthma.

5.1. Introduction.

Airway cooling and to a lesser extent airway drying were observed in chapter 3 to promote bronchoconstriction in hyperventilation induced asthma. In terms of respiratory heat exchange a graded response to heat loss was found. A cooler expirate in asthmatics was measured compared to that in normal subjects undergoing the same hyperventilation challenges. It was proposed that the intra challenge events could cause an airway wall jacket effect thereby attenuating the passage of heat from the blood capillary plexus to the mucosa. If present this jacket phenomena could be due to hyperventilation induced oedema and/or hypersecretion; both of which have been identified by other workers to be present in asthma (section 3.7).

Hyperventilation has been used as a model of the respiratory heat loss arising during exercise. Attenuation of heat loss has been associated by other workers (section 3.1) with a protective effect in asthma. The methods employed in the hyperventilation series (chapter 3) have been applied to the exercise regime. The aim of this study was threefold:

i) to determine whether a graded response to respiratory heat exchange pertains in exercise;

ii) to measure the airway cooling phenomena during exercise in exercise sensitive asthmatics and

iii) to assess the protective effect of tropical air inhalation during exercise in terms of respiratory heat exchange rate.

5.2. Tropical air generation.

Tropical air was generated using the long axis air conditioning process described in chapter 4. Figures 5.01 and 5.02 illustrate the Mk2 device. The water film delivery head, downtube and exhaust cup were identical to that described in section 4.3. Water was delivered tangentially to the internal surface of the downtube rather than perpendicular as in the Mk1 model. This facilitated a spiral flow in the water film and produced uniform and complete distribution over the inside surface of the downtube. Bending of the downtube was reduced by strapping a beam of 12 x 20 mm wood along the conditioner's major axis. Located under the exhaust cup was a perspex block which was machined to form a non - rebreathing assembly. This is illustrated in figure 5.03. Due to its close proximity to the exhaust cup the valve became heated and thereby prevented inspiratory air condensate formation. The actual valve elements were spring loaded discs as used in the Mk2 non - rebreathing valve.

The inlet air supply line incorporated a kink at the entrance to the conditioner, in order to enhance internal air turbulence. With a water film inlet temperature of 50°C and a flowrate of 1.2 l/min the exit air condition was 32-34 °C; 95-100 %RH at 150 l/min airfow. This grade of air was droplet free and considered suitable for the purpose of attenuating respiratory heat exchange.

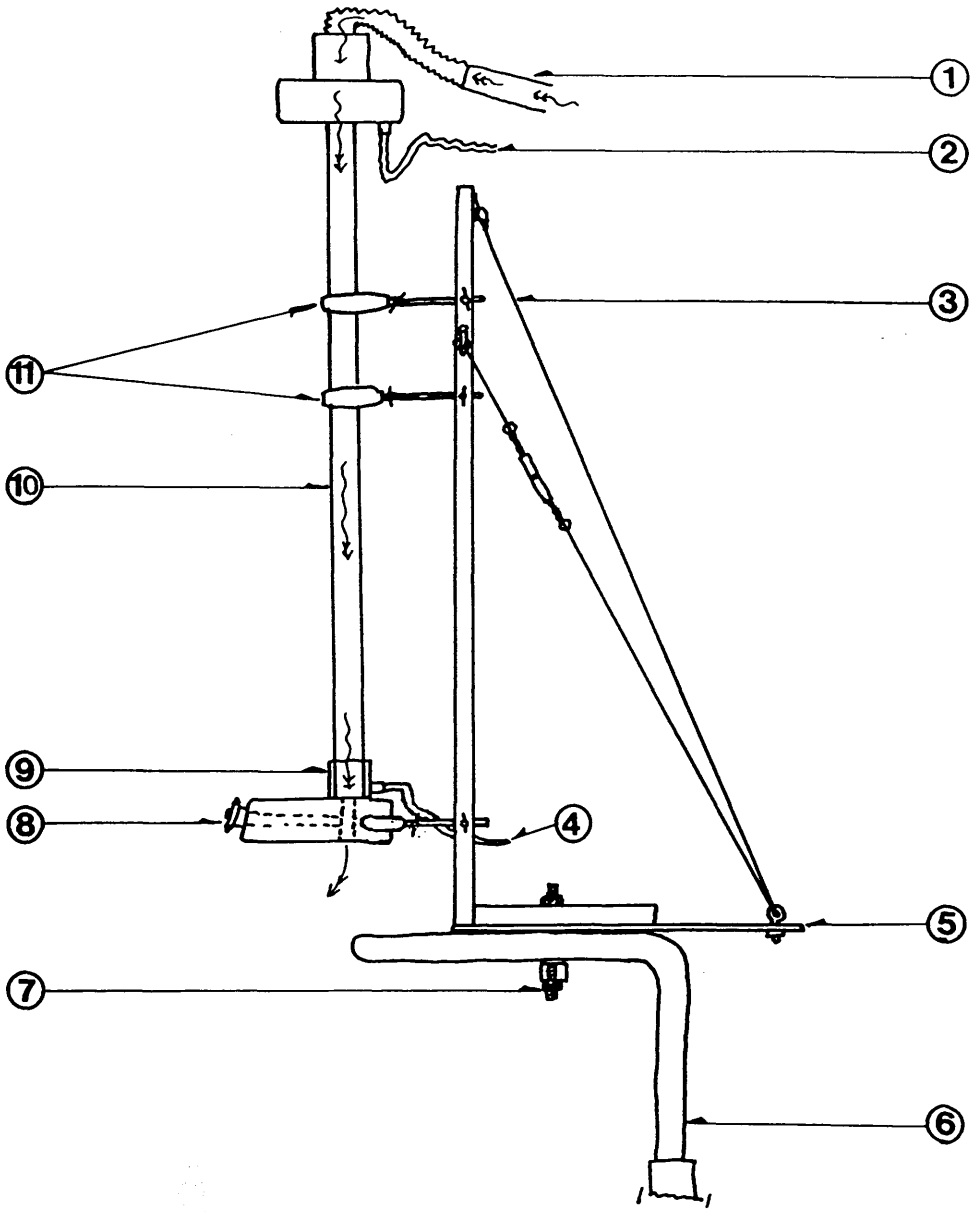

1 Air inlet
2 Water film inlet
3 Mast stay
4 Water film outlet
5 Deck
6 Treadmill handle bar
7 Deck locking bolt
8 Mouthpiece and non rebreathing valve
9 Exhaust cup
10 Downtube
11 Height & pitch clamps

Figure 5.01: The Mk2 long axis air conditioner.

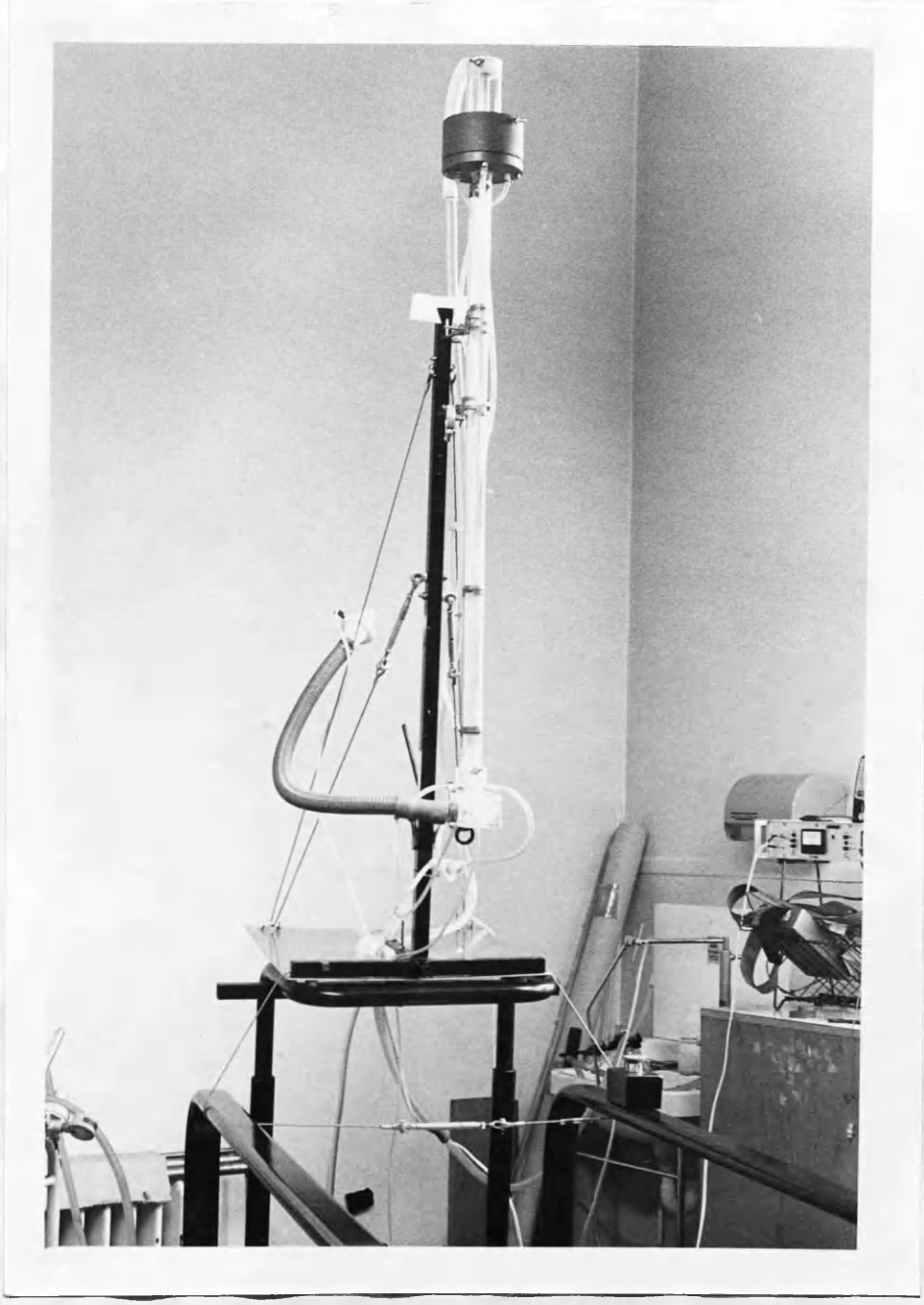

Figure 5.02: The Mk2 long axis air conditioner mounted on the treadmill.

Figure 5.03: Perspex non rebreathing valve which bolted onto the conditioner exhaust port. The valve discs were scavenged from an existing unit.

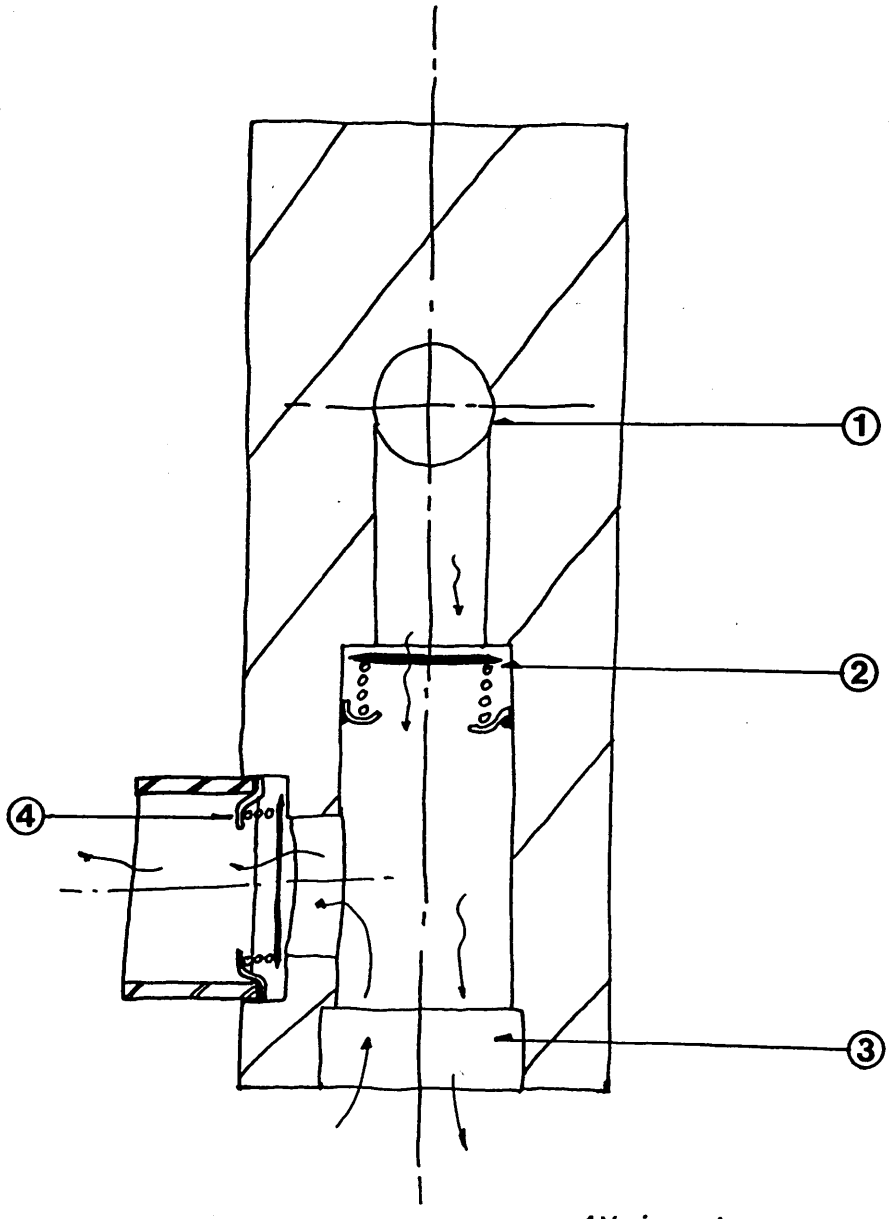

1Main airstream exit
2Inspiratory port
3Mouthpiece socket
4Expiratory port.

Long axis air conditioner non - rebreathing valve assembly. Full size, between valve dead space 38 ml.

5.3. Method.

Eleven patients (4 male) using inhaled anti asthma drugs on a daily basis were enrolled for the study. Informed consent was obtained from each prior to the tests.

The experiment required four separate visits to the laboratory. During each the participant orally inhaled either ambient; dry; cold or droplet free tropical air. The grade of air administered on a particular visit was randomised. Generation of the different air grades was done using the facilities described in section 2.2 (cold air and dry air) and section 5.2 (tropical air). Each type of air was delivered whilst the subjects underwent treadmill exercise. A brisk walk at a speed of 5 km/h on a 12° incline was used which was maintained for five minutes. This corresponded to the severity of challenge encountered in diagnostic exercise studies.

During the challenges breath by breath measurement of respiratory heat exchange rate was made by means of the microcomputer system described in sections 2.3 and 2.4. After the challenges subjects were transferred to a dry wedge spirometer where recordings of the changes in post challenge FEV_1 were made. Expired air temperature trends during the challenges were characterised by determining the local temperatures T_{25}, T_{150} and T_{300} described in section 3.9. The rate of airway cooling (RAC) prevalent in each test was calculated using the expression cited in section 3.10. Water loss rates (WLR) in each test were also determined using the following expression, defined by the author:

$$WLR = V(w_e - w_i)(1/1000) \quad g/min$$

where: V: Ventilation rate l/min; w_e: Mean expired water vapour content over length of trial mg/l; w_i: Inspiratory water vapour content mg/l.

Data were treated with a Student's 'T' test using a Minitab statistics programme.

5.4. Results.

Anthropometric and lung function data of the subjects is given in table 5.01. Figure 5.04 illustrates the percentage change in FEV_1 after each challenge. Two sub groups of patients were apparent. Group 1 patients (n=6) exhibited little or no reponse to the challenges. Group 2 patients (n=5) were more sensitive and were identified by a greater than 10% fall in FEV_1 to at least one of the ambient, dry or cold air exercise challenges. Tropical air was observed to confer a complete reversal in the airway response and this protective effect was significant ($p<0.05$) in group 2 patients.

Basal ventilation and ambient inspiratory air temperature were matched. Tidal expirate temperature of 30.02 ($\pm$0.5) °C was significantly lower ($p<0.05$) in group 2 subjects compared to the group 1 subjects 30.82 ($\pm$0.36)°C; presented in table 5.02.

Figure 5.05 illustrates the range of respiratory heat exchange rates measured during exercise and the post challenge changes in FEV_1. Tropical air caused an RHER of 13.2 W, identical to that encountered during tidal breathing and was followed by a 6% increase in basal FEV_1. In the other challenges a reduction in FEV_1 of up to 20% was observed in group 2 after exercise with an RHER of 53 W. Correlation between RHER and the mean change in FEV_1 for group 2 was: $FEV_1=0.266(RHER)-4.45$; $r=0.91$. During all the challenges matched ventilation rates of 33-36 l/min pertained for both groups. Data are summarised in table 5.03.

Expiration temperatures T_{25}, T_{150} and T_{300} encountered in the challenges are plotted in figure 5.06. Ambient air and dry air expirate remained at a uniform temperature for both

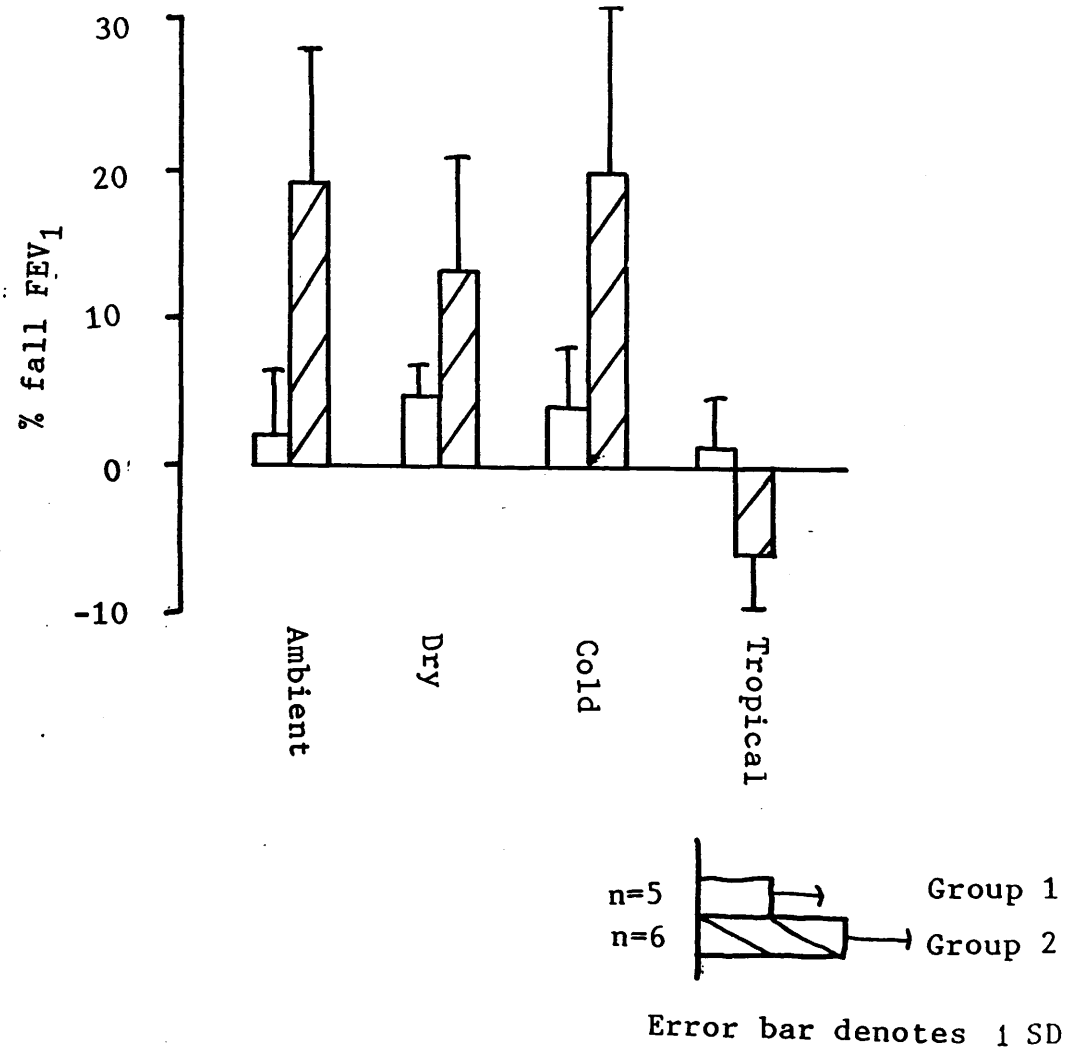

Figure 5.04: % change FEV_1 after each of the challenges.

Figure 5.05: Rate of respiratory heat exchange and % change in FEV_1 after the challenges.

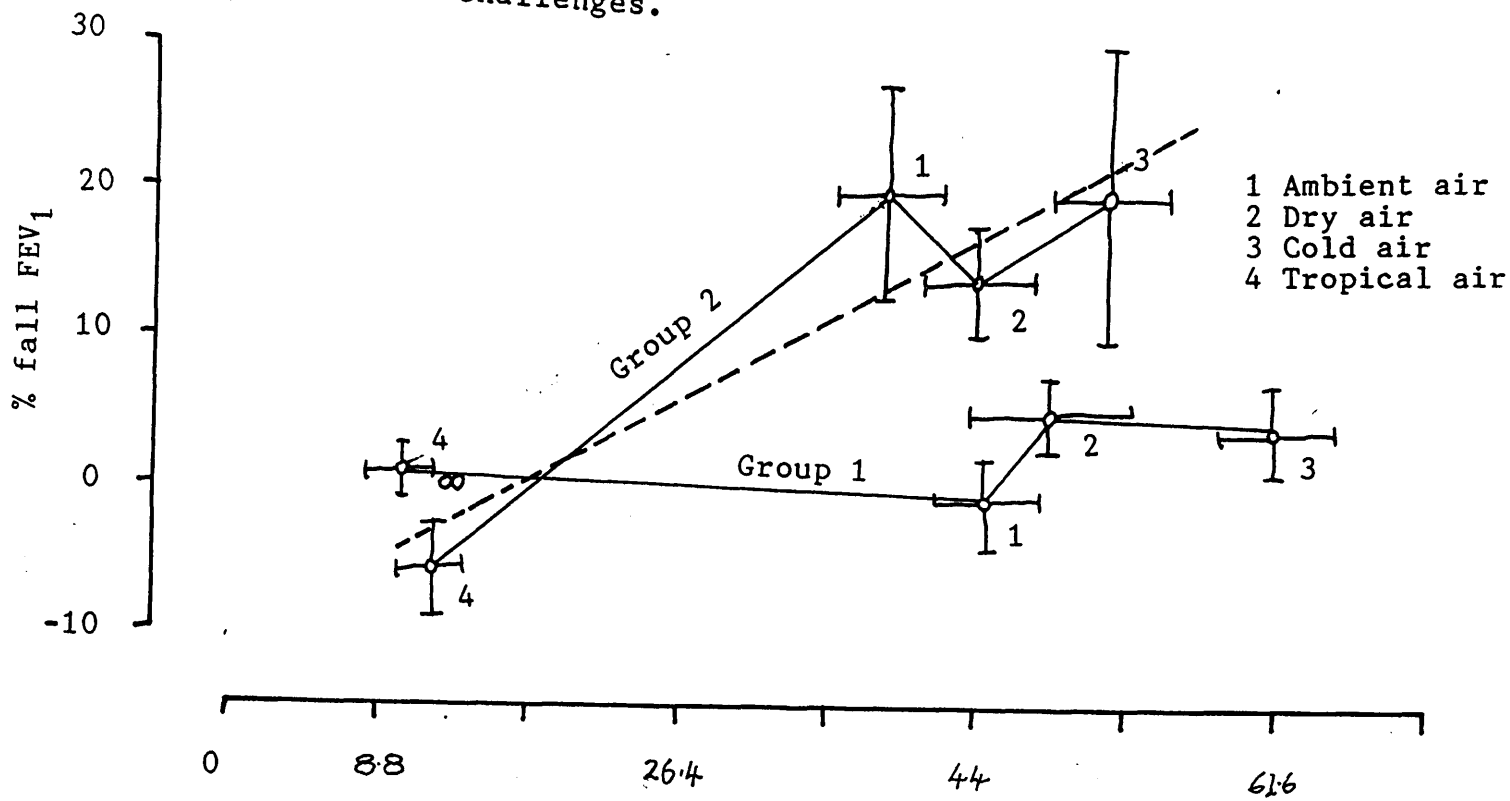

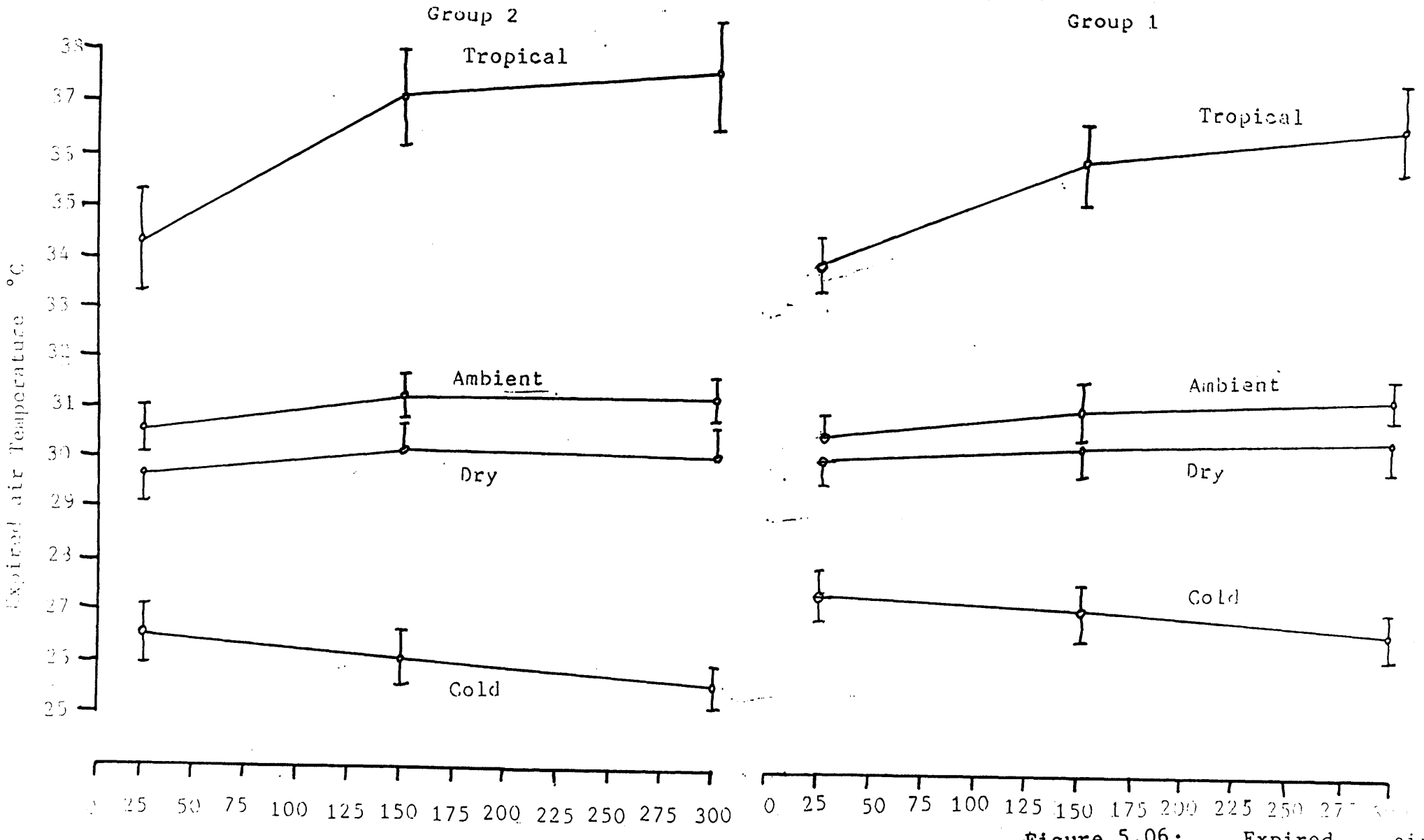

Figure 5.06: Expired air temperature throughout the challenges

groups of approximately 31°C and 30.5°C respectively. Cold air temperatures declined with progression into the test and group 2 subjects were found to have a significantly cooler ($p<0.05$) end challenge expirate (T_{300}) of 25.7 ($\pm$0.50)°C compared to group 1: 26.88 ($\pm$0.88)°C. Tropical air expiration temperatures were observed to rise throughout the challenge although no significant differences between the groups arose. Table 5.04 lists these results.

Rate of airway cooling was matched between the groups with cold air inhalation producing the highest RAC of 0.9 °C/min. Figure 5.07 illustrates the effect of progressive airway warming with tropical air breathing which lead to a 'negative cooling' RAC index of -1.5 °C/min. This was associated with a protective effect in airway response. Data are summarised in table 5.05.

Water loss rates (WLR) are plotted in figure 5.08. Between group WLR during ambient, dry and cold air challenges were similar and ranged from 0.8 to 1.05 g/min. Tropical air WLR was less than 0.35 g/min. In the group 2 patients a plateau in airway response to increasing RAC or WLR was evident, figures 5.07 and 5.08.

Tropical air inhalation attenuated respiratory heat loss to tidal levels; completely reversed airway cooling to produce a warming effect and retained at least 50% more water than would have ordinarily been expired in ambient air. It conferred complete protection to a group of five exercise sensitive asthmatics.

" Figure 5.07: Rate of airway cooling during the challenges.

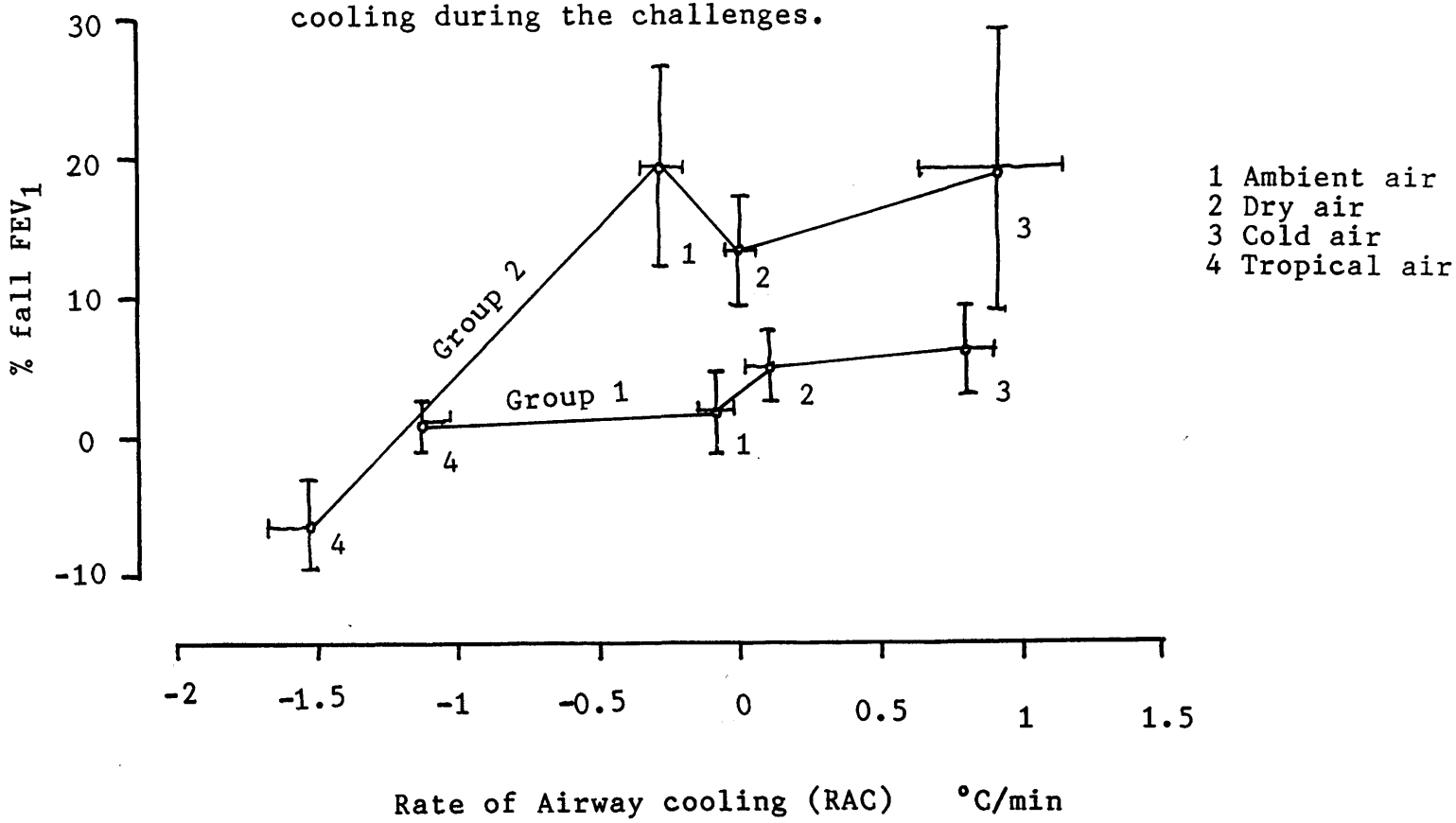

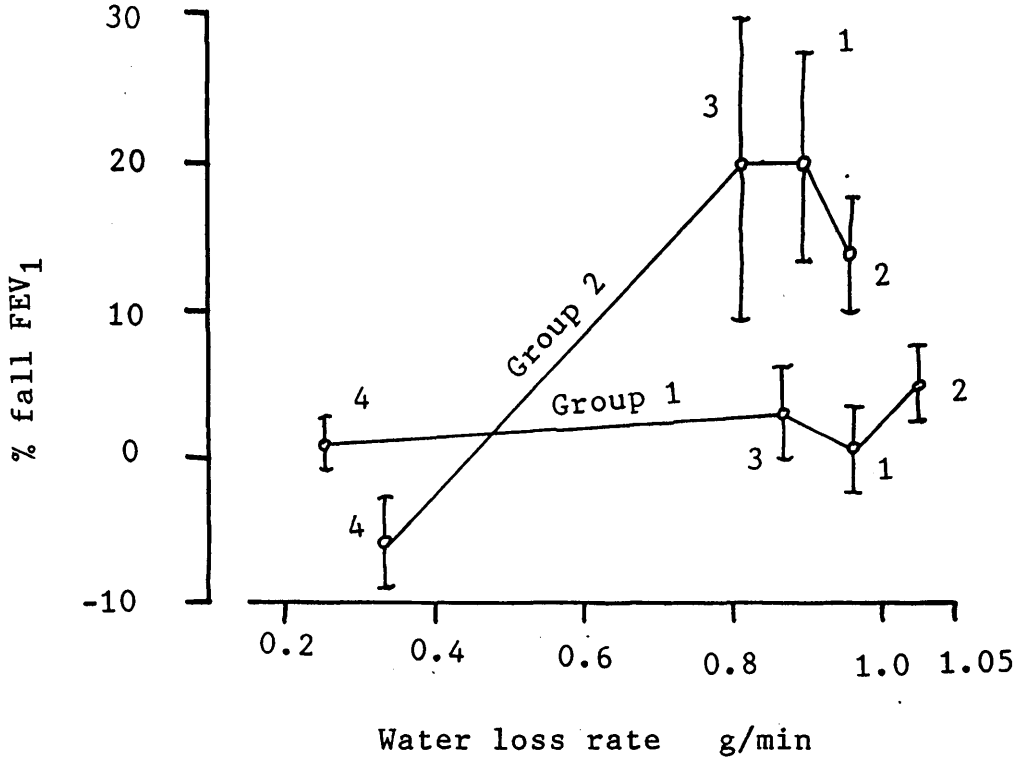

Figure 5.08: Water loss rates imposed by each challenge.

1 Ambient air
2 Dry air
3 Cold air
4 Tropical air

Table 5.01: Anthropometric and lung function data.

Subject	Sex	Age yrs	Height cm	FEV_1 l	% pred FEV_1
1 *	M	37	165	3.4	100
2 *	F	29	165	2.2	71
3 *	F	39	161	2.25	83
4 *	M	39	178	3.75	96
5 *	F	28	164	2.87	94
6	F	20	159	2.1	70
7	F	30	146	2.65	104
8	F	51	166	2.30	100
9	F	40	147	2.0	87
10	M	55	180	3.35	97
11	M	20	178	4.9	113
Overall mean (SD)		35.3 (±10.7)	164.5 (±10.9)	2.98 (±0.8)	92 (±12.7)
Group 1 (n=6)		36.0 (±13.8)	162.7 (±13.4)	2.88 (±1.01)	95.2 (±13.7)
Group 2 (n=5) '*'		34.4 (±4.9)	166.6 (±5.9)	2.89 (±0.61)	88.8 (±10.5)

'*' Denotes sub - group 2: those patients who had a >10% fall in FEV_1 to either ambient, dry or cold air challenges.

Table 5.02: Basal ventilation, T_{exp} and RHER

	Ventilation rate l/min	Expirate temp. °C	RHER W
Group 1 Mean SD	7.12 (±2.63)	30.82 (±0.33)	12.5 (±3.5)
Group 2 Mean SD	11.53 (±5.15)	30.02 (±0.51)	12.9 (±5.5)

Table 5.03: Challenge ventilation, RHER and airway response

Challenge	Ambient	Dry	Cold	Tropical
Group 1; mean ±SD				
Vent. l/min	35.85 (±4.52)	33.64 (±6.40)	34.70 (±8.57)	33.05 (±6.19)
RHER W	47.8 (±5.2)	48.4 (±11.8)	61.8 (±7.2)	10.2 (±5.6)
% Fall FEV_1	-1.0 (±6.6)	4.8 (±2.3)	3.2 (±5.3)	1.5 (±5.2)
Group 2; mean ±SD				
Vent. l/min	33.46 (±4.87)	31.25 (±7.1)	34.29 (±4.13)	35.76 (±5.79)
RHER W	38.9 (±5.5)	43.6 (±6.4)	52.3 (±4.7)	12.6 (±3.4)
% Fall FEV_1	19.6 (±16.9)	13.5 (±16.1)	19.5 (±21.6)	-6.4 (±5.9)

'-' % Fall FEV_1 denotes rise in airway response from basal value.

Table 5.04: Expired air temperatures.

Challenge Mean (SD)		Group 2 (n=5)	Group 1 (n=6)	'T' val Gp1>Gp2
Ambient	T_i	19.90 (±2.30)	17.50 (±1.84)	-NS-
	T_{25}	30.58 (±0.96)	30.50 (±0.89)	-NS-
	T_{150}	31.38 (±0.62)	31.23 (±0.64)	-NS-
	T_{300}	31.54 (±0.63)	31.40 (±0.73)	-NS-
Dry	T_i	19.55 (±1.56)	19.49 (±2.00)	-NS-
	T_{25}	29.78 (±0.74)	30.12 (±0.53)	-NS-
	T_{150}	30.23 (±0.83)	30.48 (±0.60)	-NS-
	T_{300}	30.10 (±0.68)	30.55 (±0.60)	-NS-
Cold	T_i	-17.63 (±1.38)	-18.07 (±1.41)	-NS-
	T_{25}	26.58 (±1.08)	27.57 (±0.80)	-NS-
	T_{150}	26.16 (±0.66)	27.21 (±0.85)	-NS-
	T_{300}	25.70 (±0.50)	26.88 (±0.80)	t=2.86
Tropical	T_i	33.60 (±1.56)	34.25 (±1.60)	-NS-
	T_{25}	34.34 (±2.09)	33.93 (±1.52)	-NS-
	T_{150}	37.10 (±1.87)	36.03 (±1.53)	-NS-
	T_{300}	37.64 (±1.87)	36.55 (±1.07)	-NS-

T_{25}; T_{150} and T_{300} denote local expirate temperatures, significance at $p<0.05$, -NS- not significant.

Table 5.05: Rate of airway cooling (RAC) and water loss rate (WLR).

Challenge	RAC °C/min	WLR g/min
Group 2 Mean (SD)		
Ambient	-0.27 (±0.19)	0.89
Dry	0.00 (±0.12)	0.95
Cold	0.91 (±0.80)	0.81
Tropical	-1.52 (±0.41)	0.34
Group 1 Mean (SD)		
Ambient	-0.08 (±0.18)	0.96
Dry	0.07 (±0.17)	1.05
Cold	0.79 (±0.20)	0.87
Tropical	-1.15 (±0.27)	0.24

'-' RAC denotes progressive temperature increase of the expirate.

5.5. Discussion.

Exercise induced asthma is known not to be prevalent in all asthmatics and treadmill testing is only one means of diagnosis. The protective effect of tropical air inhalation was anticipated in those subjects with EIA. This followed from the observations of Weinstein (1976)[22], Chen & Horton (1977)[23] and Bar-Orr (1977)[24], described in section 3.1.

The ventilation rate achieved by the subjects during these exercise tests was 33-36 l/min whereas in the hyperventilation series this was up to 50 l/min. It was noted in section 3.12 that a plateau in airway response could be interpreted from hyperventilation challenges in the range 18-53 W RHER. The higher rates of heat loss encountered with the 60 l/min target ventilation level rendered the response spectra more linear. In the present exercise series it is presumed that this threshold rate of heat loss was not obtained and the responses to ambient, dry and cold air were thus similar. Essentially the challenges were sub maximal.

The progressive air warming, figure 5.06, and reversal of RAC during tropical air exercise, figure 5.07, implies a complete absence of upper airway cooling or drying. Under these circumstances the expired air condition was presumably not unlike that of alveolar air. These measurements were considered to be accurate because condensate in the non - rebreathing valve was confined downstream of the expiratory port. The unit was directly heated in the contacting region between the valve block and the conditioner exhaust cup which also preserved the air condition of the inspirate.

A post challenge 're cooling' burden would have followed the tropical air test. Ambient air temperature was 19 °C and tropical air temperature was 34 °C giving rise to a 15 °C cooling gradient. The presence of post exertional ventilation would have enhanced the stress effect of 're

cooling'. A 're warming' burden of 36 °C after cold air (-17 °C) would have arisen. No rewarming would have occured with the ambient and dry air tests. McFadden (1986)[37] has suggested that re warming is important in the production of EIA following investigations involving cold air and exercise. The present work suggests that re warming per se cannot explain the similar airway responses which followed cold, dry and ambient air challenges as it was only apparent after cold air. If a post exertional thermal stress is a contributory factor to EIA then a re cooling burden after the tropical air challenge can reasonably be expected to promote bronchoconstriction. This was not observed.

It is possible that the action of cold air breathing during exercise initiates the events which lead to bronchoconstriction. Rewarming exacerbates the thermal stress on the airway. The protective effect of tropical air inhalation during exercise renders any post challenge re cooling burden irrelevent. The author suggests that it is the intra challenge events in the airway which are important.

Airway drying rates of 0.34 g/min arose during the tropical air challenge whereas between ambient and cold air challenges the rate was 0.8-1.05 g/min. Tidal water loss rates of 0.29 g/min were calculated. The rates of airway cooling were indeed reversed during tropical air breathing and presumably the expirate herein was at a temperature not unlike the alveolar air. All five subjects derived benefit from breathing tropical air. Due to the disparate range of responses to a challenge prevalent in the asthmatic population this can only be considered as an encouraging trend. Presumably there will be those asthmatics who will derive no benefit from the action of tropical air. In thermal terms the airway would have been in a neutral state.

The expired air temperatures during the cold air exercise

test in the group 2 patients were lower than those of group 1. A similar trend was observed in the the hyperventilation test series (section 3.10) in normals and asthmatics. The thermodynamic explanation for this was an airway jacketing effect caused by hyperventilation or exercise induced oedema and/or hypersecretion in the asthmatics. The thermal events witnessed in the present work may be evidence of the initialisation of the bronchoconstriction measured after the challenges.

Table 5.04 summarises the end challenge temperatures (T_{300}) encountered in group 2 asthmatics for the present five minute exercise challenge and that in the asthmatics who participated in the five minute hyperventilation challenge, described in section 3.9. The hyperventilation data is taken from table 3.11 at the 30 l/min target which closely approximates the ventilatory range encountered in the exercise challenge. The exercise group exhibited a higher T_{300} than their hyperventilating counterparts during ambient air breathing presumably because of increased pulmonary circulation and vaso-dilation. Dry air temperatures were similar for both groups. Inspiratory temperature of both grades of air was matched. Cold air in the exercise group resulted in a lower temperature expirate than with the hyperventilating patients. This arose despite a marginally warmer inspirate in the exercise group and is inconsistent with the vasodilatory effect expected in exercise. However the exercise subjects were more sensitive to the same level of thermal burden and there may have been an increased airway jacket (via oedema, section 3.11.1). This would have attenuated heat transfer from the blood capillary plexus regardless of vasodilation. Indeed the basal expirate temperature in the exercise group was about 0.5°C cooler than in the hyperventilation group. A pre challenge airway jacket may therefore have been present.

Figure 5.09 compares the mean post challenge airway responses encountered in each group. The correlation for

Figure 5.09: Comparison between hyperventilation and exercise induced asthma.

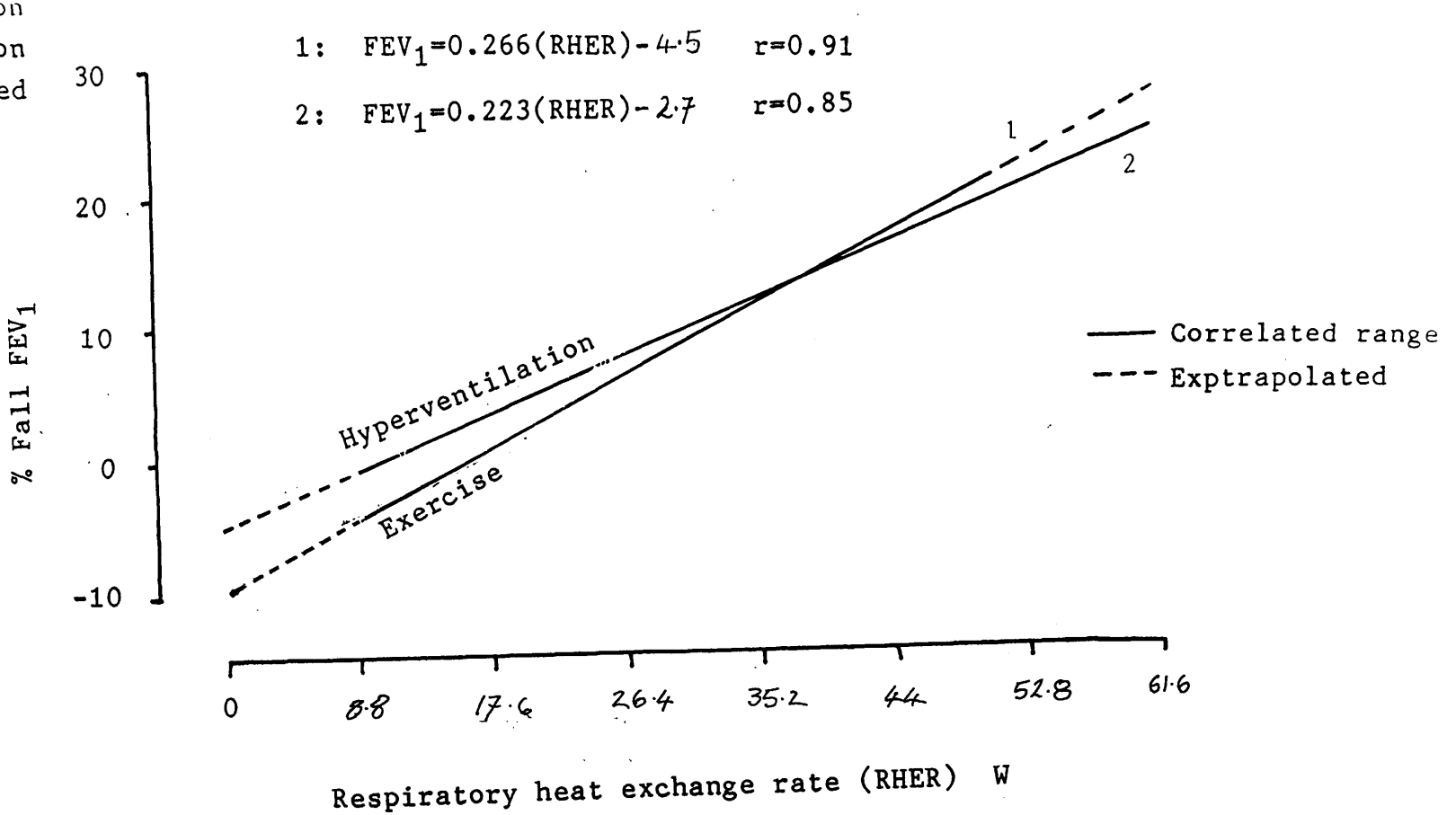

exercise group was $\%FEV_1$=0.266(RHER)-4.5, r=0.91 and for the hyperventilation group $\%FEV_1$=0.223(RHER)-2.7, r=0.85. The standard error of the mean (SEM) for the correlations were (coefficient, constant): 0.023, 0.95 (exercise) and 0.016, 0.55 (hyperventilation). The comparison is tempered by the intra group compatibility. However if this trend does pertain for all exercise sensitive asthmatics then hyperventilation is a not only a good model of exercise induced heat loss but also one of exercise induced bronchoconstriction. Hyperventilation could therefore be applied to subjects in whom exercise could be hazardous.

Table 5.04
Comparison of exercise and hyperventilation data

	Exercise		Hyperventilation (Table 3.11 30 l/min)	
Test	T_i	T_{300}	T_i	T_{300}
Ambient	19.9 (±2.3)	31.34 (±0.63)	19.88 (±1.55)	31.08 (±0.41)
Dry	19.55 (±1.56)	30.1 (±0.68)	20.89 (±2.08)	30.09 (±0.6)
Cold	-17.63 (±1.38)	25.7 (±0.50)	-22.63 (±0.95)	26.26 (±1.58)

% Fall FEV_1	Exercise	Hyperventilation
Ambient	19.6 (±16.9)	12.0 (±7.6)
Dry	13.5 (±16.1)	15.7 (±15.3)
Cold	19.5 (±21.6)	13.9 (±4.1)

Basal:	Exercise	Hyperventilation
T_{exp} °C	30.02 (±0.33)	31.45 (±0.63)
Vent l/min	11.53 (±5.15)	12.63 (±6.2)

5.6. Summary.

For a fixed rate of mechanical work the airway reponse to ambient, dry and cold air was similar. The linearity of heat exchange rate and airway response was again inferred although the achieved ventilation rates imply that the exercise challenges were sub-maximal. Tropical air inhalation was associated with a reversal in airway response and conferred heat exchange rates identical to that encountered in tidal respiration. A cooler expirate was identified at the end of cold air inhalation in the exercise sensitive group. This was interpreted as evidence of the airway jacketing phenomena; proposed in section 3.10.1.

Chapters 6 and 7 describe two series of invasive measurments of intra thoracic air temperature and mid tracheal air humidity. The measurements were made in order to supplement the laboratory findings by locating the in vivo sites of maximal heat transfer and quantifying the regional fluxes of water through the airway mucosa.

6. In vivo measurement of intra thoracic air temperature.

6.1. Introduction.

It was observed in chapters 3 and 5 that the primary index of lung function, the percentage fall in FEV_1 after a challenge, varied directly with the rate of respiratory heat loss imposed on the airway. This was expressed both in terms of rate of heat loss and rate of airway cooling. Of interest are the airway zones enduring the principal cooling (and drying) stress. The following describes a direct measurement of intra thoracic air temperature made during a diagnostic bronchoscopy. The work is pending publication, Farley & Patel (1988)[48]. The tests were done in order to provide more reliable data of the in vivo air temperature distribution and also as a 'dry run' invasive measurement procedure for the mid tracheal air humidity study described in chapter 7.

6.2. Past work.

Webb (1951)[49] inserted a thermocouple directly into the mouth and nose of resting subjects breathing ambient air. It was concluded that the expirate was "several degrees below 37.5°C". Inspired cold air (-4°C) was estimated to yield an expired pharyngeal temperature of 25°C. The possibility of mucus accumulation on the probe or contact with the airway wall was not commented upon. Moisture on the sensor would have caused wet bulb depression and an underestimate of the local air temperatures.

Cole (1953)[50] reported a pharyngeal air temperature of between 31°C to 33°C following inspiration of conditioned air in the range -30°C to +50°C using a discontinuous sampling procedure. This involved sucking inspiratory air

samples from the oropharynx into a vessel containing silica gel (Cole 1953)[51]. Cole (1954)[52] also inserted thermistor bead temperature sensors into the upper airway and concluded that the air was almost fully conditioned by that portion of the airway proximal to the pharynx.

Ingelstedt (1956)[53] has recorded ambient tidal respiratory air temperature at the larynx in the range 32.3°C-36.4°C using thermocouple elements inserted through the crico-thyroid cartilage. The procedure is detailed in section 7.2. No upstream disturbance of the airway arose but the invasive technique employed permitted evaluation of air temperature at only 1 airway station and was ethically questionable.

The apposition of the trachea with the oesophagus and the ease with which a thermocouple lead wire may be swallowed has attracted measurement of body core temperature with a view to relating observations to respiratory heat exchange. Cranston et al (1954)[54] have observed an esophageal temperature profile in normals which ranged between 36.5°C to 37.3°C at locations 25 cm to 50 cm respectively from the lips. Saltin and Hermansen (1966)[55] used the technique to obtain oesophageal temperature at the level of the diaphragm during a cycle ergometery test in ambient air. Temperatures of 36.6°C (resting) and 38.5°C (exercise) were obtained and presumed to correspond to those at the trachea. Deal etal (1979)[56] passed two 'T' type thermocouples into the oesophagus of normal and asthmatic exercise volunteers. During cold air inhalation and cycle ergometery retro-tracheal temperature (RTT) fell from 37°C to 33°C whereas the retro-cardiac temperature (RCT) remained stable. Changes in RTT were assumed to be an index of airway cooling at the trachea.

The retro tracheal temperature measurement technique does not provide direct information of intra thoracic heat transfer. However combined with a simultaneous recording of tracheal wall temperature the RTT method could be useful in

Figure 6.01: In vivo air temperature distribution, after McFadden (1985).

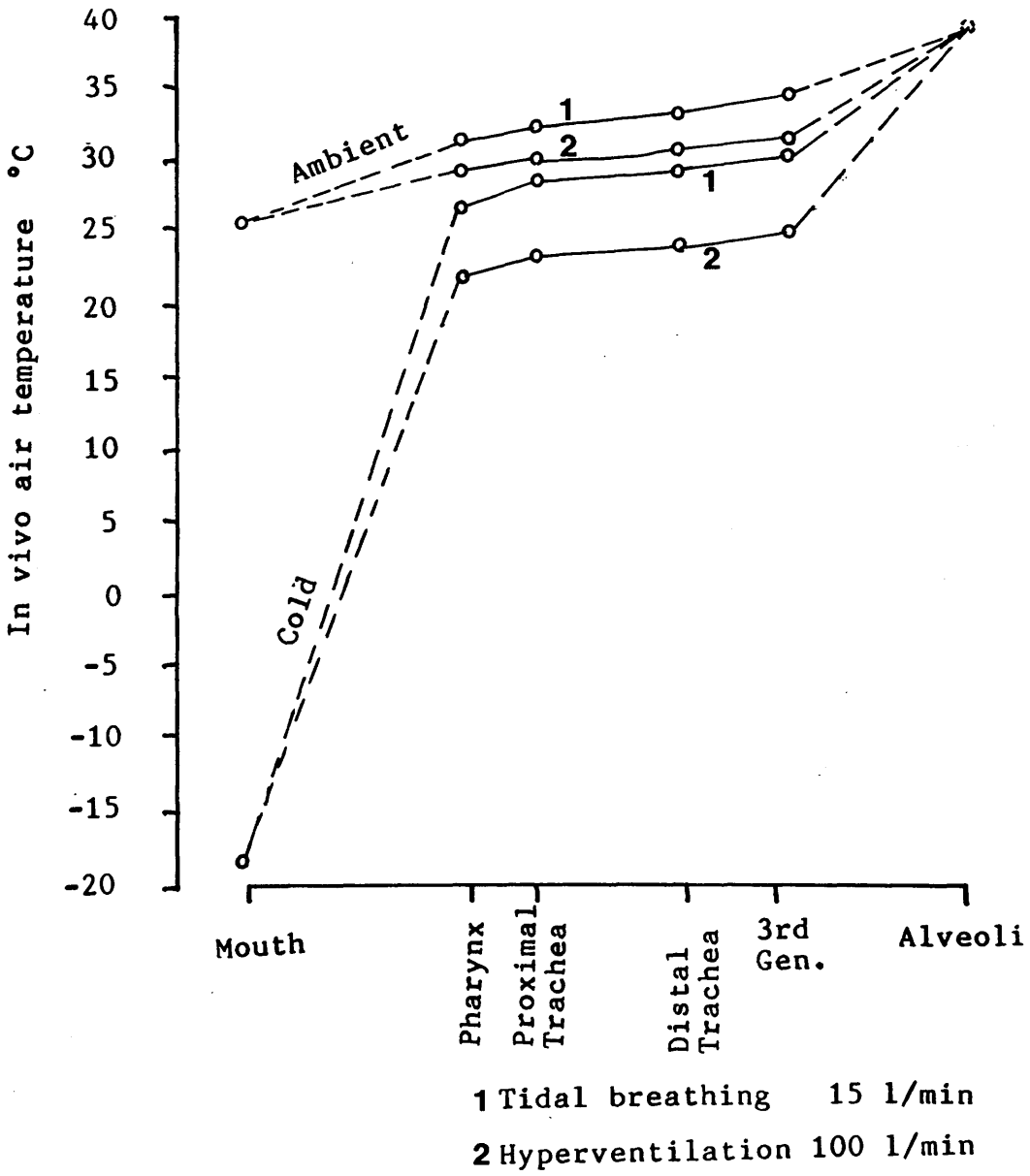

quantifying the long term tissue cooling phenomena during a challenge and the heat fluxes within the body core.

Following the RTT study by Deal et al (1979)[56], McFadden et al (1985)[57] have used a purpose built thermistor bead instrumented catheter probe to record intra thoracic air temperatures. This was inserted into the airways of normal subjects and simultaneous measurement was made at seven sites of airway temperature between the mid trachea and sub segmental airway. The subjects maintained a ventilation target by inhaling from a continuously filled rubber bladder of known volume. During cold air (-18°C) hyperventilation an inspiratory temperature of 25°C was found at the sub segmental airway whereas in ambient air this was 34°C. The corresponding ambient inspiratory temperature at the pharynx was 32°C. The results are summarised in figure 6.01. Due to the nature of the device doubt exists as to whether probe contact with the airway was present. Any local hot or cold spot on the airway wall, such as a thermistor embedded into the airway or one on which an accumulation of mucus had occurred, could only be detected in the extreme case of a completely invariant signal from the probe. The investigative technique was ethically dubious because it required an invasive procedure without direct benefit to the participant. At the time of writing the seven thermistor catheter is the only known measurement of intra thoracic air temperature. Its attraction lies in the simultaneous recording of seven airway sites. However the technique used to achieve target ventilation did not permit on line data acquisition of airflow and due to the ethical problem described the invasive procedure could not be repeated by other workers.

It was considered that a useful contribution could be made by the direct measurement of intra thoracic air temperature using an alternative invasive but ethically acceptable approach.

6.3. Method.

In vivo measurement of air stream temperature was performed at the end of a routine fibre-optic bronchoscopy on 11 patients: mean age 67.1 (±0.7) years, 3 female. These investigations were done in order to obtain tissue biopsies for inspection. Patient data are given in table 6.01. Informed consent was obtained and the procedure approved by the hospital ethical committee.

A 1 mm^2 fibreglass insulated 'T' type thermocouple was passed down the bronchoscope suction channel to protrude not more than 2.5 cm from the distal channel aperture. The thermocouple had been previously found to have a response time of under 50 msec to a 10°C step increase in temperature, (section 2.3.2.). Patients breathed quietly ambient air nasally through a face mask which vented through a pneumotachograph flowhead, (Mercury F300L and amplifier CS5). The bronchoscope was routed into the nasal cavity via an aperture in the mask. Four subjects also inhaled cold air (-17.5°C, 1 mg/l) delivered at 120 l/min to a perspex non rebreathing valve (Gas Messung type 72, figure 2.09.), and was produced using the facility described in chapter 2. During the cold air test condensate formation within the pneumotachograph was avoided by siting it downstream of the expiratory port, although this omitted recording the inspiratory portion of respiration.

The flowhead electromanometer and thermocouple amplifier output signals were digitised using the 'Microlink' and sampled at 25 Hz by software written in MSBASIC by the author. Data aquisition was programmed to last 10 seconds during which the recordings were saved in a memory array prior to storage on the microcomputer hard disc.

The bronchoscope was introduced into the airway via the nose and passed to the sub segmental bronchi at the 3rd generation airway in the right lower lobe. It was progressively withdrawn to the following sites where

recordings were made: the main carina; the proximal trachea distal to the vocal chords; the pharynx proximal to the epiglottis and finally the nares. The air temperature at the nares was recorded by inserting the thermocouple directly into the inspiratory air stream through the face mask aperture. Figure 6.02 illustrates the in vivo measurement stations which were located by the bronchoscope operator.

Throughout the trial the bronchoscopist ensured that the thermocouple was not in contact with the airway wall and that no mucus accumulated on the probe tip. The investigation added approximately 10 to 15 minutes to the bronchoscopy.

Table 6.01: Patients.

Subject	Age yrs	Sex	Reason for bronchoscopy.
1	69	M	Biopsy
2	50	M	Biopsy
3	62	M	Laser surgery
4	71	M	Biopsy
5	74	M	Biopsy
6	72	F	Biopsy
7	72	M	Biopsy
8	72	M	Biopsy
9	62	M	Biopsy
10	71	F	Biopsy
11	63	F	Biopsy
Mean (SD)	67.1 ($\pm$7)		

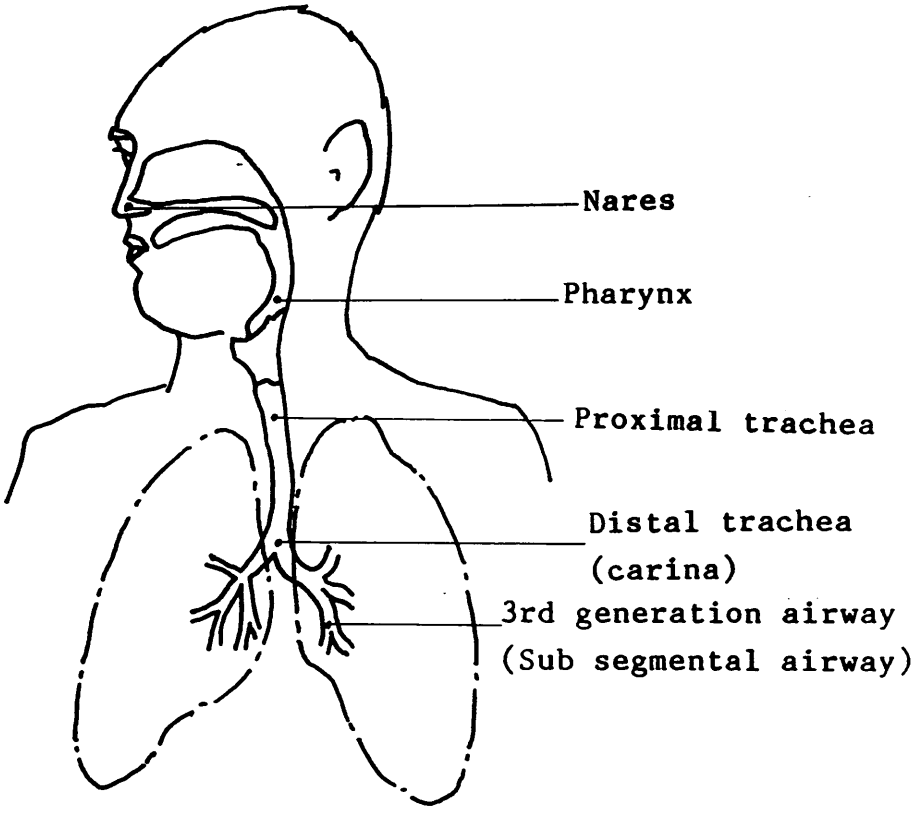

Figure 6.02: In vivo measurement locations. These were sighted by the bronchoscopist during the test.

6.4. Results.

Ambient air temperature in the theatre was measured immediately prior to the bronchoscopy to be 23.3 (±0.1)°C 48% RH, 10.2 mg/l. Cold air temperature was -17.5 (±1.3)°C and 1 mg/l.

Data analysis was by a Minitab statistics programme. This was used to detect the maximum, minimum and zero sample values and convert the spectra of real air flowrate into its root mean square (RMS) equivalent.

During ambient air breathing RMS air flow was 15.9 (±8.8) l/min (inspiration) and 10.9 (±4.7) l/min (expiration). With cold air breathing the RMS expiratory air flow rate was 17.3 (± 4.2) l/min. Figure 6.03 shows the variation in air stream temperature and respiratory air flow observed at the proximal trachea for one subject in ambient air. During early and late inspiratory phases relatively low air flowrates were encountered. The period of peak inspiratory air flow was associated with the lowest air stream temperature and was characterised by a lag of about ½ second (range 0.4-0.6 s) with air flow leading the minimum temperature. A similar phenomenon was evident between expiratory air flow and the maximum temperature encountered.

Figure 6.04 illustrates the typical spectra of air stream temperature during one respiratory cycle in ambient air at the different in vivo measurement locations. Free stream temperature was found to increase with progression into the airway and a corresponding reduction in the inspiratory-expiratory temperature difference arose. Inspiration temperature was taken to be the minimum observed at any site and ranged between 37.7 (±0.6)°C at the third airway generation and 35.8 (±0.8)°C at the pharynx during ambient air inhalation. These temperatures were 37.0 (±0.6)°C and 32.1 (±1.0)°C respectively during cold air breathing. Expiration temperatures were taken to

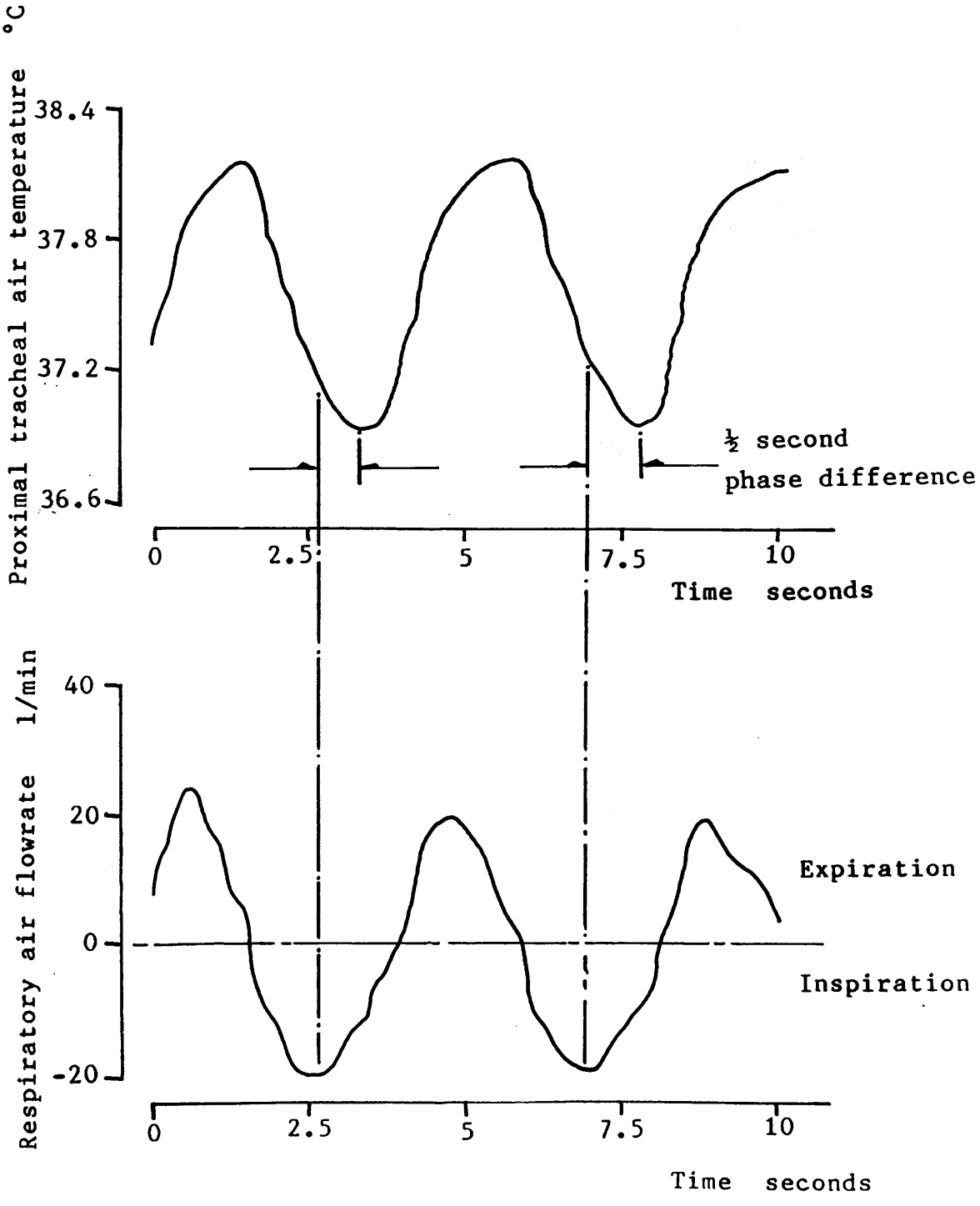

Figure 6.03: In vivo air temperature obtained at the proximal trachea with respiratory air flowrate tracings.

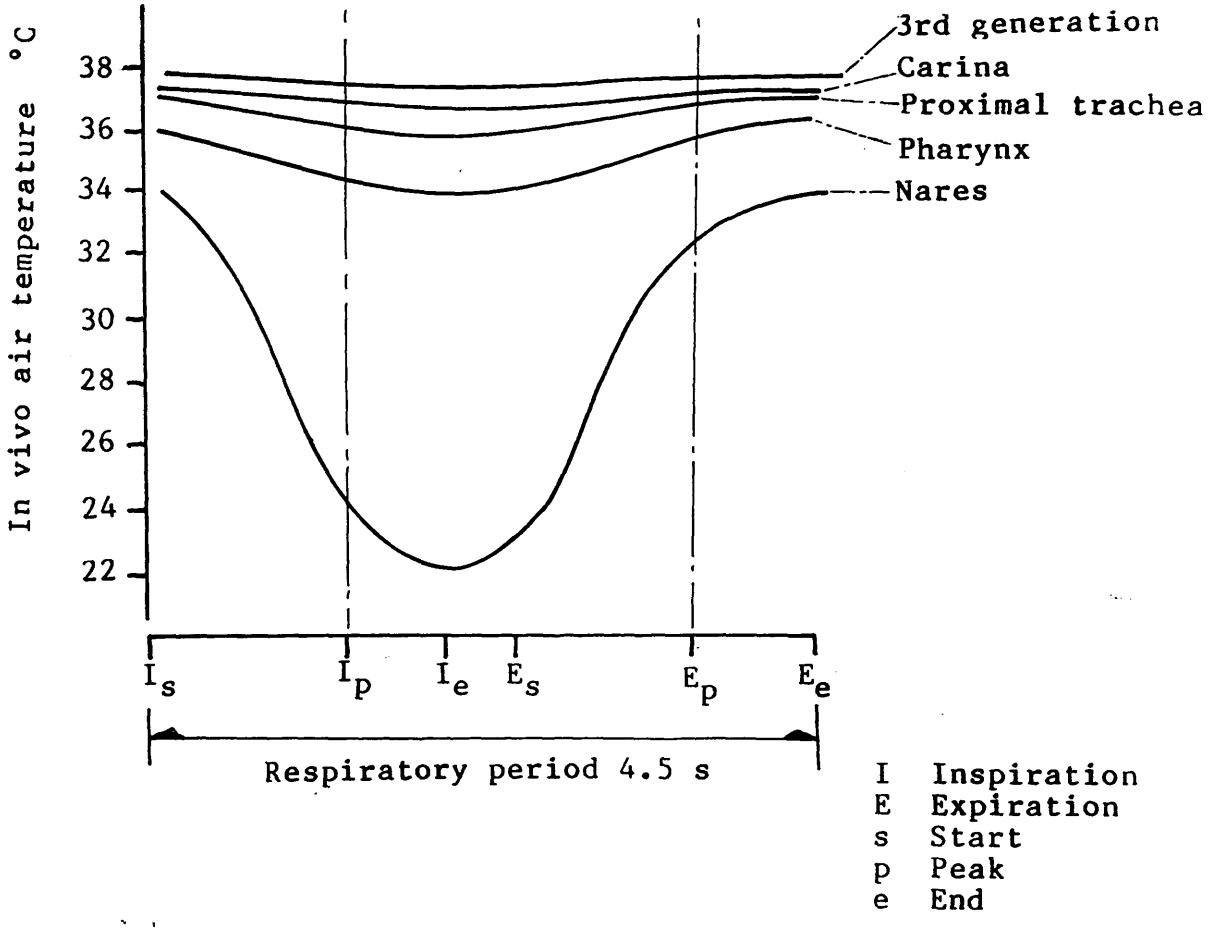

Figure 6.04: Typical spectra of air stream temperature obtained over one respiratory cycle.

be the maximum observed at any site and in ambient air breathing ranged between 38.2 (±0.6)°C at the third airway generation and 37.2 (±0.7)°C at the pharynx. The corresponding temperatures during cold air breathing were 38.1 (±0.5)°C and 36.6 (±0.3)°C respectively. Expired air temperatures at the nares were 34.0 (±1.2)°C (ambient) and 32.9 (±1.2)°C (cold).

The change in air temperature with depth into the airway is illustrated in figure 6.05. Data were subjected to an analysis of variance using the Minitab statistics package. Significant differences ($p<0.05$) in inspiration air temperature between ambient and cold air breathing were found at the pharynx and proximal trachea. Table 6.02 summarises the group temperature data and table 6.03 the ventilation data.

Table 6.02: Summary of in vivo temperature data.

Station:	Nares	Pharynx	Top of Trachea	Base of Trachea	3rd Gen. Airway.
Temperature mean (SD) °C					
Ambient inspired	23.2 (±0.1)	35.8 (±0.8)	36.6 (±0.4)	37.2 (±0.6)	37.7 (±0.6)
Ambient expired	34.0 (±1.2)	37.2 (±0.7)	37.9 (±0.6)	38.1 (±0.7)	38.2 (±0.6)
Cold inspired	-17.1 (±1.3)	32.7 (±1.0)	35.4 (±0.7)	36.6 (±0.6)	37.0 (±0.6)
Cold expired	32.9 (±1.2)	36.6 (±0.3	37.2 (±0.5)	37.8 (±0.5)	38.1 (±0.5)

Figure 6.05: Axial change in air temperature with airway location.

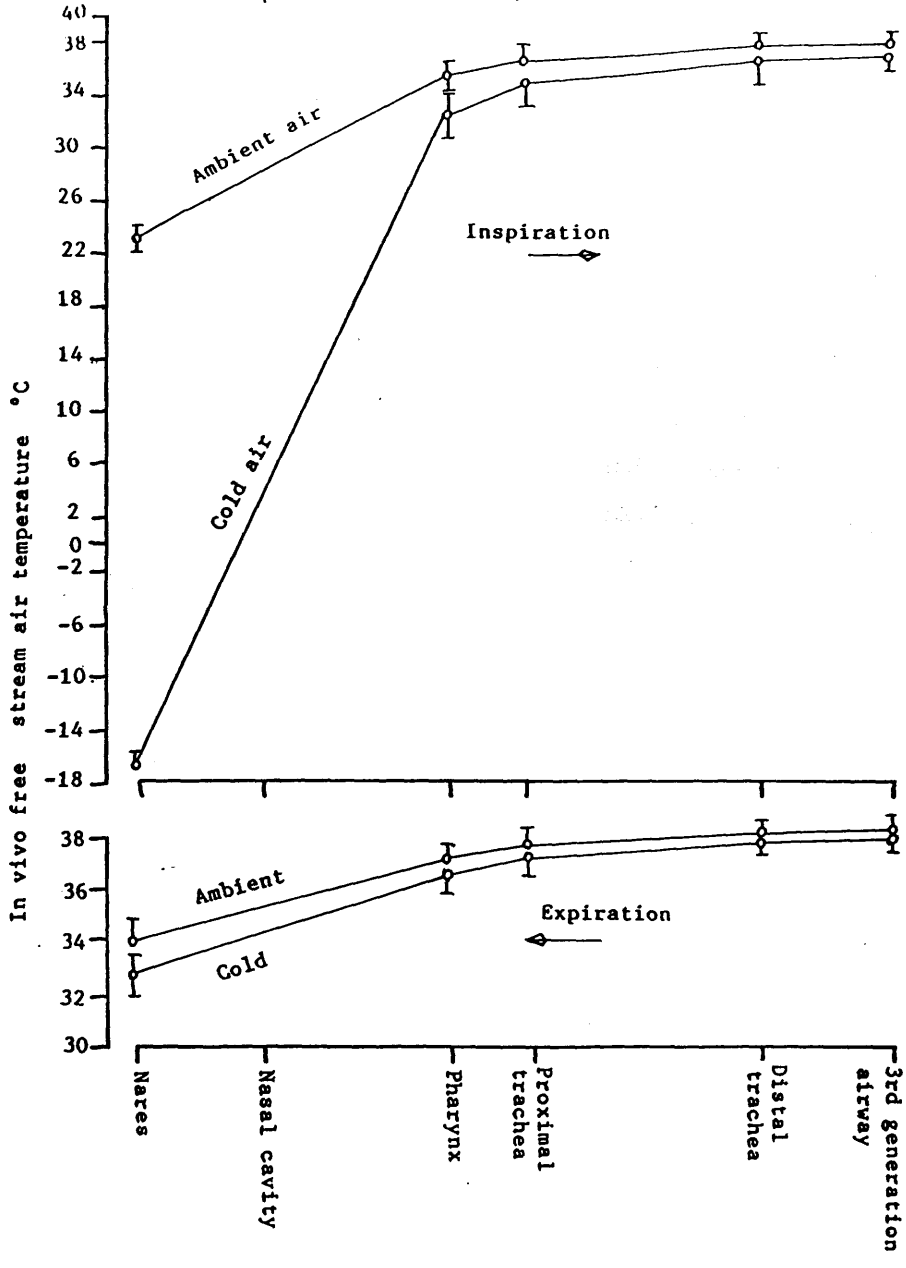

Table 6.03: Ventilation rates encountered.

Challenge	Inspiration l/min	Expiration l/min
Ambient (n=11)	15.9 (±8.8)	10.9 (±4.7)
Cold (n=4)	--	17.3 (±4.2)

6.5. Discussion.

Obstruction of the airway lumen by the bronchoscope will have undoubtedly disturbed the in vivo air flow in two ways. It will have reduced the contact time between air and airway wall by increasing the local air speed, thereby inhibiting heat transfer to the free stream. The bronchoscope will have also held open the larynx during the examination. In geometrical terms this area is similar to a venturi and serves as a focus for turbulence which would normally improve mixing of the inspirate against the trachea. The errors arising from both may not be substantial. Figure 6.05 shows that the majority of air warming during tidal breathing can be seen to have occurred proximal to the pharynx even with an obstructive presence. Flow through a normally constricted larynx and discharging into the trachea would not contribute much more to the overall air warming process. Air turbulence sustained by the diverging nature of the bronchial tree can be expected to cause greater heat transfer rates in this region. However the volume of air in any bronchial segment reduces as the tree branches towards the alveoli and the surface area of tissue available for air conditioning rises. The thermal stress or recurrent inspiratory cooling imposed on a tissue element herein will be less than that experienced

by a similar element in the nasal - pharyngeal zone.

Measurements of expired air temperature for cold air breathing concur with the 29°C-32°C range cited in the oral ventilation study by Tessier et al (1986)[58], whereas at ambient conditions Anderson et al (1985)[59] report an expired air temperature range of 32°C-34°C. The slightly higher expiration temperatures recorded at the nares in the present study are attributed to the close proximity of the thermocouple to the nostril when passed through the facemask.

The data for tidal breathing are slightly higher than described by McFadden et al (1985)[58], shown in figure 6.01, although a similar oral - pharyngeal heating role was evident. In the present work inspiration occurred nasally thus air was exposed to the additional surfaces of the nasal cavity and naso-pharynx.

The presence of the bronchoscope in the airway allowed continuous observation of the thermocouple hot junction and permitted ease of cleaning a mucus contaminated probe. Figure 6.06 illustrates the apparent variation in air stream temperature for the thermocouple in obvious contact with the airway wall. The recording was taken from the subject for whom the freestream tracing was illustrated in figure 6.03. The contacting thermocouple exhibits similar characteristics throughout the respiratory period but at an elevated temperature. Without knowledge of the contact between the probe and airway the finding can be explained by the lower ventilation rate encountered. However this was within the tidal range for the group. Although incidental to the purpose of the investigation the example serves to illustrate that airway wall temperature is not invariant. It is likely that these temperature fluctuations will be attenuated with greater impression of the probe into the epithelium.

The observation of a thermal lag between minimum air temperature and peak inspiratory air flowrate is

Figure 6.06: Embedded thermocouple tracings.

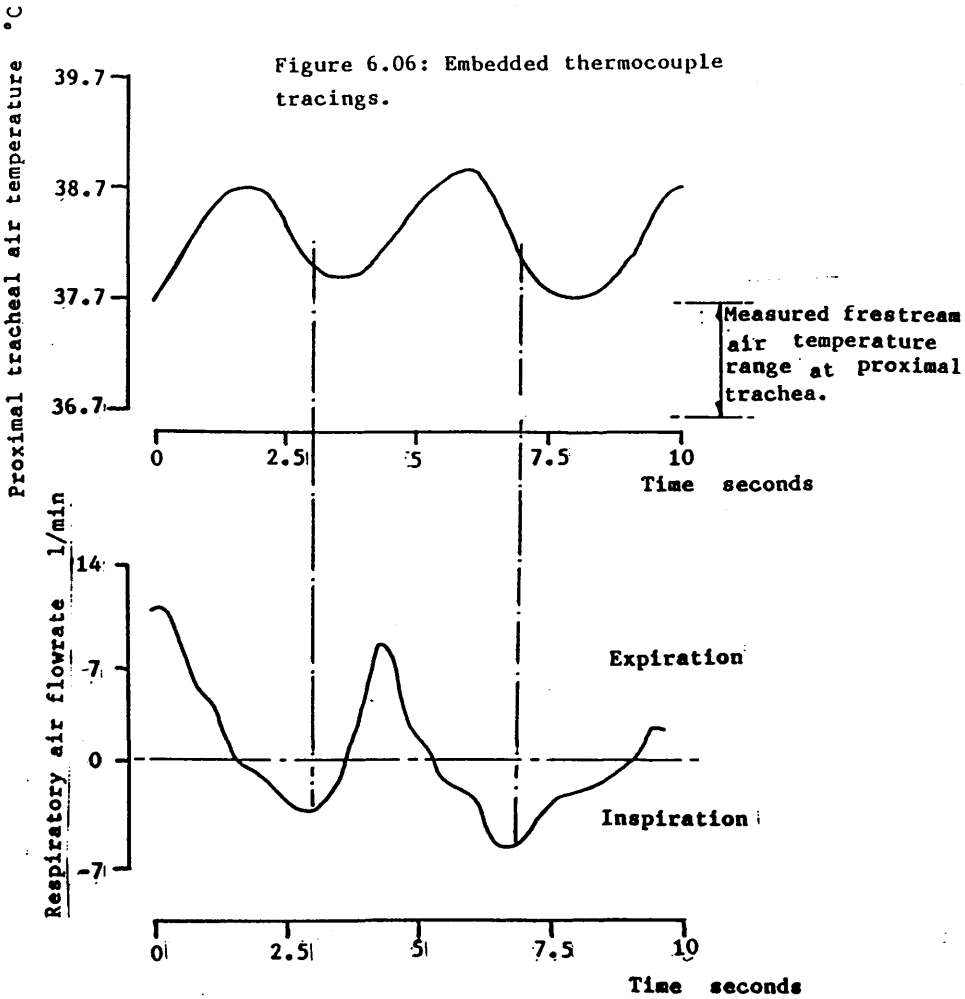

unexceptional. Many physical systems exhibit a similar response to a forcing function. The magnitude of the lag, (about ½ second in a respiratory period of 4.5 seconds), is equivalent to an angular phase difference of 40°. The low thermal conductivity of air, ($k_{air}=2.6x10^{-2}$ W/m K, 1/20th k_{water}), mitigates against immediate heat exchange from the airway wall. A more instructive test could be the simultaneous measurement of airway wall temperature, air stream temperature and air flowrate.

An investigation of this type would present ethical and technical problems. To the authors knowledge only one measurement approximating the above has been made: Ray et al (1987)[60] in the canine airway. A caged probe comprising a mass spectrometer sampling tube and thermistor bead was passed into the trachea of anaesthetised dogs. Two spring loaded miniature cantilevers located on the cage pressed thermistors into the tracheal wall allowing simultaneous measurement of airstream temperature, humidity and wall temperature. Cold and dry air inhalation were found to produce a similar airway wall cooling effect. Air flowrate measurements were not made and the depth of probe impression into the epithelium was not alluded to.

The in vivo inspiratory ambient air temperature profile found in the present work is plotted in figure 6.07 together with that found for laminar airflow midstream in the long axis air conditioner described in section 4.4.1. The axial scale is based upon the anatomical measurements of Hanna and Scherer (1986)[4]. Of the two, the human airway warms the inspirate faster presumably because of improved air wall mixing caused by geometry dependent turbulence. Both profiles are characterised by an early rapid air warming phase derived from the thermal gradient between their respective freestream and wall.

Maximal cooling, (and presumably drying), effects of inhaled air will be in the airway zones exposed first namely the mouth or nose, throat and upper tracheal region.

Figure 6.07: Comparison of air warming in the airway and the long axis air conditioner.

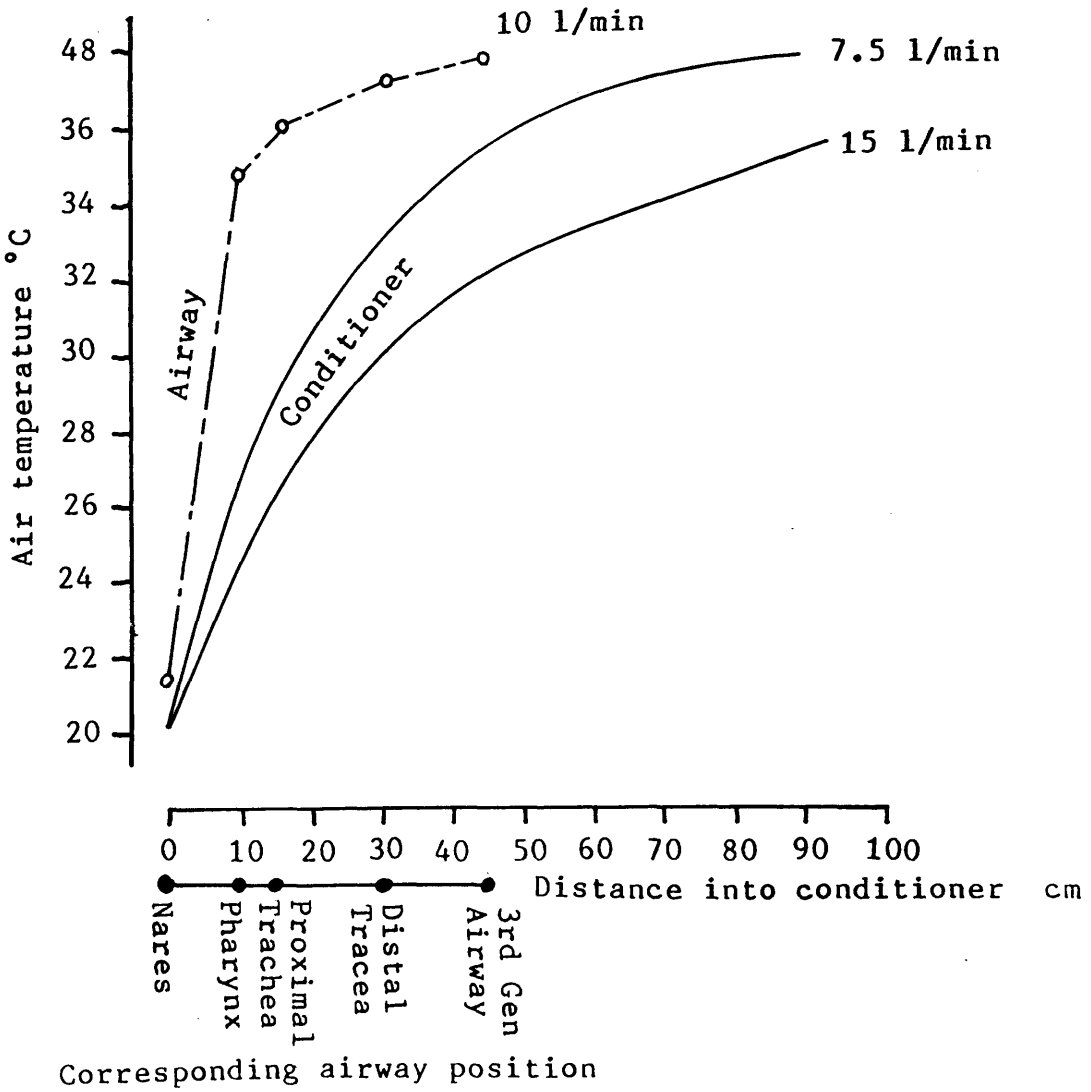

Although high respiratory air flowrates have been previously found to delay the overall air warming process into the sub segmental level, (figure 6.01), the upper airway and in particular the larynx will remain the predominant air conditioner. Moreover the long term effect of hyperventilation will be to give the airway wall less time to recover heat and moisture from its underlying blood capillary plexus and lead to enhanced cooling of the structural tissues. In so doing the upper airway may be the site of a trigger for a subsequent bronchial response to heat loss.

7. In vivo measurement of airway humidity.

7.1. Introduction.

The role of respiratory heat exchange in provoking bronchoconstriction in asthma sufferers has aroused controversy. Two schools of thought have emerged emphasising the primary importance of either airway cooling or airway drying in the biological mechanisms underpinning the response.

The main advocate of cooling, E R McFadden, cites the thermal events present in the airway as a stimulant of thermoceptors in the epithelium. Measurements of in vivo warming of inspired cold air and a rapid post challenge airway rewarming phenomena indicated increased activity of the airway vasculature in asthmatics: McFadden et al (1986)[37] and Gilbert (1987)[61]. Calculations of airway water loss therein assumed a flash saturation process of inspired air at the mid trachea, justified by bronchoscopy observations in normals during a hyperventilation exercise, (E R McFadden, personal communication). The author does not accept this as an argument for general full saturation of inspired ambient air at the mid trachea because fog formation cannot arise in a simultaneous natural convection-evaporation process without external cooling. It is possible that the observations made were either due to direct misting on the bronchoscope or the subtle effect of nasally inspired air mixing with cooler orally inspired air. The error magnitude of the flash saturation assumption was not alluded to.

Conversely, S Anderson, the protagonist of airway drying proposes that airway water loss leads to osmotic changes in the epithelium thereby producing favorable conditions for the release of mediators and subsequent bronchoconstriction: Anderson (1984)[27] and Anderson et al

(1985)[59]. Calculations therein showed that there is insufficient water available to condition an ambient inspirate from a stationary boundary of supra mucosal water estimated to range between 1u to 20u in thickness. The predictions were dependent upon estimating the airway boundary thickness and assuming it to be stagnant. Without a reliable measurement of intra thoracic airway humidity no knowledge of the regional trans epithelial water flowrate was available.

The findings of the present work have indicated a role for both airway drying and airway cooling in asthma (section 3.10). Air warming was observed to predominantly occur in the upper airway (section 6.5). Presumably this predominance of air warming is accompanied by a similar air drying role, observed by the simultaneity of heat and moisture exchange in the long axis model (section 4.5). In addition, as airway drying is known to modify the muco-ciliary beat frequency it was considered that a useful contribution could be made by the accurate measurement of intra thoracic airway humidity to determine the trans - epithelial flux of water.

7.2. Past work.

Few workers have attempted to to record in vivo inspired air water vapour content primarily because of limitations in the response time, stability and miniaturisation of transducers.

Ingelstedt (1956)[53] attempted a direct measurement of in vivo laryngeal air temperature and dew point temperature using a miniaturised thermocouple hygrometer. The invasive method employed was ethically dubious and not an option for the present study: it required insertion into the crico-thyroid membrane of a 2mm cannula through which the hygrometer was passed into the laryngeal airway. Assembled the hygrometer measured 1.7mm OD, the wet bulb being formed

from rayon silk wrapped "tightly" about a thermocouple element. Subjects were required to withdraw the device using a camera cable release mechanism if coughing was anticipated. The hygrometer and release mechanism are illustrated in figure 7.01. A response time of less than 2 seconds to a 25% step change in air humidity was evaluated for the device by means of a novel slide valve arrangement linking two reference atmospheres. For tidal nasal breathing inspiratory laryngeal air condition was found to be 32.3°C 98% RH, 34.9 mg/l. The corresponding air condition following oral inspiration was 30.5°C 90% RH, 29.1 mg/l. Expired air condition at the larynx was found to be 36.4°C 100% RH 44.5 mg/l. Respiratory airflow was determined simultaneously with the recordings using an inductive plethysmograph.

A problem with the wetted wick hygrometer is derived from the need for an adequate water supply to maintain a moist wet bulb. During the above tests it was necessary to withdraw the hygrometer from the airway and refill its reservoir every 5 or 6 breaths. Inadequate wetting of the wet bulb would cause overestimates of the air humidity. Moreover wet bulb devices have a response time dependent on air speed. They require air speeds of between 2 m/s and 40 m/s in order to achieve a full wet bulb depression Rodgers and Mayhew (1983)[47]. Although the response time of the above hygrometer was evaluated in an air speed of 1.5 m/s the tidal respiratory air speeds encountered could have been predominantly less than this. For a laryngeal diameter of 1 cm and assuming an RMS inspiratory air flowrate of 10 l/min the local RMS air speed about the probe would have been 2.12 m/s. Section 2.4.3 illustrated how air flowrates (and thus airspeeds) less than the RMS level are present for 40% of the respiratory phase. It is possible that inadequate evaporation from the wet bulb arose. This possibility was not alluded to. Low rates of evaporative cooling from the wet bulb would have also overestimated air

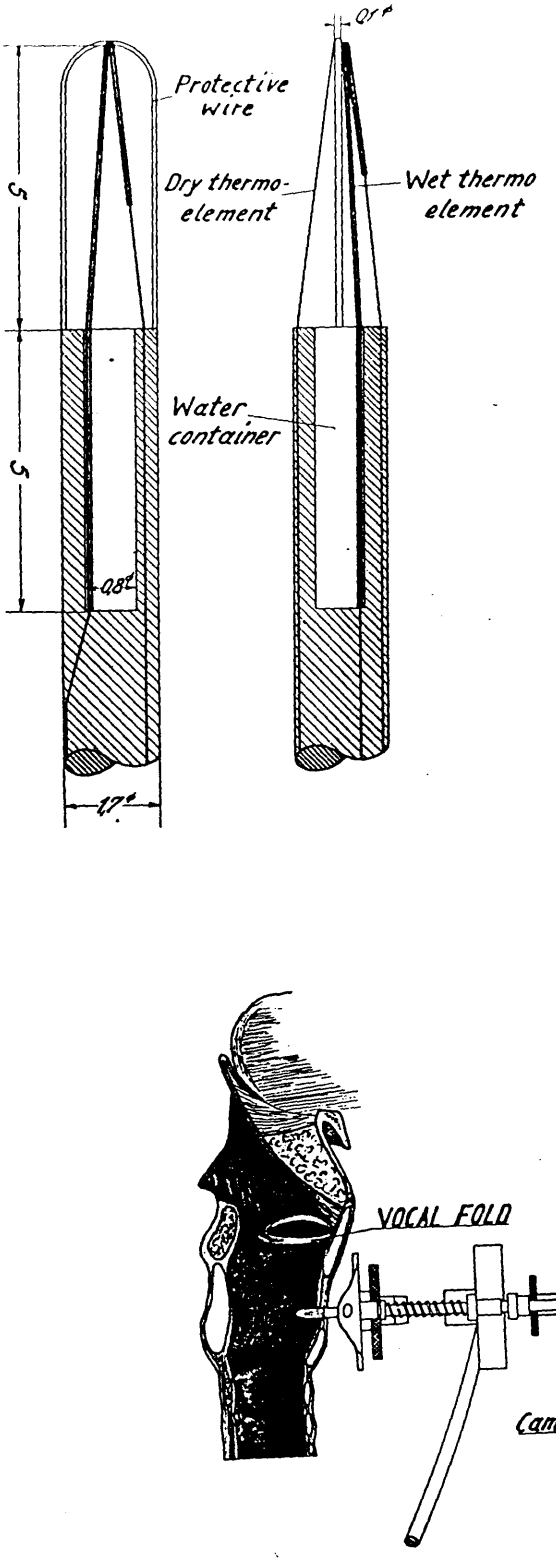

Figure 7.01: Ingelstedt's wetted wick thermocouple and invasive method. The camera release was taped to the neck and supported by the subject.

humidity.

An indirect technique by Cramer (1957)[62] involved sucking small known volumes of air from the choana (rear wall of the nares) during tidal inspiration in normal volunteers. Samples passed through a thin electrically heated tube containing a thermocouple and terminated at a vessel containing magnesium perchlorate which thereafter dried the air. The weight of this vessel was compared with its pretest value, the difference being due to the addition of inspiratory water. Figure 7.02 illustrates the device. Measurement of the air temperature in the suction tube and the mass of water added to the drying agent allowed an estimate to be made of nasal inspired air humidity. This was 32°C 80% RH, 28.1 mg/l in ambient air.

Weighing the drying agent made the technique indirect and non-continuous. Moreover no mention was given as to how the sampling process was synchronised with inspiratory airflow. Inadvertent sampling of the expirate would have undoubtably increased the measured "inspiratory" air humidity.

A variant on this technique by Dery et al (1967)[63] involved sampling inspiratory air at the mid tracheal level. Inspired moisture content was derived by recording the drop in surface temperature on a cooled mirror following condensation of the air to its dew point. A tube containing a micro thermocouple was introduced into the airway of anaesthetised subjects undergoing surgery wherein the temperature of mid tracheal air was recorded. The tube was then substituted for a 4 mm suction catheter. Inspiratory air samples were prevented from condensing on the catheter wall by the presence of a heater wire which terminated, with the catheter, at the dew point detector. The apparatus, shown in figure 7.03, had an unspecified response time of 0.25 second. Mid tracheal air temperature was measured to be 35°C 85% RH, 35.5 mg/l during tidal ambient breathing. Respiratory airflow was estimated prior to intubation by timing the period required to deflate a

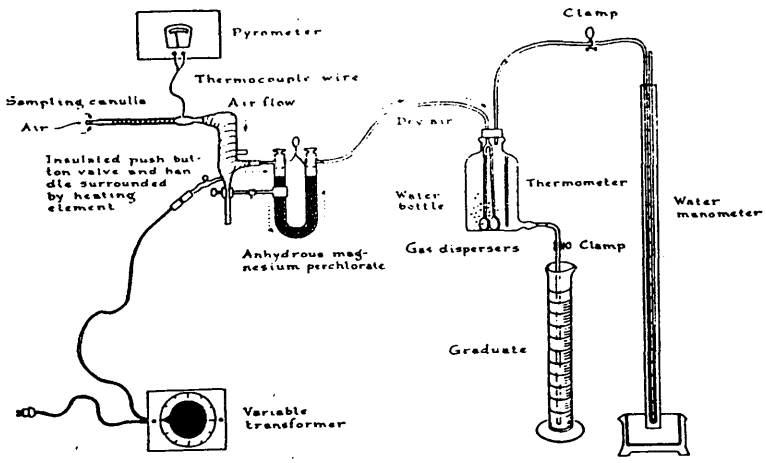

Schematic diagram of apparatus assembled and ready for sampling.

Figure 7.02: Cramer's heated tube suction method. Problems with inadequate response time and sample breath synchrony were likely.

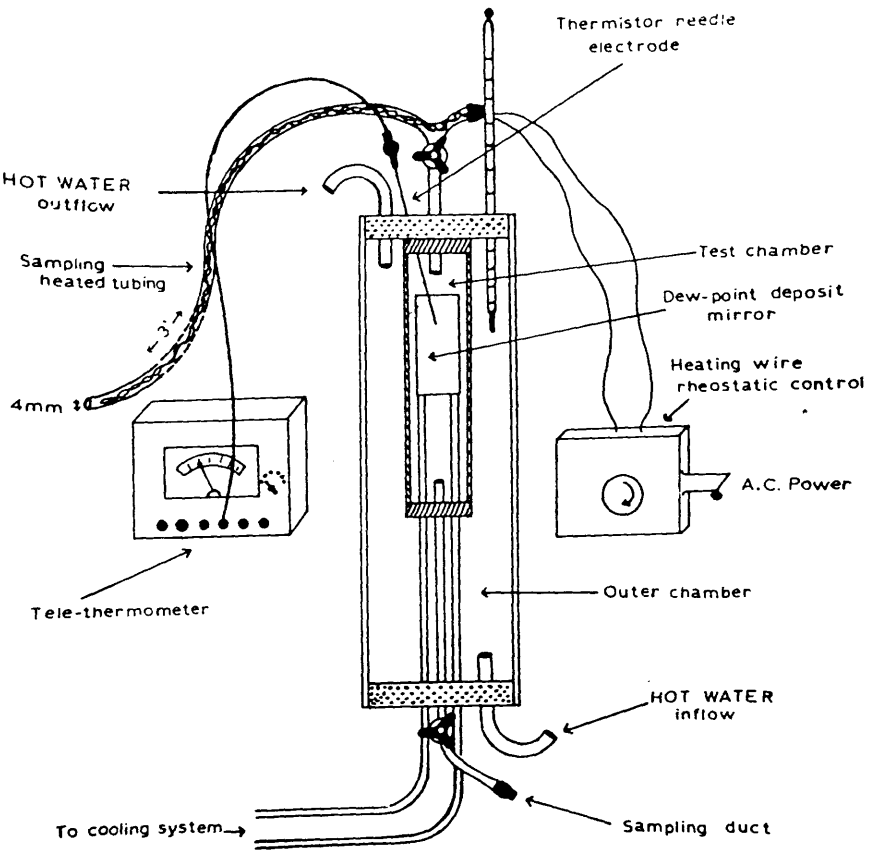

A simplified sketch of the general assembly.

Figure 7.03: Dery's heated tube suction system. The cooled mirror dew point detector would have had a fast response time. Problems with sample breath synchrony were likely.

balloon of known volume.

Extubation with the thermocouple tube followed by intubation with the suction catheter would have exposed the airway to additional irritation and as a measurement strategy was error prone. Essentially the derivation of the air condition relied upon two unrelated parameters, namely a measurement of mid tracheal air temperature followed by a measurement of the sample dew point temperature. Again the problem of sample synchronisation with the inspirate was present.

The problems associated with the in vivo measurements described are derived from the transducers available. Direct invasive recordings have presented ethical problems and previous indirect methods are constrained by sample - breath synchronisation and potential water vapour loss by condensation in the suction tube.

An overview of the principal electronic methods available for remote air humidity measurement follows, several of which lend themselves to the present application.

7.3. Methods of air water vapour determination.

Automatic and electronic methods of air water vapour measurement have developed primarily to meet the demands of the chemical process industry. Four techniques have been identified some of which lend themselves to miniaturisation and microcomputer compatibility.

Water vapour removal methods operate by totally drying an air sample. Keidel (1956)[64] describes an instrument based on the measurement, by electrolytic dissociation, of airborne water present in a gas flowing through a dessicant. Moisture extraction and determination of the masses of air and water present obstacles to miniaturisation.

Direct methods utilise physical differences between the test gas and a completely dry reference sample. Ultra

violet and infrared light absorption sensors are included in this category although they require special optics and a long light absorption path. They are not conducive to miniaturisation but do offer excellent response characteristics which are alluded to by Ray et al (1987)[61] in a mass spectrometer based air humidity study of the canine airway.

Saturation methods involve either cooling the test sample of air until dew formation occurs (condensation method) or by adding a quantity of water until the same state is reached (evaporation method). A simple wetted wick swing hygrometer is a saturation device wherein evaporative cooling of the wick depresses the bulb temperature to dew point. An adequate water supply and thermal insulation of the wet bulb element hinder the miniaturisation and response time of these types of sensor. Semiconductor saturation devices combine the role of cooling, dew detection and temperature measurement in one unit. Reitgen (1981)[65] describes a Peltier cooler, (a semiconductor cooling element), bonded to a capacitive temperature sensor used to continuously determine the dew point temperature (DPT) of a test gas. Figure 7.04 illustrates the device. The capacitor was configured as two interdigitated electrodes deposited on a glass substrate. As condensate formed on it so the capacitance of the device altered due to the large dielectric constant of water. Commercial electronic saturation sensors use a platinum resistance wire as the temperature sensor and of those considered so far are the most easily miniaturised and packaged. This kind of sensor has the disadvantage of not measuring relative humidity directly but rather dew point temperature. Errors in converting this into %RH can arise: At the time of writing a typical commercial solid state dew point sensor ("Dewmatic", MCM Ltd, Wetherby, UK) had a 0.3°C accuracy in DPT measurement which at ambient conditions yields an error of approximately 4%RH and a full

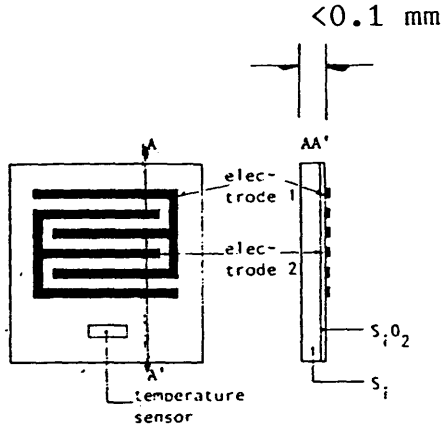

Figure 7.04: Capacitive semiconductor dew point sensor, after Reitgen (1981).

scale response time of 15 seconds.

Absorption methods depend upon the diffusion of water vapour into a hygroscopic solid which acts as a dielectric between permeable electrodes. The quantity of water passing through the electrodes is dependent upon the vapour pressure gradient between the atmosphere and dielectric. Commercial absorption sensors comprise an organic polymer dielectric sandwiched between gold, chrome or nickel electodes one of which is deposited on a metallised glass plate for mechanical rigidity. A typical gold film absorption sensor ("Humidicap" 1638 HM, Vaisala OY, Helsinki Finland) has an advertised full scale response time of less than 5 seconds to an 85%RH step change in stagnant air. This is illustrated in figure 7.05. The small size and fast response of this type of sensor made it an ideal choice for the present in vivo air humidity investigation.

7.4. Design limitations.

The final choice of design for the humidity probe was determined by four factors which were largely born of the bioengineering nature of the study. These were ethical committee approval for the investigation; simplicity of use; sterility and safety.

7.4.1. Ethical committee approval.

Existing UK hospital ethical committee guidelines do not permit invasive measurements in humans solely for the purposes of pure research. Patient safety and comfort are of paramount importance and such research must be confined to that of an appendage to routine invasive treatment. Consequently the first design consideration was how to incorporate the in vivo humidity measurements in to an existing clinical situation.

The construction of a practical Humicap sensor

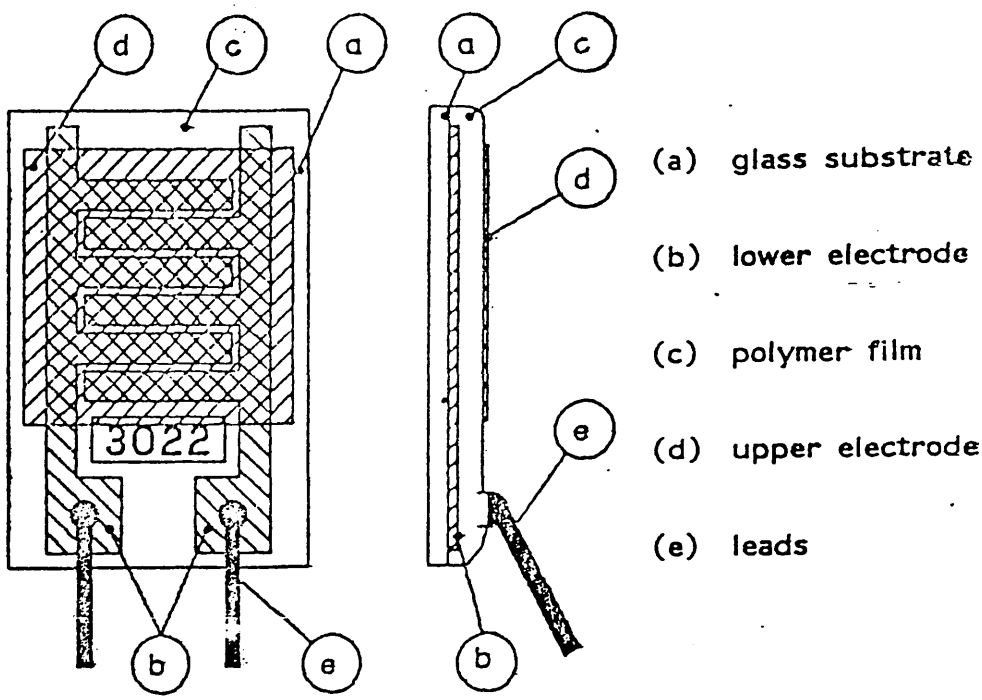

The construction of a Humicap sensor

Figure 7.05: The Viasala humidity element, 'Humidicap' chosen for the present application.

Anaesthetised patients undergoing general orthopaedic surgery were considered to be the best available for the study. Throughout the course of their operation a sterile endotracheal (ET) tube, is inserted into the airway between the mouth and mid trachea. This maintains an open airway and ensures full inhalation of the anaesthetic gas. About the circumference of the ET tube at its tracheal end an inflatable cuff forms a seal with the airway. At the mouth the ET tube is connected to the anaesthetic gas supply. A deeply anaesthetised patient will, after disconnection from the anaesthetic gas, remain anaesthetised for about 5 minutes. Thus there exists a 'window' during which a humidity probe could be inserted into the airway of an anaesthetised patient via the ET tube during ambient air breathing. The technique is described in more detail in section 7.6.1.

This procedure was acceptable to the hospital ethical committee and it became the basis for the engineering of the probe.

7.4.2. Simplicity of use

The limited period during which in vivo measurements could be made demanded a probe and experimental procedure which would both minimise patient exposure to the test and permit a 'second run' at the measurements. Experience from the in vivo temperature investigation highlighted the need for the latter as data could be easily corrupted by patient coughing or mucus accumulation on the sensor. Moreover an easy to use device would engender confidence in the anaesthetist who would be inserting the probe into the airway and therefore be more likely to generate a successful outcome.

Attention to the speed of use also focussed on the data collection software which would drive the experiment. Again, experience from the in vivo temperature

investigation showed how time consuming responding to programme prompts can be during an operating theatre based investigation.

7.4.3. Sterility and mechanical properties.

An important consideration was the ability to clean and sterilise the probe in an operating theatre. This would have to be done prior to use on each patient. The method chosen was to immerse the probe in hibitane solution, (ICI Cheshire, UK), rinse in cold water and dry by exposure to bottled dry air. The device was then stored in a sterile ET tube. This cleaning procedure was found not to disturb the calibration of the probe which was checked against the ambient condition immediately prior to the measurements. On enquiry at the at the Orthopaedic Surgical Department of the Western Infirmary an operating time of between 1½ to 2 hours was anticipated during which pre insertion cleaning could be done.

Mechanical flexibility, cohesive and tensile strength were also essential features of the design. In order to conform to the anterior posterior radius of the upper airway the material housing the humidity sensor had to bend through an angle of at least 90°. In vivo cohesion between the components was vital and of paramount concern to the ethical committee.

The final design choice for the humidity probe comprised two sub assemblies compression fitted together. These were a unidirectional leaflet valve located at one end of a flexible clear rubber tube which housed the sensing elements.

7.5. Description of apparatus.

7.5.1. Probe configuration.

A small two wire capacitive absorption sensor (Vaisala OY Finland, model 1638HM) was selected for the probe. It had an advertised response time of less than 5 seconds to an 85% step change in stagnant air humidity and measured 6 mm x 4 mm. This sensor and its amplifier were adapted from a commercial remote humidity transmitter (Vaisala HMD20U) designed for mounting in air conditioning duct work. The device originally comprised a cylindrical sensor housing (250 mm long x 10 mm OD) screwed into the amplifier casing. An initial attempt to increase the length of lead wire servicing the sensor radically attenuated the sensitivity of the element, despite advice from the manufacturer and this modification was not pursued.

Figures 7.06 and 7.07 illustrate the invivo humidity probe designed and built by the author for this study. The humidity sensor and a polythene insulated 'T' type thermocouple were housed at one end of a 312 mm long x 8 mm OD clear rubber catheter. Five wedge shaped incisions into the catheter at the sensing end allowed air mixing against the transducers. Five incisions appeared to be the maximum possible without compromising the mechanical integrity of the probe. A small unidirectional leaflet valve, fabricated from a 8.5mm OD plastic barrel and an acetate disc, was also compression fitted to the sensing end to protect the transducers from mucus invasion during the intubation phase. The end diameter of the assembled probe was 9mm OD. A 50mm length of humidity sensor lead wires projected from the amplifier end of the catheter and these were each terminated with a brass pcb pin which plugged directly on to the amplifier circuit board, modified to accept these pins.

The pcb pins allowed passage of the catheter housing and

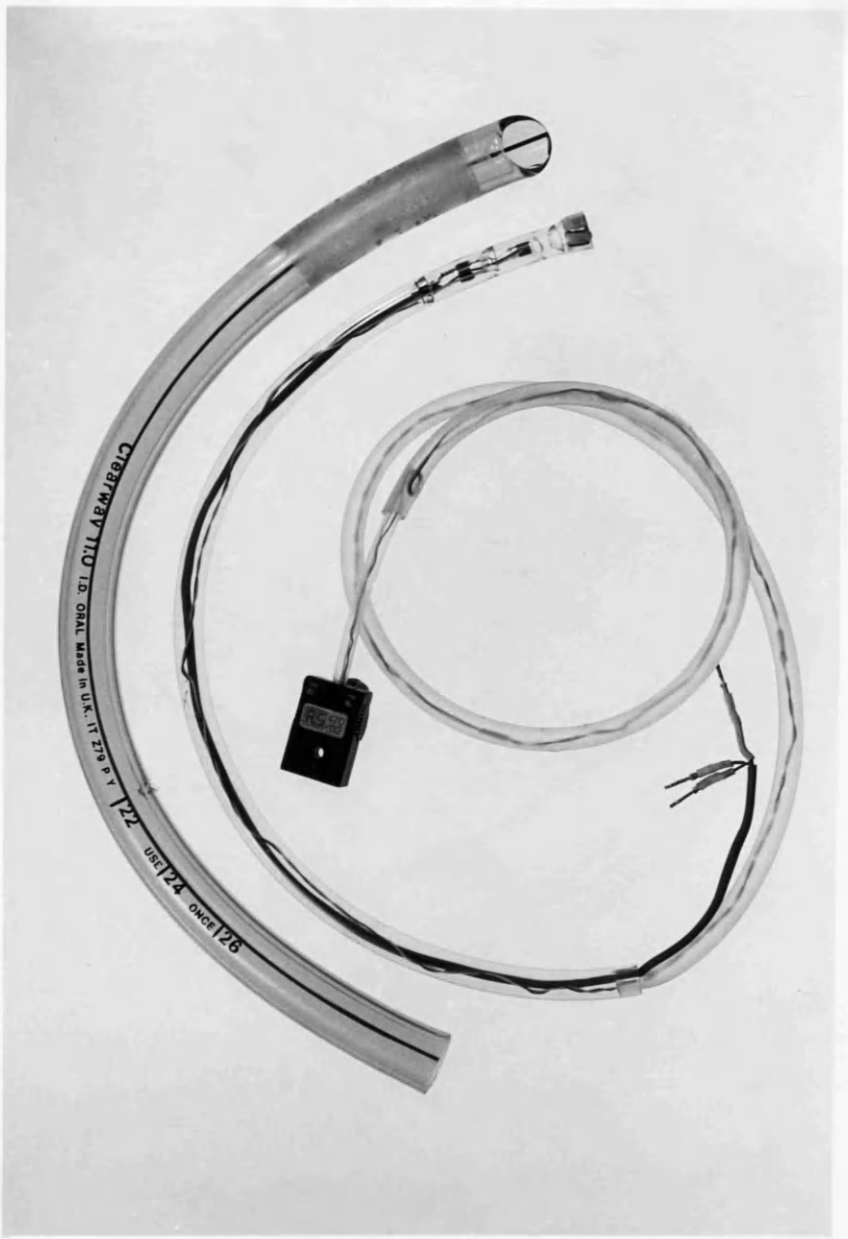

Figure 7.06: Upper airway air humidity and air temperature probe shown by an 11 mm ID ET tube. The tube is graduated in mm. The 3 pcb pins pass through the ET tube during intubation.

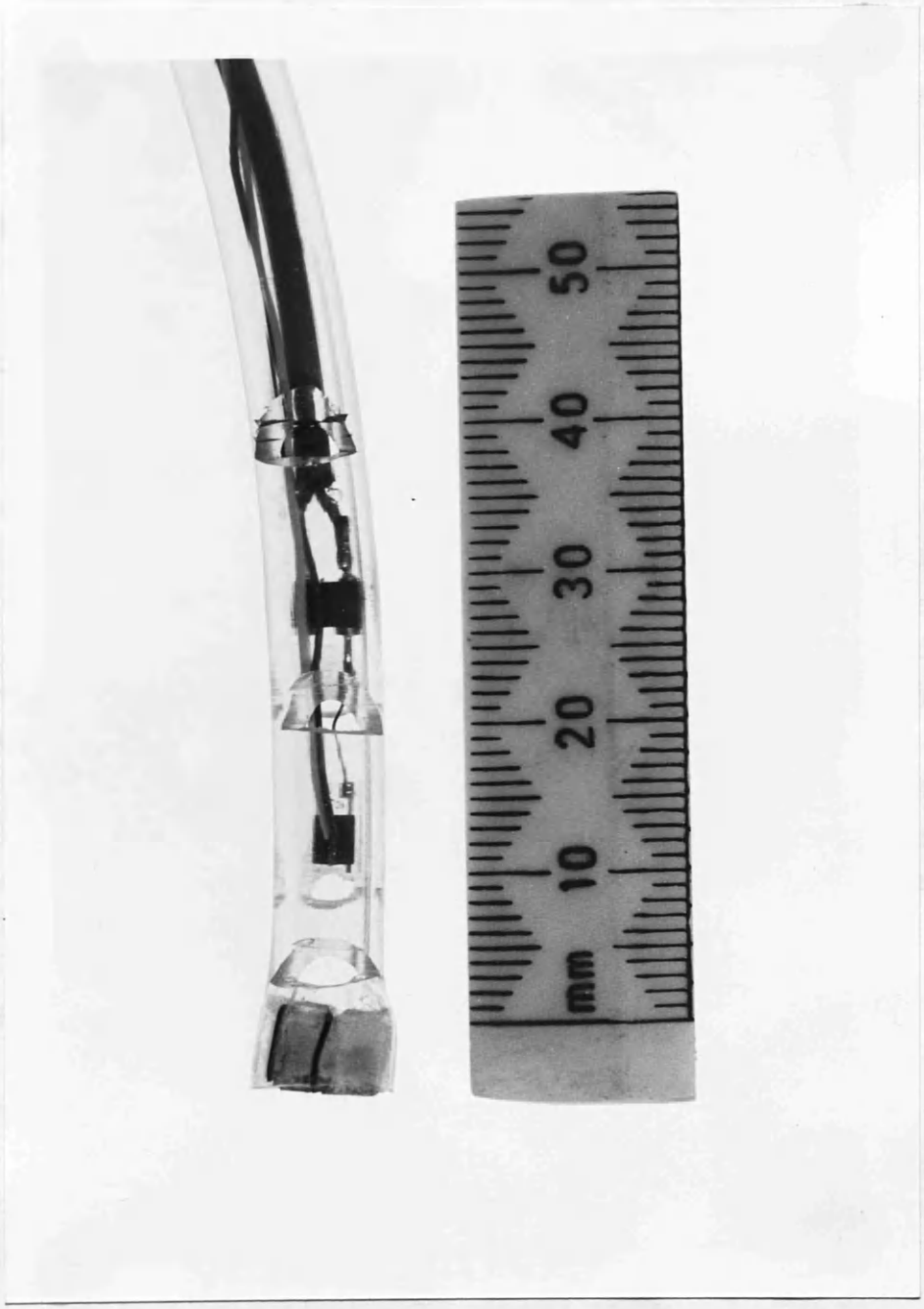

Figure 7.07: Detail of the sensing end of the humidity probe. The thermocouple is sited above the 'Humicap' both surrounded by air entry incisions. At the probe end the unidirectional valve is visible.

humidity sensor lead wires through an 11mm ID endotracheal tube. A standard copper chromel plug terminated the thermocouple lead wires 400mm beyond the catheter sufficient to accomodate the length of the ET tube.

7.5.2 Data aquisition software.

Software was written in MSBASIC to sample air temperature and humidity at a rate of 25 Hz. During the aquisition period data were stored in a 500 sample capacity memory array and after, replayed and written to a named file on the microcomputer's hard disc. Replaying the sample values after the data collection period maximised the aquisition rate and allowed determination of a successful test. The software then loaded a new file name from a magazine of preset names for subsequent data storage and returned to the data collection prompt. This feature economised the need to interact with the microcomupter whilst in the operating theatre and was derived from earlier experience with the invivo temperature measurement. A full software listing is given in appendix 13.

7.6. Performance evaluation of humidity probe.

7.6.1. Calibration.

Calibration of the probe was done by exposing it to a range of constant humidity and temperature environments. Some of these were generated by mixing to a slush consistency distilled water and salts in a purpose built sealed isothermal vessel supplied by Vaisala OY (calibrator HMK-11). The salts used and their resulting reference atmospheres at ambient temperature were: Lithium Chloride 12% RH; Sodium Chloride 76% RH and Potassium Sulphate 97% RH. Entry into the calibrator by the probe was through an aperture 25 mm above the slush, illustrated in figure 7.08.

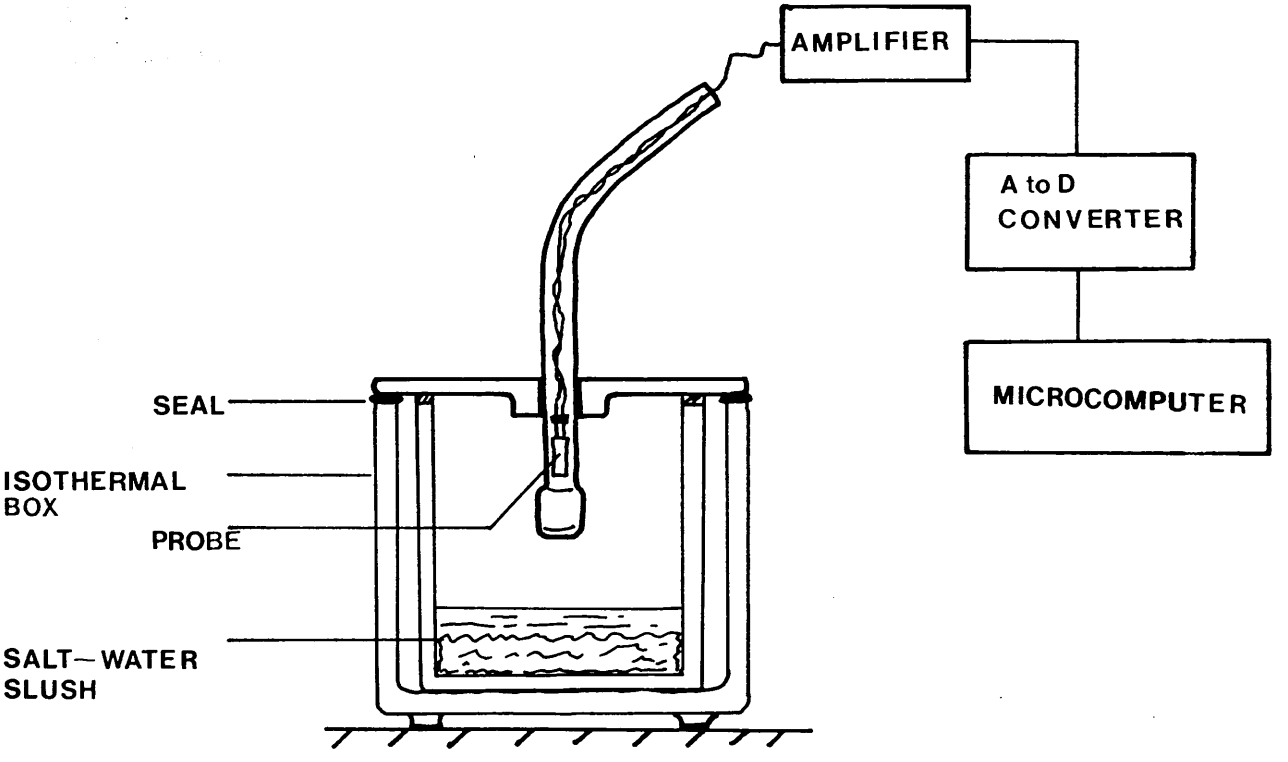

Figure 7.08: Calibration of probe using the saturated salt method.

Each mixture was allowed to stabilise for 24 hours in an unventilated room with the probe in place, after which the analogue to digital conversion number was recorded with the corresponding reference humidity. In addition the probe was exposed to dry bottled air (0% RH) and also stood in ambient air in the range 20% RH to 55% RH, the actual humidity of which was determined by a swing hygrometer, (Gallenkemp Ltd).

Figure 7.09 illustrates the graph of calibration humidity versus the analogue to digital conversion number (Y) obtained using the 'Microlink'. Throughout the measurements the calibration temperature was 21.4°C (SD $\pm$0.6). This was obtained for 15 samples and in the range 0% RH to 97% RH. In the range 12% RH to 97% RH the calibration was characterised by its linearity, the regression equation for this being Y=1203+1.82(%RH), r=0.96 $p<0.05$ and 2% error at full scale deflection, determined using a Minitab statistics programme. An overall curvilinear characteristic was apparent in the range 0% RH to 97% RH. The regression equation derived for the linear region was used to predict the humidity detected by the probe during the in vivo investigation because sub ambient humidities were not anticipated.

On communication with the Vaisala company it was discovered that the advertised response time of 5 seconds for an 85% RH step change in humidity pertained to an unshielded sensor in stagnant air. The presence of a housing could hinder mixing of the control air against the sensor and moreover did not reflect the dynamic conditions present in the human airway. Two tests are described to determine the water vapour absorption and desorption times of the probe.

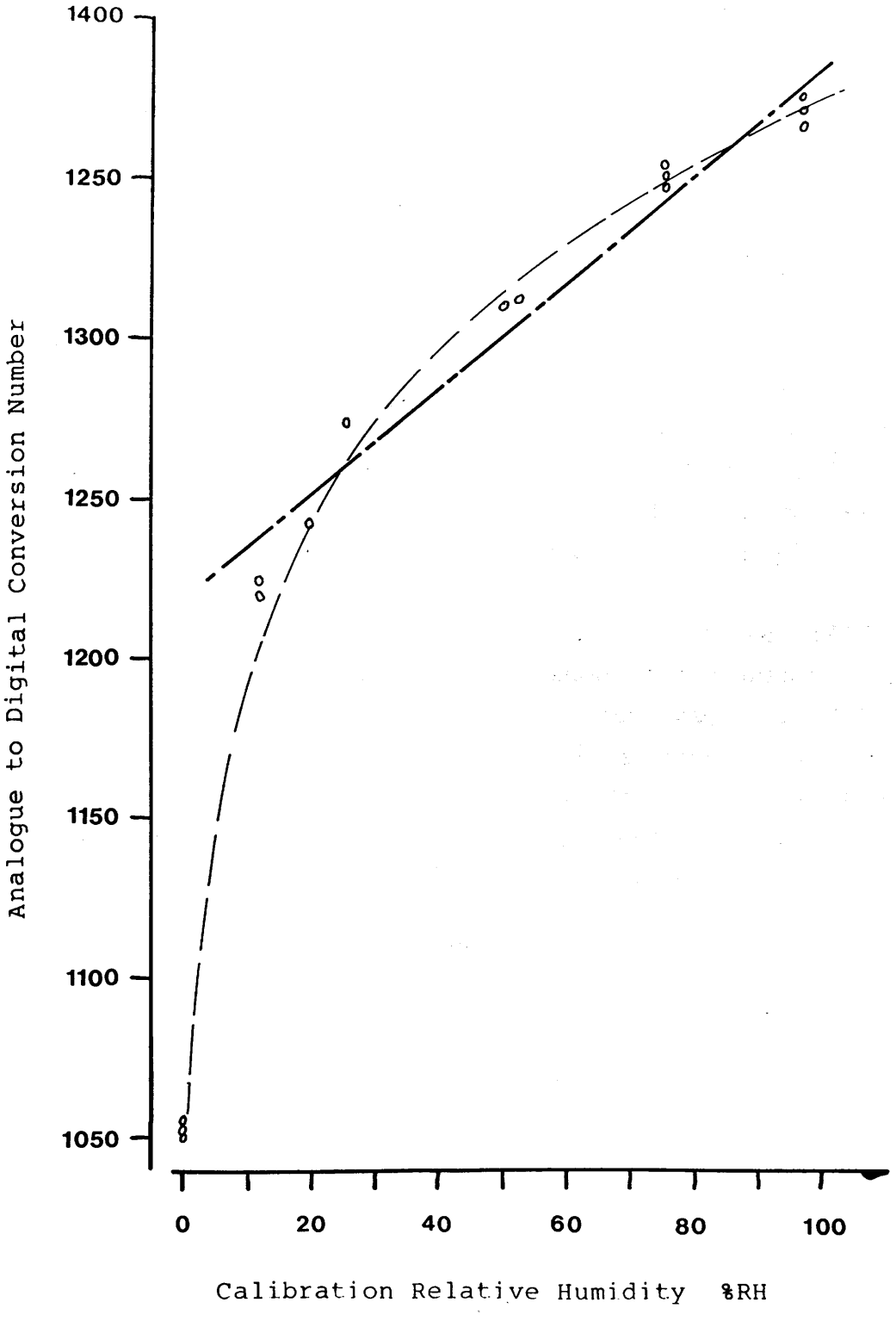

Figure 7.09: Calibration curve for the probe.

7.6.2. Step response: Absorption test.

7.6.2i. Method.

In order to do this the Long Axis Air Conditioner described in section 4 was utilised. Figure 7.10 shows how this step test was done. By varying the axial location in the downtube of the conditioner air inlet pipe so the length of boundary water film exposed to the air stream could be altered, in turn varying the exit air humidity. Immediately downstream of the air exit port was glued a thin plastic barrel 60 mm long and 35 mm OD. This acted as a control environment into which the humidity probe was manually plunged via an oblique aperture in the plastic barrel.

The water film entry temperature was set to 37°C, (similar to the body core), and maintained at a flowrate of 1.5 l/min, which by experiment had been found approximately to preserve an isothermal boundary along the downtube. Ambient air at 21°C 54% RH was pumped through the device by a rotary compressor (Edwards UK, ECB8) at an air flowrate of 100 l/min, determined by an electromanometer (Mercury, CS5 and flowhead F300L). Five target air humidities were selected which ranged between 62%RH and 94%RH. These resulted in step increases in air humidity of between 5% RH and 40% RH.

The apparatus was allowed to run for 1 hour prior to commencing the tests. This allowed thermal stabilisation of the hot water supply feeding the device. Target air humidity was set by placing the probe into the control environment and adjusting the axial position of the inlet, after which the probe was withdrawn and allowed to stabilise in ambient conditions.

Step testing was performed by manually plunging the probe through the oblique aperture into the control environment where it remained for 15 s. Following this the

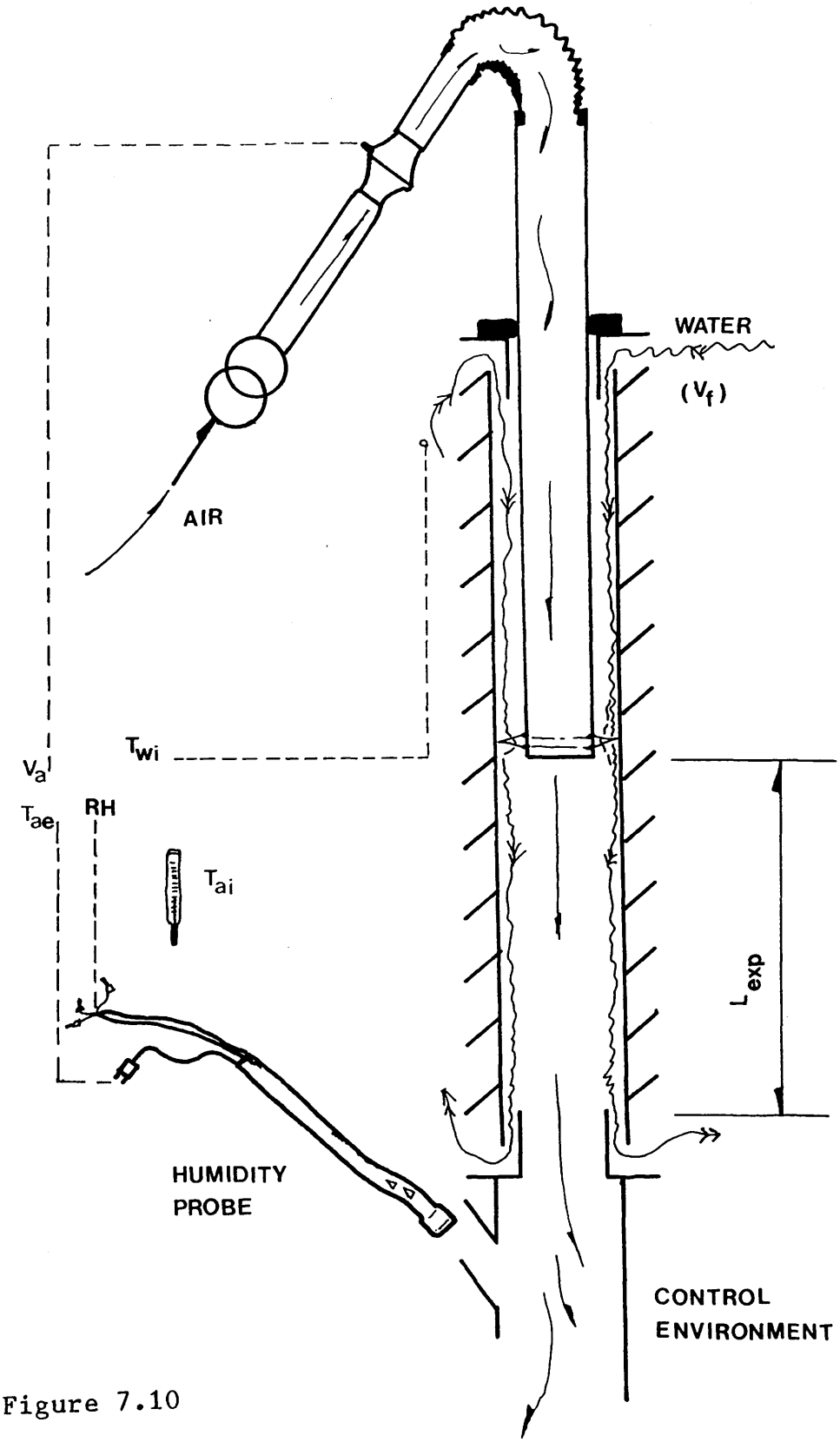

Figure 7.10

Humidity probe step test via long axis humidification.

T_{ai} : Inlet air temp; T_{ae}: Exit air temp; T_{wi}: Inlet water film temp; RH: Relative humidity; V_a : Air flowrate; V_f : Film flowrate; L_{exp}: air-water exposure length.

humidity probe was removed and allowed to equilibrate with ambient air. This procedure was repeated three times at each film exposure length.

Software, in MSBASIC, sampled outputs from the the absorption sensor amplifier and thermocouple amplifier every 38 msec (26 Hz) during the step test via the Microlink data aquisition system described in section 2.3.1. Data were written to a memory array and transferred onto mini disc after the test.

7.6.2ii. Results.

Mean ambient air temperature throughout the test was 26.6°C ($\pm$0.18) 55.1% RH $\pm$1.31, 14.2 mg/l. The mean exit temperature of the control air was 26.5°C (SD $\pm$0.3°C). Figure 7.11 illustrates the exit air humidity recorded for the range of boundary water exposure lengths used for the test. This was found to be linear in the range 5 cm to 36 cm exposure length: $\%RH_{exit}=56.8+1.06(L_{cm})$ ($r=0.97$ $p<0.05$).

Target humidity was evaluated by calculating the mean value prevalent in the last 7 seconds of the test. This was done because the exit air humidity would vary slightly associated with eddying along the downtube. The mean air humidity was consistently greater than 95% of the maximum humidity encountered. Figure 7.12 illustrates a typical first order response obtained for the probe during a 40% RH step test which is characterised by minor fluctuations superimposed onto the overall rise. The response time for each step test was determined by noting during which sample cycle the recorded air humidity began to rise and that sample cycle when the mean target humidity was achieved.

For a 40% step change in relative humidity the probe achieved this target value in under 1.4 seconds. A linear relationship between step size and response time (t) was found using a Minitab statistics programme, $t=0.958+0.0107(\%RH)$ ($r=0.95$ $p<0.05$) and is illustrated in

Figure 7.11: Exit air water vapour content and exposure length for the long axis conditioner.

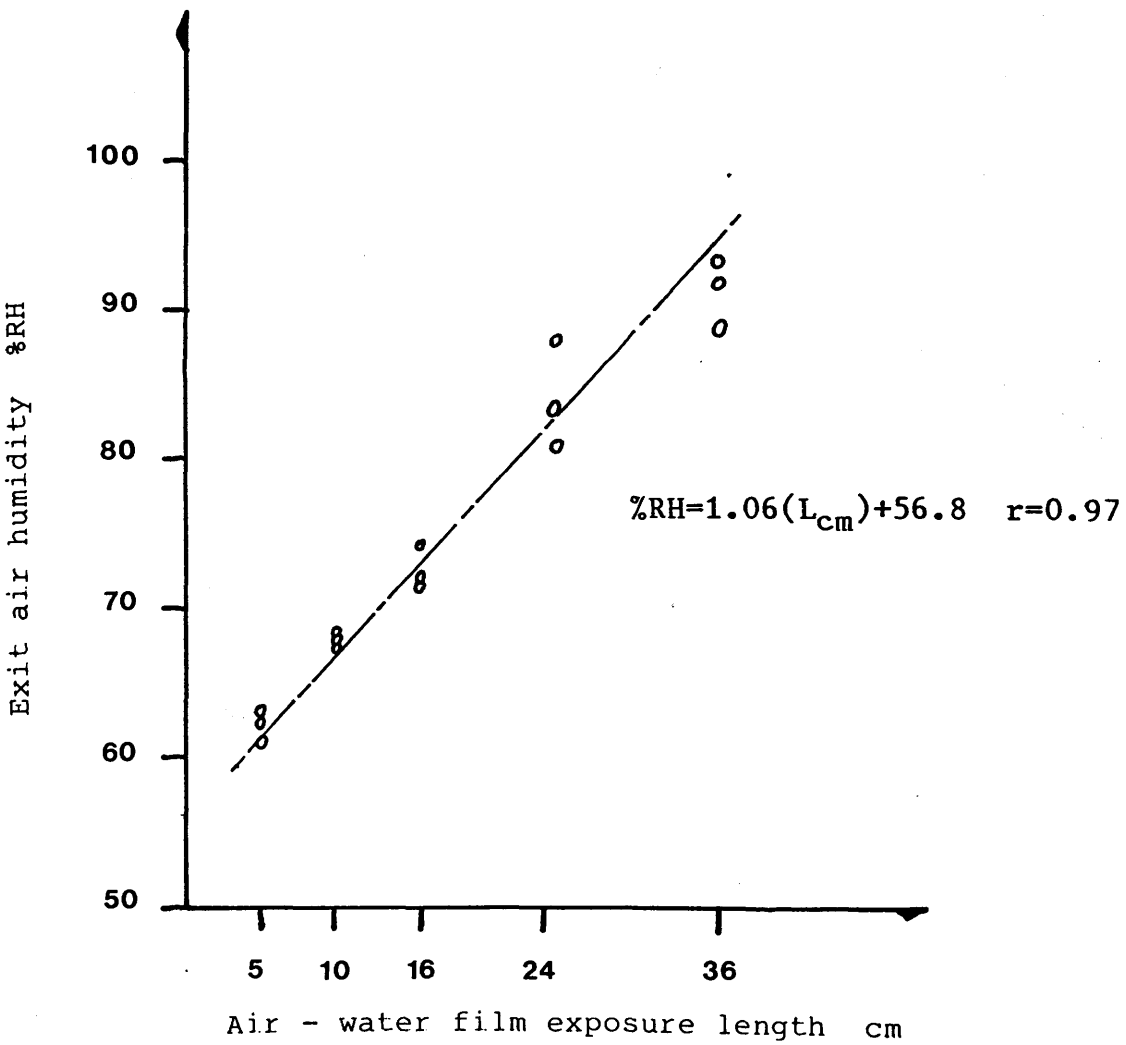

Figure 7.12: Step response characteristics in absorption and desorption.

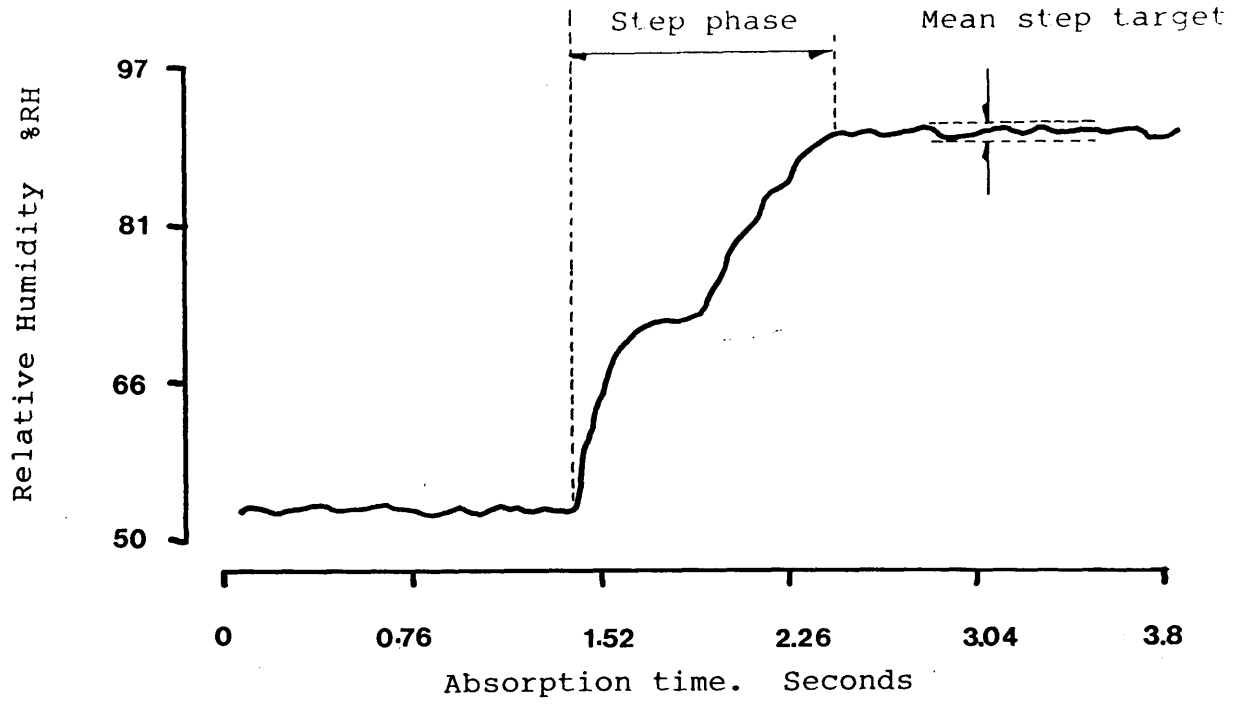

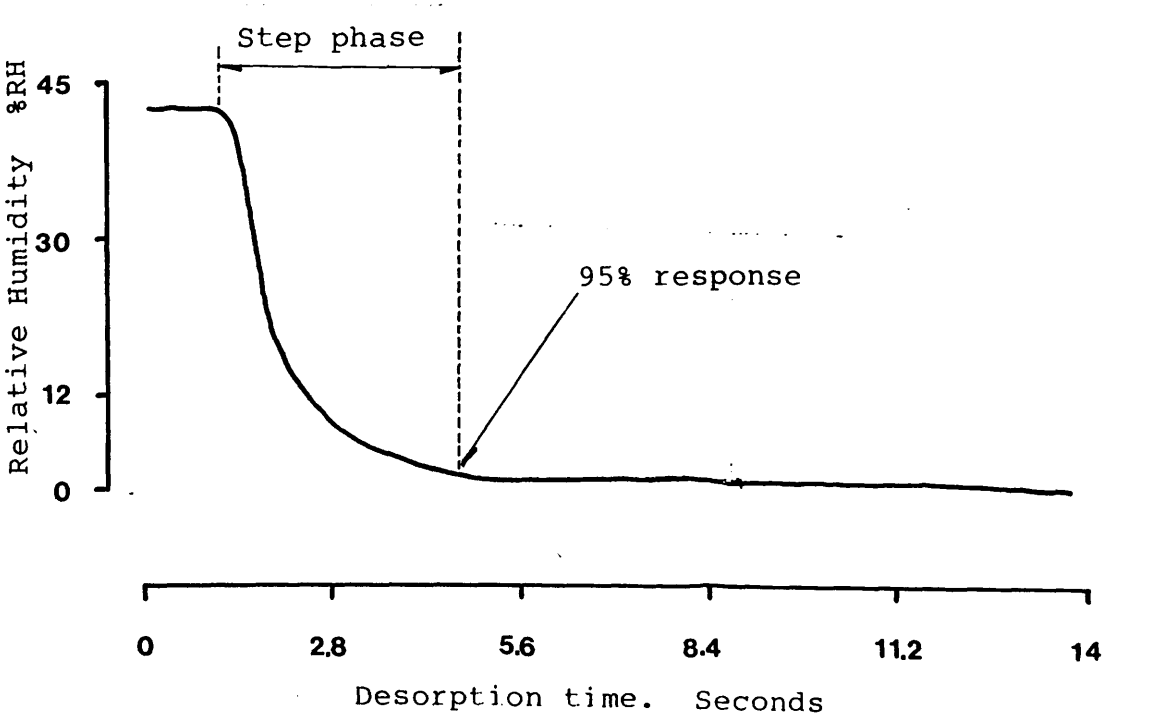

figure 7.13.

These data are pertinent to moisture absorption by the sensor. Its desorption time following exposure to a dry air stream was also evaluated.

7.6.3. Step response: Desorption test.

7.6.3i. Method.

Data collection software used to record the instantaneous air condition during the desorption test was identical to that used in the absorption test. Figure 7.14 shows how the test was carried out. The probe was inserted into an 11mm ID tube connected to the regulator outlet of a 3600 litre bottle of dry air (BOC Ltd, Glasgow, UK) taken to have zero absolute water content (0% RH). The probe was allowed to equilibrate with ambient air after which the regulator valve was spun open to achieve an air flowrate of 15 l/min. This was calculated to yield a velocity of 2.6 m/sec through the connecting tube. The procedure was repeated 7 times.

7.6.3ii. Results.

Mean air temperature throughout the test was 23.9°C (+0.1) with an ambient air humidity of 44%RH ($\pm$0.0). Figure 7.12 shows a typical desorption response which is characterised by an absence of minor fluctuations apparent in the absorption test. The 95% desorption time was evaluated using the method described for the absorption test and was found to be 3.56sec ($\pm$0.27) for a step size of 44%RH.

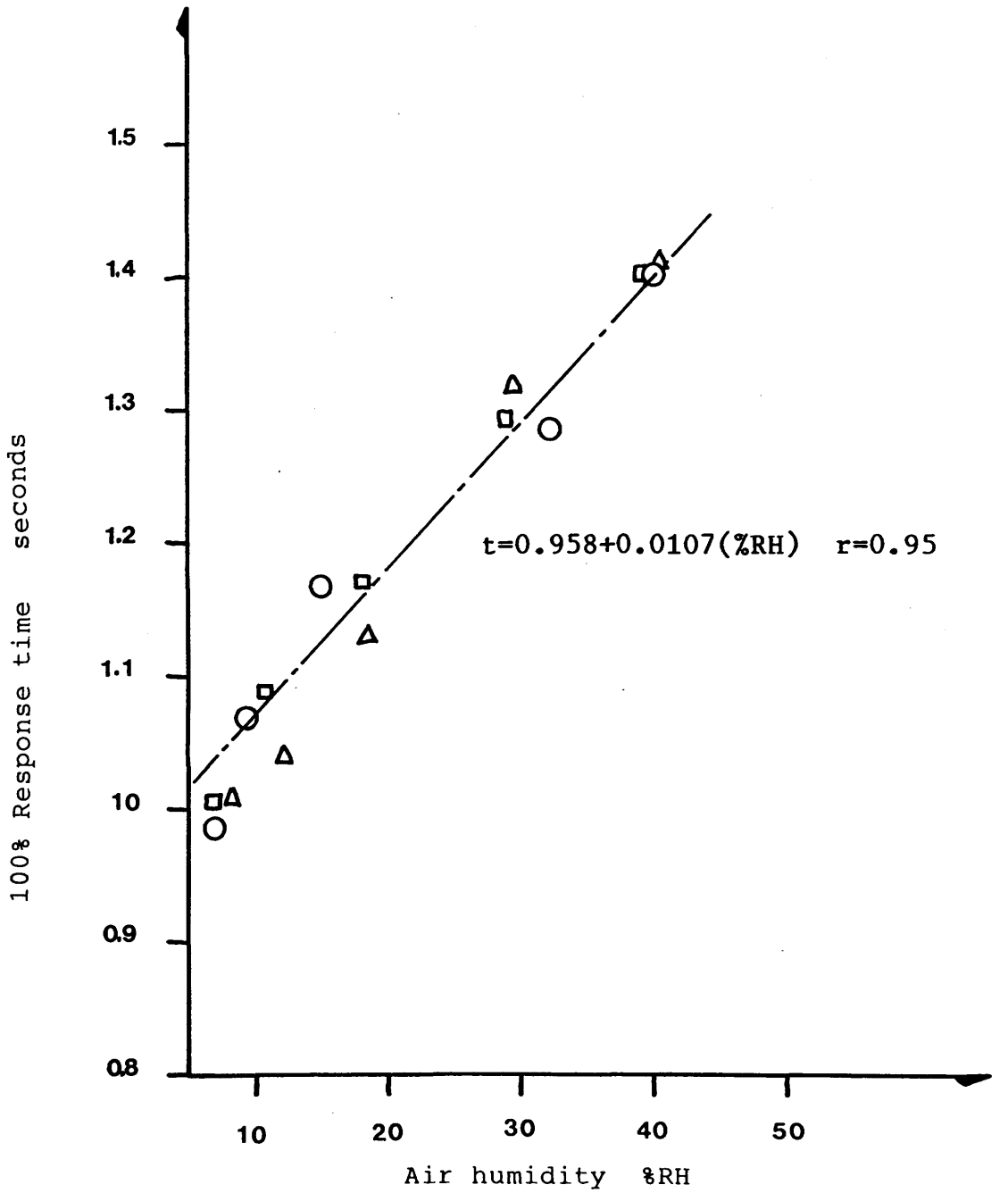

Figure 7.13: 100% response time vs step size in absorption.

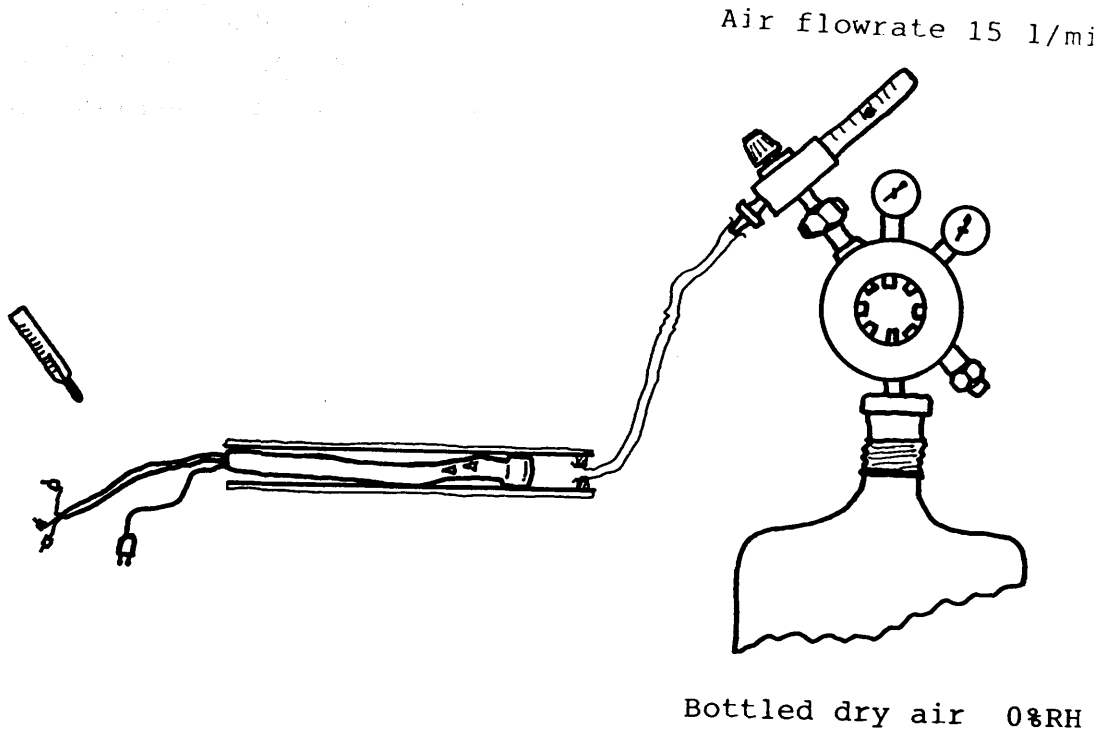

Figure 7.14: Desorption step test method. The probe was allowed to stabilise and the regulator valve then spun open.

7.6.4. Suitability for use.

In vivo air condition was estimated to vary within in the ambient - full saturation range in unison with inspiration and expiration. Figure 6.03 illustrates a tidal inspiration period of 2.5-3 s with a total respiratory phase of 5-6 s. Thus the response time obtained for the probe in either absorption or desorption mode was considered adequate for the purpose of direct in vivo measurements.

7.7. In vivo investigation.

7.7.1. Patients and intubation procedure.

Mid tracheal air humidity was measured in 4 male and 2 female patients, mean age 47.3 years ($\pm$19.8) and without respiratory disorders, immediately after orthopaedic surgery whilst under general anaesthesia. These subjects represented the best available opportunity for invivo measurements. Patient data are given in table 7.01 Hospital ethical committee approval and individual informed consent were obtained.

Anaesthesia was induced with intravenous propofol and endotracheal intubation was facilitated with suxemethonium. Anaesthesia was maintained with 1% to 2% enflurane and 50% nitrous oxide in oxygen at a total fresh gas flow of 2 l/min. The patients breathed spontaneously via a circle system incorporating an Ohmeda Mark 5 carbon dioxide absorber (BOC Ltd, Glasgow UK). At the end of surgery the anaesthetised patient was reintubated with an 11 mm ET tube if required after breathing 100% oxygen for 1 minute.

Once steady state breathing in ambient air had resumed the ventilation rate through a face mask was determined using a pneumotachograph, (Mercury CS5 and flowhead F300L), connected to the microcomputer. After a data aquisition

period of 20 s the face mask was removed and the humidity probe inserted into the airway via the ET tube. The patient was then extubated leaving the probe 20 cm into the airway, corresponding to the level of the mid-trachea. The probe was connected to its humidity and thermocouple amplifiers and data aquisition commenced for 20 seconds, limiting the entire procedure to 2 minutes. At the end of the sampling phase the probe was withdrawn from the airway and cleaned in the manner described in section 7.4.3.

7.7.2. Results.

Mid tracheal air humidity and temperature tracings, shown in figure 7.15 illustrate the typical variation in air condition encountered throughout a respiratory cycle. Table 7.02 summarises the measured air condition in each patient.

Ambient air condition in the theatre immediately prior to the tests was, mean (SD), 23.2°C (±0.34), 46% RH (±0.24) and 9.7 mg/l (± 0.49). Inspired air humidity was taken to be the minimum encountered and expired to be the maximum. Inspiratory airflow recordings were converted into their RMS equivalent and ranged between 4.3 l/min to 22.1 l/min. Inspiratory air temperature at the mid trachea ranged between 34.9°C to 36.1°C and air humidity 78% RH to 94% RH. Mid tracheal expired air was consistently saturated with water vapour, 100% RH and ranged in temperature between 35.8°C to 37.2°C.

Air-mucosa water exchange was computed on the basis of a saturated alveolar air condition of 37.5°C, 47 mg/l and a saturated expirate of 32°C, 35 mg/l. Equations 1 to 4 summarise how the water exchange in the airway was evaluated:

Wi_{MT} - Wi : Upper airway inspiratory water loss.
47 - Wi_{MT} : Lower airway inspiratory water loss.
We_{MT} - 47 : Lower airway expiratory water gain.
35 - We_{MT} : Upper airway expiratory water gain.

where : 'Wi' = inspired water content, 'We' = expired water content and 'MT' = mid trachea. Alveolar air was assumed to contain 47 mg/l and the expirate at the mouth 35 mg/l, based on a body core temperature of 37.5°C and expirate of 33°C.

For calculation and descriptive purposes 'upper airway'

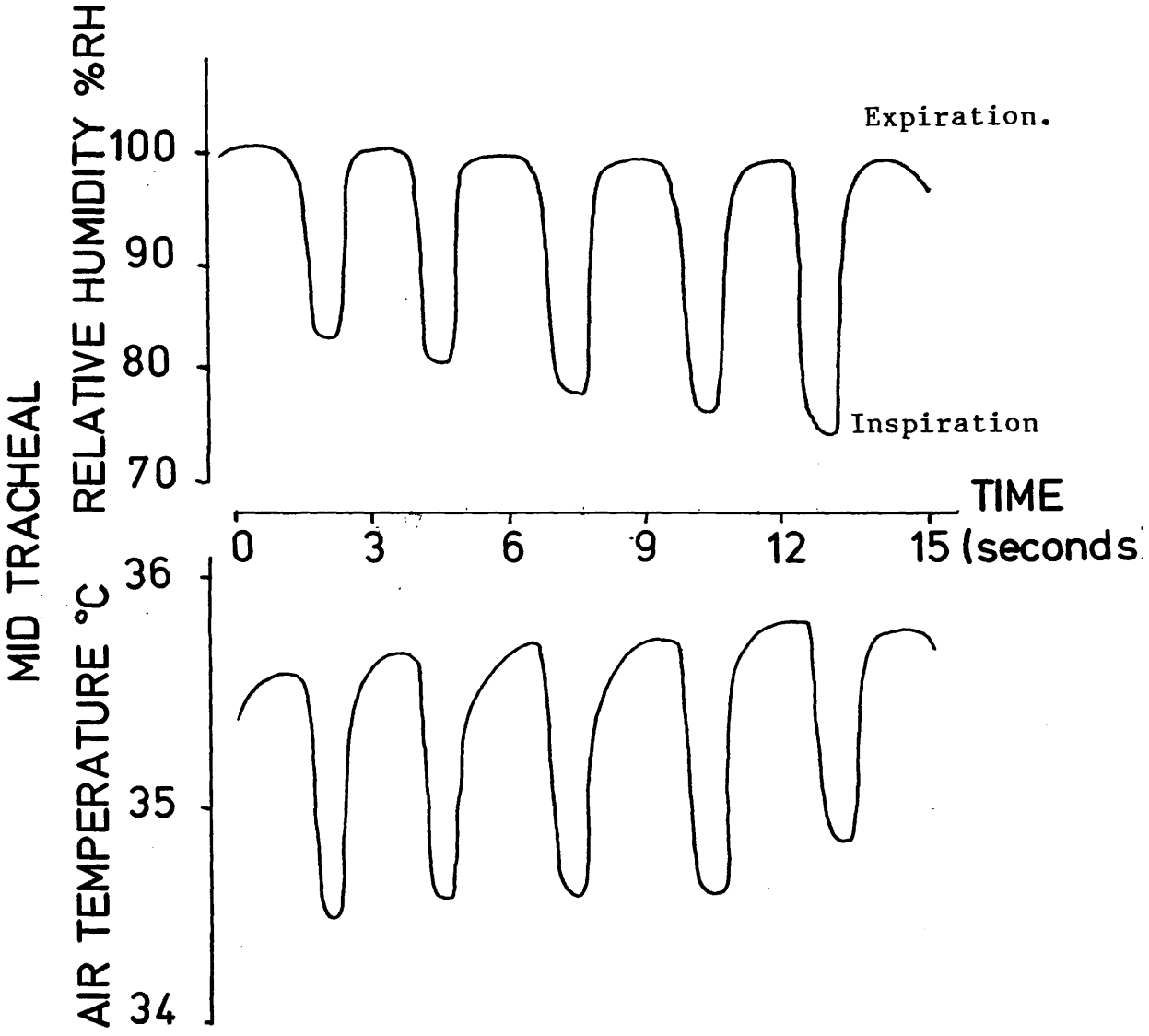

Figure 7.15: Mid tracheal air humidity and temperature trachings.

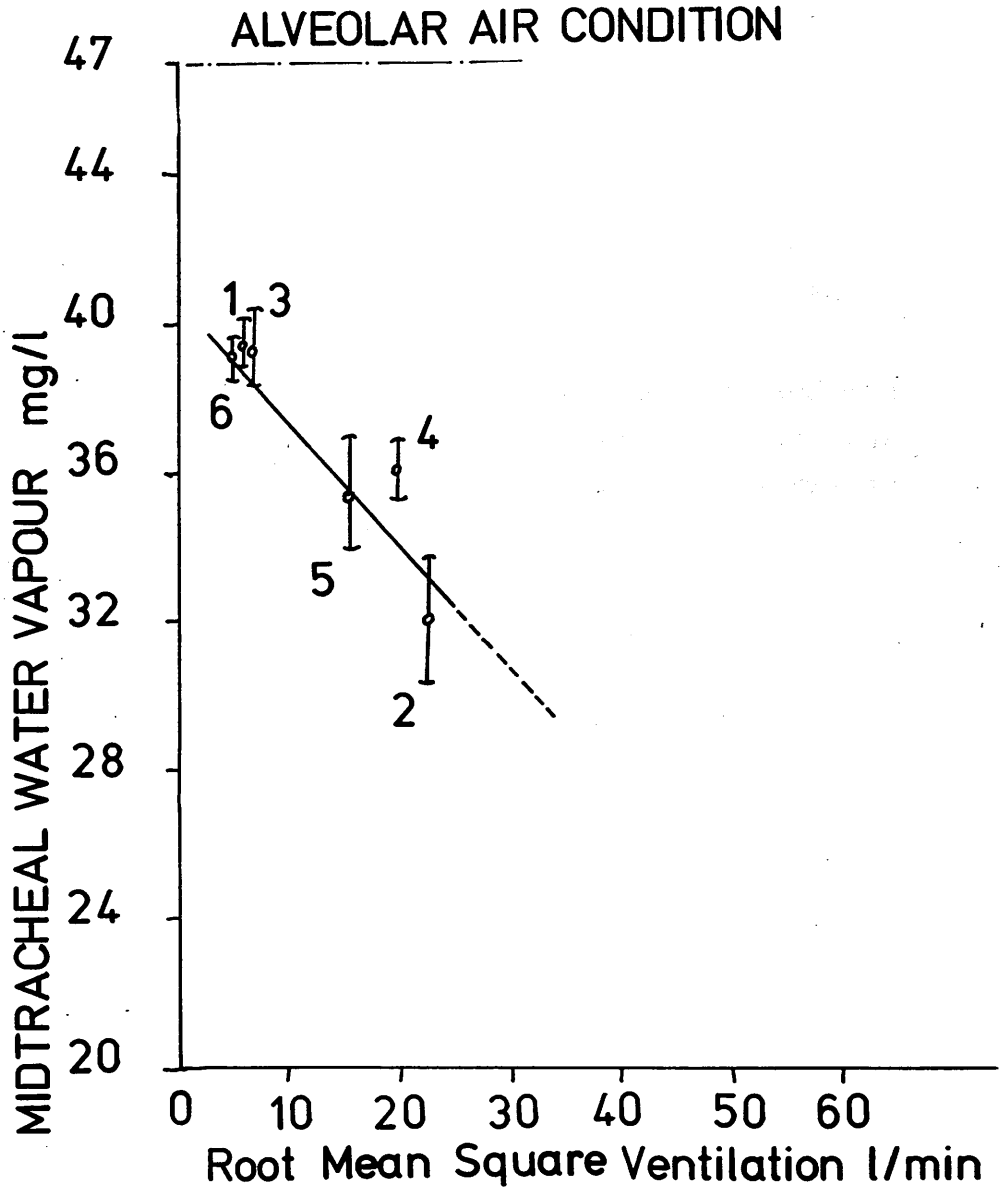

Figure 7.16: Mid tracheal water vapour content and ventilation rate obtained from each subject. Extrapolation of this relation suggests a reversal in regional airway drying roles.

implies the portion of the airway proximal to the mid trachea and 'lower airway' that distal to the mid trachea. Equations 3 and 4 yield negative answers implying the transfer of water back onto the airway.

Thus upper airway inspiratory water loss for patient 1 was computed as 30.1 mg/l, shown in table 7.03, by subtracting the measured tracheal condition from the ambient.

Upper airway inspiratory water loss was found to be 27.3 mg/l ($\pm$3.06) accounting for 72.9% ($\pm$7.4) of the total airway inspiratory drying. Expired water vapour recovery was in the upper airway was 9.7 mg/l ($\pm$1.12) or 80.6% ($\pm$9.4) of the total.

For the group an inverse linear relation between mid tracheal water vapour content and RMS air flowrate was found, (%RH=40.9-0.325(V_{RMS}), r=0.9, p<0.05), illustrated in figure 7.16.

Table 7.01: Patients and surgical procedure.

Subject	Age	Sex	Procedure.
1	28	F	Manipulation of femur
2	27	M	Manipulation of femur
3	32	M	Excision of radial head
4	57	M	Implantation of tibial pin
5	60	M	Implantation of tibial plate
6	80	F	Implantation of tibial plate
Mean	47.8		
(SD)	$\pm$19.8		

Table 7.02: in vivo air condition.

Subject	T_i °C	RH_i %	w_i mg/l	V_{rms} l/min	T_e °C	RH_e %	w_e mg/l
1	34.9	96	39.5	5.0	36.7	100	45.3
2	34.9	78	32.1	22.1	35.8	100	43.1
3	36.1	90	39.4	5.3	36.5	100	44.6
4	36.2	82	36.1	20.7	37.2	100	46.5
5	35.9	82	35.5	15.5	36.6	100	43.6
6	35.1	94	39.0	4.3	36.0	100	43.6
Mean	35.5	87	36.9	12.2	36.4	100	44.6
(SD)	(±0.5)	(±6.7)	(±2.7)	(±7.6)	(±0.46)	(0)	(±1.12)

T: Temperature; RH: Relative humidity; w: Water vapour content; i: inspiration and e: expiration.

Table 7.03: Derived regional water vapour contents.

Patient	W_i mg/l	Wi_{MT} mg/l	We_{MT} mg/l	UA loss mg/l	UA recovery mg/l
1	8.8	39.5	45.3	30.7	-10.3
2	10.3	32.1	43.1	21.8	-8.1
3	9.8	39.4	44.5	29.6	-9.5
4	9.5	36.1	46.5	26.6	-11.5
5	10.1	35.5	45.1	25.4	-10.1
6	9.5	39.0	43.6	29.5	-8.6
Mean (±SD)	9.6 (±0.5)	36.9 (±2.7)	44.6 (±1.1)	27.3 (±3.1)	-9.6 (±1.1)

Patient	LA loss	LA recovery	% UA of total: Loss.	Gain.
1	7.5	-1.7	80	85.8
2	14.9	-3.9	59.4	67.5
3	7.6	-2.5	79.6	79.1
4	10.9	-0.5	70.9	95.8
5	11.5	-1.9	68.9	84.2
6	8.0	-3.4	78.7	71.5
Mean (±SD)	10.1 (±2.7)	-2.3 (±1.1)	72.9 (±7.4)	80.6 (±9.4)

Notation:

W Water vapour content mg/l
i Inspired
e Expired
MT Mid trachea
UA Upper airway
LA Lower airway

Trans mucosal water flow based on the mean ventilation rate (V) of 12.2 l/min:

UA flow = (UA loss - UA recovery)V
= (27.3 - 9.6)12.2 = 215.9 mg/min = <u>0.22 ml/min</u>
LA flow = (LA loss - LA recovery)V
= (10.1 - 2.3)12.2 = 95.6 mg/min = <u>0.1 ml/min</u>

7.7.3. Discussion

Invasive physiological measurements are limited by ethical and technical considerations. Anaesthetised subjects without respiratory disorders and undergoing orthopaedic surgery were considered the best possible choice of patient for the study. Factors mitigating against the natural state of the airway were derived from the presence of the probe .

Modification of the airflow patterns and water vapour uptake would have arisen with the probe in vivo. The additional surface area of the catheter on which expired condensate could form would increase the amount of surface water available in the upper airway and cause overestimates of mid tracheal air humidity. This may have been partially offset because the obstruction of the lumen by the probe would cause a decrease in the air mucosa contact time. However at the resting ventilation rates encountered, this advantage is likely to have been minimal.

Measurement of inspiratory airflow rate prior to sampling in vivo humidity avoided the heat and moisture exchanger effect of a face mask and the anticipated problem of achieving a good facial seal with the probe. The breathing pattern of the patients did not perceptibly change during invasive monitoring and the RMS air flow values are taken as representative of these throughout the experiment. The marginal trend of decreasing inspiration humidity in figure 7.15 suggests the onset of recovery during the procedure.

Figure 7.15 indicates a phase of air subsaturation prevalent during early expiration and inspiration which is most likely due to the dead space volume in the airway. As this volume of air is exhaled or inhaled so the corresponding air condition oscillates between 100% RH and about 80% RH.

Group mid tracheal expired air contained 44.7 mg/l of which 9.7 mg/l would have been returned to the relatively

cooler upper airway, whereas a recovery of 2.3 mg/l was calculated for the lower airway (table 7.03). Inspiratory water losses were 27.7 mg/l in the upper airway and 10.1 mg/l in the lower yielding water deficits 17.8 mg/l and 7.8 mg/l respectively. For the group mean tidal ventilation rate of 12.2 l/min this represents loss rates of 0.22 ml/min (upper airway) and 0.1 ml/min (lower airway) which presumably corresponds to the regional transport of water through the mucosa. The calculation is described in table 7.03.

Anderson (1984)[27] has proposed a water loss rate in excess of 0.41 ml/min as necessary to provoke hyperventilation induced asthma. The cold air hyperventilation challenge described in section 3.4 was followed by a 20% reduction in FEV_1 after exposure to a water loss rate of 1.05 ml/min, some five times the rate currently evaluated for tidal breathing.

Increasing ventilation reduces the air-mucosa contact time in the upper airway and would lead to a reduction in the quantity of water evaporated from any given airway location. Extrapolation of the present data, using the regression equation shown in figure 7.16, to an RMS air flowrate of 60 l/min suggests a reversal in the relative amounts of inspiratory water delivered by the upper and lower airway: 11.7 mg/l vs 25.6 mg/l whereas previously at 12.2 l/min these were 27.1 mg/l vs 10.1 mg/l respectively. The prediction is inevitably a lower bound on what is likely to arise during hyperventilation for two reasons. Greater airway cooling would increase the amount of expiratory water recovered by condensation and improved upper airway air-mucosa mixing from air turbulence would increase the local rates of drying. However the extrapolation serves to illustrate that without compensation by the increased transport of water through the epithelium the result of sustained hyperventilation would be the gradual drying of the the mucosa and the shift

of air conditioning deeper into the airway.

Drying of the epithelium has been observed by Forbes (1973)[66] to reduce mucus flow and by Tsuda et al (1977)[67] to cause structural changes to the ciliated bronchial epithelium. In addition a decline in the ciliary beat frequency has been reported by Horstmann (1977)[7] following exposure to dry air. Thus long term airway drying encountered in hyperventilation induced asthma can be expected to interfere with the important mucociliary clearance activity.

7.8. Summary.

It is apparent that mid tracheal air is not fully saturated with water vapour during tidal inspiration. The level of saturation will inevitably decline further with hyperventilation. The rate of trans epithelial water flow in the upper airway is exceeded during the thermal burdens used to challenge the airway and mucociliary drying is expected. The structures proximal to the mid trachea are conducive to efficient air-mucosa mixing and similar to the observations of intra thoracic air temperature it is here that the maximal mucosal drying and water recovery will initially occur.

8. Conclusion.

8.1. Work done.

The hypothesis upon which the research was based proposed that the rate of airway heat exchange could be correlated with changes in FEV_1.

Rate dependancy was found both in hyperventilation (chapter 3) and exercise (chapter 5). The correlations between airway response and RHER were:

$\%FEV_1 = 0.226(RHER) - 10.2$ r=0.91, exercise n=5
SEM's: 0.023, 2.15 (coefficient, constant)

$\%FEV_1 = 0.223(RHER) - 6.2$ r=0.85, hyperventilation n=7
SEM's: 0.016, 1.26 (coefficient, constant)

In each the responses were independent of the means by which the thermal burden was produced. Thus a 20% fall in FEV_1 followed an RHER of 130W whether caused by cold air, dry ambient air or ambient air inhalation. Airways response has been previously associated with RHER[18,20]. To the author's knowledge the observation of a similarity between hyperventilation and exercise induced asthma with regard to RHER is new.

Inhalation of warm humidified air conferred protection from exercise induced asthma in agreement with other workers[22,41]. The present work has for the first time quantified the actual RHER present in tropical air breathing and compared this to the spectra of thermal burdens imposed by other grades of air. Attenuation of RHER by breathing long axis conditioned air was followed by an absence of bronchoconstriction in five exercise sensitive asthmatics. The tropical air was associated with resting

values of RHER during exercise (15W). It reversed the direct rate of airway cooling leading to an expirate temperature of 37.6°C whereas with cold air breathing this was 25.7°C (table 5.04). Similarly it facilitated retention of at least 50% more water than would have been ordinarily expired in ambient air.

The site of maximal respiratory heat transfer was determined from invasive measurements of airway temperature and humidity.

The most rapid rates of air warming were found to occur in the upper airway (chapter 6). The numerical model (section 4.5) showed that simultaneous heat and water vapour transfer was dependent upon the concentration gradients between the airway boundary and freestream. Thus high rates of air warming and humidification occur in those regions in proximity to the unconditioned inspirate. Comparison of the longitudinal air warming profile in vivo with that found for the long axis air conditioner (figure 6.07) illustrated the contribution of airway geometry to the initial phase of air warming. Geometrical variance serves to increase the heat and mass transport coefficients (h_c, k_c) giving rise to local variations in the rates of cooling and drying.

Trans mucosal water flow was estimated to be 0.22 ml/min in the upper airway, accounting for 70% of the total airway drying during tidal conditions. Alone this is over half the total airway drying proposed necessary for hyperventilation induced asthma[27]. The primary drying burden was placed on the airway structures proximal to the trachea in agreement with the in vivo temperature findings. The subsaturated state of tidally inspired air at the mid trachea implies that some lower airway drying can be expected during hyperventilation (figure 7.16).

8.2. Possible implications.

The group sizes of subjects used in this study are small and the findings interpreted as an encouraging trend. The rate dependancy of airway response to heat loss lends credence to the possibility of a sensory initiator in the production of exercise or hyperventilation induced asthma. The similar responses found between hyperventilation induced asthma and exercise induced asthma with regard to the imposed RHER cannot at present be explained by a common biochemical initiator[35,36] (section 3.7). If the similarity between each holds for the majority of exercise sensitive asthmatics then hyperventilation could be used to model the effect of exercise in patients in whom heart disorders are present.

Chapter 1 described the presence of a variety of receptors located in the sub mucosa. Presumably drying of the mucosa not only leads to evaporative cooling but also may interfere with the muco cilary beat action by increasing the viscosity of the mucus[7,66,67]. It is conceivable that a change in mucus viscosity and cilary beat frequency could itself directly irritate the airway.

The upper airway, proximal to the trachea, can be presumed to host the sensory initator to heat loss induced asthma. This region is well ciliated and populated by numerous mucus secreting glands. A progressively drier wall surface develops with depth into the airway. The venturi like geometry of the larynx would serve to promote turbulance and thereby increase local rates of epithelial cooling and drying. Laryngeal mobility is known and during an asthmatic episode has been proposed as a choke point causing restricted expiratory airflow[5]. Combined with the possibility that the tracheobronchial nerve supply is derived from the larynx[9] a local laryngeal heat loss

stimulus could presumably lead to a direct 'knock on' response for the entire airway. Mechanical irritation of the larynx is known to promote asthma although at variance with this an attempt to block EIA by anaesthesia of the larynx was inconclusive[34]. Until the sensory pathways serving the airway are better understood the 'knock on' process remains speculative.

8.3. Future Work.

8.3.1. Clinical.

A larger asthmatic population must be exposed to the hyperventilation and exercise challenges before a confident assertion regarding the similarity of HIA and EIA can be made. The present work compared unrelated individuals and challenges. A less error prone approach would be the development of a protocol involving one group of patients exposed to hyperventilation and exercise.

The possibility of a modification in expired air temperatures in asthmatics could be explained by an airway jacket effect of hypersecretions arising during the thermal burden. Variations in asthmatic expirate temperature compared to normals have not been previously reported. If present such a phenomena would presumably exclude the possibility of post challenge airway rewarming as a stimulus for asthma.

8.3.2. Development.

Since completing the programme of work the author has built a Mk3 non rebreathing valve. The device has a dead space of less than 12 ml and operates by means of a divided bidirectional polythene leaflet assembly, similar to a double flap occluder. Initial measurments with the device indicate tidal expirate temperatures of 33-34°C. A similar

rate of airway cooling has been found in cold air hyperventilation using the device compared to the Mk2, thus its primary advantage apears to be in the low ventilation rate regime. Design and development is continuing.

8.3. Conclusions.

1. The rate of airway heat loss correlates directly with the post challenge fall in FEV_1.

2. Minimising the rate of airway heat loss prevents post challenge fall in FEV_1.

3. The site of maximal airway cooling and drying is located in the stuctures proximal to the mid trachea.

Appendix 1
Thermocouple response test: step interval.

The reader is referred to figure 2.10. Assuming no contact by the impact mass with the cylinder wall and negligible piston - cylinder friction the impact velocity (v_m) of the mass will be, from momentum theory:

$$v_m = [u^2 + 2.g.s]^{\frac{1}{2}} \quad m/s, \qquad .....1$$

where u: inital mass velocity, 0 m/s
g: acceleration (gravity), 9.81 m/s^2
s: distance fallen, 0.14 m

so v_m = 2.75 m/s

From conservation of momentum the combined initial momentum of the piston and mass is the same as the momentum of the mass just prior to impact, thus:

$$M_m.v_m = (M_m + M_p).u_p$$

Where M_m: impact mass 31 g
M_p: piston mass 5.5 g
v_m: impact velocity 2.75 m/s
u_p: initial combined velocity (?)

so u_p = 2.33 m/s

The terminal piston velocity is given from equation 1 where s=0.001m (step distance):

Therefore v_p = 2.33 m/s. With an average step velocity of 2.33 m/s the step time s/v_p was T = 0.5 msec.

APPENDIX 2

```
10 REM program name STEP
20 REM Rob Farley, 300686.....v1
30 REM Step test response of T Type thermocouple
40 REM Approximate sampling speed... 1 sample/20msec
50 REM
60 REM
70 REM
80 DEF SEG=0
90 DEF SEG=PEEK(641)*256+PEEK(640)
100 NUI488=&H103
110 NU0488=&H106
120 DIM A(400)
130 PRINT CHR$(27)+"E"
140 PRINT CHR$(27)+"E"
150 INPUT"Enter name of data file";N$
160 OPEN N$ FOR OUTPUT AS 2
170 REM
180 REM
190 REM
200 TOUT%=20
210 NS%=1
220 PA%=7
230 ST%=0
240 PRINT CHR$(27)+"E"
250 PRINT" "
260 REM
270 REM
280 REM
290 Q$="P"
300 REM Cold junction temperature measurement
310 Q$=INKEY$
320 IF Q$=" " THEN GOTO 470
330 PRINT"HIT SPACE BAR TO START SAMPLING"
340 C%=15: FL%=16: SA%=8
350 CALL NU0488 (TOUT%,ST%,FL%,NS%,C%,SA%,PA%)
360 FL%=17
370 CALL NUI488 (TOUT%,ST%,FL%,NS%,X%,SA%,PA%)
380 V=(X%-1024)*.0025/100
390 R=100*(.5+V)/(.5-V)
400 CJ=(R-100)*2.5707
410 CJ=(INT(CJ*100)/100)
420 PRINT"Cold junction temperature..... ";CJ
430 PRINT" "
440 GOTO 310
450 REM
460 REM
470 GOSUB 560
480 GOSUB 680
490 CLOSE£2
500 PRINT" "
510 PRINT"Type RUN to sample again NB>>>>NEW FILE NAME"
520 END
530 REM
540 REM
550 REM
560 REM
570 FOR I=0 TO 399
580 SA%=8: FL%=16
590 CH%=2
600 CALL NU0488 (TOUT%,ST%,FL%,NS%,CH%,SA%,PA%)
610 FL%=17
620 CALL NUI488 (TOUT%,ST%,FL%,NS%,X%,SA%,PA%)
630 A(I)=X%
640 NEXT
650 RETURN
660 REM
670 REM
680 REM
690 PRINT" "
700 PRINT "COLD JUNCTION TEMPERATURE "CJ
710 PRINT" "
720 II=1
730 FOR I=0 TO 399
740 PRINT" "
750 ZZ=A(I)
760 V=(ZZ-1024)*.0025/100
770 V=V*1000000!
780 V0=38.680238£*CJ
790 V0=V0+.0141277001£*CJ*CJ
800 V=V+V0
810 T1=.027401364£*V
820 T1=T1-.000000437843 64£*V*V
830 T1=(INT(T1*100))/100
840 PRINT T1,I
850 WRITE£2,I,T1
860 NEXT
870 RETURN
```

```
10 REM Respiratory heat exchange estimation based on fully
20 REM saturated expired air.
30 REM programme name RHE5
40 REM Rob Farley.......090288.....v5
50 DEF SEG =0
60 DEF SEG = PEEK(641)*256+PEEK(640)
70 NUI488 = &H103
80 NU0488 = &H106
90 PRINT CHR$(27)+"E"
100 HR=0
110 RT=0
120 CLK=0
130 PRINT"Sampling of cold air, ambient air and exercise"
135 PRINT"Use TARGETING calibrated pneumotachograph"
140 PRINT"  "
150 INPUT"Name of data file....NAME.DAT";N$
160 PRINT
170 OPEN N$ FOR OUTPUT AS 2
179 MM=1
180 PRINT
181 PRINT"Enter meter multiplier:"
182 PRINT"x0.3..... 3"
183 PRINT"x1..... 1"
184 INPUT MJ
185 IF MJ=3 THEN MM=.24096
186 IF MJ=1 THEN MM=.8
187 IF MM=1 THEN 180
190 INPUT"Enter current atmospheric pressure in mm Hg ";PAT
200 PAT=PAT*1013.25/760
210 PRINT
220 PRINT"To enter ambient air temperature and moisture content......1"
230 PRINT"To sample cold air.....2"
240 INPUT B
250 IF B=1 THEN 270
260 IF B=2 THEN 300 ELSE 220
270 INPUT"Enter inspiratory air temperature xC ";T1
280 INPUT"Enter inspiratory moisture content kg/kg ";AMC
290 INPUT"Equivalent moisture content mg/l";MCW
300 INPUT"Sample every Nth breath: Enter N ";BC
310 PRINT"    "
320 S$="0"
330 INPUT"Hit RETURN to commence data aquisition";S$
340 TOUT%=100
350 PA%=7: NS%=1: ST%=0
360 IF CLK MOD 20=0 THEN GOSUB 410
370 GOTO 480
380 REM
390 REM
400 REM
410 PRINT CHR$(27)+"E"
420 PRINT"Time";TAB(7)"Ti";TAB(11)"Te";TAB(16)"Flow";TAB(23)"We";TAB(29)"Wi";
TAB(34)"RHER";TAB(41)"RHE";TAB(47)"RHET";TAB(54)"HR";TAB(60)"ExP"TAB(65)"TVol";
430 RETURN
440 REM
450 REM
460 REM
470 REM
480 REM Cold junction temperature measurement
490 CH%=15: FL%=16: SA%=8
500 CALL NU0488 (TOUT%,ST%,FL%,NS%,CH%,SA%,PA%)
510 FL%=17
520 CALL NUI488 (TOUT%,ST%,FL%,NS%,X%,SA%,PA%)
530 V=(X%-1024)*.0025/100
540 R=100*(.5+V)/(.5-V)
550 T0=(R-100)*2.5707
560 T0=INT(T0*100)/100
570 REM
580 REM
590 REM
600 REM Monitoring flowrate
610 X%=0: SA%=1
620 CALL NUI488 (TOUT%,ST%,FL%,NS%,X%,SA%,PA%)
630 IF B=1 THEN 770
640 REM Monitoring cold air inlet temperature
650 SA%=8: FL%=16: CH%=1+16*3
660 CALL NU0488 (TOUT%,ST%,FL%,NS%,CH%,SA%,PA%)
670 FL%=17
680 CALL NUI488 (TOUT%,ST%,FL%,NS%,T1%,SA%,PA%)
690 V=(T1%-1024)*2.5
700 V0=38.68023£*T0
710 V0=.0141277001£*T0*T0+V0
720 V=V+V0
730 T1=.02740136£*V
740 T1=T1-.0000004384364£*V*V
750 T1=INT(T1*10)/10
760 REM Test for trigger value.
770 IF X%>20 THEN GOSUB 860
780 IF X%>20 THEN GOSUB 1480
790 IF Q$=" " THEN 2160
800 GOTO 340
810 REM
820 REM
830 REM
840 REM
850 REM Temperature & flow capture.....RMS derivation
860 FLOW=0
870 TEMP=0
880 C%=0
890 V0%=0
900 Y%=X%
910 WHILE Y%>20
920 Y%=0
930 FL%=17
940 SA%=1
950 CALL NUI488(TOUT%,ST%,FL%,NS%,Y%,SA%,PA%)
960 FL%=16: SA%=8: CH%=48
970 CALL NU0488(TOUT%,ST%,FL%,NS%,CH%,SA%,PA%)
980 FL%=17
```

APPENDIX 3

```
990 CALL NUI408 (TOUT%,ST%,FL%,NS%,T%,SA%,PA%)
1000 SA%=4
1010 CALL NUI408(TOUT%,ST%,FL%,NS%,VN%,SA%,PA%)
1020 C%=C%+1
1030 TEMP=T%*1%+TEMP
1040 FLOW=Y%*Y%+FLOW
1050 IF VN%>V0% THEN V0%=VN%
1060 WEND
1070 REM
1080 REM
1090 REM
1100 FLO=SQR(FLOW/C%)
1110 FLOW=INT(FLO*MM*100)/100
1120 TEMP=SQR(TEMP/C%)
1130 V=(TEMP-1024)*2.5
1140 V0=38.680238£*T0
1150 V0=.0141277001£*T0*T0+V0
1160 V=V+V0
1170 T=.027401364£*V
1180 T=T-.0000043784364£*V*V
1190 T=INT(T*10)/10
1200 T2=T
1205 IF MJ=3 THEN V0%=INT(V0%/3)
1210 TVOL=CINT(V0%*.723)/100
1220 TMASS=TVOL*1.255/1000
1230 ZZ%=CINT((CVOL+TVOL)*100)
1240 CVOL=ZZ%/100
1250 ITIM=C%*.058
1260 ZZ%=CINT(ITIM*100)
1270 ITIM=ZZ%/100
1280 REM
1290 REM
1300 REM
1310 REM
1320 REM Calculation of moisture content based on Murray equation
1330 REM and psychrometric constant. Full saturation assumed.
1340 REM
1350 REM
1360 K=EXP(17.269388£*T/(T+237.3))
1370 P=6.108*K
1380 MC=INT((.622*P/(PAT-P))*10000)/10000
1390 W2=MC
1400 ROD=-.0046*T+1.2922
1410 MC=ROD*1000*W2
1420 MC=INT(MC*10)/10
1430 RETURN
```

```
1440 REM
1450 REM
1460 REM
1470 REM
1480 REM Calculation of inlet/outlet enthalpies and RHE
1490 FLUU=FLOW/60
1500 M=FLUU*1.255/1000
1510 FLUU=INT(FLUU*100)/100
1520 IF B=1 THEN 1560 ELSE 1640
1530 REM
1540 REM
1550 REM Super zero inlet parameters
1560 W1=AMC
1570 CPM1=1.004+W1*1.88
1580 HFG1=2500-T1/30*70
1590 H1=CPM1*T1+W1*HFG1
1600 GOTO 1810
1610 REM
1620 REM
1630 REM Sub zero inlet parameters
1640 H1=-1*((-35-T1)/(-29)*(-34.5)+34.86)
1650 W1=EXP(.0946382*T1)
1660 W1=INT(.003788*1000000!*W1)/1000000!
1670 ROD=-.0046*T+1.2922
1680 MCC=ROD*1000*W1
1690 IF T1<=0 THEN  GOTO 1800
1700 K=EXP(17.269388£*T1/(T1+237.3)): REM saturated cold air >0xc
1710 P=6.108*K
1720 W1=INT((.622*P/(PAT-P))*10000)/10000
1730 CPM1=1.004+W1*1.88
1740 HFG1=2500-T1/30*70
1750 H1=CPM1*T1+W1*HFG1
1760 ROD=-.0046*T+1.2922
1770 MCC=ROD*1000*W1
1780 REM
1790 REM
1800 REM Calculation of outlet parameters and RHE
1810 CPM2=1.004+W2*1.88
1820 HFG2=2500-T2/30*70
1830 H2=CPM2*T2+W2*HFG2
1840 ENTH=H2-H1
1850 YZ=TMASS*ENTH*1000
1860 ZZ%=CINT(YZ)
1870 RHE%=ZZ%
1880 YZ=M*ENTH*1000
1890 ZZ%=CINT(YZ)
1900 RHER%=ZZ%
1910 RHET=RHET+RHE%/1000
1915 RHET=INT(RHET*100)/100
1920 IF B=1 THEN MCI=MCW ELSE MCI=MCC
1930 MCI=INT(MCI*10)/10
1940 REM
```

```
1950 REM
1960 REM Heart rate measurement...BPM
1970 SA%=2: FL%=17: X%=0
1980 CALL NUI488 (TOUT%,ST%,FL%,NS%,X%,SA%,PA%)
1990 YZ=X%/3.7097
2000 HR%=CINT(YZ)
2010 REM
2020 REM
2030 KT=KT+1
2040 IF KT MOD BC=0 THEN 2050 ELSE 2140
2050 IF CLK=0 THEN TYME=TIME
2060 CLK=CLK+1
2070 TIM=TIME-TYME
2080 REM
2090 REM
2100 REM
2110 WRITE£2,TIM,T1,T2,FLUU,MC,MCI,RHER%,RHE%,RHET,HR%,ITIM,TVOL,CVOL
2120 PRINT TIM;TAB(6)T1;TAB(10)T2;TAB(16)FLUU;TAB(22)MC;TAB(28)MCI;TAB(33)RHER%;TAB(40)RHE%;TAB(46)RHET;TAB(53)HR%;TAB(59)ITIM;TAB(6
5)TVOL;TAB(72)CVOL
2130 HR=0
2140 Q$=INKEY$
2150 RETURN
2160 REM
2170 REM
2180 REM
2190 PRINT"  "
2200 PRINT"End of programme"
2210 PRINT"File saved is.............";N$
2220 CLOSE£2
2225 PRINT"Remember to switch off CO2"
2230 END
2240 Q$="P"
2250 GOTO 340
2260 CLOSE£2
2270 PRINT"end of programme"
2280 END
```

APPENDIX 4

Water content of fully saturated air
Actual, based on Jone and Stoecker (1981)
Predicted, based on Gardner (1972), section 2.4.4.

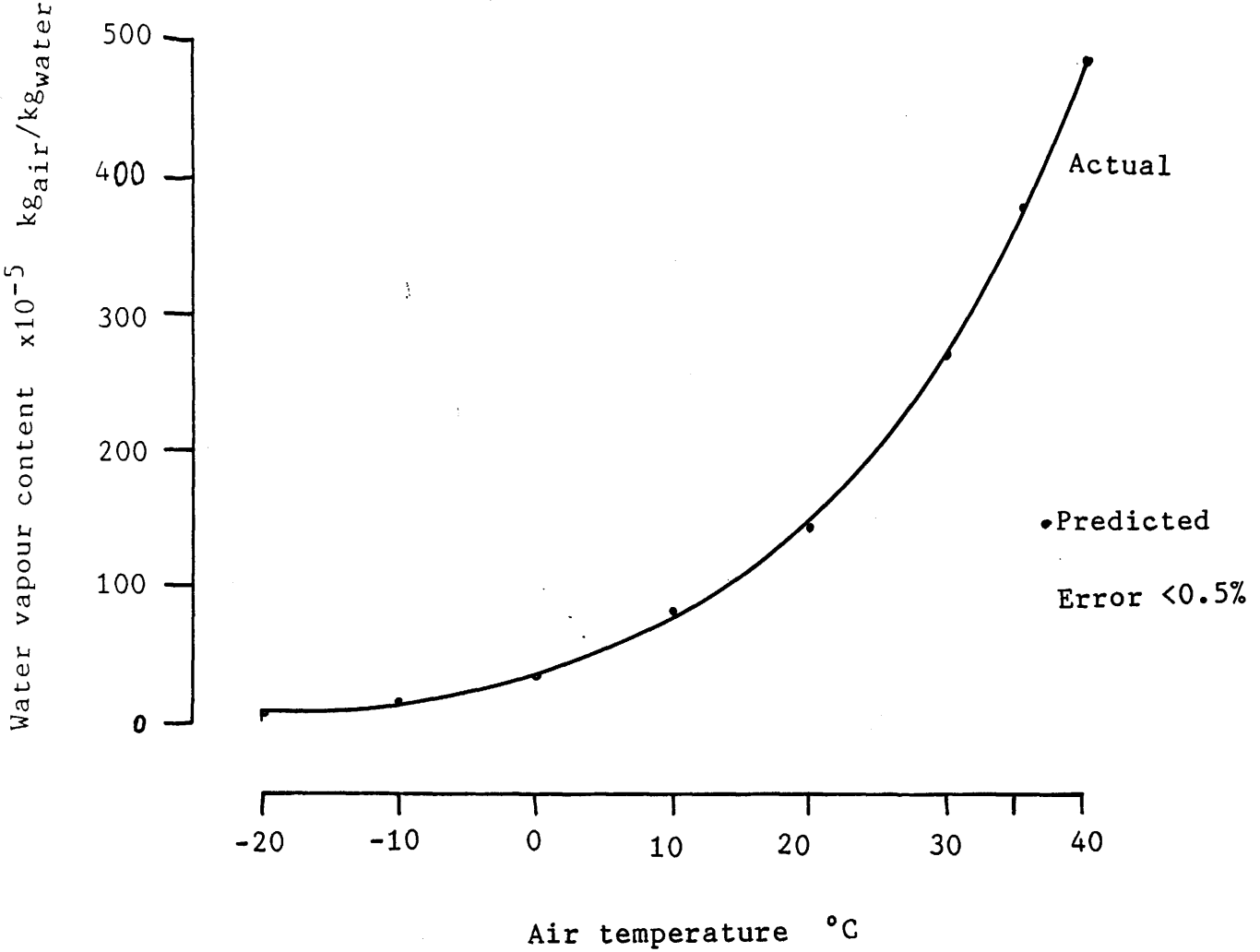

APPENDIX 5

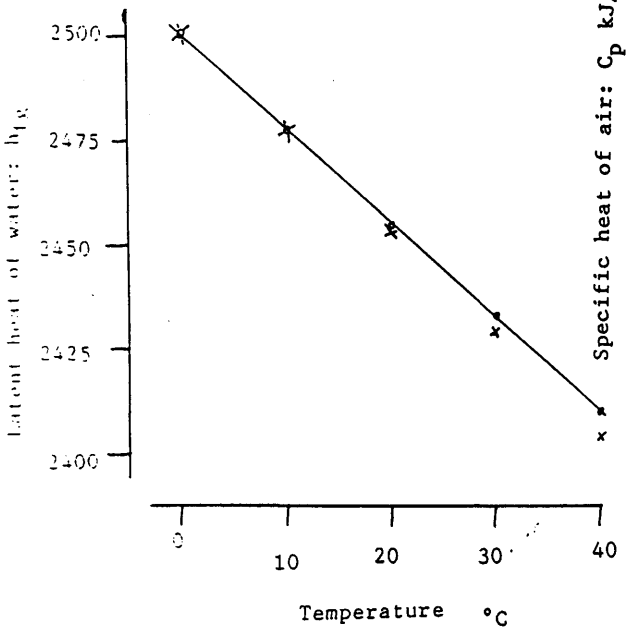

$h_{fg} = 2500 - (T/30).(70)$ kJ/kg

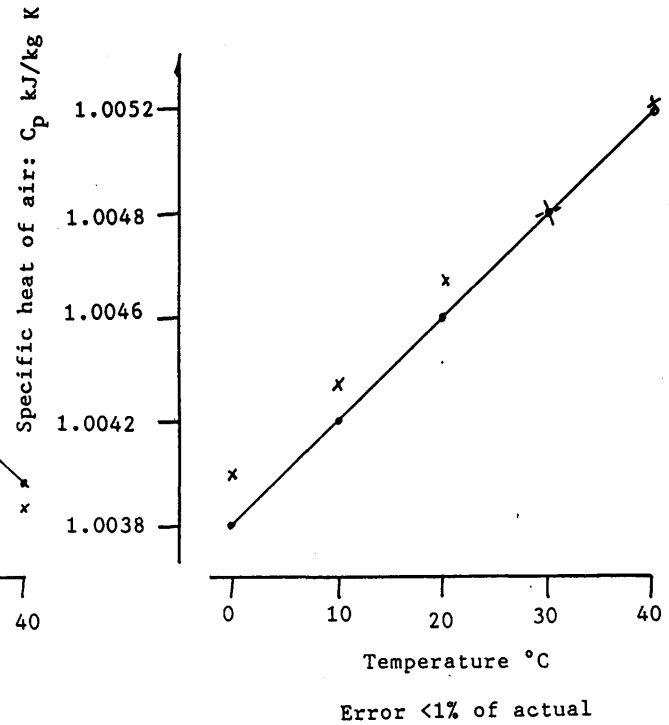

Error <1% of actual

Linear interpolation based on Rodgers and Mayhew (1979).

$C_p = 1.0049 - (0.0022).(300 - T)/(75)$;
where T = air temperature: kelvin

APPENDIX 6

Enthalpy condition of air at subzero temperatures
Linear interpolation: H = 34.5/29.(-35 - (T)) + 34.86 kJ/kg
based on Jones & Stoecker (1981)

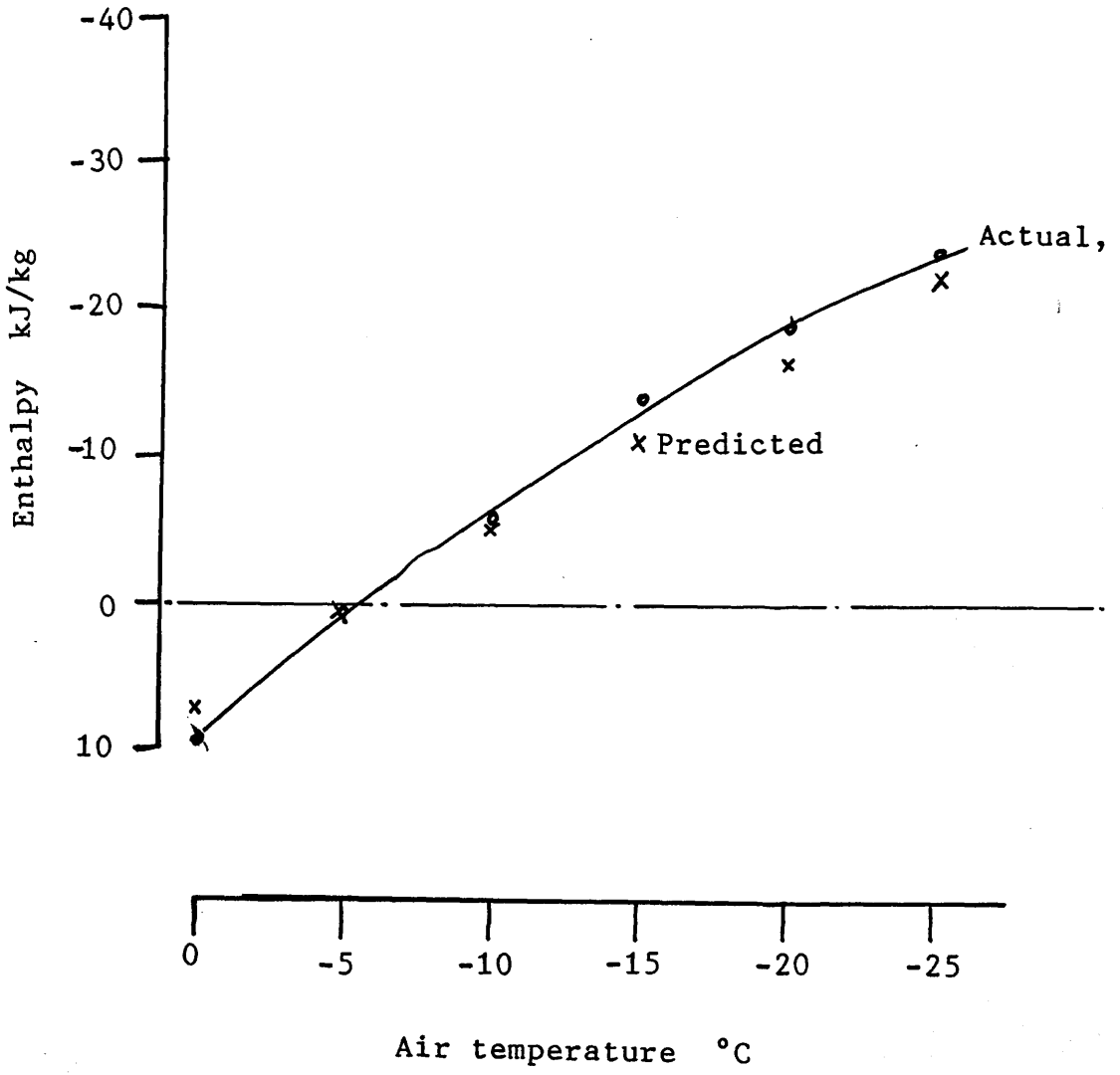

Appendix 7

Passage time and thickness of water film through long axis air conditioner.

The reader is referred to figure 4.09. It is assumed that there is no rippling on the film surface, negligible evaporative mass loss of water occurs compared to the bulk flow and that the mass flow of water at inlet is constant.

The volumetric water flow through the annular cross section occupied by the film is:

$$V = [\pi.d^2/4 - \pi.(d-2t)^2/4].L/T_w \qquad m^3/s.....1$$

where d: downtube internal diameter 0.024 m
L: downtube length 0.965 m
t: film thickness (?)
T_w: film passage time (?)

Expanding equation 1 and ignoring square terms:

$$V = \pi.dtL/T_w \qquad m^3/s \qquad .....2$$

Now $T_w = L/v$, v: film velocity.

Therefore two unknowns: T_w and t.

Passage time.

The total passage time (T) through the conditioner was 3.2 ($\pm$0.21) s, found by injecting a 10 ml bolus of blue ink into the spray head (figure 4.02). The device consumed 5 l water in 213.5s yielding $V = 2.4 \times 10^{-5}$ m^3/s. The length (L_{ex}) of the four exhaust tubes from the base of the down tube was 1.295 m and each had a internal diameter of 3.9 mm (determined volumetrically). Thus the volume (v_i) of

each exhaust tube was 1.2×10^{-5} m^3. The water velocity (v_{ex}) in four such tubes was:

$v_{ex} = V/(4.v_i)$, or 0.5 m/s

and the exhaust passage time was $T_{ex} = L_{ex}/v_{ex}$ or

$T_{ex} = 2.59$ sec

Thus the passage time in the working section (T_w) was

$T_w = T - T_{ex}$, or 0.57 s, (approximately 0.6 sec).

Film thickness

Rearranging equation 2:

$t = T_w.V/(\pi.d.L)$ and substituting values yields:

$t = 1.88 \times 10^{-4}$ m, (approximately 0.2 mm).

Appendix 8

Mass, momentum and energy balance arising in long axis air conditioner.

Figure 4.09 illustrated the thermal and mass gradients between the unconditioned air stream and water film. The total heat transferred to the air is a combination of latent and sensible heats; Q_L and Q_S. The notation for the following derivations is largely given in section 4.7. Where this is not so the symbol is explained in the text.

Applying the Newton rate equation (4.5.2)

$Q_S = h_c.A.(T_f-T_a)$ W, or dividing by A

$q_S = h_c.(T_f-T_a)$ W/m^2 sensible heat flux.

The flux N (mol/cm^2 s) of water molecules from a boundary region of air above the water film to the free stream is descibed by the Fick rate equation (Welty et al 1984) where:

$N = k_c.(c_f-c_a)$ mol/cm^2 s

The water content of this boundary layer of air is estimated on the basis of full saturation at the temperature of the water film using the Gardner relation described in 2.4.4:

$W_f = 0.622 \cdot P_w/(P_{atm}-P_w)$ kg/kg or

$w_f = W_f/8.85x10^{-4}$ mg/l or

$c_f = (5.556x10^{-8}).w_f$ mol/cm^3

thus the latent heat flux is:

$q_L = h_{fg}.N.M_w$ W/m^2 latent heat flux

and total heat flux q_t is q_S+q_L:

$q_t = h_c.(T_f-T_a) + h_{fg}.N.M_w$ 1

$N = kc.(c_f-c_a)$ 2

$c_f = (5.556x10^{-8}).w_f$; via the Gardner equation 3

Equations 1-3 describe the thermodynamic state of the air at one axial site in the conditioner. A complete model of long axis air conditioning requires that all axial sites be described. To do so involves extrapolating the known state prevalent at the current site into the next occurring site. A numerical predictor corrector process is used based upon a mass balance (to predict water vapour concentration) and an energy balance (to predict temperature).

Mass balance.

Using the principle of conservation of momentum the water vapour uptake is estimated as follows.

From figure 4.09 the volumetric uptake in water between stations 1 and 2 is c_2-c_1 (mol/cm^3). In the control volume the surface area available for water exchange is dx.P (cm^2) and for a vapour flux N the rate of water uptake will be N.dx.P (mol/s). For air flowing with a velocity v (m/s) the volumetric flow is v.A (cm^3/s). Therefore the volumetric uptake is:

$N.P.dx/(v.A)$ mol/cm^3 , or:

$c_2-c_1 = N.P.dx/(v.A)$ mol/cm^3 4

From equation 2 the gain equation (4) can be rewritten:

$c_2-c_1 = P/(v.A).k_c.(c_f-c_a).dx$ or

$$v.dc_{1,2}/dx = P/(A).k_c.(c_f-c_a) \quad \ldots\ldots\ldots\ldots 5$$

Equation 5 is the mass balance which describes the axial rise in water vapour content.

Energy balance .

Using the principle of conservation of energy the gain in energy of the air between stations was estimated as follows.

The gain in enthalpy (energy content) of the the air is derived from the transfer of heat and mass to the freestream. In volumertic terms the energy gain between stations is $E_{1,2}$ where $E_{1,2} = C_{pa}.\rho.(T_2-T_1)$ J/cm^3. $E_{1,2}$ comprises the energy content present in the air and the water vapour.

The heat flux from the boundary air is described by the Newton Rate Equation: $q_s = h_c.(T_f-T_a)$ $(J/cm^2\ s)$. The volumetric gain in energy is thus derived from sensible heat and is dependent on the surface area avaliable for heating, similar to equation 4. Thus the volumetric energy gain from air heating is: $P.dx/(v.A).h_c.(T_f-T_a)$ (J/cm^3).

The mass of water gained by the control volume was previously given by equation 4. The enthalpy or energy content associated with the water vapour is $C_{pw}.(T_f-T_a)$ (J/kg). Thus the volumetric energy gain from humidification is:

$P.dx/(v.A).N.C_{pw}(T_f-T_a).M_w$ (J/cm^3)

Combining the energy content of air and water vapour yields:

$E_{1,2} = P.dx/(v.A).h_c.(T_f-T_a) + P.dx/(v.A).N.C_{pw}(T_f-T_a).M_w$

or tidying the expression:

$$C_{pa}.\rho.(T_2-T_1) = P.dx/(v.A).(h_c + N.C_{pw}.M_w).(T_f-T_a).dx$$

or

$$v.dT_{1,2}/dx = P/(C_{pa}.\rho.A).(h_c + N.C_{pw}.M_w).(T_f-T_a) \quad .....6$$

Equation 6 is the energy balance which describes the axial rise in air temperature between stations. Appendix J. describes the predictor - corrector algorithm used to solve equations 5 and 6.

Appendix 9

Numerical predictor - corrector (P-C) algorithm to evaluate mass and energy balances.

The conservation of mass and energy equations are stated:

$$dc_{1,2}/dx = [P/(A).\ k_c.(c_f-c_a)]/v \qquad .....5$$

$$dt_{1,2}/dx = [P/(C_{pa}.\ .A).(h_c+N.C_{pw}.M_w).(T_f-T_a)]/v \qquad .....6$$

Solution to the mass balance precedes the energy balance because equation 6 requires knowledge of c_2 via the flux N.

Let the RHS of 5 be $f(c_i)$. The i+1th state (c_{i+1}) is to be determined. The predictor corrector process operates by first guessing c_{i+1} and then iteratively refining the guess. The predictor - corrector (P-C) method used was the simplest available termed the Nystrom trapezoidal rule P-C, given in Nakamura (1977). The predictor, an Euler guess was:

$$c_a'(i+1) = c_a(i) + h\ .\ f(c_a(i)) \qquad .....7$$

where c_a' = estimated concentration at the i+1th site
c_a = actual concentration at the ith site
h = small axial length between sites i & i+1.

Refinement of the Euler guess follows using the corrector:

$$c_a(i+1) = c_a(i) + h/2\ .\ [f(c_a'(i+1)) + f(c_a(i))] \qquad .....8$$

where $c_a(i+1)$ is the refined estimate. This new solution is replaced in $f(c_a(i+1))$ and the cycle repeated. Numerical convergence was obtained after 4 iterations.

Evaluation of T(i+1) was by using an identical algorithm.

Appendix 10
Derivation of h_c from experimental data

The derivation of section 4.5.2 is summarised:

$$q_{sen} = m.C_p.(T_2-T_1) = 0.02102\ (V)(T_2-T_1) \quad W$$
$$q_{conv} = h_c.A.(T_f-T_a) \quad W$$

$q_{conv} = q_{sen}$, thus $h_c = m.C_p.(T_2-T_1)/A.(T_f-T_a)$;

where T_a = midpoint air temperature between stations.

Example

Data for the example is taken from the 7.5 l/min test. The film temperature was 38.7 °C. At 0 cm the inlet air temperature was 20 °C and at 10 cm the temperature was 28.08 °C. From equation 5 (section 4.5.2) the midpoint temperature is 24.04 °C.

$$q_{sen} = 0.02102\ .\ (7.5).(28.08-20)$$
$$= 1.274\ W$$

The internal surface available for heat transfer over a 10 cm length was: $A = 0.1(\pi.D)$; where D = 23 mm. Thus $A = 7.23 \times 10^{-3}\ m^2$

Therfore h_c is:

$$h_c = 1.274/[7.23 \times 10^{-3}.(38.7-24.04)]$$
$$= 12.04\ W/m^2\ K$$

Summary data for h_c.

Station cm	T_1 °C	T_2 °C	h_c W/m^2 K
7.5 l/min: (T_f=38.7 °C)			
0 - 10	20	28.08	12.04
10 - 20	28.08	31.34	7.88
20 - 30	31.34	35.01	14.55
30 - 40	35.01	36.99	16.0
40 - 50	36.99	37.65	10.46
50 - 60	37.65	37.85	4.59
60 - 70	37.85	38.14	6.67
70 - 80	38.14	38.33	8.83
80 - 90	38.33	38.49	12.17
		Mean (±SD)	10.35 (±3.5)
15 l/min (T_f=38.6 °C)			
0 - 10	20	26.15	17.29
10 - 20	26.15	29.03	11.41
20 - 30	29.03	30.77	8.73
30 - 40	30.77	32.15	8.43
40 - 50	32.15	33.93	13.96
50 - 60	33.93	34.97	10.94
60 - 70	34.97	35.75	10.22
70 - 80	35.75	36.18	7.16
80 - 90	36.18	36.79	14.68
		Mean (±SD)	11.43 (±3.1)

Station cm	T_1 °C	T_2 °C	h_c W/m^2 K
30 l/min (T_f=38.44 °C)			
0 - 10	20	23.96	21.0
10 - 20	23.96	26.72	18.4
20 - 30	26.72	28.2	11.72
30 - 40	28.2	28.75	4.86
40 - 50	28.75	29.54	7.49
50 - 60	29.54	30.6	11.08
60 - 70	30.6	31.2	7.17
70 - 80	31.2	32.06	10.99
80 - 90	32.06	32.6	7.7
		Mean (±SD)	11.2 (±5.1)
50 l/min (T_f=38.3 °C)			
0 - 10	20	22.46	20.96
10 - 20	22.46	26.26	39.65
20 - 30	26.26	26.93	8.33
30 - 40	26.93	27.87	12.54
40 - 50	27.87	28.45	8.32
50 - 60	28.45	28.75	4.5
60 - 70	28.75	29.37	9.76
70 - 80	29.37	29.62	4.21
80 - 90	29.62	30.67	18.75
		Mean (±SD)	14.1 (±10.5)

Station cm	T_1 °C	T_2 °C	h_c W/m^2 K
100 l/min (T_f=37.66 °C)			
0 - 10	20	22.12	34.81
10 - 20	22.12	25.39	63.68
20 - 30	25.39	26.4	22.95
30 - 40	26.4	27.38	24.1
40 - 50	27.38	27.7	8.34
50 - 60	27.7	28.2	13.53
60 - 70	28.2	28.97	22.16
70 - 80	28.97	29.52	16.93
80 - 90	29.52	30.19	16.29
		Mean (±SD)	24.7 (±15.0)

Appendix 11
Transport coefficients k_c and h_c and the Chilton - Colburn analogy.

Solution to equations 5 and 6 requires knowledge of the initial condition of the air (T_a, c_a); boundary air condition (T_f, c_f); the air speed (v); conditioner geometry (dx, P) and the transport coefficients k_c and h_c. h_c was derived from experimental data, presented in section 4.5.2.

'k_c' was estimated using the dimensionless convective heat and mass transport analogy derived from experimental work by Chilton and Colburn (in Welty 1984) also quoted in 4.5.2. Their work is summarised as follows, notation is given in section 4.7.

$Sh = 0.332 \cdot Re^{\frac{1}{2}} \cdot Sc^{0.333}$ or

$Sh/(Re \cdot Sc) \cdot Sc^{0.666} = 0.332\ Re^{-\frac{1}{2}} = jD$, the j factor for mass transfer.

Where Sh: Sherwood no. relating convective mass transfer and diffusivity; $Sh = k_c.L/D_{ab}$

Re: Reynolds no. relating viscosity and momentum; $Re = (L.\rho.v)/u$

Sc: Schmidt no. relating molecular diffusivity of momentum and mass; $Sc = u/(\rho.D_{ab})$

The analogous relation for heat transfer was found to be

$Nu_x = 0.332 \cdot Re^{\frac{1}{2}} \cdot Pr^{0.333}$ or

$Nu_x/(Re \cdot Pr) \cdot Pr^{0.666} = 0.332 \cdot Re^{-\frac{1}{2}} = jH$, the j factor for heat transfer.

Where Nu_x: Nusselt no. relating conductive and convective heat transfer; $Nu_x = h_c.L/k_t$

Pr: Prandtl no. relating molecular diffusivity of momentum and heat; $Pr = u.C_{pa}/k_t$

Now jD = jH; thus:

$$Nu_x/(Re \cdot Pr) \cdot Pr^{0.666} = Sh/(Re \cdot Sc) \cdot Sc^{0.666};$$

which reduces to : $h_c/(\rho.C_{pa}).Pr^{0.66} = k_c.Sc^{0.66}$

or $k_c = h_c/(\rho.C_{pa}).(Pr/Sc)^{0.666}$.

This relation was used to determine k_c in the long axis numerical model, shown at line 450 of the listing in appendix 12.

APPENDIX 12

```
REM Rob Farley, 11-3-88, Programme name LAXMOD
REM Predictor corrector estimate of LAX performance.
PRINT CHR$(27)+"E"
PRINT"Predictor corrector estimate of internal heat transfer in LAX"
PRINT
PRINT
INPUT"Enter airflow through model  l/min ";VE
FLO=VE/(60*(1000)): REM m^3/sec
INPUT"Enter inlet air temperature through model   xC ";TA1
TINSP=TA1
INPUT"Enter moisture content of inlet air   MG/L ";MCI
CA1=MCI*.000001/18: REM mol/cm^3
CINSP=CA1
REM Film temperature 38xC (TFMAX), vapour content 0.043 kg/kg 48.6 mg/l
TFMAX=38
CFMAX=48.6*.000001/18: REM mol/cm^3
TF=38
REM
REM
REM Constants.....
KC=.0262: REM Thermal conductivity of air.......W/m K
NU=1.461E-05: REM Kinematic viscosity.......m^2/s
MU=1.241E-05: REM Dynamic viscosity.........kg/m s
MW=18: REM Molecular weight of water vapour.......kg/kmol
CPW=4178: REM Specific heat of water..........J/kg K
RO=1.177: REM Ambient air density.............kg/m^3
CP=1004: REM Specific heat of air.............J/kg K
REM
REM
REM Modelling........
REM
REM
LENG=.1: DIA=.023
PH=LENG/10
AH=DIA*3.1416/4
PH=DIA*3.1416
VEL=FLO/AH
FOR I=1 TO 9
REM
PRINT"  "
INPUT"Enter hc..... ";HC
FOR CNT=1 TO 10
DAB=(.0915*(TA1+273.2))/10000: REM Diffusion of water vapour in air.....m^2/s
SC=DAB/NU: REM Schmidt number
PR=MU*CP/KC: REM Prandtl number
REM Mass transfer based on Chilton Colburn
REM Analogy...p613 Welty et al Mass, Energy & Mom'm Transfer 1983.
REM
REM
REM
ZH=PH*KC/(AH*VEL)
REM Predictor corrector loop.....  (moisture)
CA2G=CA1+H*ZH*(CFMAX-CA1)
FOR JJ=1 TO 4
CA2=CA1+H/2*ZH*(CFMAX-CA2G)+H/2*ZH*(CFMAX-CA1)
CA2G=CA2
NEXT JJ
REM
REM
REM
NH1=KC*100*(CFMAX-CA1)
YH1=HC+CPW*MW*NH1*10
NH2=KC*100*(CFMAX-CA2G)
YH2=HC+CPW*MW*NH2*10
REM Predictor corrector loop..... (temperature)
TA2G=TA1+H*(ZH/KC)*YH1/(RO*CP)*(TFMAX-TA1)
FOR JJ=1 TO 4
TA2=TA1+H/2*ZH/(KC*RO*CP)*YH2*(TFMAX-TA2G)+H/2*ZH/(KC*RO*CP)*YH1*(TFMAX-TA1
TA2G=TA2
NEXT JJ
REM
REM
REM
CD=(CA1-CINSP)/(CFMAX-CINSP)*100
CD=(INT(CD*100))/100
TD=(TA1-TINSP)/(TFMAX-TINSP)*100
TD=(INT(TD*100))/100
HFG1=2500-TA1*70/30: REM Enthalpy kJ/kg
Q1=HC*(TFMAX-TA1)+NH1*MW*HFG1: REM Rate of heat transfer mW/cm^2
Q1=INT(Q1*10)/10
FX=NH1*18000: REM Film - stream vapour flux mg/cm^2 s
WVC=CA1*18/.000001: REM mg/l
PRINT I,CNT,TA1,WVC
TA1=TA2: CA1=CA2
NEXT CNT
REM
REM
REM
NEXT I
END
```

APPENDIX 15

```
10 REM Program name ORDEX .1 Rob Earley 190887 Brightwood.
20 REM Invivo measurement of laryngeal temperature, inspiration humidity and flow.
30 PRINT CHR$(27)+"E"
35 REM Dec 1987 calibration.... RH=(X%-1286)/1.07
40 PRINT" Program samples temperature, humidity and flow"
60 FOR JJ=0 TO 500: NEXT JJ
70 PRINT CHR$(27)+"E"
80 DEF SEG = 0
90 DEF SEG = PEEK(&411)*256+PEEK(&410)
100 NUI488 = &H1C3
110 NU0488 = &H106
115 INPUT"SIZE  ",SIZE
120 DIM A%(SIZE)
130 DIM B%(SIZE)
140 DIM C%(SIZE)
150 PRINT"      "
160 PRINT"CONS multiplier........"
170 PRINT"x0.3.......... 3
180 PRINT"x1.0.......... 1
190 INPUT M%
200 IF M%=1 THEN CONST=.8
205 IF M%=1 THEN GOTO 220
210 IF M%=3 THEN CONST=.24096 ELSE GOTO 160
220 TOUT%=100
230 PA%=7: NS%=1: ST%=0
240 PRINT CHR$(27)+"E"
250 INPUT"Enter name of data file";N$
260 OPEN N$ FOR OUTPUT AS 2
270 REM
280 REM
290 REM Cold junction temperature measurement
300 CH%=15: FL%=16: SA%=8
310 CALL NU0488 (TOUT%,ST%,FL%,NS%,CH%,SA%,PA%)
320 FL%=17
330 CALL NUI488 (TOUT%,ST%,FL%,NS%,X%,SA%,PA%)
340 V=(X%-1024)*.0025/100
350 R=100*(.5+V)/(.5-V)
360 T0=(R-100)*2.5707
370 T0=INT(T0*100)/100
380 V0=38.680238E*T0
390 V0=.0141277001E*T0*T0+V0
400 PRINT T0
410 O$="PP"
420 REM Humidity probe on
430 SA%=3: X%=0
440 CALL NUI488 (TOUT%,ST%,FL%,NS%,X%,SA%,PA%)
450 RH=(X%-1203)/1.82
460 RH=INT(RH*10)*.1
470 SA%=8: FL%=16: CH%=10+16*3
480 CALL NU0488 (TOUT%,ST%,FL%,NS%,CH%,SA%,PA%)
490 FL%=17
500 CALL NUI488 (TOUT%,ST%,FL%,NS%,T%,SA%,PA%)
510 V=(T%-1024)*.0025/1000
520 V=V*1000000!
530 V=V+V0
540 T=.02740136E*V
550 T=T-.00000043784364E*V*V
560 T=INT(T*10)/10
570 PRINT TAB(5) RH;TAB(15) T
580 FOR JJ%=0 TO 100: NEXT JJ%
590 Q$=INKEY$
600 IF Q$=" " THEN 610 ELSE 410
610 PRINT CHR$(27)+"E"
620 PRINT" COLLECTING DATA"
630 REM
640 FOR I%= 1 TO SIZE
650 REM Temp........
660 SA%=8: FL%=16: CH%=10+16*3
670 CALL NU0488 (TOUT%,ST%,FL%,NS%,CH%,SA%,PA%)
680 FL%=17
690 CALL NUI488 (TOUT%,ST%,FL%,NS%,TI%,SA%,PA%)
700 REM Humidity....
710 SA%=3: X%=0
720 CALL NUI488 (TOUT%,ST%,FL%,NS%,X%,SA%,PA%)
730 SA%=1: Y%=0
740 CALL NUI488 (TOUT%,ST%,FL%,NS%,Y%,SA%,PA%)
750 A%(I%)=TI%
760 B%(I%)=X%
770 C%(I%)=Y%
780 NEXT I%
790 REM
800 REM
810 REM
820 REM Replay of arrays
830 FOR I%=1 TO SIZE
840 A=A%(I%)
850 V=(A-1024)*.0025/1000
860 V=V*1000000!
870 V=V+V0
880 T=.02740136E*V
890 T=T-.00000043784364E*V*V
900 T=INT(T*10)/10
910 RH=B%(I%)-1203
920 RH=RH/1.82
930 RH=INT(RH*10)*.1
935 FLO=C%(I%)*CONST
940 FLO=INT(FLO*100)/100
950 WRITE£2,I%,T,B%(I%),RH,FLO
960 PRINT TAB(2) I%;TAB(10) T;TAB(20) B%(I%);TAB(30) RH;TAB(40) FLO
970 NEXT I%
980 CLOSE£2
990 PRINT" "
1000 PRINT N$"  Saved"
1005 PRINT"  "
1006 PRINT"New settings....(End)....N"
1007 PRINT"Old Settings.............O"
1008 INPUT"Enter.................";SET$
1009 IF SET$="N" THEN GOTO 1013
1010 IF SET$="O" THEN GOTO 240
1011 PRINT"Incorrect entry"
1012 GOTO 1005
1013 PRINT" "
1014 PRINT"End of program"
1015 PRINT"  "
1016 END
```

References

1. Best CH, Taylor NB, "The physiological basis of medical practice" 8th edition, The Williams & Wilkins Company; 1984.

2. Crofton J, Douglas A, "Respiratory Disease" 3rd edition, Blackwell Scientific Publications; 1981.

3. Tortora GJ, Anagnostakos NP, "Principles of Anatomy and Physiology" 4th edition, Harper & Row Publishers; 1984.

4. Hanna LM, Scherer PW, "Measurement of local mass transfer coeffficients in a cast model of the human respiratory tract", Trans. ASME, Journal of Biomechanical Engineering; 1986, 108: 12-18.

5. Engel LA, "The respiratory function of the larynx and upper airway", Pleanary Symposium: British Thoracic Society Summer Meeting; 1987

6. Weibel ER, "Morphometry of the human lung", New York Acedemic; 1964

7. Horstmann G, Iravani J, Norris-Melville G, Richter HG, "Influence of temperature and decreased water content on the ciliated bronchial epithelium", Acta Otolaryngologica; 1977, 84: 124-131.

8. Barnes PJ, "Pulmonary vascular smooth muscle: In vitro pharmacology" (abstract), Joint meeting: Societas Europaea Pneumologia & Societas Europeaea Physiologiae Clinicae Respiratoriae; Paris, September 1986.

9. Balliere, Tindall and Cox: In Best & Taylor (1); 1137-1149

10. Sakula A, "A History of Asthma", Journal of the Royal College of Physicians, London; 1988, 1: 36-44

11. Clark TJH & Godfrey S, "Asthma", Chapman Hall Medical; 1983.

12. Andrews G, "Disease rampant in inner city flats"; The Guardian, Guardian Newspapers Ltd; 15th December 1986.

13. Hedges S, "Take a deep breath", The Guardian, Guardian Newspapers Ltd; 24th April 1986.

14 Hodgkinson N, "Asthma drugs could kill, say specialists", Glasgow Herald, Outram Press Ltd; 12th October 1986.

15. Millar JS, Nairn JR, Unkles RD, McNeil RS, "Cold air and ventilatory function", British journal of Diseases of the chest; 1965, 59: 23-27.

16. Simonsen BG, Jacobs FM, Nadel J, "Role of the autonomic nervous system and the cough reflex in the increased responsiveness of airways with obstructive airways disease", Jounal of clinical Investigation; 1967, 46: 1812-1818.

17. Strauss RH, McFadden ER, Ingram RH, Jaeger JJ, "Enhancement of exercise induced asthma by cold air breathing", New England Journal of Medicine; 1977, 297: 743-747.

18. Deal ER, McFadden ER, Ingram RH, Strauss RH, "Role of respiratory heat exhange in exercise induced asthma", Journal of Applied Physiology; 1979, 46: 467-475.

19. Magussen H, Ruess G, Jorrres R, Kessler K, "Protective effect of disodium chromoglycenic acid on inhalative thermal burden in asthma", Prax. Klin Pneumol; 1983, 37: 364-371

20. Rose-Innes AC, "Low temperature laboratory techniques", English Universities Press; 1973 1: 29 & 246.

21: Gardner WR, "Comments on the 'field capacity' and 'permanent wilting point' concepts". Proceedings of the Symposium on Thermocouple Psychrometers, ed Brown RW & Haveren BPV; Utah University 1972 1: 246.

22. Weinstein RE, Anderson SA, Krale P, Sweet LC, "Effects of humidification on exercise induced asthma (EIA)", Journal of Allergy and Clinical Immunology; 1976, 56: 250-251.

23. Chen WY, Horton DJ, "Heat and water loss from the airways in EIA", Respiration; 1977, 34: 305-313.

24. Bar-Or Y, Neuman I, Doton R, "Effects of dry and humid climates on EIA in children and adolescents", Journal of Allergy and clinical Immunology; 1977, 60: 163-178.

25 McFadden ER, Denison DM, Waller JR, Assoufi B, Peacock A, Sopwith T, "Direct recordings of the temperature in the tracheobronchial tree in normal man", Journal of Clinical Investigation; 1982, 69: 200-205.

26 Silverman M, Anderson SD, "Standardisation of exercise tests in asthmatic children", Journal of Allergy and Clinical Immunology; 1972, 52: 119-209.

27 Anderson SD, "Is there a unifying hypothesis for exercise induced asthma", Journal of Allergy and Clinical Immunology; 1984: 73,660-665.

28 Hahn A, Anderson SD, Morton R, Black JL, Fitch KDA, "Reinterpretation of the effect of temperature and water content of the inspired air in exercise induced asthma", American Review of Respiratory Disease; 1984, 130:575-579.

29. Ben Dov I, Bar-Yishay E, Godfrey S, "Refractory period after exercise induced asthma unexplained by respiratory heat loss", American Review of Respiratory Disease; 1982, 175: 530-534.

30. Assoufi B, Dally M, Lozewicz S, Newman-Taylor A, Denison DM, "Absence of refractory period of cumulative effect of cold air hyperventilation", Thorax; 1986 (abstract) 41: (3) 238.

31. Lee TH, Nagakura T, Cromwell O, Brown MJ, Carson R, Kay AB, "Neutrophil chemotactic activity and histamine in atopic and non atopic subjects after exercise induced asthma", American Review of Respiratory Disease; 1984, 129: 409-412.

32. Deal ER, Wasserman M, Sater NA, Ingram RH, McFadden ER, "Evaluation of the role played by mediators of immediate hypersensitivity in exercise induced asthma", Journal of Clinical Investigation; 1980, 65: 659-665.

33. Farley RD, Albazzaz MK, Patel KR, "Role of cooling and drying in hyperventilation induced asthma", Thorax; 1988, 43: 289-294.

34. Tullet WM, Patel KR, Berkin KE, Kerr JW, "Effect of lignocaine, sodium chromoglycate and ipratropium bromide in exercise induced asthma", Thorax; 1982,37: 737-740.

35. Barnes PJ , Brown MJ, "Venous plasma histamine in exercise and hyperventilation induced asthma in man", Clinical Science; 1981, 61: 159-162.

36. Nagakura T, Lee TH, Assoufi K, Newman-Taylor J, Denison DM, Kay AB, "Neutrophil chemotactic factor in exercise and hyperventilation induced asthma", American Review of Respiratory Disease; 1983, 128: 294-296.

37. McFadden ER, Lenner KAM, Strohl KP, "Post exertional airway rewarming and thermally induced asthma", Journal of Clinical Investigation; 1986, 78: 18-25.

38. Farley RD, Patel KR "Rate of airway cooling in hyperventilation induced asthma", Proceedings: American Review of Respiratory Disease (abstract); 1988

39. Spencer H, "Asthma", in "Pathology of the Lung", Pergammon Press, 2nd edition; 1973.

40. Lopez-Vidriero MT, Reid L, "Asthma", Chapman Hall Medical, 2nd edition; 1983: 79-95.

41. Gravelyn TR, Capper M, Eschenbacher W, "Effectiveness of a heat and moisture exchanger in preventing bronchoconstriction in subjects with asthma" Thorax; 1987,42: 877-880.

42. Lichtiger M, Moya F. "Introduction to the practice of anaesthesia", Harper and Row Publishers; 1974: 454-457.

43. Cheah KP, Davis CN, "The spinning top aerosol generator. Improving the performance.", Journal of Aersol Science, 1984; 15: 741-751.

44. Gilland ER, Sherwood TK, "Diffusion of vapours into airstreams", Industrial and Engineering Chemistry; 1934, 36: 516-523.

45. Hanna LM, Scherer PW, "A theoretical model of heat and water vapour content in the human respiratory tract", Trans. ASME, Journal of Biomechanical Engineering; 1986, 108: 19-27.

46. Welty JR, Wicks CE, Wickson RE, "Fundamentals of Momentum, Heat and Mass Transfer", Wiley, 3rd edition; 1984.

47. Rodgers GFC, Mayhew YR, "Engineering Thermodynamics, Work and Heat Transfer", Longman, 3rd edition; 1983.

48. Farley RD, Patel KR, "Comparison of air warming in the human airway with a thermodynamic model", submitted: Medical and Biological Engineering and Computing.

49. Webb P, "Air temperatures in respiratory tacts of resting subjects in cold", Journal of Applied Physiology; 1951, 4: 378-382.

50. Cole P, "Some aspects of temperature, moisture and heat relationships in the upper respiratory tract", Journal of Laryngology and Otology; 1953, 67: 449-459.

51. Cole P, "Further observations on the conditioning of respiratory air", Journal of Laryngology and Otology; 1953, 67: 669-681.

52. Cole P, "Recordings of respiratory air temperature", Journal of Laryngology and Otology; 1954, 68: 295-307.

53. Ingelstedt S, "Studies of the conditioning of air in the respiratory tract", Acta Otolaryngologica (Supplementum); 1956, 131: 1.

54. Cranston W, Gerbrandy J, Snell S, "Oral, rectal and oesophageal temperatures and some factors affecting these", Journal of Physiology; 1954, 126: 347-358.

55. Saltin B, Hermansen L, "Oesophageal, rectal and muscle temperature during exercise", Journal of Applied Physiology; 1966, 21: 1757-1762.

56. Deal ER, McFadden ER, Ingram RH, Jaeger JJ, "Oesophageal temperature during exercise in asthmatic and non asthmatic subjects", Journal of Applied Physiology; 1979, 46: 484-490.

57. McFadden ER, Pichuro BM, Bowman HF, Ingenito E, Burns S, Dowling N, Solway J, "Thermal mapping of the airways of humans" Journal of Applied Physiology; 1985, 58: 564-570.

58. Tessier P, Cartier A, L'Archeveque J, Ghezzo H, Martin R, Malo JL, "Within and between day reproducibility of isocpnic cold air challenges in subjects with asthma", Journal of Allergy and Clinical Immunology; 1986, 78:379-387.

59. Anderson SD, Schoffel RE, Black JL, Daviskas E, "Airway cooling as the stimulus to exercise induced asthma, a re-evaluation", European Journal of Respiratory Disease; 1985, 67: 20-30.

60. Ray D, Strek M, Ingenito, E, Schumacher P, Solway J, "Airway wall cooling is similar during warm dry air hypernea", American Review of Respiratory Disease; 1987, (abstract) 135, 4 A95.

61. Gilbert IA, Foulke JM, Lenner KA, McFadden ER, "Direct assesment of the temperature and water flux in the respiratory tract of asthmatics during exercise", American Review of Respiratory Disease; 1987, (abstract) 135 (4) A90.

62. Cramer II, "Heat and moisture exchange of the respiratory mucus membrane", Annals of Otology, Rhinology and Laryngology; 1957, 66: 327-343.

63. Dery R, Jaques A, Clavert M, "Heat and moisture patterns during anaesthesia with the semi closed system", Canadian Anaesthesia Society Journal; 1967, 14: 287-298.

64. Kiedel FA, "A novel and inexpensive instrument for accurate analysis of traces of water", Pittsburgh Conference on Analytical Chemistry and Applications; 1956.

65. Reitgen PPL, "Solid state humidity sensors", Sensors and Actuators; 1981, 2: 85-89.

66. Forbes AR, "Humidification and mucus flow in the intubated trachea", "British Journal of Anaesthesia; 1973, 43: 874-878.

67. Tsuda T, Nogachi H, Takuim Y, Aochi O, "Optimum humidification of air administered to a tracheostomy in dogs", British Journal of Anaesthesia; 1977, 49: 965-976.

68. Stoecker WF, Jones JW, "Refrigeration and Air Conditioning" McGraw Hill; 1982, 2nd edition.

69. Nakamura S, "Computational Methods in Engineering and Science - With Applications to Dynamics and Nuclear Systems", John Wiley; 1977.

70. Farley RD, Patel KR, " A microcomputer based facility for use in the diagnosis of thermally induced asthma", Journal of Engineering in Medicine; 1989, 203 issue H1.